A Dynamic Circadian Protein-Protein Interaction Network

DISSERTATION

zur Erlangung des akademischen Grades
doctor rerum naturalium
(Dr. rer. nat.)
im Fach Biologie
eingereicht an der

Mathematisch-Naturwissenschaftlichen Fakultät I
der Humboldt-Universität zu Berlin
von

Diplom-Biologe Thomas Wallach

Präsident der Humboldt-Universität zu Berlin
Prof. Dr. Jan-Hendrik Olbertz

Dekan der Mathematisch-Naturwissenschaftlichen Fakultät I
Prof. Stefan Hecht PhD

Gutachter: 1. Prof. Dr. Hanspeter Herzel
2. Prof. Dr. Achim Kramer
3. Prof. Dr. Martha Merrow

Tag der mündlichen Prüfung: 21. September 2012

INDEX

INDEX OF THE APPENDIX

ABBREVIATIONS

aa	amino acid(s)
AD	activation domain
AHR	aryl hydrocarbon receptor
AKT1	v-akt murine thymoma viral oncogene homolog 1
Amp	amplitude
aq. dest.	*aqua destillata*
AR	androgen receptor
ar	arrhythmic
ARNT	aryl hydrocarbon receptor nuclear translocator
ARNTL	aryl hydrocarbon receptor nuclear translocator-like 1
ARNTL2	aryl hydrocarbon receptor nuclear translocator-like 2
ASH2L	absent, small, or homeotic-like (*Drosophila*)
ATF1	activating transcription factor 1
ATN1	atrophin 1
ATRX	alpha thalassemia/mental retardation syndrome X-linked
BATF	basic leucine zipper transcription factor
BCA	bicinchonin acid
BHLHB2	basic helix-loop-helix family, member e40
BHLHB3	basic helix-loop-helix family, member e41
BIND	Biomolecular Interaction Network Database
BIOGRID	Biological General Repository for Interaction Datasets
Bis-Tris	Bis(2-hydroxyethyl)amino-tris(hydroxymethyl)methan
BMAL1	brain and muscle ARNTL
BMAL2	brain and muscle ARNTL2
bp	base pair
BP	biological processes
BSA	bovine serum albumin
BTRC	beta-transducin repeat containing
Byr	billion years
CA2	carbonic anhydrase II
cAMP	cyclic adenosine monophosphate
Cat. no.	catalog number
cc	correlation coefficient
CCA1	circadian clock associated 1
cDNA	complementary DNA
CEBPA	CCAAT/enhancer binding protein, alpha
CEBPG	CCAAT/enhancer binding protein, gamma
CHD4	chromodomain helicase DNA binding protein 4

CHEK1	checkpoint kinase 1
CHX	cycloheximide
CIPC	circadian protein
CK1/2	casein kinase 1/2
CLOCK	circadian locomoter output cycles kaput protein
CM	complete medium
CMV	cytomegalovirus promoter
CNS	central nervous system
co-IP	co-immunoprecipitation
Corr. coeff.	correlation coefficient
CREB3	cAMP responsive element binding protein 3
CREB3L1	cAMP responsive element binding protein 3-like 1
CREBBP	CREB binding protein
CREM	cAMP responsive element modulator
CRY1	cryptochrome 1 (photolyase-like)
CRY2	cryptochrome 2 (photolyase-like)
CSNK1D	casein kinase 1, delta
CSNK1E	casein kinase 1, epsilon
CSNK2A1	casein kinase 2, alpha 1 polypeptide
CSNK2A2	casein kinase 2, alpha prime polypeptide
CSNK2B	casein kinase 2, beta polypeptide
CT	circadian time points
CUL4A	cullin 4A
CUL4B	cullin 4B
D	dalton
Damp	damping
DBD	DNA binding domain
DBP	D site of albumin promoter (albumin D-box) binding protein
DDB1	damage-specific DNA binding protein 1, 127 kDa
DDIT3	DNA-damage-inducible transcript 3
DIP	Database of Interacting Proteins
DMEM	Dulbecco’s modified eagle medium
DMSO	dimethyl sulfoxide
DNA	deoxyribonucleic acid
DNMT1	DNA (cytosine-5-)-methyltransferase 1
DNMT3A	DNA (cytosine-5-)-methyltransferase 3 alpha
DNMT3B	DNA (cytosine-5-)-methyltransferase 3 beta
dNTP(s)	deoxynucleoside triphosphate(s)
DR1	down-regulator of transcription 1
DTL	denticleless homolog (*Drosophila*)
DTT	dithiothreitol

Dyn.	dynamic
E-box	enhancer box
E4BP4	E4 promoter-binding protein 4
E2F6	E2F transcription factor 6
EDTA	ethylenediaminetetraacetic acid
EED	embryonic ectoderm development
e.g.	*exempli gratia*
EP300	E1A binding protein p300
EPAS1	endothelial PAS domain protein 1
Epo	erythropoietin
ESR1	estrogen receptor 1
EtBr	ethidium bromide
Exp.	experiment
EZH2	enhancer of zeste homolog 2 (*Drosophila*)
FBS	fetal bovine serum
FBXL3	F-box and leucine-rich repeat protein 3
FBXL15	F-box and leucine-rich repeat protein 15
FBXW11	F-box and WD repeat domain containing 11
FDR	false discovery rate
FRET	fluorescence resonance energy transfer
FRQ	frequency
FW	forward
Gapdh	glyceraldehyde-3-phosphate dehydrogenase
GFP	green fluorescent protein
GIT1	G protein-coupled receptor kinase-interacting protein
GNAI1	guanine nucleotide binding protein (G protein), alpha inhibiting activity polypeptide 1
GNAI2	guanine nucleotide binding protein (G protein), alpha inhibiting activity polypeptide 2
GNB1	guanine nucleotide binding protein (G protein), beta polypeptide 1
GO	Gene Ontology
GOE	Great Oxidation Event
GPRASP1	G protein-coupled receptor associated sorting protein 1
GRWD1	glutamate-rich WD repeat containing 1
GSK3B	glycogen synthase kinase 3 beta
h	hour or human
HC	antibody heavy chain
HCFC1	host cell factor C1
HCFC2	host cell factor C2
HD	Huntington’s disease
HDAC1	histone deacetylase 1
HDAC2	histone deacetylase 2

HEPES	4-(2-hydroxyethyl)-1-piperazineethanesulfonic acid
HIF1A	hypoxia inducible factor 1, alpha subunit
His	histidine
HLF	hepatic leukemia factor
HPLC	high-performance liquid chromatography
HPRD	Human Protein Reference Database
HRP	horseradish peroxidase
htt	huntingtin
hrs	hours
HSP90AA1	heat shock protein 90 kDa alpha (cytosolic), class A, member 1
i.e.	*id est*
IgG	immunoglobulin G
IP	immunoprecipitation
k	kilo
kb	kilo base
KAT2B	K(lysine) acetyltransferase 2B
KEGG	Kyoto Encyclopedia of Genes and Genomes
lacZ	gene of β-galactosidase
LB	Luria Broth
LC	antibody light chain
Leu	leucine
LIM	Lin11, Isl-1, Mec-3
LMO3	LIM domain only 3 (rhombotin-like 2)
lp	long period
Luc	firefly luciferase
LUCA	last universal common ancestor
MCC	mutated in colorectal cancers
MED1	mediator complex subunit 1
MEN1	multiple endocrine neoplasia I
min	minute
MLL	myeloid/lymphoid or mixed-lineage leukemia (*Drosophila*)
MOPS	3-(N-morpholino) propanesulfonic acid
mRNA	messenger RNA
MYC	v-myc myelocytomatosis viral oncogene homolog (avian)
MYOD1	myogenic differentiation 1
NCOA1	nuclear receptor coactivator 1
NCOA2	nuclear receptor coactivator 2
NCOA3	nuclear receptor coactivator 3
NCOA5	nuclear receptor coactivator 5
NCOR1	nuclear receptor corepressor 1
NCOR2	nuclear receptor corepressor 2

NFIL3	nuclear factor, interleukin 3 regulated
NME1	non-metastatic cells 1, protein (NM23A)
NME2	non-metastatic cells 2, protein (NM23B)
NONO	non-POU domain containing, octamer-binding
NOS1	nitric oxide synthase 1 (neuronal)
NOS1AP	nitric oxide synthase 1 (neuronal) adaptor protein
NPAS2	neuronal PAS domain protein 2
NPAS4	neuronal PAS domain protein 4
NR0B1	nuclear receptor subfamily 0, group B, member 1
NR1D1	nuclear receptor subfamily 1, group D, member 1
NR1D2	nuclear receptor subfamily 1, group D, member 2
NR2E3	nuclear receptor subfamily 2, group E, member 3
NRIP2	nuclear receptor interacting protein 2
ORF(s)	open reading frame(s)
PAS	PER-ARNT-SIM
PASK	PAS domain containing serine/threonine kinase
PBS	phosphate buffered saline
PBST	PBS Tween
PCC	Pearson correlation coefficient
PCNA	proliferating cell nuclear antigen
PCR	polymerase chain reaction
PEG	polyethylene glycol
PER1	period homolog 1 (*Drosophila*)
PER2	period homolog 2 (*Drosophila*)
PER3	period homolog 3 (*Drosophila*)
PDGFRB	platelet derived growth factor receptor, beta
PHF1	PHD finger protein 1
PML	promyelocytic leukemia
POLA2	polymerase (DNA directed), alpha 2 (70 kD subunit)
POLR2A	polymerase (RNA) II (DNA directed) polypeptide A, 220 kDa
PPI	protein-protein interaction
PP1	protein phosphatase 1
PPP1CA	protein phosphatase 1, catalytic subunit, alpha isozyme
PPP1CB	protein phosphatase 1, catalytic subunit, beta isozyme
PPP1CC	protein phosphatase 1, catalytic subunit, gamma isozyme
PPP1R15B	protein phosphatase 1, regulatory subunit 15B
PP2	protein phosphatase 2
PPP2CA	protein phosphatase 2, catalytic subunit, alpha isozyme
PPP2CB	protein phosphatase 2, catalytic subunit, beta isozyme
PPP2R1A	protein phosphatase 2, regulatory subunit A, alpha
PPP2R1B	protein phosphatase 2, regulatory subunit A, beta

PPP2R5D	protein phosphatase 2, regulatory subunit B', delta
PPP2R5E	protein phosphatase 2, regulatory subunit B', epsilon isoform
PPP5C	protein phosphatase 5, catalytic subunit
PRKACA	protein kinase, cAMP-dependent, catalytic, alpha
PRKCA	protein kinase C, alpha
PRX	peroxiredoxin
PSMC5	proteasome (prosome, macropain) 26S subunit, ATPase, 5
PSPC1	paraspeckle component 1
PXN	paxillin
q-PCR	quantitative PCR
qRT-PCR	quantitative real-time PCR
r	rat
RAR	retinoic acid receptor
RARA	retinoic acid receptor, alpha
RASD1	RAS, dexamethasone-induced 1
RBBP5	etinoblastoma binding protein 5
RHT	rethinohypothalamic tractus
RNA	ribonucleic acid
RNAi	RNA interference
RORA	RAR-related orphan receptor A
RORB	RAR-related orphan receptor B
RORC	RAR-related orphan receptor C
ROS	Reactive oxygen species
RRE	ROR response element
RT	room temperature
RT-PCR	reverse transcriptase PCR
RV	reverse
RXRA	etinoid X receptor, alpha
SCN	suprachiasmatic nucleus
SDS	sodium dodecyl sulfate
s.d.	standard deviation
SDS-PAGE	sodium dodecyl sulfate polyacrylamide electrophoresis
sec	second(s)
SFPQ	splicing factor proline/glutamine-rich
s.e.m.	standard error of the mean
SIM	single-minded
siRNA	small interfering RNA
SOD	superoxide dismutase
sp	short period
SP1	simian-virus-40-protein-1/specificity protein 1
SPI1	spleen focus forming virus (SFFV) proviral integration oncogene spi1

STAT3	signal transducer and activator of transcription 3
SUZ12	suppressor of zeste 12 homolog (*Drosophila*)
SV40	Simian virus 40
Sym.	symbol
TAE	Tris/acetate/EDTA
TCEP	Tris(2-carboxyethyl)phosphine
TE	Tris/EDTA
TEF	thyrotrophic embryonic factor
TGFBR1	transforming growth factor beta receptor 1
TIM	timeless homolog *(Drosophila*)
TIPIN	TIMELESS interacting protein
TOC1	timing of CAB expression 1
TREX1	three prime repair exonuclease 1
Tris	Tris(hydroxymethyl)-aminomethan
Trp	tryptophan
TW	Thomas Wallach
UBE2I	ubiquitin-conjugating enzyme E2I
UNIHI	Unified Human Interactome Database
Ura	uracil
UV	ultraviolet
V	volt
v/v	volume per volume
VAV1	vav 1 guanine nucleotide exchange factor
VCL	vinculin
w/v	weight per volume
WD	tryptophan-aspartic acid
WDR5	WD repeat domain 5
WDR57	WD repeat domain 57
Y2H	yeast-two-hybrid

FIGURES

SUMMARY

Essentially all biological processes depend on protein-protein interactions (PPIs). Timing of such interactions is crucial for regulatory function. Although circadian (~24 hrs) clocks constitute fundamental cellular timing mechanisms regulating important physiological processes PPI dynamics on this timescale are largely unknown.

To elucidate so far unknown regulatory mechanisms within the circadian clockwork, I have systematically mapped PPIs among 46 circadian components using high-throughput yeast-two-hybrid (Y2H) interaction experiments. I have identified 109 so far uncharacterized interactions and successfully validated a sub-fraction *via* co-immunoprecipitation experiments in human cells. Among the novel PPIs, I have identified modulators of CLOCK/BMAL1 function and further characterized the role of protein phosphatase 1 (PP1) in the dynamic regulation of BMAL1 abundance. Furthermore, to generate a more comprehensive circadian PPI network, the experimental network was enriched and extended with additional interactions and interaction partners from literature, some of which turned out to be essential for normal circadian dynamics. The integration of circadian mRNA expression profiles allowed us to determine the interaction dynamics within our network. Systematic genetic perturbation studies (RNAi and overexpression in oscillating human cells) revealed a crucial role of dynamic regulation (*via* rhythmic PPIs) for the molecular clockwork. Furthermore, dynamic modular organization as a pervasive circadian network feature likely contributes to time-of-day dependent control of many cellular processes. Global analysis of the proteome regarding circadian regulation of biological processes *via* rhythmic PPIs revealed time-of-day dependent organization of the human interactome. Circadian PPIs dynamically connect many important cellular processes like signal transduction and cell cycle, which contribute to temporal organization of cellular physiology.

Overall, these data provide a global view and valuable resource on the circadian control of protein-protein interactions that is not only important for the circadian oscillator but also for the temporal orchestration of many essential cellular processes.

ZUSAMMENFASSUNG

Die dynamische Regulation von Protein-Protein Interaktionen (PPIs) ist wichtig für den Ablauf von biologischen Prozessen. Die circadiane Uhr, die einen ~24 Stunden Rhythmus generiert und eine Vielzahl von physiologischen Parametern steuert kann auch die Dynamik von PPIs regulieren. Obwohl es für einige der PPIs innerhalb des circadianen Oszillators Informationen über ihr tageszeitspezifisches Auftreten gibt, fehlt jedoch diese temporale Auflösung für die meisten PPIs.

Um neue Erkenntnisse über regulatorische Mechanismen innerhalb des molekularen Oszillators zu gewinnen, habe ich zunächst alle möglichen PPIs zwischen 46 circadianen Komponenten mittels eines systematischen *yeast-two-hybid* (Y2H) Screens bestimmt. Dabei habe ich 109 bis dahin noch unbekannte PPIs identifiziert und einen repräsentativen Anteil mittels Co-Immunopräzipitationsexperimenten in humanen Zellen validiert. Unter den neuen PPIs habe ich bis dahin unbekannte Modulatoren der CLOCK/BMAL1 Transaktivierung identifiziert und dabei die Rolle der Proteinphosphatase 1 (PP1) als dynamischen Regulator der BMAL1 Stabilität funktionell charakterisiert. Das experimentelle PPI Netzwerk wurde mit bereits aus der Literatur bekannten PPIs und Interaktionspartnern ergänzt. Eine systematische RNAi Studie belegte außerdem die Relevanz der aus der Literatur stammenden Interaktoren für die ~24 Stunden Periodizität. Um eine Aussage über die Dynamik der PPIs im Netzwerk treffen zu können, wurden circadiane mRNA Expressionsdaten in das PPI Netzwerk integriert. Systematische Perturbationsstudien, in denen alle Komponenten des experimentellen Netzwerkes mittels RNAi herunterreguliert oder überexprimiert wurden, zeigten eine essentielle Bedeutung für die dynamischen PPIs innerhalb des circadianen Oszillators auf. Desweiteren wurden im circadianen PPI Netzwerk funktionelle Module identifiziert, welche dynamisch organsiert sind. Durch eine systemweite Analyse des humanen Proteoms wurden viele dynamische PPIs identifiziert, die biologische Prozesse wie z.B. Signaltransduktion und Zellzyklus miteinander verbinden. Rhythmische PPIs sind daher von Bedeutung für die zeitliche Organisation zellulärer Physiologie.

Insgesamt wurden hier neue Erkenntnisse über die circadiane Dynamik von PPIs gewonnen, was zu einem erweiterten Verständnis der circadianen Uhr und ihrer Regulations-mechanismen führt.

1 INTRODUCTION

1.1 Circadian Rhythms and Chronohistory

On the first look, the beauty of life seems to be so simple and one could assume it is based on many circumstances that decide about the fate and development of organisms on our planet. But on the second look, life only could create such diversity because many processes important within an organism's life as well as among different species are precisely timed due to adaption to environmental settings.

In its ecliptic route around the sun, the earth rotates around its axis and, at every given moment, one half of the earth is in light while the other half is in darkness. These light-dark cycles define the length of day and night and are the strongest rhythmic stimuli on our planet creating the basis for a fundamental adjustment. Circadian rhythms (circadian is derived from Latin *circa* – about – and *dies* – day) are biological cycles of about 24 hours (hrs), which are conserved in nearly all living organisms from bacteria to humans.

In the past, circadian rhythms were assumed to be a passive response to the light-dark cycle, today, it is known that they are genetically determined and endogenously generated [1-3].

The first proof for the existence of intrinsic circadian rhythms and therefore their persistence under constant conditions was done in the 18th century by the French astronomer de Mairan. Observing plants kept in darkness he recorded leaf movements that continued with a daily periodicity in absence of a light-dark cycle [4]. However, it took again two centuries to prove the genetic character of circadian rhythms by demonstrating that the period length is heritable using bean plants as a model organism by experiments of Bünning in the 1930s [5].

Since the second part of the 20th century, scientist could demonstrate the existence of circadian rhythms in other species reaching from single-cell eukaryotes (Sweeny and Hastings 1957) [6], birds (Kramer 1952) [7], and humans (Aschoff and Wever 1962) [8, 9] but the genes that program the circadian system still remained obscure. The discovery of clock mutants in the fruit fly *Drosophila melanogaster* by Ronald Konopka and Seymour Benzer in 1971 was the beginning of the understanding of the molecular mechanisms underlying a circadian phenotype. In a mutagenesis screen, one gene was identified that when mutated led

to an altered circadian free-running period in pupal eclosion and locomotor activity [10]. The affected flies were called *per* mutants (*per* for *period*). Almost simultaneously the *frq* (*frq* for *frequency*) gene was discovered in the filamentous fungus *Neurospora crassa* that is a crucial regulator of conidiation rhythms [11].

The extensive knowledge of *Drosophila* and *Neurospora* genetics, together with novel molecular approaches resulted in a rapid progression unraveling the molecular mechanisms for circadian function. Although some differences exist between the model organisms the basic molecular principles resulting in circadian phenotype are common even for the mammalian molecular oscillator.

Besides circadian rhythms, many other biological rhythms can co-exist within an individual organism like rhythms in neuronal activity and seasonal or annual cycles that are present within the animal kingdom and human society (Figure 1).

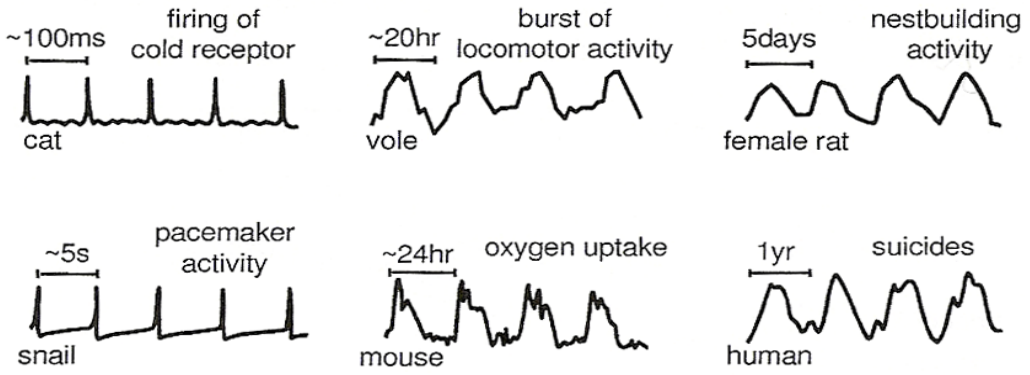

Figure 1. Examples of Biological Rhythms of Different Species and Their Periodicity.
Taken from [12].

1.2 Characteristics of Circadian Rhythms

Circadian rhythms have three principal properties:

(i) they can be entrained or synchronized to the light-dark cycle with a stable phase relationship,

(ii) they are self-sustained and persist in constant conditions like in the absence of a light-dark cycle (constant darkness) with a endogenous period that only differs slightly from 24 hrs

(free-running period), and

(iii) they are temperature compensated, *i.e*. they show only minor changes in response to changes in external temperature.

1.3 Circadian Rhythms in Human Physiology

The circadian clock affects the daily rhythm of many physiological processes. In humans, *e.g.* the sleep-wake cycle, body temperature, cognitive and motoric performance, secretion of hormones and immune function are regulated in a circadian manner [2, 13, 14].

Even though circadian rhythms have a propensity to be synchronized by cycles of light and dark (the strongest synchronization stimuli or *zeitgeber* for the circadian system), other factors – such as temperature, food intake, stress and also exercise – can effect circadian timing [15-17].

1.4 Hierarchical Organization of Circadian Oscillators

In mammals, there is a hierarchical organization of biological oscillators. The master oscillator or pacemaker that orchestrates the circadian program is located in the suprachiasmatic nucleus (SCN) in the anterior hypothalamus. The SCN is a paired nucleus of small neurons above the optic chiasm on each side of the third ventricle. The SCN receives optic input from the retina by the retinohypothalamic tractus resulting in the synchronization of SCN neurons. The entrained or synchronized SCN than coordinates the timing of so called "slave" oscillators *e.g*. in other brain areas like the cortex and in peripheral tissues like kidney and liver (Figure 2) [2].

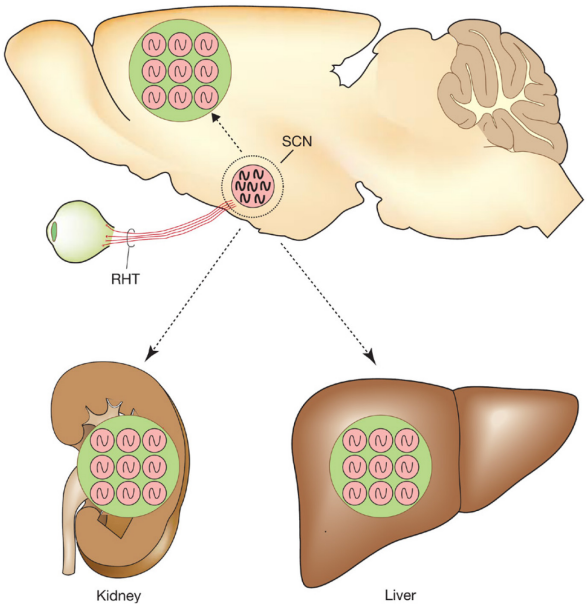

Figure 2. Hierarchical Organization of Circadian Clocks in Mammals.
The suprachiasmatic nucleus (SCN) consists of two compact cell groups above the optic chiasm and at the base of the third ventricle. The SCN receives optic input signals through the rethinohypothalamic tractus (RHT) and synchronizes circadian clocks in peripheral tissues (from [2]).

1.5 The Circadian Timing System – Input and Output Pathways

The general properties of an about 24 hrs oscillation require a system that is composed of three components (Figure 3):

(i) photoreceptors and their input to the pacemaker,

(ii) the ~24 hrs clocks/pacemakers, and

(iii) the output from the pacemakers that leads to the robust regulation of circadian physiology.

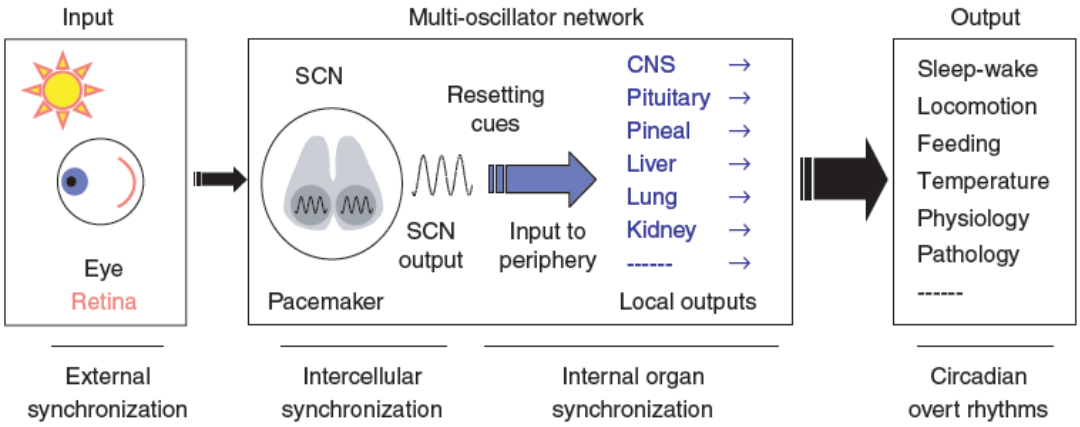

Figure 3. Overview on the Basic Organization of the Mammalian Circadian Timing System.
Taken from [18]. SCN (suprachiasmatic nucleus), CNS (central nervous system).

1.6 Molecular Clocks

In mammals and other species, the circadian oscillator is composed of interconnected transcriptional translational negative and positive feedback-loops, which generate circadian rhythms at the molecular level. Within this gene-regulatory network, a precise timing of gene expression, protein-protein interactions (PPIs) as well as posttranscriptional and post-translational modifications is essential for sustaining circadian rhythms with normal dynamics [1-3]. The interaction between the transcription factors CLOCK and BMAL1 (= ARNTL), which has been discovered in a Y2H screen [19], is crucial for the activation of the *Period* (*Per*) and *Cryptochrome* (*Cry*) genes. PER and CRY proteins form large complexes that inhibit their own transcription by binding directly to the CLOCK/BMAL1 complex during the late night (Figure 4) [20]. This fundamental principle of the negative feedback mechanism is conserved in many species and required for keeping circadian periodicity.

In the last years, many novel clock genes and modifiers have been discovered leading to a better understanding of the circadian oscillator. Especially posttranslational modifications of individual clock proteins and complexes have been recognized as crucial for circadian rhythm generation. *E.g.* effects mediated by kinases like Casein kinase 1 and 2 (CSNK1E/D isoforms, CSNK2A and CSNK2B subunits) as well as F-box proteins like FBXL3 are essential for complex formation, sub-cellular localization and degradation of circadian proteins [21-23].

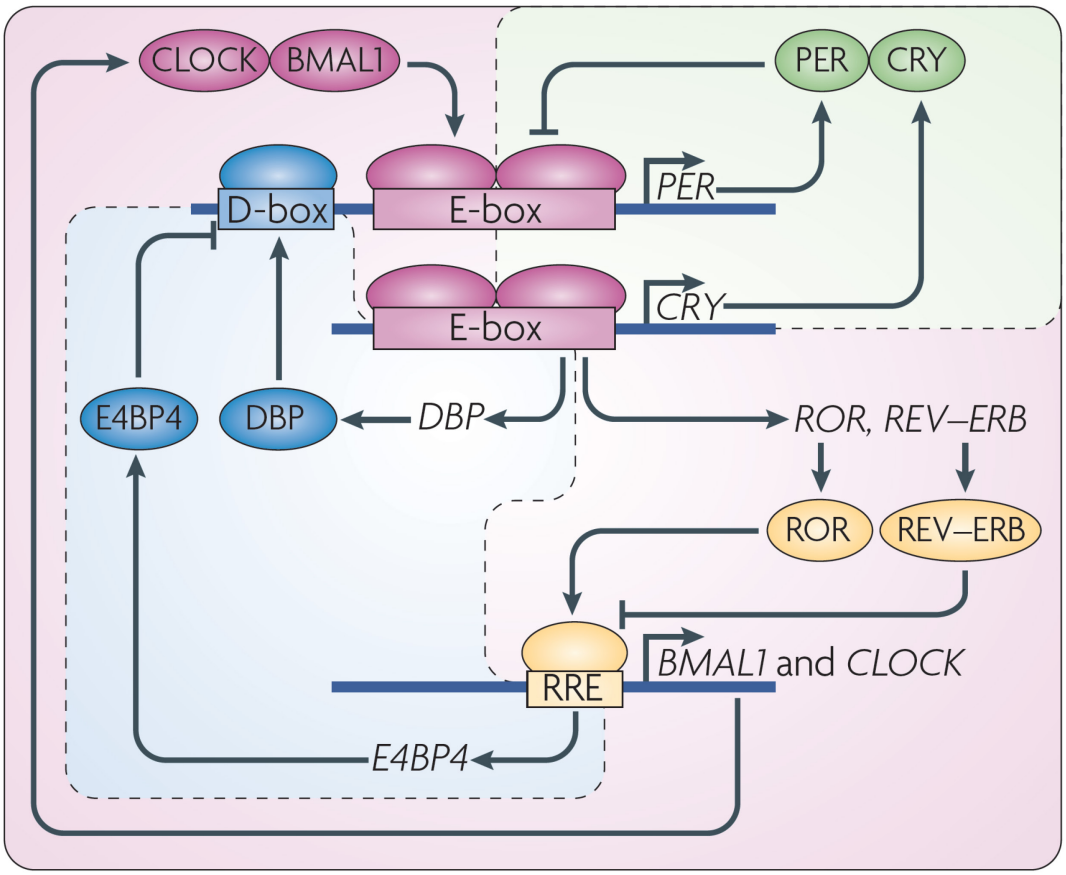

Figure 4. Basic Principle of the Mammalian Molecular Clock.
Circadian rhythms are generated *via* interconnected transcriptional and translational negative-feedback loops within various cells and tissues. At the core, the positive regulators CLOCK and BMAL1 activate the transcription of their own repressors (PERs and CRYs) by binding to enhancer elements (E-boxes) within their promoters. Later in the circadian cycle, PER and CRY proteins undergo posttranslational events and as a result, feed back with a crucial delay to inhibit their own transcription. In addition, the transcription of *CLOCK* and *BMAL1* is regulated by ROR transcriptional activators and the REV-ERB repressors *via* binding to ROR response elements (RRE). Furthermore, the activators DBP (D site of albumin promoter (albumin D-box) binding protein) and E4BP4 (E4 promoter-binding protein 4) together regulate the expression of D-box containing genes as *PER* and other clock output genes (from [3]).

Although transcription, translation and protein-protein interactions events in concert generate the circadian pace recent studies indicate that circadian rhythms can sustain even without transcriptional regulation *e.g.* in the unicellular pico-eukaryotic alga *Ostreococcus tauri* and in human red blood cells. In these cells about 24-hrs redox cycles of peroxiredoxins (antioxidant proteins) show all properties of a circadian oscillation without transcription being necessary. These rhythms are highly conserved in *Bacteria*, *Archaea* and *Eukaryota* suggesting that redox homeostasis has co-evolved within this organisms and therefore probably is a valid universal bio-marker for circadian rhythms and circadian clock evolution

after the Great Oxidation Event (GOE) on our planet (Figure 5) [24-26].

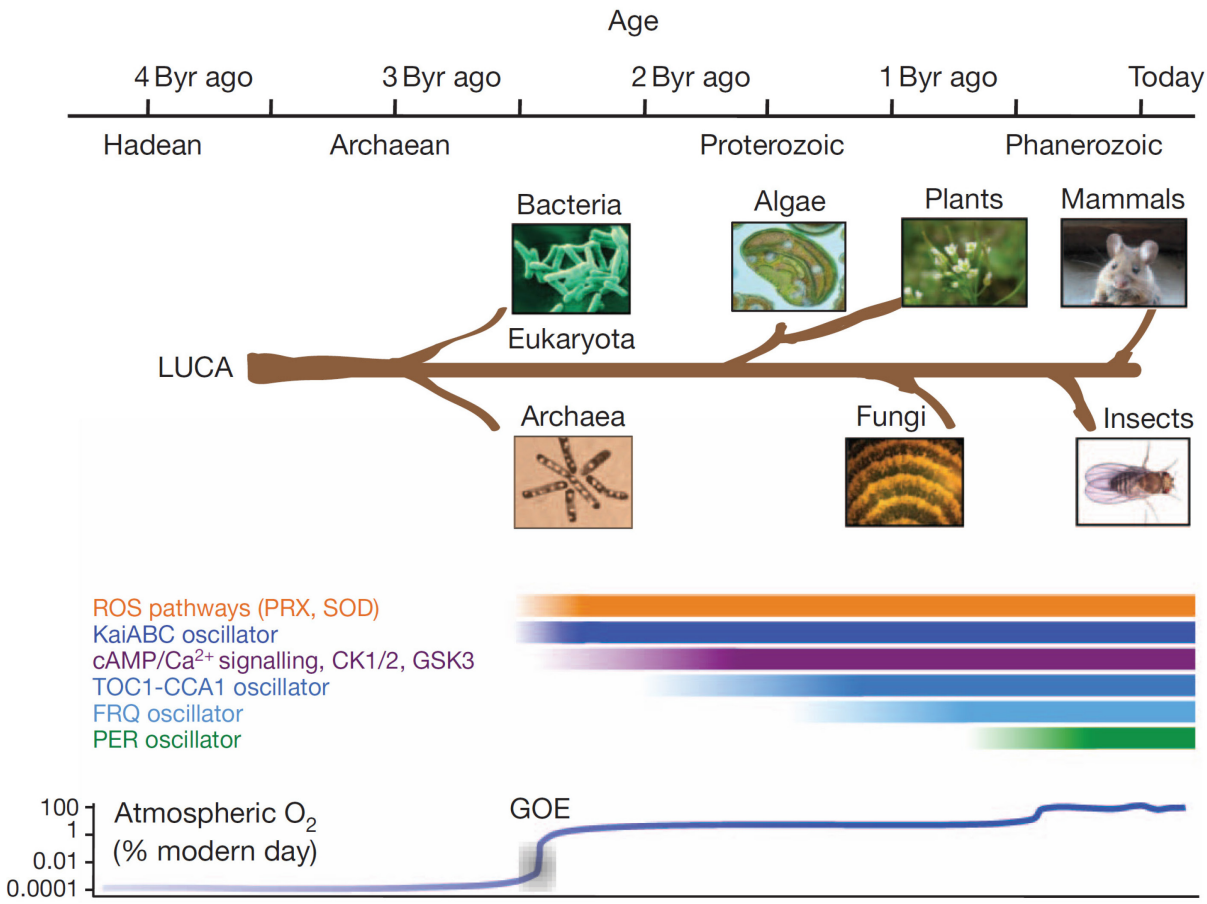

Figure 5. Evolution of the Circadian Oscillator.
Top: Timeline and geological area of illustrated species. Middle: Phylogenetic tree represents the genetic origins of the depicted phyla descending from the last universal common ancestor (LUCA). Bottom: Bars mark the time from which the depicted oscillator systems with their characteristic components have evolved. Atmospheric oxygen levels are given in percent (from [24]). Byr (billion years), cAMP (Cyclic adenosine monophosphate), CCA1 (circadian clock associated 1 circadian clock associated 1), CK1/2 (casein kinase 1/2), FRQ (frequency), GOE (Great Oxidative Event), GSK3 (glycogen synthase kinase 3), PER (period), PRX (peroxiredoxins), ROS (reactive oxygen species), SOD (superoxide dismutase), TOC1 (timing of CAB expression 1).

1.7 Systems-Level Understanding of Circadian Clocks

The molecular clock regulates a multiplicity of cellular functions. *E.g.* circadian rhythms in gene expression – 2-10% of the transcriptome in a given tissue – is under circadian control (Figure 6) [13, 27-29]. Consequently, also a large fraction of the proteome is thought to be regulated in a time-of-day dependent manner. However, large-scale data sets of the circadian proteome are still rare [29].

Recent publications using circadian microarray data derived from different mammalian

tissues provide systematic analysis of the rhythmic regulation of transcription on a systems-wide level being essential for the clock controlled regulation of cellular output processes [29, 30]. In addition, circadian metabolome analyses have uncovered that many essential physiological processes are dependent on circadian regulation indicated by *e.g*. the circadian oscillation of a variety of metabolites including the clock controlled regulation of the uracil salvage pathway [14, 31, 32].

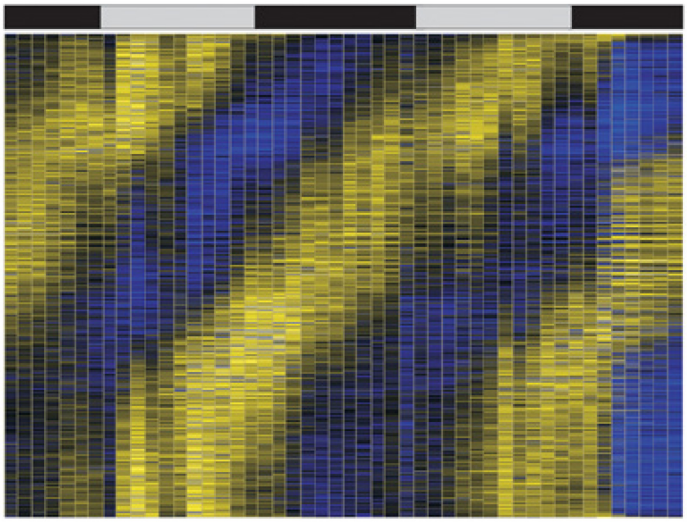

Figure 6. Circadian Microarray Transcriptome Analysis of Mouse Liver.
Lines represent individual transcript profiles. Expression data were sorted in respect to the circadian phase (from [27]). Gray bar: subjective day; black bar: subjective night.

In the last decade, different Systems Biology approaches were applied to generate a more comprehensive view of processes that result in a circadian phenotype. Transcriptome as well as proteome analyses were used to characterize circadian parameters of a multiplicity of genes in different organisms and tissues. Furthermore, large scale forward and reverse genetics screens have identified new components and modulators important for the robustness and fine tuning of circadian timing and linked the circadian clock to other biological processes like the control of immune response [13, 22, 27, 33-35]. In addition, recent studies have uncovered proportionality and paralog compensation as crucial circadian network features essentially contributing to its robustness (see Figure 7) [36, 37].

However, with the rapid progression in systems identification leading to the discovery of many novel molecular clock or clock associated components a comprehensive network view of the circadian oscillator is still missing.

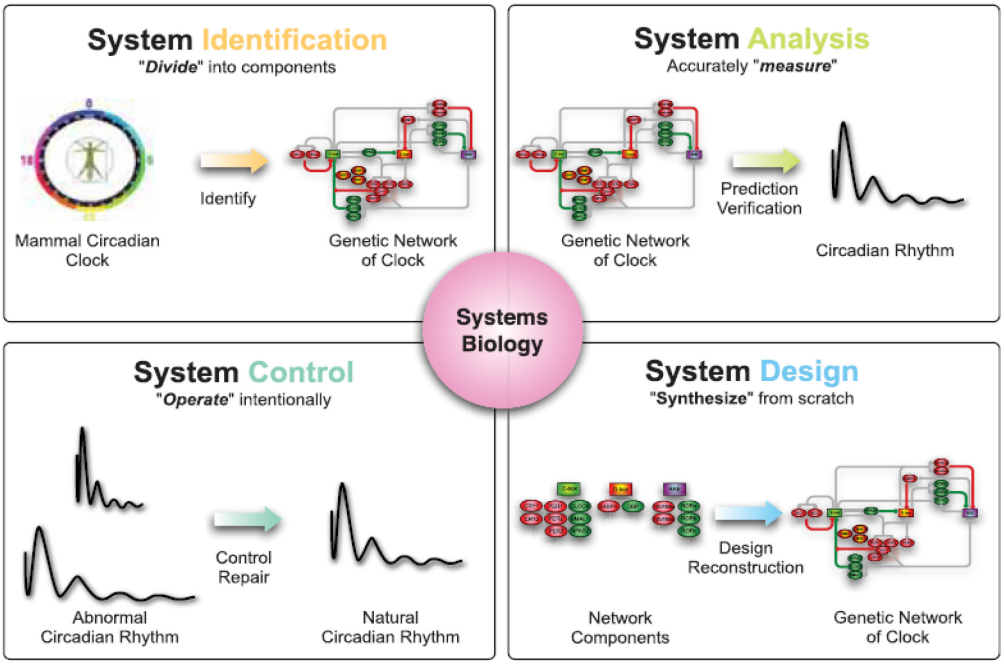

Figure 7. Four Different Levels of Systems Biology for the Molecular Oscillator.
Systems Biology can be considered as Biology after identification reaching from system analysis and control to system design (from [38]).

Another goal to understand a complex system is to map protein-protein interactions within, which represent molecular links for further functional characterization. Global human interactomes have been created using high-throughput Y2H interaction mapping providing a framework for interactors that participate in specific cellular processes and pathways or are linked to disease associated factors [39-41]. Such a network linked uncharacterized gene products and human disease proteins (ataxia) resulting in the identification of novel modulators of Wnt signaling [41]. Furthermore, a combination of a classical library and matrix (using a selection of putative interactors) based Y2H screens led to the identification and resulting mechanistic characterization of GIT1 (G protein-coupled receptor kinase-interacting protein), an enhancer of Huntingtin aggregation to Huntington's disease (HD) [39]. Experimental derived large-scale protein-protein interaction networks are the basis for the determination of a variety of topological parameters (*e.g.* network organization with highly connected components – so called `hubs´ – and the identification of functional modules *etc.*). In addition, the integration of further experimental data of network components (*e.g.* gene silencing information and expression profiles) is leading to a better understanding of the dynamic behavior of a biological network [42, 43]. Several studies propose that essentiality of

a network component correlates with its degree (number of interactions) [44]. However, these statements are currently controversially discussed since different experimental techniques and large-scale or low-scale interaction mapping do not really allow a comprehensive analysis of different network types [45].

Recently, the integration of dynamic transcriptome information of different cell cycle states in yeast or circadian transcript profiles form a hepatic cell line with protein-protein interaction data led to the identification of functional modules and their timely resolved dynamics [46, 47].

Although protein-protein interaction networks contain a large variety of information they are in the most cases static and still far away from saturation [43]. It is obvious that due to technical limitations of approaches used for interaction detection (like high-throughput Y2H mapping or mass spectrometry analysis) there will always remain a risk of false positive and negative signals. Therefore, validation of interaction screen data with an independent system turned out to be essential for network construction [43, 48].

1.8 Dynamics of Protein-Protein Interactions within the Mammalian Circadian Gene-Regulatory Network

Cellular functions are increasingly recognized to be regulated by protein complexes, thus, PPIs and their timing are predicted to be crucial for many physiological processes [49]. In most cases, in which PPIs exert a regulatory function, such interactions are transient and occur only under specific conditions, *e.g*. as a response to a signal, after binding of a co-factor or when the expression of one or both partners is induced in response to a changing cellular condition. Circadian clock regulation of cellular functions *via* PPIs can be accomplished by restricting important interactions to specific times of the day. In the circadian oscillator, many of the known PPIs also happen predominantly at specific times of the day, *e.g*. PER/CRY complexes bind to CLOCK/BMAL1 in the late night to inhibit transactivation [20]. Here, the temporal binding profile correlates with the abundance profiles of PER and CRY proteins. While these examples demonstrate the fundamental importance of precisely timed PPIs for the circadian clockwork we are still far from a comprehensive view of the PPI network among circadian oscillator proteins and their dynamics. Furthermore, the extent of a regulation of circadian output processes *via* time-of-day dependent PPIs is largely unknown.

1.9 Aim of the Study

Since the complexity of the circadian oscillator is increasing because of the identification of many new clock components and modulators in the last years, I firstly wanted to map PPIs among these components (46 candidates at the beginning of my study, July 2007) using a high-throughput interaction mapping approach in yeast. With this experimental information, I wanted to generate a more comprehensive view on the circadian protein-protein interaction network that allows me to uncover new mechanisms that are probably important for the regulation of circadian periodicity and cellular physiology.

In the second part of my study, I wanted to investigate the circadian network organization/topology and the underlying interaction dynamics on the circadian time scale *via* integration of circadian expression as well as genetic perturbation data for each network component. In addition, I wanted to focus on the identification of clock controlled regulation of cellular physiology by rhythmic PPIs.

Expected significance:

Since the large fraction of regulatory enzymes (kinases, phosphatases and F-box proteins, 22 in total) and circadian clock components or associated core clock factors (24 in total) that I have included for the construction of the circadian PPI network the interaction mapping should lead to the identification of new PPIs probably also mediating posttranslational modifications. In the last years, phosporylation of clock proteins was recognized as crucial for setting the speed of the circadian clock but not much is known about the role of phosphatases within the mammalian system. Therefore, I have included phosphatase 1 (PP1) and phosphatase 2 (PP2) subunits as candidates in my interaction experiments. My approach should lead to the discovery of many so far uncharacterized interactions and therefore serve as a valuable resource for the circadian clock community helping us to understand the mammalian molecular clockwork at the systems-level. In addition, by integrating circadian expression information to the circadian PPI network data (with the highest available temporal resolution), it should be able to create the first comprehensive view on PPI dynamics on a ~24-hrs timescale.

2 MATERIALS

2.1 Materials and Suppliers

2.1.1 Chemicals

All used chemicals were provided by the following companies:

Sigma-Aldrich (Taufkirchen, Germany)

Merck KGaA (Darmstadt, Germany) and

Carl Roth GmbH & Co (Karlsruhe, Germany).

2.1.2 Reagents

Acris	(Acris Antibodies GmbH, Herfort, Germany)
Applied Biosystems	(Forster City, USA)
Bio-Rad	(Bio-Rad Laboratories GmbH, Munch, Germany)
Calbiochem	(EMD Biosciences/Merck Biosciences, Darmstadt, Germany)
Fermentas	(GmbH, S. Leon, USA)
GIBCO	(Invitrogen Corporation, Karlsruhe, Germany)
Invitrogen	(Invitrogen Corporation, Carlsbad, California, USA)
Molecular Probes	(Invitrogen Corporation, Eugene, Oregon, USA)
MWG Biotech AG	(Ebersberg, Germany)
New England Biolabs	(New England Biolabs Inc., Ipswich, Massachusetts, USA)
NOVOUS	(Novous Biologicals, Littleton, USA)
Open Biosystems	(Thermo Fischer, St. Leon-Rot, Germany)
PIERCE	(Pierce Biotechnology Inc., Rockford, Illinois, USA)
Promega	(Promega Corporation, Madison, Wisconsin, USA)
QIAGEN	(QIAGEN GmbH, Hilden, Germany)
Roche	(Roche Diagnostics, Manheim, Germany)
SantaCruz	(Santa Cruz Biotechnology Inc., Santa Cruz, USA)
Stratagene	(La Jolla, California, USA)

2.2 Enzymes

2.2.1 Restriction Endonucleases

ApaI: (NEB, Cat. no. R0114S)

Recognition site:

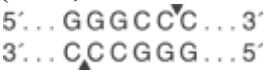

BamHI: (NEB, Cat. no. R0136 S)

Recognition site:

```
5′...G▼GATCC...3′
3′...CCTAG▲G...5′
```

BsrGI: (NEB, Cat. no. R0575 S)

Recognition site:

```
5′...G▼GATCC...3′
3′...CCTAG▲G...5′
```

EcoRI: (NEB, Cat. no. R0101 S)

Recognition site:

```
5′...G▼AATTC...3′
3′...CTTAA▲G...5′
```

HindIII: (NEB, Cat. no. R0104 S)

Recognition site:

```
5′...A▼AGCTT...3′
3′...TTCGA▲A...5′
```

SacI: (NEB, Cat. no. R0156 S)

Recognition site:

```
5′...GAGCT▼C...3′
3′...C▲TCGAG...5′
```

XhoI: (NEB, Cat. no. R0146 S)

Recognition site:

```
5′...C▼TCGAG...3′
3′...GAGCT▲C...5′
```

2.2.2 PCR Enzymes

Platinum-Pfx-Polymerase:	(Invitrogen, Cat. no. 11708-013)
DeepVent-DNAPolymerase:	(New England Biolabs, Cat. no. M0258L)
SuperscriptRNaseH:	(Invitrogen, Cat. no. 18053-017)

2.3 Technical Equipment

ABI PRISM 7000	(Applied Biosystems)
Betascout luminometer	(PerkinElmar)
Centrifuges	(Eppendorf)
ChemoCam	(Intas)
ELISA platereader	(Berthold Technologies)
Gyrorocker shaker	(Labnet International)
Infinite F200Pro	(TECAN)
Lumi Imager	(Roche)
LumiCyle	(ActiMetrix)
Microscope	(Laica)
Multichannal pipettes	(Eppendorf)
NANODrop	(Roche)

OrionII	(Berthold Detection Systems)
Pipettes	(Eppendorf)
Pipetting robot	(Biomek FX)
Spotting robot	(KBiosystems)
TOPCount	(PerkinElmar)
XCell Sure Lock Sytem	(Invitrogen)

2.4 Buffers and Solutions

RIPA buffer:
1x PBS
1% Igepal CA-630
0.5% Na-deoxicholate
0.1% SDS

co-IP buffer:
20 mM Tris-HCl, pH 8.0
140 mM NaCl
1.5 mM $MgCl_2$
1 mM TCEP
1% Triton-X-100
10% glycerine

co-IP washing buffer:
20 mM Tris-HCl
150 mM NaCl
0.5% Igepal CA-630

1x HEPES:
50 mM HEPES
140 mM NaCl
1.5 mM Na_2HPO_4
in aq. dest.; pH 7

1x NEBuffer 2:
10 mM Tris-HCl
50 mM NaCl
10 mM $MgCl_2$
1 mM dithiothreitol
pH 7.9

10x MOPS buffer:
200 mM MOPS
50 mM Na-acetate
10 mM EDTA
pH 7.0 (NaOH)

2x sample buffer:
95% formamide
0.02% SDS
0.025% bromphenol blue
0.025% xylene cyanol
0.025% ethidiumbromide

	0.5 M EDTA
DNA buffer (6x):	30% glycerine 1 mM EDTA 0.25% bromphenol blue
10x PBS:	1.37 M NaCl 27 mM KCl 100 mM Na_2HPO_4 20 mM NaH_2PO_4 in aq. dest.; pH 7.2
1x PBS:	100 ml 10x PBS ad 1 l aq. dest.
1x PBST:	1x PBS 0.25% Tween
X-GAL soultion:	156 µl X-GAL 100 µl DTT (1M) 10 ml Z-buffer
X-GAL:	20 mg/ml X-GAL in dimethyl formamide
Z-buffer:	10.6 g/l Na_2HPO_4 x 2 H_2O 5.5 g/l NaH_2PO_4 x H_2O 0.75 g/l KCl 0.25 g/l $MgSO_4$ x 7 H_2O

2.5 RNA and DNA Gel Composition

RNA gel:	0.6 g agarose 37 ml aq. dest. 5 ml 10x MOPS buffer
DNA gel:	10 mM EDTA pH 7.0 (NaOH) 5 µl of 1% EtBr on 100 ml

2.6 Commercial Assay Systems

(i) Dual-Luciferase Reporter Assay System (Promega Corporation, Madison, Wisconsin, USA). (Cat. no. E1960)

(ii) SuperSignal West Pico Chemiluminscent Substrate (Pierce Biotechnology Inc., Rockford, Illinois, USA).

(Cat. no. 34079)

2.7 DNA Marker

1 kb DNA ladder:	(NEB, Cat. no. N3232)
100 bp DNA ladder:	(NEB, Cat. no. N3231)

2.8 Bacteria

2.8.1 Bacteria Strains

DH10B	F` *mcrA* Δ-(*mrr hsd RMS-mcr BC*) φ80d*lacZ*ΔM15 Δ*lacX*74 *de recA*1 *araD*139 Δ(*ara leu*)7697 *galU galK* λ- *rpsL endA*1 *nupG* (Invitrogen)
XL1-Blue	*recA*1 e*ndA*1 *gyrA*96 *thi*-1 *hsdR*17 *supE*44 *relA*1 *lac*- F`[*pro*AB *lac*lqZΔM15 Tn*10* (Tetr) (Stratagene)

2.8.2 Media for Bacteria

LB medium:	10 g NaCl 10 g bactotryptone 5 g yeast extract ad 1 l aq. dest. autoclave
LB agar plates:	1 l LB medium 10-15 g agar (BD Biosciences) autoclave
LB selective medium:	1 l LB agar LB ampicillin 100 µg/ml ampicillin LB kanamycin 100 µg/ml kanamycin stock solutions: 100 mg/ml in 70% EtOH
S.O.C. medium:	0.5% w/v yeast extract 2% w/v tryptone 2.5 mM KCl 10 mM NaCl 10 mM $MgCl_2$ 10 mM $MgSO_4$ 20 mM D-(+)-glucose

2.9 Yeast

2.9.1 Yeast Strains

L40ccU MATa	MATa *his 3Δ200 trp1-901 leu 2-3,112 LYS 2 :: (lex Aop)4--HIS3 ura3:: (lex Aop)8 -lacZ ADE 2 :: (lexAop)8-URA3 GAL4 gal 80 can 1 cyh* 2 [39]
L40cc MATα	*MATα his3Δ200 trp1-910 leu2-3,112 ade2 LYS2::(lexAop)4-HIS3URA3::(lexAop)8-lacZ GAL4 gal80 can1 cyh* [39]

2.9.2 Media for Yeast

YPD medium:	10 g/l bacto yeast extract 20 g/l bacto peptone 20 g/l glucose
SD medium:	6.7 g/l yeast nitrogen base 20 g/l glucose 10 ml 100x aa (amino acid) per l
NBG medium:	6.7 g/l yeast nitrogen base 20 g/l glucose 0.5 M betain 10 ml 100x aa per l
GAL medium:	6.7 g/l yeast nitrogen base 20 g/l galactose 10 ml 100x aa per l

2.9.3 Amino Acids and Nucleobases for Yeast Media

Amino acids were obtained from Sigma-Aldrich, Germany (amino acid kit, Cat. no. LAA21). Adenine and uracil were obtained from Sigma-Aldrich, Germany (Cat. no. A2786-100G and U1128-25G).

Adenine (100x)	20 mg/l final concentration
Histidine (100x)	20 mg/l final concentration
Leucine (100x)	20 mg/l final concentration
Tryptophan (100x)	20 mg/l final concentration
Uracil (100x)	20 mg/l final concentration

2.9.4 Yeast Transformation Reagents

Mix I:	0.1M LiAc 1 M sorbitol 0.5x TE
Mix II:	0.1 M LiAc 2 ml 60% PEG 3350 1x TE

2.10 Human Cell Lines

2.10.1 HEK293 Cells

HEK293 cells were used for ectopic expression of recombinant proteins.

Organism	*homo sapiens* (human)
Tissue	kidney; transformed with adenovirus 5 DNA
Comments	the cells express the transforming gene of adenovirus 5
Growth properties	adherent
Morphology	epithelial
Propagation	DMEM Medium, 10% v/v FBS

2.10.2 HEK293T Cells

HEK293T cells were used for lentivirus production.

Organism	*homo sapiens* (human)
Tissue	kidney; transformed with SV40 adenovirus DNA
Comments	the cells express the transforming gene of the large T antigen from SV40 that inactivates pRb
Growth properties	adherent
Morphology	epithelial
Propagation	DMEM Medium, 10% v/v FBS

2.10.3 U2OS Cells

U2OS cells were used for dynamic circadian oscillations recordings, ectopic expression of recombinant proteins and detection of clock genes *via* q-PCR and Western blot analysis.

Organism	*homo sapiens* (human)
Tissue	bone tissue, osteosarcoma cell line
Comments	Circadian oscillating cell line [22, 35], cells express wild type p53 and Rb, but lack p16
Reporter	*Bmal1*-promoter luciferase fragment
Growth properties	adherent, contact inhibited growth
Morphology	epithelial
Propagation	DMEM Medium, 10% v/v FBS

2.10.4 Cell Culture and Reporter Media

CM (complete medium):	500 ml DMEM 50 ml FBS 5 ml penicillin/streptomycin 100x 14 ml 1M HEPES
CM (without antibiotics):	45 ml DMEM 5 ml FBS
Reporter medium:	500 ml High Glucose DMEM, phenolred free 50 ml FBS 5 ml penicillin/streptomycin, 100x 5 ml D-luciferin in DMEM, 25 mM 500 µl puromycin, 10 mg/ml or 500 µl blasticidin, 10 mg/ml
FBS (fetal bovine serum)	(Gibco, Cat. no. 10106-169)
Penicillin/streptomycin:	10.000 U/10.000 µg/ml, (Biochrom AG) Final concentration: 100 µg/ml
Blasticidin:	5 mg/ml in 1x PBS (Invitrogen, Cat. no. R210-01) Final concentration: 5-10 µg/ml
Hygromycin B:	50 mg/ml (Invitrogen, Cat. no. R220-05)

	Final concentration: 50-100 µg/ml
Kryomedia:	90% FBS 10% DMSO
Dexamethasone:	1 mM in EtOH (Sigma-Aldrich, Cat. no. D4902) Final concentration: 1 µM
Luciferin (firefly):	0.1 mM in CM (P.J.K., Cat. no. 260150) Final concentration: 1 µM
Cycloheximide (CHX):	100 mg/ml in DMSO (Sigma-Aldrich, Cat. no. C4859) Final concentration: 0.2-2 µg/ml

2.11 Protein Extraction

Phosphatase-Inhibitor-Cocktail I 100x:	(Sigma-Aldrich, Cat. no. P-2850)
Phosphatase-Inhibitor-Cocktail II 100x:	(Sigma-Aldrich, Cat. no. P-5726)
Protease-Inhibitor-Cocktail 100x:	(Sigma-Aldrich, Cat. no. P-8340)

2.12 BCA-Test for the Determination of Protein Concentration

Reagent A:	2% (w/v) Na_2CO_3 x H_2O 1% (w/v) BCA-Na_2 0.95% (w/v) $NaHCO_3$ 0.4% (w/v) NaOH 0.16% (w/v) Na_2 tartrate ad 1 l aq. dest.; pH 11.25
Reagent B:	4% (w/v) $CuSO_4$ x 5 H_2O

2.13 SDS Gelelectrophoresis

NuPAGE LDS Sample Buffer (4x):	(Invitrogen, Cat. no. NP0007)
NuPAGE 4-12% Bis-Tris Gel 1.0 mm, 10 well:	(Invitrogen, Cat. no. NP0321PK2)
NuPAGE 4-12% Bis-Tris Gel 1.5 mm, 10 well:	(Invitrogen, Cat. no. NP0335PK2)
NuPAGE MES SDS Running Buffer (20x):	(Invitrogen, Cat. no. NP0002)
MagicMark XP:	(Invitrogen, Cat. Nr. LC5602)

Laemmli buffer (6x):	0.1 ml 20% (w/v) SDS 2 ml 14 M 2-mercaptoethanol 1 ml glycerine 10 mg bromphenol blue ad 5 ml aq. dest.
10x SDS-PAGE buffer:	0.25M Tris-base 1.92 M glycine 1% (w/v) SDS pH 8.5
1x SDS-PAGE buffer:	100 ml 10x SDS-PAGE buffer ad 1 l aq. dest.
Buffer SDS-PAGE:	0.5 M Tris-HCl pH 6.8
Seperation buffer:	1.5 M Tris-base pH 8.8

2.14 Protein Blotting

NuPAGE Transfer Buffer (20x):	(Invitrogen, Cat. No NP0006-1)
Transfer buffer:	100 ml 10x SDS-PAGE buffer 20% (v/v) methanol ad 1 l aq. dest. 10x TBS: 1.37 M NaCl 100 mM Tris-Base pH 7.3
1x TBST:	100 ml 10x TBS 0.05% (v/v) Tween 20 ad 1 l aq. dest.
Blocking solution:	1x TBST 5% (m/v) dry milk (BD, Cat. no. 232100)
Detection:	SuperSignal West Pico Chemiluminscent Substrate (Pierce, Cat. Nr. 34080)
Membrane:	Nitrocellulose membrane Protan BA85, pore size 0.45 µm

	(Schleicher and Schuell, Cat. no. 10401196)
Blotting paper:	Whatman Gel Blotting Paper (Schleicher and Schuell, Cat. no. 10426982)

2.15 Agarose Gelelectrophoresis

50x TAE:	2 M Tris base 50 mM EDTA 1 M 100% asparic acid pH 8.5
1x TAE:	20 ml 50x TAE ad 1 l aq. dest.

2.16 Animals

2.16.1 Mouse Strains

C57black6 (The Jackson Laboratory, Bar Harbor, Maine, USA) strain mice were sacrefied for liver extraction.

2.16.2 Entrainment of Mice

Male C57black6 mice were entrained to a 12 hrs light dark regime. Locomotor activity was monitored by the CLOCKLAB ANALYSIS software (Actimetrix). Mice were sacrefied in free run conditions (complete darkness) at the indicated timepoints in constant darkness *via* cervical dislocation. Liver dissection was performed on ice.

2.17 Plasmids

Constructs/cell lines have either been generated during my PhD work by me (TW) or were already available from Prof. Kramer's or Prof. Wanker's group or were purchased at Imagenes.

2.17.1 ENTRY Constructs

Symbol	Clocne ID	Obtained from
hNONO	RZPDo834C104D/RZPD	[41]
hWDR5	IOH4895/RZPD	[41]
hDEC1	CCSB_14984/MGC	[41]
hNPAS2	IOH29403/RZPD	[41]
hNR1D1	ORF_SEQ_3F10	[41]
hNR1D2	ORF_SEQ_6C06/1-22	[41]
hRORA	CCSB_4928/MGC	[41]
hRORB	IOH39668/RZPD	Imagenes
hRORC	CCSB_8508/MGC	Imagenes
hNFIL3	RZPDo839B0796/RZPD	Imagenes
hEZH2	CCSB_143/MGC	[41]
hRASD1	CCSB_1134/MGC	[41]
hCSNK2A1	RZPDo839B0979/RZPD	[41]
hCSNK2A2	IOH6369/RZPD	[41]
hCSNK2B	RZPDo834F0628D/SMP	[41]
hPRKCA	IOH29644/SMP	[41]
hPRKACA	IOH26286/SMP	[41]
hPPP1CA	CCSB_3788/MGC	[41]
hPPP1CB	CCSB_4085/MGC	[41]
hPPP1CC	CCSB_7076/MGC	[41]
hPPP2CA	RZPDo834A1014D/RZPD	[41]
hPPP2CB	ORF SEQ 1H11	[41]
hPPP2R1A	RZPDo839E0974/RZPD	[41]
hPPP2R1B	RZPDo839F0390/RZPD	[41]
hPPP2R5D	IOH43173/IM/imaGenes	[41]
hPPP2R5E	IOH29856/imaGenes	[41]
hFBXL3	CCSB_14644/MGC	[41]

2.17.2 Generated Constructs and Cell Lines

2.17.2.1 HEK293 Cells Expressing Luciferase Fusions

HEK293 CLOCK-luciferase (pLenti6 backbone, Invitrogen), TW

HEK293 BMAL1-luciferase (pLenti6 backbone, Invitrogen), TW

2.17.2.2 Prey and Bait Constructs

No.	Gene	Prey config. (pACT4-DM)	Bait config. (pBTM116-D9)
1	PER1	TW	TW
2	PER2	TW	TW
3	PER3	TW	TW
4	CRY1	TW	TW
5	CRY2	TW	TW
6	NONO	TW	TW
7	WDR5	TW	TW
8	TIMELESS	TW	TW
9	CIPC	TW	TW
10	DEC1	TW	TW
11	DEC2	TW	TW
12	CLOCK	TW	TW
13	NPAS2	TW	TW
14	BMAL1	TW	TW
15	BMAL2	TW	TW
16	NR1D1	TW	TW
17	NR1D2	TW	TW
18	RORA	TW	TW
19	RORB	TW	TW
20	RORC	TW	TW
21	DBP	TW	TW
22	NFIL3	TW	TW
23	EZH2	TW	TW
24	RASD1	TW	TW
25	CSNK1D	TW	TW
26	CSNK1E	TW	TW
27	GSK3B	TW	TW
28	CSNK2A1	TW	TW
29	CSNK2A2	TW	TW
30	CSNK2B	TW	TW
31	PRKACA	TW	TW
32	PRKCA	TW	TW
33	PPP1CA	TW	TW
34	PPP1CB	TW	TW
35	PPP1CC	TW	TW
36	PPP2CA	TW	TW
37	PPP2CB	TW	TW
38	PPP2R1A	TW	TW

39	PPP2R1B	TW	TW
40	PPP2R5D	TW	TW
41	PPP2R5E	TW	TW
42	PPP5C	TW	TW
43	BTRC	TW	TW
44	FBXW11	TW	TW
45	FBXL3	TW	TW
46	FBXL15	TW	TW

2.17.2.3 pLenti6, MYC and FLAG Constructs

No.	Gene	pLenti6	pMYC-CMV-D12	pFLAG-CMC-D11
1	PER1	Prof. Kramer	TW	Prof. Kramer
2	PER2	Prof. Kramer	TW	Prof. Kramer
3	PER3	TW	TW	TW
4	CRY1	Prof. Kramer	TW	Prof. Kramer
5	CRY2	Prof. Kramer	TW	Prof. Kramer
6	NONO	Prof. Kramer	TW	TW
7	WDR5	Prof. Kramer	TW	TW
8	TIMELESS	Prof. Kramer	TW	TW
9	CIPC	Prof. Kramer	TW	TW
10	DEC1	TW	TW	TW
11	DEC2	TW	TW	TW
12	CLOCK	Prof. Kramer	TW	Prof. Kramer
13	NPAS2	TW	TW	TW
14	BMAL1	Prof. Kramer	TW	Prof. Kramer
15	BMAL2	TW	TW	TW
16	NR1D1	TW	TW	TW
17	NR1D2	TW	TW	TW
18	RORA	TW	TW	TW
19	RORB	TW	TW	TW
20	RORC	TW	TW	TW
21	DBP	TW	TW	TW
22	NFIL3	TW	TW	TW
23	EZH2	TW	TW	TW
24	RASD1	TW	TW	TW
25	CSNK1D	Prof. Kramer	TW	TW
26	CSNK1E	Prof. Kramer	TW	TW
27	GSK3B	Prof. Kramer	TW	TW
28	CSNK2A1	Prof. Kramer	TW	TW
29	CSNK2A2	Prof. Kramer	TW	TW

30	CSNK2B	TW	TW	TW
31	PRKACA	TW	TW	TW
32	PRKCA	TW	TW	TW
33	PPP1CA	TW	TW	TW
34	PPP1CB	TW	TW	TW
35	PPP1CC	TW	TW	TW
36	PPP2CA	Prof. Kramer	TW	TW
37	PPP2CB	Prof. Kramer	TW	TW
38	PPP2R1A	Prof. Kramer	TW	TW
39	PPP2R1B	Prof. Kramer	TW	TW
40	PPP2R5D	Prof. Kramer	TW	TW
41	PPP2R5E	Prof. Kramer	TW	TW
42	PPP5C	TW	TW	TW
43	BTRC	TW	TW	TW
44	FBXW11	TW	TW	TW
45	FBXL3	TW	TW	TW
46	FBXL15	TW	TW	TW

2.17.2.4 Reporter Cell Lines

No.	Expressed gene (pLenti6)	U2OS *Bmal1*-promoter luciferase reporter cells (pLenti6)
1	PER1	TW
2	PER2	TW
3	PER3	TW
4	CRY1	TW
5	CRY2	TW
6	NONO	TW
7	WDR5	TW
8	TIMELESS	TW
9	CIPC	TW
10	DEC1	TW
11	DEC2	TW
12	CLOCK	TW
13	NPAS2	TW
14	BMAL1	TW
15	BMAL2	TW
16	NR1D1	TW
17	NR1D2	TW
18	RORA	TW
19	RORB	TW
20	RORC	TW

21	DBP	TW
22	NFIL3	TW
23	EZH2	TW
24	RASD1	TW
25	CSNK1D	TW
26	CSNK1E	TW
27	GSK3B	TW
28	CSNK2A1	TW
29	CSNK2A2	TW
30	CSNK2B	TW
31	PRKACA	TW
32	PRKCA	TW
33	PPP1CA	TW
34	PPP1CB	TW
35	PPP1CC	TW
36	PPP2CA	TW
37	PPP2CB	TW
38	PPP2R1A	TW
39	PPP2R1B	TW
40	PPP2R5D	TW
41	PPP2R5E	TW
42	PPP5C	TW
43	BTRC	TW
44	FBXW11	TW
45	FBXL3	TW
46	FBXL15	TW

2.18 RNAi Constructs

RNAi constructs were obtained from Open Biosystems. Lists with the used constructs can be found in the Appenidix section.

2.19 Oligonucleotides

2.19.1 Primer for TOPO Cloning

Symbol	**Primer pairs (FW: forward, RV: reverse)**
mPER1	FW: CAC CAT GAG TGG TCC CCT AGA AGG RV: CTA GCT GGT GCT GTT TTC TTC

mPER2	FW: CAC CAT GAA TGG ATA CGT GGA CTT CTC
	RV: TTA CGT CTG GGC CTC TAT CC
mPER3	FW: CAC CAT GGA TCC CTG TGG AGA CCC
	RV: TCA ACT GGT GTC TTC TGC TGG
mCRY1	FW: CAC CAT GGG GGT GAA CGC CGT GC
	RV: TCA GTT ACT GCT CTG CCG CTG
mCRY2	FW: CAC CAT GGC GGC GGC TGC TGT
	RV: TCA GGA GTC CTT GCT TGC TG
mTIM	FW: CAC CAT GGA CTT GTA CAT GAT GAA CTG
	RV: TCA GTC ATC CTC ATC CTC AAT
mCIPC	FW: CAC CAT GGA GAG GAA AAT CCC ATC CA
	RV: CTA TAC GTC TGG GTG ATC AGA C
hDEC2	FW: CAC CAT GGA CGA AGG AAT TCC TCA
	RV: TCA GGG AGC TTC CTT TCC TG
mCLOCK	FW: CAC CAT GGT GTT TAC CGT AAG CTG TA
	RV: CTA CTG TGG CTG GAC CTT GG
mBMAL1	FW: CAC CAT GGC GGA CCA GAG AAT GGA
	RV: CTA CAG CGG CCA TGG CAA G
hBMAL2	FW: CAC CAT GGC GGC GGA AGA GGA GG
	RV: CTA GAG GGT CCA CTG GAT GT
hDBP	FW: CAC CAT GGC GCG GCC TGT GAG C
	RV: TCA CAG GGC CCC GTG CTG
mCSNK1E	FW: CAC CAT GGA GTT GCG TGT GGG AAA
	RV: TCA TTT CCC AAG ATG GTC AAA TG
hCSNK1D	FW: CAC CAT GGA GCT GAG GGT CGG GA
	RV: TCA TCG GTG CAC GAC AGA CTG
mGSK3B	FW: CAC CAT GTC GGG GCG ACC GAG AAC C
	RV: TCA GGT GGA GTT GGA AGCTGA
rPPP5C	FW: CAC CAT GGC GAT GGC GGA GGG C
	RV: TCA CAT CAT TCC TAG CTG CAG
mBTRC	FW: CAC CAT GGA CCC GGC AGA GGC GGT G
	RV: TTA TCT GGA GAT GTA GGT GTA TGT CC
mFBXW11	FW: CAC CAT GGA CCC GGC AGA GGC GGT G
	RV: TTA TCT GGA GAT GTA GGT GTA TGT CC
hFBXL15	FW: CAC CAT GGA GCA ACC GAT GGA GC
	RV: TCA GAC CTG CAG GTT GAC AA

2.19.2 Primer for q-PCR

No.	Gene	Gene ID	Cat. no.	Supplier
1	hGAPDH	2597	QT01192646	Qiagen
2	hPer1	5187	QT00069265	Qiagen
3	hPer2	8864	QT00011207	Qiagen
4	hNr1d1	9572	QT00000413	Qiagen
5	hDbp	1628	QT00055755	Qiagen
6	hPPP1CA	5499	QT00031654	Qiagen

2.20 Antibodies

2.20.1.1 Primary Antibodies

Anti-MYC	(Novous Biologicals, Cat. no. NB600-335)
Anti-FLAG	(Sigma-Aldrich, Cat. no. F3165)
Anti-BMAL1	(Michael Brunner laboratory [29])
Anti-PPP1CA	(Santa Cruz Biotechnology, Cat. no. sc-7482)
Anti-PPP1R15B	(Novous, Cat. no. NBP1-06588)
Ideotypic IgG	(Acris, Cat. no. PPP500P)
Anti-β-actin	(Sigma-Aldrich, Cat. no. A-5441)

2.20.1.2 Secondary Antibodies

Donkey anti-rabbit-HRP	(Santa Cruz, Cat. no. sc-2317)
Goat anti-rabbit-HRP	(Santa Cruz, Cat. no. sc-2030)
Goat anti-mouse-HRP	(Santa Cruz, Cat. no. sc-2005)
Donkey anti-mouse-HRP	(Santa Cruz, Cat. no. sc-2314)
Donkey anti-goat-HRP	(Santa Cruz, Cat. no. sc-2020)

2.21 Kits

Bradford Proteinassay Kit	(BioRad, Cat. no. 500-0002)
CalPhos-Kit	(BD-Biosciences, Cat. no. 631312)
FuGene 6	(Roche, Cat. no. 11815091001)
MinElute PCR-Purification Kit	(Qiagen, Cat. no. 28004)

Lipofectamin 2000	(Invitrogen, Cat. no. 11668-019)
TOPO Cloning Kit	(Invitrogen, Cat. no. K450001)
QIAprep Spin Midiprep Kit	(Qiagen, Cat. no. 12145)
QIAprep Spin Miniprep Kit	(Qiagen, Cat. no. 27104)
QIAprep Plasmid Maxi Kit	(Qiagen, Cat. no. 12163)
QIAquick PCR Purification Kit	(Qiagen, Cat. no. 28104)
QIAquick Gel Extraction Kit	(Qiagen, Cat. no. 28704)
RNeasy Purification Kit	(Qiagen, Cat. no. 74106)
RNase-Free DNase Set	(Quiagen, Cat. no. 79254)

2.22 Databases

BIND	http://binddb.org/
BIOGRID	http://thebiogrid.org/
Circadian BIOGPS	http://biogps.org/circadian/
DIP	www. dip.doe-mbi.ucla.edu/
Expasy	www.expasy.org
HD Research Crossroads	http://www.hdresearchcrossroads.org/
HPRD	www.hprd.org/
INTACT:	www.ebi.ac.uk/intact/
Ncbi	www.ncbi.nlm.nih.gov/
Cancer Gene Census	www.sanger.ac.uk/genetics/CGP/Census
UNIHI	www.UniHI/pages/unihiSearch

2.23 Software

Bioconductor:	www.bioconductor.org/
Chronostar:	In house generated software for evaluation of dynamic oscillation recordings (Dr. Stephan Lorenzen, Dr. Bert Maier)
CLOCKLAB:	Actimetrix
ClusterOne	www.paccanarolab.org/cluster-one
Cytoscape 2.8.1:	www.cytoscape.org/
ImageJ 1.44p	National Institutes of Health
LumiCyle analysis:	Actimetrix
Matlab 7.0:	Mathworks
MCODE	http://baderlab.org/Software/MCODE
MS Office:	Microsoft Word, Excel and Powerpoint

3 METHODS

3.1 RNA and DNA Techniques

3.1.1 RNA Isolation and Quantification

The template mRNA for RT-PCR was purified using the RNeasy Mini Kit from Quiagen according to the user's manual. In this system, a specialized high-salt buffer allows up to 100 µg of RNA longer than 200 bases to bind to the RNeasy silica membrane with help of speed microspin technology. In addition, an on column DNA digestion was performed using the RNase-Free DNase Set (Quiagen). RNA quantification was performrd measuring the absorbtion at 260 nm with the NANODrop (Roche) device.

3.1.2 Reverse Transcription

RT-PCR is a laboratory technique for amplifying a defined piece of ribonucleic acid (RNA) molecule. The RNA strand is first reverse transcribed into its DNA complement or cDNA (complementary DNA), followed by amplification of the resulting DNA using polymerase chain reaction (PCR). In the first step of RT-PCR, named the first strand reaction, the cDNA is made from mRNA template using dNTPs and RNA-dependent DNA polymerase (reverse transcriptase) through the process of reverse transcription. The above components are combined with designed DNA primers in a reverse transcriptase buffer at 37°C. After the reverse transcription reaction is finished, and the cDNA has been generated from the mRNA, the standard PCR, termed the second reaction can be initiated.

Reagents	**1 reaction in µl**
5x buffer	10
dNTP´s	(each 10 mM) 1
RNase inhibitor	(40 U/µl) 0,5
0.1 M DTT	5
pentadecamers	(50 µM) 5
Superscript pol.	(200 U/µl) 0.25
RNA (2 µg)	X
RNase free H_2O	Y
Σ final volume µl	50

Thermocyle program for second reaction:

Time	Temperature
50 min	37° C
15 min	70° C
∞	4°C

3.1.3 DNA Purification

Depending on the amount of plasmid DNA needed, the desired vector construct was amplified. Bacteria were cultured in 4, 50 or 200 ml of LB growth medium plus ampicillin or kanamycin at 37°C with agitation (200 rpm) overnight. Qiagen mini-, midi- or maxi-kit was used to purify the vector DNA. The concentration of the DNA solution was measured at 260 nm. Quality of DNA was also assumed by running 0.5 µg of plasmid on an agarose gel after enzymatic digestion.

3.1.4 Agarose Gelelectrophoresis

Agarose gels were prepared by dissolving 0.6 g of agarose in 60 ml of 1x TAE buffer for a 1% w/v gel. For a 2% gel, double the amount of agarose was used. Once the agarose solution cooled to approximately 50°C, 1 µl of ethidium bromide (EtBr; 10 mg/ml) was added. The DNA samples were diluted in 6x loading buffer and loaded onto the gel. 10 µl of 1 kb or 100 bp DNA ladder was loaded and used as a size standard. Electrophoresis was run at 130 V for approximately 15-30 min, depending on the size of the expected products. The separated DNA was visible under ultraviolet (UV) light due to the DNA intercalation property of EtBr.

3.1.5 Enzymatic Digeston

0.5 µg of DNA were incubated with 1x NEBuffer 2 supplemented with 100 µg/ml bovine serum albumin (BSA) at 37°C for at leats 1 h. 10 µl of sample were mixed with 2 µl of 6x DNA loding buffer and agarose gels were run as described above.

3.1.6 PCR

PCR is a scientific technique in molecular biology to amplify a single or a few copies of a piece of DNA generating copies of a particular DNA sequence.The method relies on thermal cycling, consisting of cycles of repeated heating and cooling of the reaction for DNA melting and enzymatic replication of the DNA. Primers are short DNA fragments containing sequences complementary to the target gene and enable selective and repeated amplification.

Topo cloning of ENTR vectors was performed using theTOPO Cloning Kit (Invitrogen, Cat. no. K450001) according to the manufacturer's manual.

PCR reaction for amplification of gene of interest.

Reagents	**1 reaction in µl**
DNA template	10-100 ng
10x PCR buffer	5 µl
50 mM dNTPs	0.5 µl
Primers	100-200 ng each
ad H_2O	49 µl
Taq Polymerase	(1 unit/µl) 1 µl
Σ final volume	50 µl

PCR program:

Step	**Time**	**Temperature**	**Cycles**
Initial denaturation	2 min	94°C	1x
Denaturation	1 min	94°C	1x
Annealing	1 min	55°C	25x
Extension	1 min	72°C	1x
Final extension	7 min	72°C	1x

TOPO reaction:

Reagents	**1 reaction in µl**
PCR product	0.5-4 µl
Salt solution	1 µl
ad. H_2O	5 µl
TOPO vector	1 µl
Σ final volume	7.5 µl

3.1.7 Quantitative PCR

Real-time PCR, also called quantitative real-time PCR (q-PCR/qRT-PCR) is a laboratory technique based on PCR, which is used to amplify and simultaneously quantify a targeted DNA molecule. For one or more specific sequences in a DNA sample, Real-Time PCR enables both detection and quantification. The quantity can be either an absolute number of copies or a relative amount when normalized to DNA input or additional normalizing genes. 8 µl of cDNA template, 2 µl of specific primer mixture and 10 µl of ready-to-use mastermix (Fermantas) were placed into a 96-well plate. 96-well plates were sealed and centrifuged before starting the q-PCR reaction using the ABI 7000 q-PCR cycler.

Reagents	**1 reaction in µl**
20x universal mastermix	10
Primer/probe mix	2
cDNA (1:10 dilution)	8
Σ volume	20

Cycler program:
2 min 50°C
10 min 95°C
15 sec 95°C
1 min 60°C 40x
∞ 8°C

3.1.7.1 Quantification and Evaluation

The quantification of the mRNA transcripts was done using the $2^{-\Delta\Delta Ct}$- method (see also [22]).

(i) Means of gene Ct triplicates were generated.
(ii) Normalization to reference control (*Gapdh*).
(ii) Ct target gene - Ct *Gapdh* = ΔCt sample
(iv) Normalization to a calibrator
(v) ΔCt sample - ΔCt calibrator = ΔΔCt
(vi) Calculation with $2^{-\Delta\Delta Ct}$

3.2 Bacterial Transformation

Competent cells were slowly defrosted for 15 min on ice. 1-5 µl of ligation mixture were added to 25 µl of bacterial competent cells (Invitrogen, Top10 super competent cells) followed by an incubation period on ice of 20 min. The transformation mixture was then incubated for 90 sec at 42°C and immediately chilled on ice for 2 min. 250 µl of S.O.C (Invitrogen) medium were added to the mixture and incubated for 30 min with agitation at 37°C. The mixture was then centrifuged for 1 min (5,000 x *g*). The bacterial pellet was resuspended in 50 µl of the supernatant and plated on LB medium plates containing 100 µg/ml ampicillin or kanamycin. The bacteria were grown at 37°C over night.

3.3 Yeast Transformation

Yeast strains were grown in 2 ml YPD medium overnight. After the addition of 28 ml YPD medium, cells were grown to reach the optic desity (OD600) of 0.6-0.8. Cells were centrifuged at 3,000 x *g* for 5 min. Pellets were washed with 10 ml 1x TE and resuspendend in Mix I followed by incubation for 10 min at RT. 40 µl of yeast cells of each transformation condition were mixed with 0.5 µg of DNA, 5 µg fish sperm DNA and 320 µl of Mix II and incubated for 30 min at 30°C. Heat shock was performed after the addition of 30 µl of DMSO for 7 min at 42°C. Cells were plated on selective medium for 4 to 6 days.

3.4 Protein Techniques

3.4.1 Cell Culture

Human cell lines were maintained at 37ºC in humidified atmosphere containing 5% CO_2 unless otherwise stated. Cells were grown in Dulbecco's modified Eagle's medium (DMEM) supplemented with 10% FBS, 2 mM L-glutamine, 50 U/ml penicillin and 0.25 µg/ml streptomycin. Monolayer cells were split 1:10 and 1:20 at 70-80% confluence. To dislodge the cells, cell medium was removed from tissue culture dish, cells were rinsed once with 1x PBS and incubated in Trypsin-EDTA solution (Gibco) for 2-4 min at RT. Cells were then suspended in complete DMEM and split into 10 cm dishes.

Subculturing procedures were carried out in a laminar flow hood in a sterile environment

using medium and reagents that were all pre-warmed to 37ºC.

3.4.2 Whole Cell Protein Extraction

Mammalian or mouse cells were washed twice with ice-cold 1x PBS and extracted with RIPA or co-IP buffer. Total cell extracts were incubated on ice for 30 min and then centrifuged at 13,000 x *g* for 15 min at 4ºC to pellet the insoluble cell debris. The supernatant fraction was then removed and used for cellular protein analysis.

3.4.3 Transient Transfection

Cells were seeded at 1.2×10^6/60-mm dishes at least 12 hrs prior to transfection. For other well sizes, the cell number was adjusted proportionally. Transient transfection was performed with 1-5 µg of total DNA using Lipofectamine 2000 reagent (Invitrogen) or FuGene 6 (Roche) according to the manufacturer's recommendations. For each transfection, DNA and 3x the amount of transfection reagent were separately diluted in 100 µl of Opti-MEM I Reduced Serum Medium or serum free medium (Gibco). Mixtures were incubated for 10-45 min at RT, combined and then left at RT for the next 30 min to allow the formation of DNA-liposome complexes. DNA-liposome complex solution was overlaid onto the cells. Following incubation, the medium was replaced with complete DMEM and transfected cells were grown for the next 24-48 hrs.

3.4.4 Protein Quantification

The BCA Assay is based on the reduction of Cu^{2+} to Cu^{1+} by protein in an alkaline medium and the highly sensitive and selective colorimetric detection of the cuprous cation using bicinchoninic acid (BCA).

For the determination of the protein concentrations, BCA Protein Assay Reagent A and BCA Protein Assay Reagent B (Pierce) were mixed in the proportion 50:1. 10 µl of BSA standards (0.1 µg/µl, 0.5 µg/µl, 1 µg/µl, 2 µg/µl, 6 µg/µl) and protein samples were added to 500 µl BCA (A + B) solution following 30 min incubation at 37°C. 200 µl of each sample were placed into a 96-well plate and the protein concentration was appointed using a plate reader device. Samples were diluted to a 1x concentration with the NUPAGE SDS Sample Buffer (4x)

(Invitrogen) containing 0.8% 2-ß mercaptoethanol (Sigma) and boiled for 5-10 min.

3.5 High-Throughput Interaction Mapping

3.5.1 Selection of Candidates for the Y2H High-Throughput Interaction Mapping

For the generation of the circadian protein-protein interaction network, all currently described circadian as well as assumed components in mammals were considered at the start of the study (July 2007). Furthermore, suggested candidates based on gene homology and orthology from other species (*Drosophila*, *Neurospora*) were included. *E.g*. to complete the set of well-established kinases within the molecular oscillator like CSNK1E/D and GSK3B [1], recent studies indicated the involvement of the mammalian PRKCA [50] and PRKACA described in the *Neurospora* system [51] to be important to regulate circadian rhythms. In addition, based on at this time unpublished findings of [22] CSNK2 subunits as well as FBXL3 [21, 22, 35, 52] were also considered for systematic interaction mapping. *Fbxl15*, the mammalian homolog of *Drosophila Jetlag* [53] and the long isoform of mammalian TIMELESS (TIM) [54] were also selected as potential candidates. PPP2 catalytic subunits and the mammalian regulatory subunits closely related to *Drosophila Widerborst* were as well included for high-throughput interaction experiments (for list of candidates see below).

3.5.2 Generation of the Y2H Matrix

18 circadian clock genes were amplified *via* PCR and TOPO cloning (Invitrogen) was performed according to the manufacturer's protocol to generate a Gateway^{TM} compatible entry clone collection. Primer pairs and source of additional 29 entry constructs are shown in the Materials section. All 46 open reading frames (ORFs) were sub-cloned into bait (pBTM116-D9) and prey destination vectors (pACT4-DM), respectively [39, 41]. DNA quality was controlled by digestion in the attR1/attR2 sites of yeast destination vectors and gene identity of ORFs was ensured by sequencing.

3.5.3 Automated Y2H Screening

The *L40ccαMATα* yeast strain was independently transformed with prey plasmids encoding

the *Gal4* transcription activation domain (N-terminal fusions) while the bait plasmids containing the *LexA* DNA binding domain hybrids (N-terminal fusions) were introduced into the L40ccU *MAT*a strain, respectively. All constructs were tested for auto-activation of the three reporters (*his3*, *ura3* and *lacZ*) by co-transformation of baits or preys with constructs harboring only the transcription activation or DNA binding domain in four independent repetitions in 96 wells. 13% (6 baits) of the constructs have strongly activated the reporters by themselves and were excluded from the Y2H matrix screen. For each of the six independent interaction matings, 50 µl of the liquid cultures of the *MAT*a yeast strain were placed into 384-micro titer plates by a pipetting robot (Biomek FX) while the prey colonies were stirred from solid selective medium into the liquid cultures using a spotting robot (KBiosystems). The yeast mixtures were then spotted onto YPD (yeast complete medium) agar plates and incubated for at least three days at 30°C. After the mating procedure, colonies were automatically transferred into 348 wells containing SDII liquid (-Leu, -Trp) selective medium and transferred to SDII agar for selection of diploid yeast followed by incubation at 30°C for at least two days. Diploid yeasts were again stirred into liquid and subsequently spotted on solid selective SDIV agar plates (-Leu, -Trp, -Ura, -His) as well as nylon membranes placed on SDIV agar plates. After 6 days at 30°C, β-Galactosidase assays were performed with the colonies that grew on membrane. Digital images were taken. Growth and β-Galactosidase activity was analyzed using the Visual Grid (GPC Biotech) software [39, 41]. Because of a very low mating efficiency of mPER2 (prey configuration) and mCRY2 (bait configuration) matings with yeast expressing all 45 components were individually performed for these two candidates in 96-well format in six independent experiments. In case that interaction of two components occurred in both the bait and prey configuration the conformation with the highest interaction score was selected for representation. Yeast strains expressing BHLHB2 (= DEC1) could not successfully mate with strains expressing BTRC, FBXW11, NPAS2 and PRKCA. In addition, yeast strains expressing PRKCA were not mating with BHLHB2 or PPP2R1B expressing strains.

3.5.4 X-GAL Assay

Yeast colonies were grown on membranes (MicronSeparations Inc.) placed on solid SDII or SDIV medium for 3-6 days at 30°C. Membranes harboring colonies were shock-frosted with

liquid niriogen for 5 min and defrosted at RT. This procedure was repeted for 2-4 times. Membranes were placed on 3 MM Whatman paper in a dish and incubated for 2-6 hrs with the X-GAL solution. If *lacZ* was expressed in the yeast cells blue stainig of the colonies demonstrated β-Galactosidase activity. Within this process the clear 5-brom-4-chlor-3-indolyl-β-D-galactoside of β-Galactosidase is cleaved into the blue 5-brom-4-chlor-indigo.

3.5.5 Cryoconservation of Yeast Cells

Yeast cells were grown in NBG medium overnight and frozen at -80°C.

3.5.6 Scoring of Interactions Detected in Yeast

Interactions were scored based on their reproduction rate in six independent repetitions. The ratio of positive colony growth on SDIV or positive colonies for β-Galactosidase activity and the corresponding mating controls on SDII medium was calculated and represented in percent. For example, Clock and Bmal1 were six times positive for interaction on SDIV medium underlying six successful matings for diploid yeast on SDII (6 x SDIV positive/6 x SDII positive x 100 = 100% - all of tested interactions have been detected). The analogs calculation was performed for β-Galactosidase activity. Values > 50% were scored with 2 points, values between 25% and 50% were scored with one point and values < 25% were scored with 0 points. Final score is represented by the sum of score points for SDIV growth selection and β-Galactosidase activity. 90 interactions have received 4 points and were classified as high score, 41 interactions with 3 or 2 points were defined as medium score and 19 interactions have received 1 point and were therefore categorized as low score. PER3, TIMELESS, NR1D1, PRKCA, PPP5C, BTRC and FBXL3 showed no interactions in yeast cells.

3.6 Validation of New CLOCK and BMAL1 Interactions in Mammalian Cells

3.6.1 Co-Immunoprecipitation (Co-IP) Experiments in HEK293 Cells

Immunoprecipitation (IP) is a technique of precipitating an antigen out of solution using an antibody specific to that antigen. This process can be used to identify protein complexes present in cell extracts (co-IP), by targeting a protein believed to be in the complex. The

complexes are brought out of solution by antibody-binding proteins isolated initially from bacteria, such as Protein A and Protein G. These can also be coupled to sepharose beads that can easily be isolated out of solution *e.g*. by centrifugation. After washing, the precipitate can be analyzed using mass spectrometry, western blotting, or enzymatic activity measurements.

HEK293 cells were lentivirally transduced with constructs expressing Clock or Bmal1 luciferase fusion proteins in the pLenti6 backbone (Invitrogen). Cells stably expressing luciferase fusions were transiently transfected with N-terminal MYC-tagged components (pc-myc-CMV-D12) using FuGene 6 (Roche) or Lipofectamine 2000 (Invitrogen) according to the manufacturer's protocol. 48 hrs after transfection cells were harvested in co-IP buffer containing a protease inhibitor cocktail (P-8340, Sigma-Aldrich). Lysates with one million luciferase counts were subjected for co-IP experiments. Input counts of 5 µl lysate were detected with the Beta Scout (PerkinElmer) device using 25 µl of LARI (Promega) as a substrate containing reagent for 10 sec. Pull-downs were performed with 2 µg of an anti-MYC (NB600-335, Novous Biologicals) or an isoform specific ideotypic (PPP500P, Acris Antibodies) antibody with G PLUS-agarose beads (Santa Cruz Biotechnology) *via* overnight incubation at 4°C and constant agitation. Beads were washed three times in 250 µl co-IP washing buffer. Luciferase activity of beads pellets was measured as performed for input detection. Beta Scout background values were subtracted for all conditions. Validation experiments were performed at least twice with comparable results.

3.6.2 Input Detection of MYC-Tagged Components *via* Western Blot

Lysates used for co-IP experiments containing MYC-tagged proteins were denatured in SDS-loading buffer (Invitrogen) for 10 min at 95°C. Separation was performed by SDS-PAGE with 4%-12% Bis-Tris gels (Invitrogen). Proteins were transferred to nitrocellulose membrane (0.45 µm) using a tank transfer system (wet transfer). For one gel, one sheet of membrane and two sheets of chromatography paper were cut to size of the gel. The gel, membrane, paper and two foam pads were equilibrated in the transfer buffer for 5 min, assembled into a stack, and placed in the tank blotting gear with membrane side facing the anode. SDS-denaturated proteins are negatively charged and move from the gel to the membrane. The transfer was run for 60 min at 90 V. The buffer was cooled with an ice block to prevent overheating during the transfer. Membranes were incubated with an anti-MYC antibody (NB600-335, Novous

Biologicals) according to the manufacturer's protocol. For standard Western blots, the membrane was blocked in PBS(T) with 5% nonfat dry milk for 1 h at RT or overnight at 4°C. After washing in PBS(T) (3x 5 min)m, the membrane was placed in the primary antibody solution and gently shaken overnight at 4°C. The membrane was then washed in PBS(T) (3x 5 min) and incubated with the HRP-conjugated secondary antibody (Santa Cruz Biotechnologies) for 1 h at RT. After another washing step in PBS(T) (3x 5 min), chemiluminescence reaction (see below) was performed with Super SignalWest Pico substrate (Pierce). Protein bands were visualized using the ChemoCam (Intas) detection system.

3.6.3 Enhanced Chemiluminescence Immunodetection

This method, developed by Amersham, was subsequently used for all antibody detection because of the speed of the reaction and the exclusion of radioactivity. ECL is a light emitting, nonradioactive method for the detection of immobilised specific antigens with antibodies conjugated to horseradish peroxidase (HRP). The system utilises a chemiluminescent reaction in that immunoreactive proteins were detected by enhanced chemiluminescence. Equal volumes of Super SignalWest Pico substrate solution 1 and 2 (Pierce) were mixed and added to the membrane. The reaction was allowed to proceed for 1 min at RT and excess of HRP substrate was removed. Chemiluminescence was detected as described above.

3.7 Genetic Perturbation Studies in Oscillating Cells

3.7.1 Production of Lentiviruses in Flasks

HEK293T cells were trypsinized using Trypsin/EDTA (BIOCHROM AG, Cat. no. L2143) for ~5 min at 37°C from an almost confluent 175 cm^2 culture flask (culture time < 6 weeks). Cells were seeded in a 175 cm^2 or 75 cm^2 flask in equal parts in 25 ml or 12.5 ml cell culture medium. Next day, cells were transfected with packaging plasmid and lentiviral vector. Culture medium was replaced prior tranfection. 17.5 µg or 8.4 µg of lentiviral expression plasmid (RNAi or overexpression vectors), 12.5 µg or 6 µg of psPAX and 7.5 µg or 3.6 µg pMD2G plasmid were mixed and the volume was adjusted to 1095 µl or 526 µl with the supplied H_2O (solution A). 155 µl or 74 µl of supplied 2 M Calcium solution (CalPhos-Kit, BD-Biosciences, Cat. no. 631312) was added to solution A. Transfection sample was mixed

by carefully vortexing solution B (1250 µl or 600 µl of 2x HBS) while adding drop wise solution A. Mixtures were incubated for 20 min at RT. 2.5 ml or 1.2 ml of each transfection solution were added to almost confluent HEK293T cells growing in one 175 cm^2 or 75 cm^2 flask. Cells were incubated overnight at cell culture conditions. Medium was replaced the next day and the first supernantant was harvested into a 50 ml tube and stored on ice overnight. Flasks were refiled with the equivalent amount of new cell culture medium. 24 hrs later, the remaining supernantant was harvested into the corresponding 50 ml tube and tubes were spinned at 4,100 x *g* for 15 min to remove cell debris. Supernatant was passed through a 0.45 µm filter (SARSTEDT, Cat. no. 83.1826) to remove remaining cell particles and used directly for lentiviral transduction of reporter cells or was frozen down to -80°C in working aliquots.

3.7.2 Production of Lentiviruses in 96-Well Plates

HEK293T cells (culture time < 9 weeks) in log phase were trypsinized with Trypsin/EDTA (BIOCHROM AG, Cat. no. L2143) for ~5 min at 37°C. $30*10^3$ cells were seeded in 100 µl medium per well on clear 96-well plates (BD Falcon, Cat. no. 353072). Constructs were prepared in 96-well format with ~0.14 µg/µl of DNA in HPLC H_2O. Two 15 ml tubes with 2.75 ml OptiMEM (GIBCO, Cat. no. 31985) each were prepared. Tube A contained 11 µg psPAX and 6.6 µg pMD2G plasmid while tube B 55 µl Lipofectamin 2000. Reagents were incubated for 5 min at RT. 25 µl of tube A reagent were transferred onto 96-well PCR V-bottom microtiter plate (Costar, Cat. no. 3363) using a multichannal pipette. 1 µl of prediluted DNA was transferred anlogous in the same 96-well PCR microtiter plate. 96-well plates were sealed with adhesive tape (Roth, Cat. no. EN83.1), mixed, and centrifuged with ~400 x *g* (using max. 2x 4 plates per run) for 1 min. Next, 25 µl of tube B were transferred onto the 96-well PCR microtiter plate. Plates were sealed with adhesive tape and mixed well followed by centrifugation at ~400 x *g*. Mixtures were incubated for 20-40 min at RT. Transfection mix was then transferred to 96-well microtiter plate with HEK293T cells. Next day, supernatant was removed from HEK293T cells with a NUNC immuno-washer device (NUNC, Cat. no. 470175) with a 9.5 mm comb depth and medium was replaced with 150 µl fresh culture medium.

3.7.3 Lentiviral Transduction in 96-Well Plates

U2OS BLH TD1 2K5 reporter cells [22, 35] (culture time < 9 weeks) grown in log phase (one

175 cm^2 flask) were trypsinized with trypsin/EDTA for ~5 min at 37°C. Reporter cells (20 * 10^3/well) were seeded in 50 µl culture medium plus 32 µg/ml protamine-sulfate (final concentration 8 µg/ml) in white 96-well plates. Viral particles containing supernantant from HEK293T cells (see previous section) were filterd using MultiScreen HTS filter plates (Milipore, Cat. no. MSFBN6B50), which were placed on top of a white 96-well culture plate (NUNC, Cat. no.136101) by spinning at 3,000 x *g* for 1 min. Next, GFP expression (in the case of GIPZ constructs) of the HEK293T cells was measured with the Infinite F200Pro device (TECAN). Next day, supernatant was removed from reporter cell plate using the NUNC immuno-washer and replaced with 150 µl fresh culture medium plus puromycin (10 µg/ml) or blasticidin (10 µg/ml).

3.7.4 Dynamic Oscillation Monitoring

Cells were synchronized by adding 50 µl of dexamethason solution (Sigma-Aldrich, Cat. no. D4902, solubilized in EtOH) to reporter cell plate, using a multichannel pipette. After a 15-30 min incubation time at at 37°C with 5% CO_2. The reporter cell plate was washed twice with 150 µl prewarmed PBS/well (using the immuno-washer). During the second wash with PBS on plate, GFP expression of the U2OS cells was measured (for GIPZ constructs) with the Infinite F200Pro device (TECAN). Finally, 150 µl of reporter medium per well were added to the plate and plates were sealed with Diamont Seal (Abgene, Cat. no. AB-0812) and the ALPS 50 device (Abgene) (2x with 165°C for 3 sec). Luminescence recording in TopCount luminometer (PerkinElmar) was started.

3.7.5 RNAi-Mediated Gene Silencing

Lentiviruses delivering RNAi (pGIPZ) constructs (Open Biosystems, Huntsville AL) were produced in HEK293T cells in a 96-well-plate format essentially as described above. Virus containing supernatants were filtered using Acro-Prep filterplates (Milipore). U2OS reporter cells (with a stably integrated 0.9 kb *Bmal1* promoter fragment) [22, 35] were transduced with 100 µl virus filtrate plus 8 µg/µl protamine sulfate (Sigma, Munich, Germany) in white 96-well plates (Nunc, Langenselbold, Germany). After one day, medium was exchanged to puromycin (10 µg/ml) containing medium. Three days later, cells were synchronized with dexamethasone (1 µM) for 30 min. Bioluminescence was recorded for 5 to 7 days in a

TopCount luminometer (PerkinElmer) with a stacker unit (sampling rate: ~30 min). RNAi data for 88 network neighborhood genes are part of a genome-wide screen (n = 1). RNAi experiments for clock core and regulatory components (45 genes; no RNAi construct was available for DEC1 in our library) were performed in three independent experiments (independent virus productions) with 20 non-silencing pGIPZ constructs per 96-well plate serving as controls.

3.7.6 Overexpression

U2OS reporter cells were lentivirally transduced with 46 ORFs in pLenti6 backbone (Invitrogen). After ten days of positive selection with blasticidine (10 μg/ml) (Invitrogen), bioluminescence was recorded as described above. PRKACA overexpression caused cell lethality. Experiments were independently performed three times. Cells expressing GFP (pLenti6) (n = 10 per plate) were considered as controls.

3.7.7 Data Analysis and Phenotypic Score

Network neighborhood (88 genes): period values were determined using an in-house programmed software (Chronostar), which basically performs a detrending by division of individuals data 24-hrs-running average and gives parameter estimations by fitting of a cosine wave function: y=a*exp(b*t)*cos(2 *pi * t * 24/c + d) where a = amplitude, b = damping, c = period and d = phase. The reliability of fitted parameters was determined by the correlation coefficient (cc). This software allows batch-processing of large quantities of circadian bioluminescence datasets. Curve fits with cc-values < 0.86 where considered as not reliable and marked for visual inspection. Those datasets which could not be described properly by above cosine function where excluded from further analysis. Datasets with cc < 0.86 and an arrhythmic characteristic where labeled as arrhythmic. Individual period values where normalized on global period effects of lentiviral load as determined by GFP fluorescence (Infinite F200pro, Tecan, Austria) of U2OS cells right before bioluminescence recording, as well as on optimized plate mean value (arbitrarily set to 24 hrs). This optimized mean value was determined by an iterative process, where extreme values (more than two standard deviations away from the respective actual mean) were excluded. We considered only those values as altered phenotypes, which deviated at least 0.5 hrs from an optimized mean value of

the respective plate. We evaluated 88 genes from circadian network neighborhood. For 82 genes, we found at least one targeting construct in our pGIPZ library (this was not the case for the genes: CEBPA, DDIT3, EP300, HSP90AA1, NOS1 and PXN). Genes from the network neighborhood, which showed at least two RNAi constructs with similar period phenotype, *i.e.* extreme period changes in the same direction or one period phenotype plus one arrhythmic phenotype, where considered as neighborhood hits.

Clock core and regulatory components (46 genes): data were analyzed as described above. Period differences to control values (mean of 20 non-silencing controls/plate for knockdowns; mean of 10 GFP expressing controls/plate for overexpression) within individual plates of > 0.5 hrs were considered as altered phenotypes. Amplitude and damping values that were more than 2.5 standard deviations different from the mean of the controls were considered as significant. Time series with a bad fit to a cosine function, *i.e.* a $cc < 0.8$ for knockdowns and $cc < 0.9$ for overexpression were classified as arrhythmic. Arrhythmic phenotypes were confirmed or rejected by visual inspection of the corresponding raw data.

Phenotypic score: Oscillations classified as arrhythmic based on bad fit to a cosine function (see above) were scored with 4 points. Period between 0.5 hrs and 1 h different from controls, between 1 h and 2 hrs, and more than 2 hrs were scored with 1, 2 or 3 points, respectively. Low amplitude and high damping were scored with 1 point and not assigned if a phenotype was already classified as arrhythmic. Phenotypic scores represent the sum of points from knockdown and overexpression experiments for an individual component in all categories.

3.8 Dual-Luciferase Reporter Assay System

In the Dual-Luciferase Reporter Assay System (DLR) from Promega, the activities of the firefly and Renilla luciferases are measured sequentially from a single sample. The firefly luciferase reporter is measured first by adding LAR II reagent to generate a "glow-type" luminescent signal. After quantifying the firefly luminescence, this reaction is quenched and the Renilla luciferase reaction is initiated by adding Stop and Glo reagent to the same tube. The Stop and Glow reagent also produces a "glow-type" signal from the Renilla luciferase, which decays slowly over the course of the measurement. This assay sytem was used for the co-transactivation experiments and BMLA1-luc and CLOCK-luc stability measurements (see below).

3.9 CLOCK/BMAL1 Co-Transactivation Assay

An artificial 6 *E-box* luciferase reporter (pGL3, Promega), Clock/Bmal1 (pDEST26, Invitrogen) and individually all discovered CLOCK and BMAL1 interactors and their paraloges (pLenti6, Invitrogen) that have been found by high-throughput interaction mapping in yeast were transiently transfected with Lipofectamine 2000 (Invitrogen) according to the manufacturer's protocol in HEK293 cells. CLOCK/BMAL1 co-transactivation assays were performed as previously described [19, 55]. Normalization was performed to Renilla-luciferase signals in lysates. Equal DNA amounts in transfections were ensured by the addition of *lacZ* DNA in the corresponding backbone. Signal detection was performed with the Dual-Luciferase Reporter Assay (Promega) in the Orion II Luminometer plate reader (Berthold Detection Systems). Experiments with all candidates were independently performed three times. A fourth repetition was only performed with candidates that showed consistent results in the previous repetitions (n = 3). Regulatory and scaffolding subunits were co-transfected with their corresponding catalytic subunits to simulate functional holoenzymes. Overexpression of candidates had no effect on the reporter alone.

3.10 Co-IP with Endogenous Components from Mouse Liver

Animals were sacrificed at circadian time points (CT) CT12 or CT0 for liver preparation. Lysates were generated and co-IPs were performed as described for Y2H validation. Co-IPs and Western blot analysis were performed with an anti-BMAL1 antiboby (kindly donated by the M. Brunner laboratory; specificity was intensively characterized using *Bmal1* knock out mouse tissue [29] or an anti-PPP1Cα antibody (sc-7482, Santa Cruz Biotechnology)). Controls were performed with the following ideotypic antibodies (sc-3878, sc-2037 Santa Cruz Biotechnology). 100 µg of total lysate were loaded as input controls. 500 µg of protein were subjected for immunoprecipitation experiments.

3.11 BMAL1 and CLOCK Stability Measurements

3.11.1 Protein Stability Measurement of BMAL1-and CLOCK-Luciferase Hybrids

HEK293 cells stably expressing BMLA1 or CLOCK luciferase fusions (as generated for

interaction validation experiments) were lentivirally transduced with pLenti6 PPP1CA or tGFP DNA in 24-well format. 48 hrs after transfection, luciferase activity in lysates was detected as described for the co-transactivation assays.

3.11.2 Endogenous BMAL1 Levels in the Presence of PPP1CA

Steady-state: U2OS *Bmal1*-promoter luciferase reporter cells stably expressing PPP1CA or GFP (pLenti 6, Invitrogen) were harvested in RIPA buffer containing protease inhibitor cocktail (P-8340, Sigma-Aldrich). 30 µg of total lysate were loaded for Western blot analysis as performed in 2.1 using the anti-BMAL1 antibody from M. Brunner's laboratory. Membranes were probed with an anti-Actin IgG (A-5441, Sigma-Aldrich) as loading controls. Quantification was performed with ImageJ 1.44p software (National Institutes of Health).

Cyclohexamide (CHX) time series: U2OS cells – as described above – were treated with CHX (C4859, Sigma-Aldrich) using a 0.71 mM final concentration. Cells were harvested at the following selected time points: 3 hrs, 4 hrs, 5 hrs and 6 hrs. Western blotting and incubation with antibodies were performed as described above.

3.12 Network Visualization

Network was depicted using the Cytoscape 2.8.1 software as available at www.cytoscape.org/.

3.13 Bioinformatics Analysis

Bioinformatics analyses were conceptionally designed by me and performed by Dr. Matthias Futschik and Dr. Ravi Kalthur (Universtiy of Algarve, Faro, Portugal). I have performed network topology analysis (network properties and cluster analysis using Cytoscape 2.8.1 sofware) as well as KEEG pathway analysis. I and Dr. Matthias Futschik have written the following Methods section.

3.13.1 Construction of Protein-Protein Interaction Networks form UNIHI

For network analyses, proteins were indexed by corresponding human Entrez Gene IDs. For a

proteome-wide interaction network, data curated in the original databases HPRD (binary interactions only), DIP, BIND, BIOGRID and INTACT as stored in the UNIHI4 version were integrated [56]. This generated a global network of 9,982 proteins and 45,775 interactions. The network was used to identify additional interactions between the proteins in the circadian network (PPIs among 46 components (clock core and regulatory components)) as well as to assess the molecular context of the circadian network. First, the global protein networks were examined for overlap (common proteins and interactions) with the circadian PPI network. Identified additional interactions between the 46 components were added to enlarge the circadian PPI network. Furthermore, we included proteins interactions based on a literature review that we conducted.

3.13.2 Determination of Periodic Expression

To identify periodic expression patterns, the data set by [27] measuring gene expression in mouse liver was utilized. The microarray dataset includes consecutive sampling over 48 hrs (with intervals of 1 h) for 45,101 probe sets. These probe sets correspond to 21,308 unique mouse Entrez Gene identifiers. For derivation of probe set intensities, the RMA method as implemented in the Bioconductor *affy* package was utilized.

To evaluate the periodicity, the expression vectors mRNA profiles were standardized and subsequently corresponding Fourier scores for a periodicity of 24 hrs were calculated. The Fourier score is defined as

$$F[x] = \sqrt{\left(\sum_i (\cos(2 \cdot \pi \cdot t_i/T) \cdot x_i\right)^2 + \left(\sum_i (\sin(2 \cdot \pi \cdot t_i/T) \cdot x_i\right)^2}$$

where x is the standardized expression vector (mean(x) = 0; sd(x) = 1) for the gene, T is the period (in our case 24 hrs), and x_i is the measured expression at time point t_i. Statistical significance (*i.e.* false discovery rate (FDR)) was derived through comparison using randomly permutated time series [57]. The expression analysis was performed using the Bioconductor *cycle* package.

3.13.3 Interactions and Expression of Regulatory Proteins

To compare the number of interactions of regulatory and non-regulatory proteins in the human interactome, we first calculated the number of interactions for each protein in the global protein-protein interaction networks derived from UNIHI database. For the classification of regulatory proteins, we utilized gene annotation from the GO database. Proteins whose corresponding genes were associated with the GO category `Regulation of biological process´ (GO:0050789) were assigned as regulatory proteins (n = 4,635). The remaining proteins were classified as non-regulatory (n = 5,347). Subsequently, the numbers of interactions of proteins in both groups were compared. We observed that regulatory proteins tend to have more interactions than non-regulatory proteins. The mean number of interactions for regulatory proteins was 12.74, whereas non-regulatory proteins have in average only 5.64 interactions. Statistical testing demonstrated that this difference is highly significant (Wilcoxon test: $p < 10^{-15}$).

We also examined the relationship between periodic expression and number of interactions. First, we calculated the number of interactions for human proteins for which the mouse ortholog is showing significant periodic expression (FDR < 0.01; n = 2,468). The average number was 11.31 interactions compared to 8.81 for proteins with a mouse orthologs that are not periodically expressed (n = 5,011). The difference is statistically highly significant (Wilcoxon Rank test; $p < 10^{-10}$) indicating that proteins with periodic expression tend to have more interactions compared to constitutively expressed proteins. Secondly, we examined whether the reverse is valid *i.e.* interaction-rich proteins tend to be periodically expressed. To this end, we classified proteins with more than 50 interactions as interaction-rich (n = 762), and compared their periodic expression with proteins that have less than 5 interaction (n = 6,654). Notably, almost 42% of the interaction-rich proteins were periodically expressed compared to only 29% for interaction poor. Statistical evaluation of the difference by Chi-squared test indicated a high significance ($p < 10^{-5}$).

3.13.4 Identification of Dynamic/Rhythmic Protein-Protein Interactions

To obtain an approximation of the dynamics of PPI in the network, we assumed that the abundance A_C of the complex C formed by two interacting proteins $P_{1,2}$ through a PPI is

proportional to the expression E of $P_{1,2}$. Thus, the abundance $A_C(t)$ over time can be approximated by the product of expression vectors mRNA profiles $E_{P1}(t) * E_{P2}(t)$ which was then associated with the corresponding PPI between P_1 and P_2. As proxy for the expression, the transcript levels over time were utilized, thus

$$PPI_{12} \sim A_C(t) \approx c * A_{P1}(t) * A_{P2}(t) \rightarrow A_C(t) \approx E_{P1}(t) * E_{P2}(t).$$

The statistical significance of the product of expression vectors mRNA profiles was calculated in the same manner as for simple expression vectors (*i.e.* using the Fourier-score and permutated time series as background model) after standardization (*i.e.* mean($E_{P1} * E_{P2}$) = 0; sd($E_{P1} * E_{P2}$) = 1). Additionally, a phase was assigned to a periodic interaction through shifting a cosine (with periodicity 24 hrs) along the time axis and measuring the overlap of the expression levels with the cosine curve. PER1-3 mRNA profiles were shifted + six hrs (see [20]). The time shift leading to a maximum overlap was considered as the phase α of the PPI and ranges from 0 to 24 hrs.

3.13.5 Dynamic Interactions between Biological Processes in the Circadian Protein-Protein Interaction Network

To examine the dynamic coupling between biological processes in the circadian network, we first selected the processes, which were examined in the analysis. Biological processes (BP) and their associated genes (or respectively proteins) were given by the annotation in Gene Ontology (GO, www.geneontology.org). Here, we chose processes, for which associated proteins were overrepresented in the circadian network. For calculation of statistical significance of enrichment, hypergeometric test (which is equivalent to Fisher´s exact test) with subsequent Benjamini-Hochberg for multiple testing was utilized. A FDR cut-off of 0.25 for significance was set.

A well-known difficulty in the interpretation of enrichment analysis for GO categories is occurrence of highly overlapping terms. This is caused by the hierarchical structure of GO: significance of enrichment in children terms frequently result in significance of their parent terms (*e.g.* significance in proteins linked to the term `Intracellular signal transduction´

contribute to the statistical enrichment of proteins in the term `Signal transduction´). To reduce the set of significant terms to a smaller and less redundant set of terms, we used following filtering procedure: Categories were excluded if the majority of included genes (*i.e.* more than 50%) had been associated with a single category having less genes. This procedure generally led a reduced set of more specific categories facilitating inspection of results. Applied to the 134 genes included in circadian network and the full set of categories for biological processes derived from GO through the Bioconductor GO package, 16 significant categories with a minimum size of 10 associated genes were derived.

Next, we counted the number of interactions between proteins for all possible pairs of processes. Also, the number of dynamic interactions (with a significance of periodicity of FDR < 10^{-5}) was counted. Using the calculated numbers, we tested whether dynamic interactions were over-represented in the total set of interactions between a pair of categories using Fisher's exact test with subsequent Benjamini-Hochberg adjustment for multiple testing. A network of biological processes was then constructed based on the significance for the enrichment in dynamic interactions between categories.

For the reduced set of GO categories, setting a threshold for significance of FDR < 0.1 resulted in a network with 12 links between 11 processes. The central position is constituted by the BP category `Circadian rhythm´ which is linked to the 10 other categories by dynamic interactions.

3.13.6 KEGG Pathway Analysis of Components of the Network Neighborhood

The circadian network neighborhood was examined for enriched KEGG (Kyoto Encyclopedia of Genes and Genomes) pathways. To this end, the 88 proteins in the neighborhood were annotated with pathway information derived from KEGG through the Bioconductor KEGG package. The significance for enrichment was calculated using the hypergeometric test, which is equivalent to the Fisher's exact test. Pathways with less than 5 associated proteins from the network neighborhood were excluded. For multiple testing, an adjustment by the Benjamini-Hochberg method was conducted and FDR were derived. A threshold of FDR < 0.25 was applied.

3.13.7 Overlap with Reference Gene Sets

Significance was calculated using the hypergeometric test with the complete lists of genes included in the global network as reference set.

The overlap with the Cancer Gene Census (www.sanger.ac.uk/genetics/CGP/Census) of 427 genes is:

- for the clock core and regulatory components (46 proteins): EZH2, NONO, PER1; three genes; $p = 0.10$
- for the full extended network (134 proteins): AKT1, ATF1, CEBPA, CREBBP, DDIT3, EP300, EZH2, HLF, HSP90AA1, MEN1, MLL, MYC, NCOA1, NCOA2, NONO, PER1, PML, RARA, SFPQ, SUZ12; 20 genes, $p = 2.8 * 10^{-8}$
- for the neighborhood only (88 proteins): AKT1, ATF1, CEBPA, CREBBP, DDIT3, EP300, HLF, HSP90AA1, MEN, MLL, MYC, NCOA1, NCOA2, PML, RARA, SFPQ, SUZ12; 17 genes; $p = 3.8 * 10^{-9}$

The overlap with the HD Research Crossroads (www.hdresearchcrossroads.org) gene list of 692 HD-relevant genes is:

- for the clock core and regulatory components (46 proteins): CSNK2A1, CSNK2B, GSK3B, NR1D1, PPP1CA, PRKACA, PRKCA, RORB; eight genes; $p = 0.0012$
- for the full extended network (134 proteins): for the full extended network (134 proteins): AKT1, AR, CREBBP, CSNK2A1, CSNK2B, GANI1, GNB1, GSK3B, HDAC1, HDAC2, HSP90AA1, NCOR1, NOS1, NPAS4, NR1D1, POLR2A, PPP1CA, PRKACA, PRKCA, RORB, RXRA, SP1, UBE2I; 23 genes; $p = 1.6 * 10^{-6}$
- for the neighborhood only (88 proteins): AKT1, AR, CREBBP, GANI1, GNB1, HDAC1, HDAC2, HSP90AA1, NCOR1, NOS1, NPAS4, POLR2A, RXRA, SP1, UBE2I; 15 genes; $p = 7.2 * 10^{-5}$

3.13.8 Identification of Structural Modules

In order to identify dense local sub-networks (*i.e.* structural modules), two algorithms were

used: 1. The MCODE algorithm (http://baderlab.org/Software/MCODE) and 2. The ClusterOne algorithm (www.paccanarolab.org/cluster-one). For both algorithms, their Cytoscape implementation was utilized. The two methods are similar in their general procedure, *i.e.* to detect first dense local networks and them to expand them.

Significance of periodicity of interaction is represented by edge color with red representing highly significant (FDR < 10^{-5}) and yellow/white representing low significance of periodic expression. Similarly, edge width represents also the significance of periodicity of interaction with larger width representing higher significance. Yellow circles highlight rhythmic RNA profiles; circle width corresponds to significance of periodic expression. Calculation of significance of functional enrichment was based on Fisher's exact test with Benjamini-Hochberg adjustment using the annotation provided by the GO Bioconductor package.

3.13.8.1 MCODE Modules

To identify structural modules using the MCODE algorithm, the node score cutoff parameter was set to 0.05. For other parameter, the default values (Version 1.32) were used. This parameter setting led to small structural modules facilitating their inspection. In total, nine clusters were identified, five of which were simple triangles and disregarded in the subsequent analysis. The top four modules are as follows:

1. Module

This module obtained rank 1 and a score of 3. The score produced by MCODE is the average number of distinct interactions per protein. It includes seven proteins and 21 interactions. Five proteins are significantly (FDR < 0.01) periodically expressed. The GO terms `Histone methyltransferase complex´ (FDR < $10^{-11}$; five genes: ASH2L, HCFC1, MEN1, MLL, RBBP5) and `Transcription from RNA polymerase II promoter´ (FDR = 0.0008; five genes: ASH2L, HCFC1, HCFC2, MEN1, MLL) are significantly enriched.

2. Module

This module obtained rank 2 and a score of 2. It includes five proteins and ten interactions. The GO term `Transcription from RNA polymerase II promoter´ (FDR= 0.004; four genes: CEBPG, DDIT3, HLF, TEF) as well as the Pfam family `Basic region leucine zipper´ (FDR < 10^{-10}); four genes: CEBPG, DDIT3, HLF, TEF) are significantly enriched.

3. Module

This module obtained rank 3 and a score of 1.8. It includes five proteins and nine interactions. The GO terms `Transcription coactivator activity´ (FDR = 0.0016; three genes: KAT2B, NCOA1, NCOA2) and `Positive regulation of transcription from RNA polymerase II promoter´ (FDR = 0.0004; four genes: AR, HIF1A, NCOA1, NCOA2) are significantly enriched.

4. Module

This module obtained rank 4 and a score of 1.5. It includes eight proteins and twelve interactions. The GO terms `Chromatin modification´ (FDR < $10^{-4}$; five genes: CHD4, EED, EP300, HDAC1, HDAC2), `Transcription factor binding´ (FDR < 10^{-4}; six genes: AHR, CHD4, EP300, HDAC, HDAC2, NCOR2), `Negative regulation of transcription´ (FDR < 10^{-3}; four genes: EED, HDAC2, NCOR2, UBE2I) are significantly enriched.

3.13.8.2 ClusterOne modules

Besides MCODE, we used the ClusterOne Cytoscape plugin to detect structural modules. For the detected modules, the density, quality and p-value of the modules are reported. Density of a structural module is defined by the number of observed interactions within the module divided by the maximum number of possible interactions. The quality of a module is the number of internal interactions divided by the sum of internal interactions and interactions with proteins outside the module. The p-value is based on a one-sided Mann-Whitney U test distinguishing internal interactions and interactions with proteins outside the module. More details are available at http://www.cs.rhul.ac.uk/home/tamas/assets/files/cl1/cl1-cytoscape-0.92.html.

1. Module

This module has ten proteins connected by 24 interactions. It obtained a density of 0.54, a quality of 0.57 and a p-value of 0.003 by the ClusterOne algorithm. The GO terms `Rhythmic process´ (FDR < $10^{-4}$; four genes: DBP, HLF, NFIL3, TEF) and `RNA polymerase II transcription factor activity´ (FDR < 10^{-3}; four genes: BATF, CEBPA, DBP, TEF) as well as the Pfam family `Basic region leucine zipper´ FDR < 10^{-18}; seven genes: CEBPA, CEBPG, DBP, DDIT3, HLF, NFIL3, TEF) were significantly enriched.

2. Module

This module has nine proteins connected by 20 interactions. It obtained a density of 0.56, quality of 0.58 and a p-value of 0.004 by the ClusterOne algorithm. The GO terms `Transcription from RNA polymerase II promote´ (FDR = 0.00013, six genes: CEBPG, DDIT3, DR1, HLF, NFIL3, TEF), `Transcription corepressor activity´ (FDR < 10^{-3}; three genes: DDIT3, DR1, NFIL3) as well as the Pfam family `Basic region leucine zipper´ (FDR < 10^{-11}; five genes CEBPG, DDIT3, HLF, NFIL3, TEF) are significantly enriched.

3. Module

This module has 18 proteins connected by 77 interactions. It obtained a density of 0.50, quality of 0.42 and a p-value of 0.01 by the ClusterOne algorithm. The KEGG pathways `Circadian rhythm – mammal´ (FDR < $10^{-7}$; five genes: BHLHE40, BHLHE41, CRY1, CSNK1E, CLOCK) and `Wnt signaling pathway´ (FDR < 10^{-5}; seven genes; CSNK1E, CSNK2B, PPP2CA, PPP2R1A, PPP2R1B, PPP2R5D, PPP2R5E) as well as the GO term `Protein phosphatase type 2A complex´ (FDR < 10^{-5}; four genes: PPP2CA, PPP2R1A, PPP2R5D, PPP2R5E) are significantly enriched.

4. Module

This module has nine proteins connected by 21 interactions. It obtained a density of 0.58, quality of 0.53 and a p-value of 0.015 by the ClusterOne algorithm. The GO terms `Response to DNA damage stimulus´ (FDR = 0.0017; four genes; CUL4B, CUL4A, DDB1, DTL) and `Nucleotide excision repair´ (FDR < 10-5; 3 genes; CUL4B, CUL4A, DDB1) as well as the Pfam family `WD domain, G-beta repeat´ (FDR < 10-6; five genes: DTL, GRWD1, RBBP5, SNRNP40, WDR5) are significantly enriched.

5. Module

This module has 17 proteins connected by 68 interactions. It obtained a density of 0.50, quality of 0.407 and a p-value of 0.015 by the ClusterOne algorithm. The GO terms `Histone acetyltransferase activity´ (FDR < $10^{-8}$; five genes: CREBBP, EP300, KAT2B, NCOA3, NCOA1), `Positive regulation of transcription from RNA polymerase II promoter´ (FDR < 10^{-8}; nine genes: AR, EP300, HDAC1, HIF1A, MYOD1, NCOA1, NCOA2, RXRA, SP1) as well as the KEGG pathways `Notch signaling pathway´ (FDR < $10^{-5}$; five genes; CREBBP, EP300, HDAC1, KAT2B, NCOR2), `Pathways in cancers´ (FDR < 10^{-4}; eight genes: AR,

CREBBP, EP300, HDAC1, HIF1A, PML, RXRA, STAT3) and `Huntington's disease´ (FDR < 10^{-3}; five genes: CREBBP, EP300, HDAC1, POLR2A, SP1) are significantly enriched.

6. Module

This module has 18 proteins connected by 78 interactions. It obtained a density of 0.51, quality of 0.43 and a p-value of 0.02 by the ClusterOne algorithm. The KEGG pathways `Circadian rhythm – mammal´ (FDR < $10^{-10}$; six genes: BHLHB2 (= DEC1), BHLHB3 (= DEC2), CLOCK, CRY1, CSNK1E, PER2) and `Wnt signaling pathway´ (FDR < 10^{-4}; six genes: CSNK1E, CSNK2B, FBXW11, PPP2R1B, PPP2R5D, PPP2R5E) are significantly enriched.

7. Module

This module has 18 proteins connected by 77 interactions. It obtained a density of 0.50, quality of 0.41 and a p-value of 0.025 by the ClusterOne algorithm. The KEGG pathways `Circadian rhythm – mammal´ (FDR < $10^{-21}$; ten genes: BHLHB2, BHLHB3, CLOCK, CRY1, CRY2, CSNK1D, CSNK1E, PER1, PER2, PER3) and `Wnt signaling pathway´ (FDR < 10^{-4}; six genes CSNK1E, CSNK2B, FBXW11, PPP2R1B, PPP2R5D, PPP2R5E) are significantly enriched.

3.14 Dynamic Interactome

To examine circadian coupling between processes on a systems-wide level, all PPIs of the compiled human interactome (n = 45,775) were assessed for dynamic behavior. Human proteins were mapped to their orthologs in mouse. As previously for the circadian network, the periodicity of interactions was based on the expression data for mouse liver over the time span of 48 hrs. In total, the dynamic behavior of 30,413 interactions could be determined. For the remaining interactions, either corresponding gene expression data was not available or the mouse orthologs could not been found.

For the determination of significance in periodic expression, the described Fourier-based approach with random permutations as background model was used. A threshold of FDR < 10^{-5} was set. This resulted in the identification of 2,788 significantly dynamic interactions. The full lists of interactions containing the human proteins and their mouse orthologs, corresponding gene symbols, significance of periodic expression and offset of

individual interactions partners as well as of the interaction can be found in the Appendix section.

For evaluation, which biological processes are connected in a dynamical manner, we performed an enrichment analysis for the 1,979 proteins with dynamic interactions. The analysis was based on their GO slim annotation. To obtain non-redundant set of categories for biological processes, the previously described filtering procedure was used, *i.e.* categories are excluded if the majority of included genes are associated with a single category having less genes. We obtained 27 biological processes with a significant enrichment of FDR < 0.25. Next, we mapped the dynamic interactions to the corresponding biological processes. As before, the significance of over-representation of dynamical interactions between categories was calculated. Connections, which were significantly dynamical enriched, were displayed as network. Transcription and signal transduction were detected to be central hubs in the network of processes coupled by dynamic interactions. In contrast, processes like `Cellular homeostasis´ and `Lipid metabolism´ tended to be linked to other processes *via* static interactions.

As an alternative approach to examine, which biological processes tend to be linked by the dynamic interactions, we compared the wiring of the observed interaction network with randomized versions of it. For randomization, the degree distribution of each protein was conserved. To this end, the interaction between protein pairs were randomly switched, *i.e.* interactions between protein pairs A-B and C-D were changed to A-C and B-D. Every interaction was repeatedly switched in average 100 times. For the randomized networks, the number of dynamic interactions between the biological processes were counted and compared with the observed network. Altogether, 1,000 randomized networks were independently generated. We found that for 26 pairs of biological processes, the numbers of dynamic interactions were higher than in any of the randomized network. This number of pairs increased if we relax the requirement. We obtained 52 pairs if we required that the number of dynamic interactions between processes should not be higher in ten out of the 1,000.

Data regarding the dynamic interactome analysis will be available as online supporting material of my publication (Wallach T, Schellenberg K, Maier B, Kalathur R, Porras P, Wanker EE, Futschik M, Kramer A. Dynamic Circadian Protein-Protein Interaction Networks Reveal Temporal Organization of Cellular Functions. *In preparation*).

4 RESULTS

4.1 Large-Scale Y2H Interaction Analysis with Circadian Clock Components

To systematically map the PPIs within the circadian clock regulatory network, I performed a matrix-based Y2H screen in yeast with 46 known or assumed clock or clock-associated components. In this screen, each potential interaction was tested individually in six replicas minimizing the risk of false negatives (see Figure 8 A, B; Figure 9 A) [39, 41]. After excluding transcriptionally autoactive components, I have performed 11,040 individual Y2H experiments monitoring growth on selective medium and β-galactosidase activity as readouts for interaction (Figure 8 C and Figure 9 A to C).

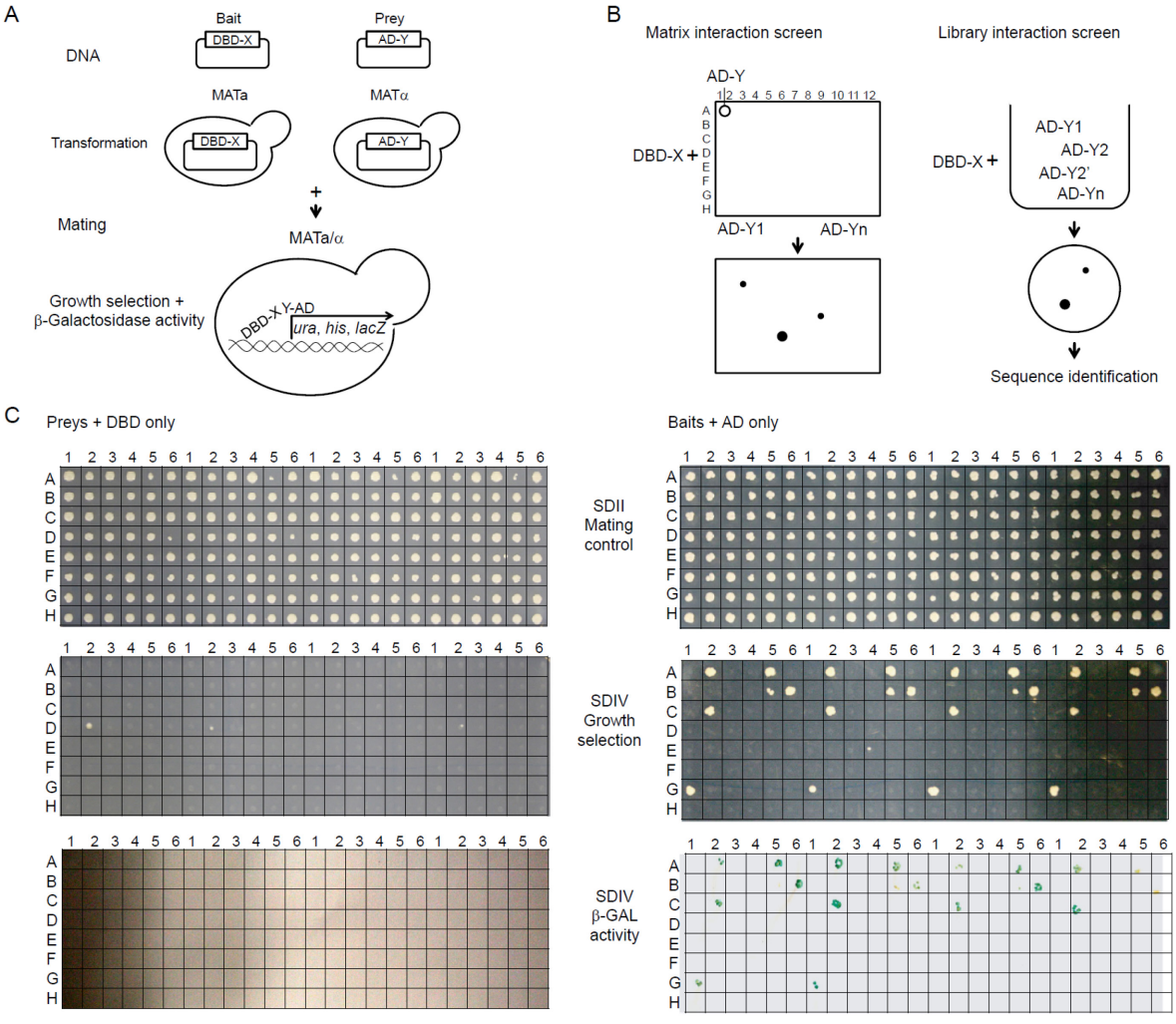

Figure 8. The Yeast-Two-Hybrid (Y2H) Approach.
(A) Principle of the Y2H screen. Y2H is a genetic approach where two interacting proteins can reconstruct a functional transcription factor, which leads to the activation of several reporter genes (*ura*, *his*: growth selection on minimal medium; *lacZ*: β-Galactosidase activity). One interactor – X – is fused to a DNA binding domain (DBD: LEXA; bait configuration), while the other – Y – to a transcription activation domain (AD: GAL4; prey configuration). Both hybrids are transformed into different yeast strains (MATa or MATα). Interaction of X and Y is detected after mating *via* activation of reporter genes.
(B) Left: Matrix-based Y2H screening. Defined bait and prey fusions allow performing several repetitions of an interaction screen. Matrix position reveals positive interaction pairs without the necessity of sequence identification. Right: Library-based Y2H screening. Bait is presented to prey library containing redundant sequences. Growth competition and sequencing are required for the identification of interactors.
(C) Auto-activation test for 46 circadian clock components. Left: Yeast strains containing preys were mated with a yeast strain expressing the DBD only. Results are shown for four independent mating experiments. NPAS2 (position D2) showed weak auto-activating properties (weak growth on selective medium, no *lacZ* expression) and was included for high-throughput interaction mapping. Right: Auto-activation test for baits. Yeast containing baits were mated with a yeast strain expressing the AD only. PER2 (A2), BMAL1 (A5), NR1D1 (B5), NR1D2 (B6), RORB (C3) and PPP2CA (G1) showed strong auto-activation of all reporters leading to exclusion of these components in the bait configuration from further interaction experiments.

Based on the reproducibility, the putative interactions were sorted into sets with high, medium and low confidence (Figure 9 B and C). Thereby, 150 interacting protein pairs that occurred at least in two independent experiments were identified, of which I rated 90 as high-score, 41 as medium score and 19 as low-score interactions (Figure 9) (for details on scoring see Methods section). While I could reproduce a large number (41 in total) of previously described interactions (*e.g.*, CLOCK-BMAL1, PERs-CRYs, CRYs-BMAL1), 109 PPIs among circadian clock proteins were new (see Appendix section). For example, I detected high-score interactions between DEC1/2 and CRY1/2, medium-score interactions between CLOCK and RORB, CLOCK and the α-catalytic subunit of protein phosphatase 1 (PPP1CA) as well as between BMAL1 and WDR5 and low-score interaction between CLOCK and RORC (Figure 9 B and C, Figure 10 A).

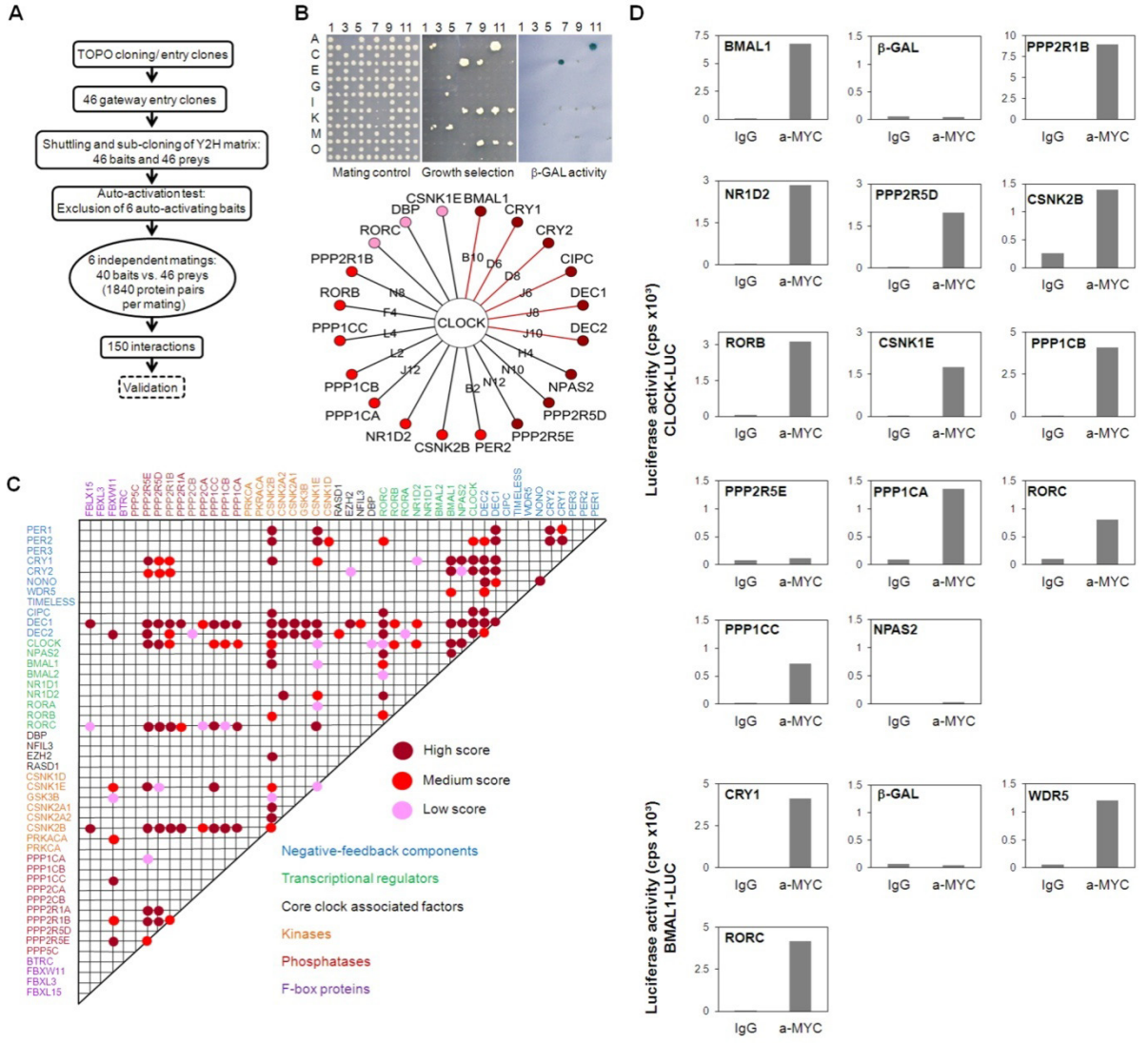

Figure 9. Systematic Interaction Mapping between 46 Circadian Clock Proteins and Associated Components.

(A) Flow chart of matrix based high-throughput Y2H interaction screen.

(B) CLOCK interactors: Mating controls (top left) on selective medium (-Leu, -Trp) demonstrate that yeast cells have simultaneously expressed bait and prey fusion proteins. When proteins interact, several reporter genes (top middle: *his*, *ura* for growth selection, top right: *lacZ* for β-galactosidase activity assay) are activated. Bottom: Detected interactions for CLOCK protein with circle color representing interaction score (see (C)) and position of representative colonies. Red lines show CLOCK interactions that were previously discovered in yeast.

(C) Detected interactions in yeast. Circles represent interactions between two components not differentiating between bait and prey configuration, circle color denotes interaction score based on the reproduction rate within six independent repetitions.

(D) Validation of new CLOCK and BMAL1 interactions in mammalian cells. HEK293 cells stably expressing CLOCK- or BMAL1-luciferase fusion proteins were transiently transfected with the indicated MYC-tagged components. Co-immunoprecipitations were performed with an anti-MYC or an ideotypic antibody as a control. Luciferase activity measurements (cps – counts/10 sec) demonstrate the presence of luciferase fusions in the immunoprecipitates. MYC-β-galcactosidase fusions served as negative, MYC-BMAL1 and MYC-CRY1 as positive controls, respectively. Depicted are representative results of at least two independent experiments with similar results.

4.2 Validation of CLOCK and BMAL1 Interactors Detected in Yeast

To test whether the PPIs discovered in yeast also occur in mammalian cells, co-immunoprecipitation experiments in HEK293 cells were performed.

As representatives for the novel PPIs, I focused on the interactions of the transcriptional activators CLOCK and BMAL1 – central players within the circadian clock gene-regulatory network – whose functional modulation by interacting proteins is likely to be highly relevant for normal circadian rhythms. Twelve of the 14 (*i.e.* 85%) novel CLOCK and BMAL1 interactions found in yeast were validated using co-IP (Figure 9 D and Figure 10 B and D), suggesting that a substantial proportion of all interactions identified in yeast are also detectable in mammalian cells.

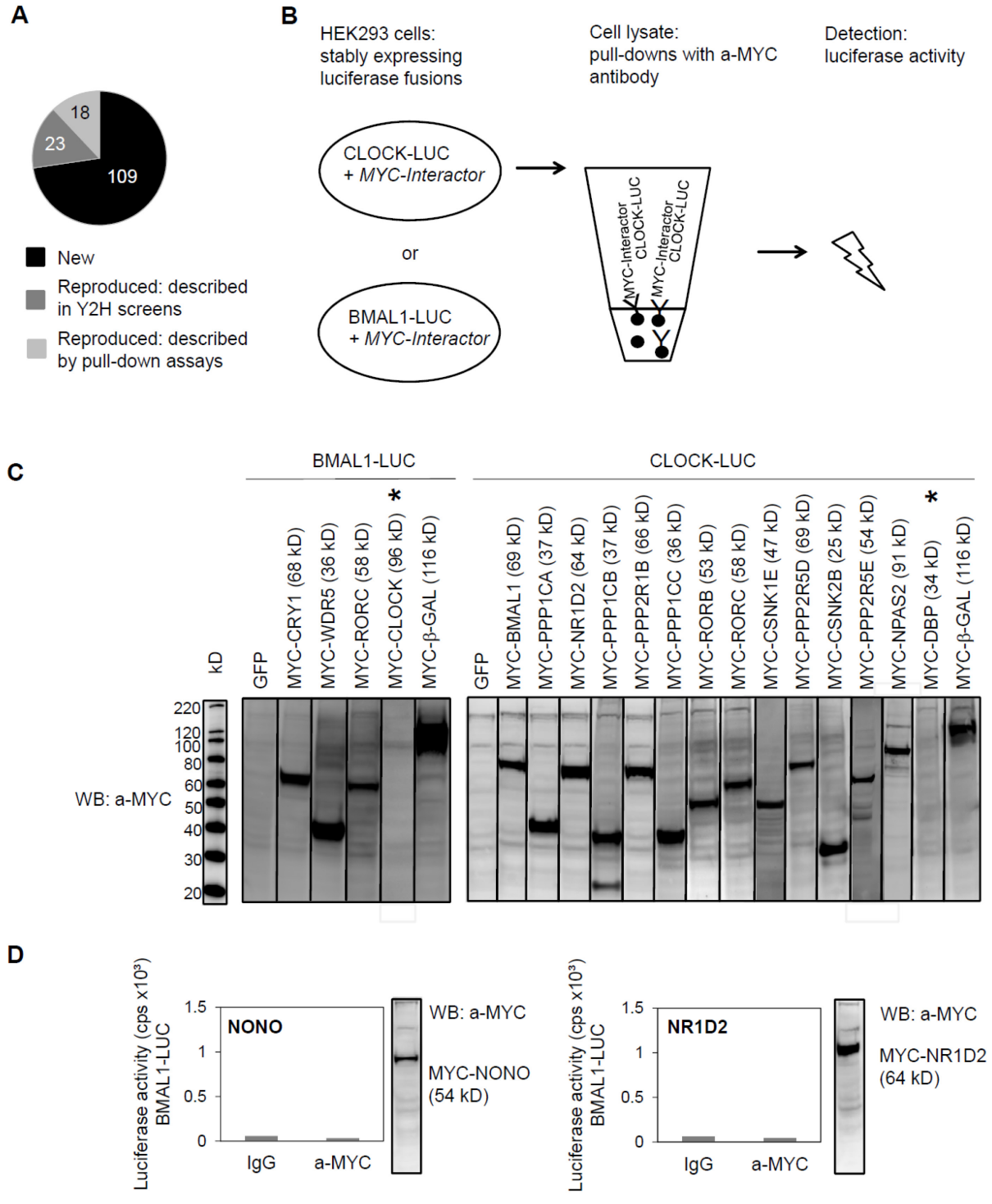

Figure 10. Reproduction Rate of Y2H Screen and Validation of CLOCK and BMAL1-Interactions in Mammalian Cells.

(A) 109 interactions that occurred in the matrix-based Y2H screen were so far uncharacterized. 23 interactions were previously found in library based Y2H screens and reproduced with our approach, whereas 18 interactions were reproduced that were detected previously by other approaches (not in yeast cells).

(B) Principle of co-IP experiments. HEK293 cells stably expressing CLOCK or BMAL1 C-terminal luciferase fusions were transfected with MYC-tagged interactors. Lysates containing one million luciferase counts were subjected to IP experiments. Pull-downs were preformed with an anti-MYC antibody or an ideotypic antibody in (beads) controls. After washing, beads pellets were incubated with a luciferin containing reagent and luciferase activity was measured (for details see Methods).
(C) Input detection *via* Western blot analysis. 25 µg of total lysate were loaded per lane as an input control. MYC-fusions were detected with an anti-MYC antibody. The results for the co-IP as performed in Figure 9 D are shown. CLOCK and DBP fusions could not be detected in lysates as MYC (*), FLAG or V5-hybrids (not shown). Expected protein size (from Expasy database) is shown in brackets.
(D) NONO and NR1D2 were not detected as direct BMAL1 interactors in yeast. Co-IP experiments as performed for validation with BMAL1-LUC and MYC-NONO or MYC-NR1D2 also show no interaction in mammalian cells using the validation system. Western blots show input controls as performed in (C).

4.3 Enrichment, Extension and Topology Analysis of the Circadian PPI Network

To understand the structure and the organizing principles of the complex web of interactions occurring between circadian clock components, we created an interaction network using our novel Y2H interaction data together with previously published interactions among these components. In addition, we extended this network by adding known interacting proteins (direct `neighbors´) of our network components (except regulatory components such as kinases, phosphatases and F-box proteins, which are known to be involved in many other cellular processes) to get an idea how the circadian PPI network is embedded in the cellular interactome (Figure 11). Thereby, a large PPI network with 134 components and 625 PPIs was created consisting of a circadian clock core (24 components), regulatory components (22 components) and the neighborhood (Figure 12).

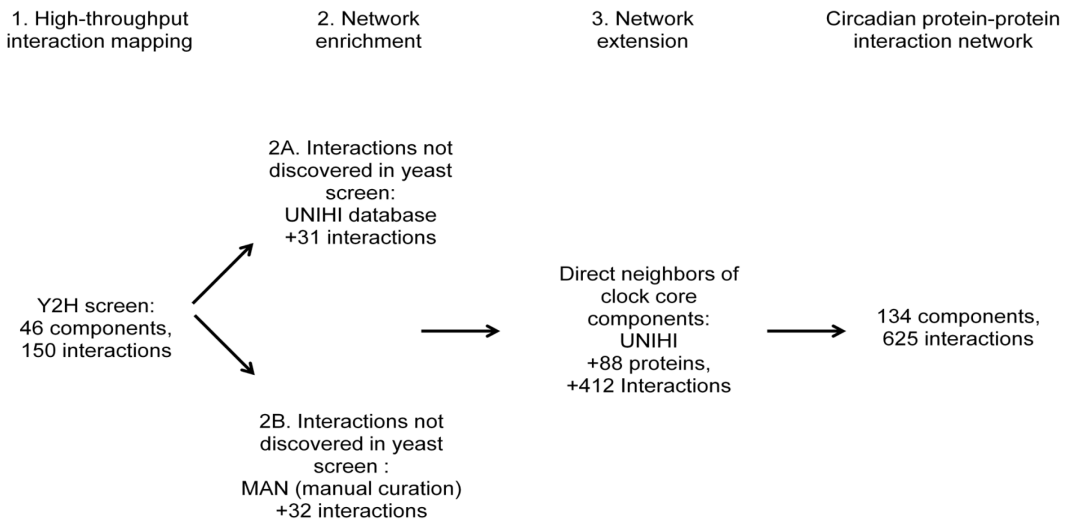

Figure 11. Construction of the Circadian Protein-Protein Interaction Network and Topology Analysis. Enrichment and extension of the circadian protein-protein interaction network. The experimentally derived network was firstly enriched by adding previously described interactions (Y2H screen false negatives) from literature and extended by the direct neighbors of clock core components as stored in the UNIHI database. This resulted in the construction of a circadian protein-protein interaction network consisting of 134 proteins and 625 interactions.

For this network, a mean shortest path length between any two proteins of 2.8 links was calculated, *i.e.* most proteins are very closely linked to each other indicating a `small world´ type of network [58]. Like many other PPI networks [42], the circadian network has `scale-free´ properties, *i.e.* it is a network, for which the distribution of the number of interactions (`degree´) for each protein follows a power law – many proteins have few and few proteins have many interactions. On average each component has 8.4 interaction partners, however, 11 proteins are highly connected with more than 20 interactions (*e.g.* CLOCK, BMAL1, PER2, CREBBP, DEC1, AR, HDAC1). Network topology analysis, further revealed that the circadian network is hierarchically organized, *i.e.* highly connected components (so-called `hubs´) link network regions with less connected components, which themselves tend to form clusters (Figure 12).

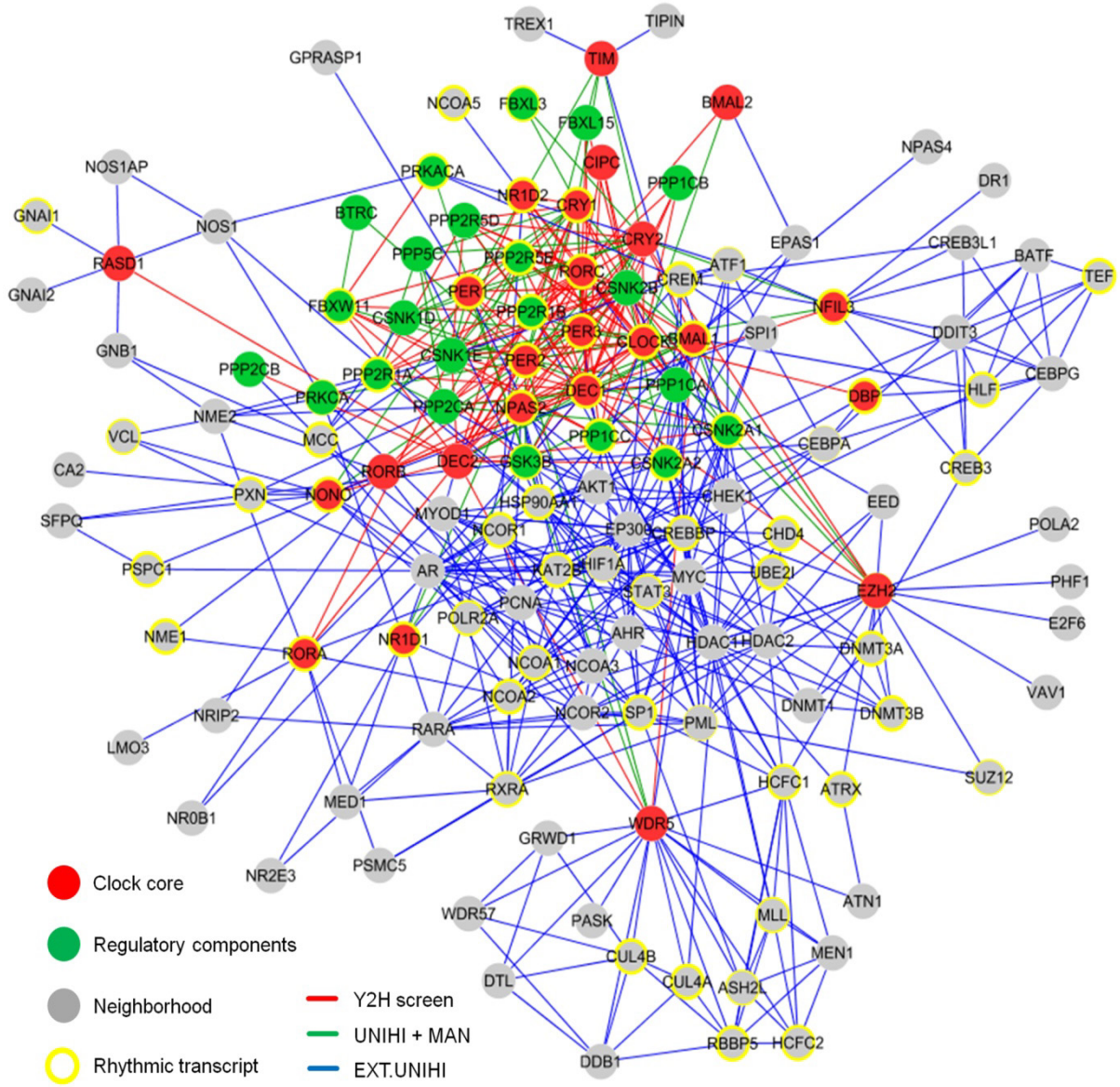

Figure 12.The Circadian Protein-Protein Interaction Network.
The circadian interaction network integrates different interaction sources and visualizes 134 proteins with 625 interactions. Proteins are displayed as nodes with the node color indicating the type or role of the corresponding protein. Red lines (edges) are interactions discovered by high-throughput interaction mapping in yeast. Green lines represent previously described (but not discovered in the Y2H screen), as stored in the UNIHI database and/or described in literature (MAN – manually curated). Blue lines show interactions of network extension (EXT – stored in UNIHI), *i.e.* between clock core and regulatory components and neighborhood components. Yellow border highlights components with a rhythmic transcript detected in murine liver [27]. Border width represents the significance for rhythmic expression. Visualization was performed using Cytoscape 2.8.1 (www.cytoscape.org). 64 self-self interactions are excluded from graph. Dr. Matthias Futschik performed the circadian transcript expression analysis.

4.4 Characterization of the Circadian Clock Network Neighborhood

Proteins in the direct network neighborhood that interact with circadian clock core components might be relevant for regulating clock output functions, but could also include yet unknown proteins important for modulating the circadian clock machinery; *i.e.* I have hypothesized that they might be clock components themselves. To test the latter possibility, the expression of 88 neighborhood genes was systematically downregulated by RNAi in human U2OS cells (as a part of a already performed global RNAi mediated screen for new clock genes by Maier *et al*., unpublished data). These cells have been shown to possess robust circadian rhythms in cell culture, which were monitored *via* a stably integrated *Bmal1* promoter-luciferase reporter construct [22, 35]. Together, we identified 21 components of the neighborhood that altered circadian period in oscillating human cells by at least 0.5 hrs (Figure 13) (for all identified genes also see Appendix section). For example, downregulating the cell-cycle kinase CHEK1 (that interacts with TIMELESS and CK2) significantly shortened the circadian period by more than 1 h, while downregulating the DNA helicase binding protein CHD4 (that interacts with RORC) lengthened it. In addition, knocking down the androgen receptor (AR), which interestingly has many interaction partners (including CREBBP, GSK3B, HDAC1, NCOR1/2, NONO and UBE2I), also resulted in a shortening of the circadian period by almost one hour. Together, the relatively high number of clock modulating components in the network neighborhood indicates the presence of yet uncharacterized mechanisms in the molecular circadian oscillator.

In addition to being novel clock components, proteins in the network neighborhood might also connect specific cellular processes to circadian control by means of directly interacting with clock components. Such interactions are likely time-of-day dependent, which may be accomplished by rhythmic abundance levels of one or both of the interaction partners. Therefore, I have hypothesized that the whole network but also the neighborhood alone are significantly enriched in components with rhythmic abundance levels. This is indeed the case – at least if we consider (due to the lack of protein abundance data) mRNA expression profiles of network components in mouse liver tissue – the circadian transcriptome with highest available temporal (1 h) resolution [27]. Of the 134 network components, 65 (49%) show a significantly rhythmic mRNA expression profile, a highly significant enrichment when compared to a random selection of genes from this expression data set ($p < 10^{-6}$; Chi-

squared test). This is not surprising since the network as a whole contains many circadian oscillator components, which are known to be rhythmically transcribed. However, if we analyze the neighborhood separately, we still find a significant enrichment ($p < 10^{-4}$; Chi-squared test) in components that are rhythmically transcribed: of the 88 components in the neighborhood, 38 (43%) are rhythmically expressed (Figure 12, yellow circles) suggesting that PPIs in the circadian clock network might indeed be a means to mediate rhythmic control of cellular physiology. The extraction of rhythmic transcripts from liver data and statistics were performed by Dr. Matthias Futschik.

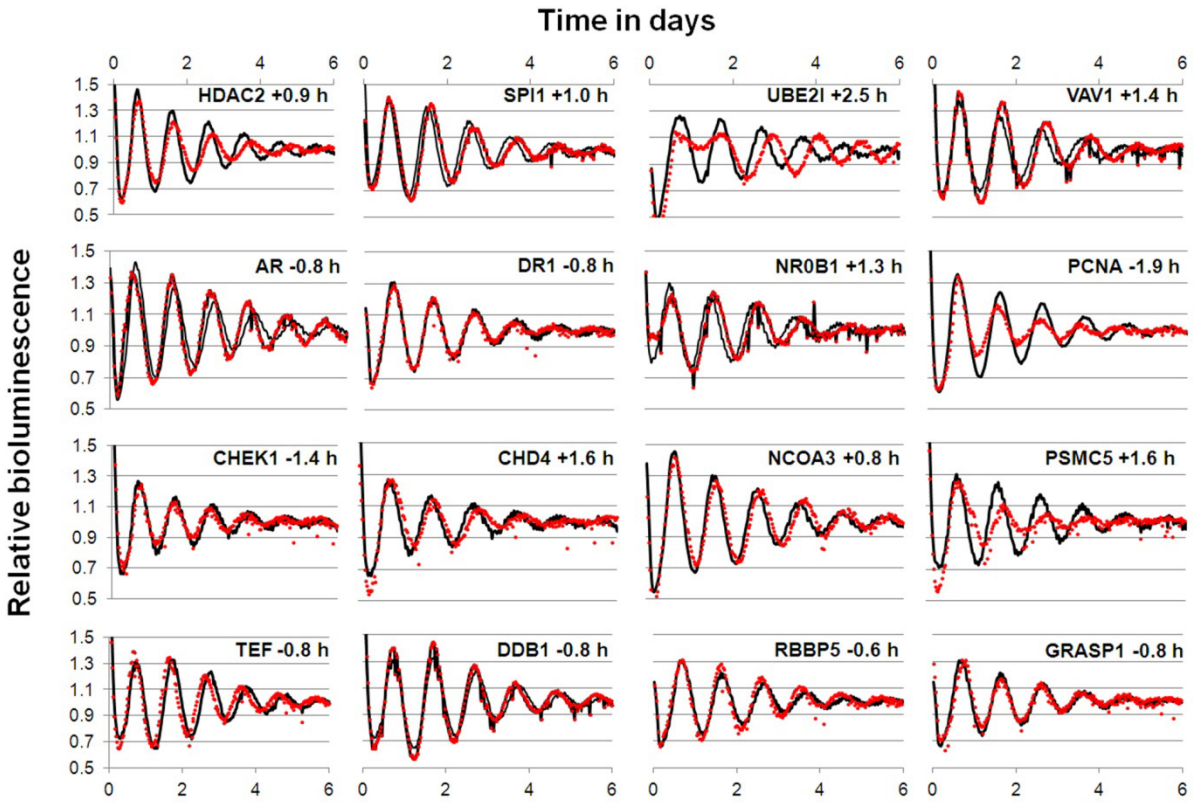

Figure 13. Network Neighborhood Contains Clock Modulating Components.
Systematic RNAi-mediated downregulation of network neighborhood genes in dexamethasone-synchronized U2OS cells harboring a Bmal1-promoter luciferase reporter. Shown are altered oscillation dynamics (red curves) for 16 genes achieved by individual RNAi constructs. For twelve genes, two RNAi constructs resulted in similar phenotypes, for nine genes, only one construct was available in our laboratory library. Black curves are controls representing the mean values of at least 80 irrelevant constructs. Period deviations from controls are shown.
I have conceptionally designed the screen for new clock components in the network neighborhood and prepared the figure. Data presented here are part of a genome-wide RNAi mediated screen for clock genes of Maier *et al*. unpublished data.

4.5 A Dynamic Circadian PPI Network

At what time of day do the PPIs in the circadian network occur or – in other words – can we elucidate dynamic properties of our (still static) network? Again, hypothesizing that a PPI more likely happens at times, when the interaction partners are co-expressed, we again used mouse liver transcriptome data [27] as a validated proxy for protein abundance [59] – an approach successfully used also for the yeast interactome [60]. To first test this hypothesis for PPIs in general (*i.e.* beyond our circadian network), we compared the Pearson correlation coefficient (PCC) of transcript levels (as a measure for co-expression) for all pairs of interacting proteins present in the UNIHI interactome database and for which we have time-resolved expression data [27] with the PCC of randomly chosen pairs. Interestingly, we found that interacting proteins are significantly more likely to be expressed at similar circadian times (PCC > 0.5 with PCC ranging from -1 to 1; $p < 10^{-15}$ Chi-squared test; Figure 14 A left). These data suggest that circadian co-expression may be a common feature in cellular systems to restrict regulatory interactions to specific times of the day. This assumption is supported by the fact that proteins with many interaction partners – which are known to exert regulatory functions – are more likely to be rhythmically expressed ($p < 10^{-10}$; Wilcoxon Rank test) and *vice versa*, *i.e.* proteins with rhythmic transcripts have statistically more interaction partners than constitutively expressed proteins ($p < 10^{-5}$; Chi-squared test). Interestingly, also the circadian PPI network displays these properties: interaction between proteins occurs more likely when both proteins are co-expressed in time (Figure 14 A right).

Based on our results above, we assume that many PPIs happen at specific times of the day. Therefore, we assigned to each PPI in our network a circadian phase, at which the corresponding components are likely to interact based on their transcript expression. To this end, we approximated the abundance of the complex of two proteins as the product of their expression profiles. Derived time series for the interaction complexes were subsequently examined for 24-hrs periodicity with a stringent threshold ($FDR < 10^{-5}$) resulting in a dynamic circadian PPI network with 190 individual protein pairs that likely interact at specific circadian phases (Figure 14 B). Interestingly, PPIs seem to be distributed over the whole circadian cycle. Beyond the dynamic interactions that occur among circadian core components, we identify many time-of-day specific putative regulatory interactions within the neighborhood. For example, the lysine acetyltransferase KAT2B binds to the nuclear receptor

coactivator NCOA1 – two proteins involved in transcriptional regulation – during the late day, which may hint to a time-of-day specific function of these proteins. Nevertheless, we are aware that the restriction to transcript (and not protein) profiles and also a potential competitive nature of the possible interactions pose limitations to this analysis. However, such a framework offers the possibility to globally analyze processes controlled by circadian PPIs in a time-specific manner. The analysis concerning network dynamics was conceptionally designed by me and the analyses were performed by Dr. Matthias Futschik.

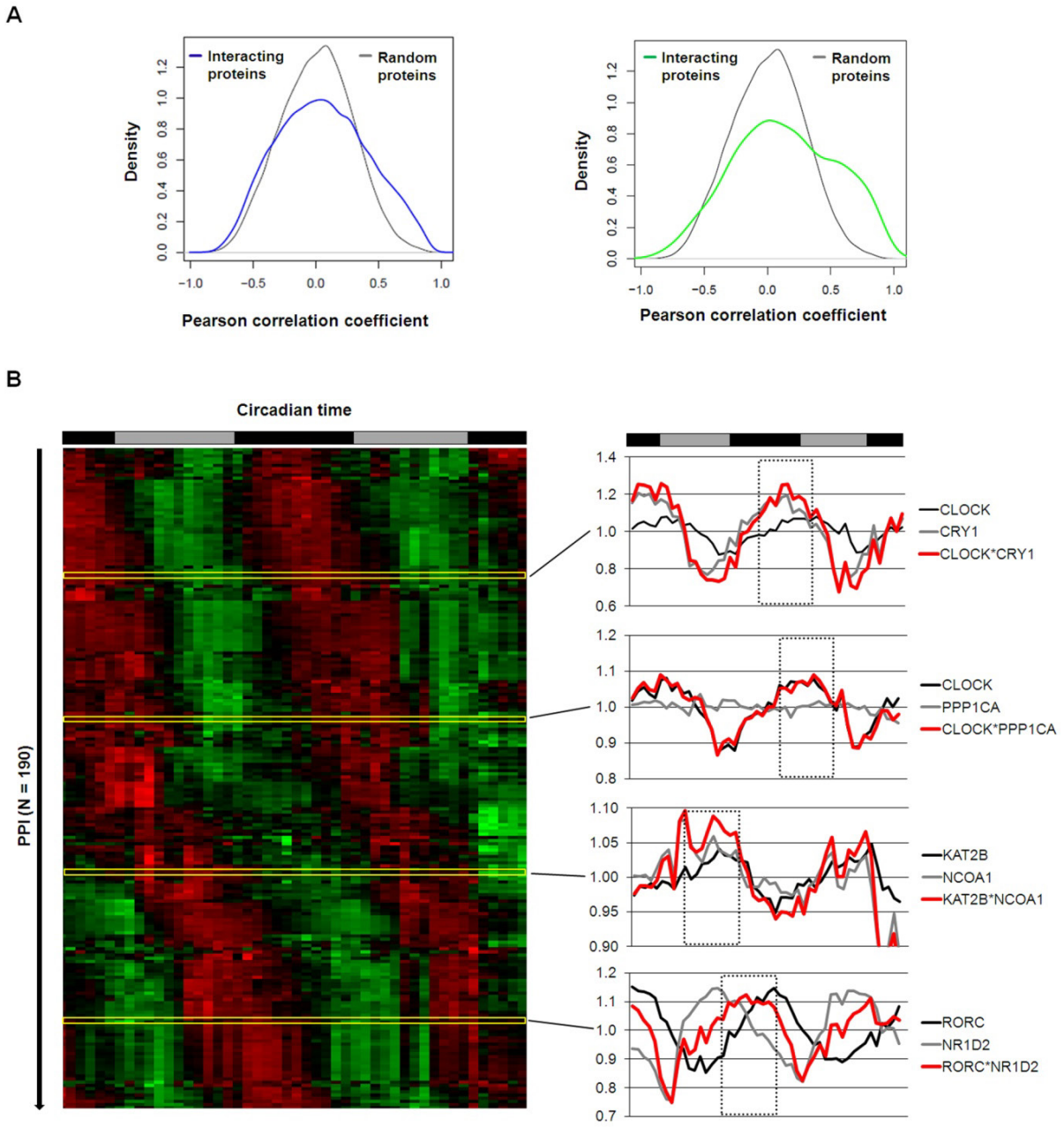

Figure 14. Interaction Dynamics within the Circadian Protein-Protein Network.
(A) Interacting proteins are more likely to be co-expressed in time. Left: Co-expression of all proteins, for which literature-derived PPI information is stored in the UNIHI database, was calculated using the Pearson correlation coefficient (PCC) based on published circadian liver transcriptome data [27] and were compared with randomly selected protein pairs. Among interacting proteins co-expressed proteins (*i.e.* a PCC > 0.5) are significantly overrepresented (Chi squared test: $p < 10^{-15}$). 13% of interacting proteins have a PCC > 0.5 compared to 4% for random pairs. Right: Analogous analysis performed for the circadian PPI network. Interacting proteins that are co-expressed (PCC > 0.5) are highly overrepresented (Chi squared test: $p < 10^{-15}$; 22% compared to 4% with PCC > 0.5).
(B) Left: Heat map representing the dynamics of PPI (lines: 190 interactions) based on their liver RNA expression level. Interactions were classified as rhythmic if the product of their expression vectors shows highly significant periodic expression (FDR < 10^{-5}). Black and grey bars represent subjective night and day, respectively. Right: Representative examples for four interaction pairs and their corresponding predicted interaction phase. Red lines represent products of individual transcript profiles of two interacting proteins (black and grey lines). Dotted rectangles highlight likely phase of interaction. I have conceptionally designed the analyses and prepared the figure. Dr. Matthias Futschik preformed the presented analyses.

4.6 Role of Dynamic Interactions for the Circadian Oscillator

Network components interacting with many partners – so-called `hubs´- not only have important organizing properties in scale-free networks; they are also (controversially) discussed to be more essential for life (at least in yeast, *Drosophila* and *C. elegans*; [44]).

To test, whether in our network dynamic interactions and/or `hub´ proteins are essential for the trait `circadian rhythmicity´ – *i.e.* for generating and maintaining circadian rhythms – I have correlated circadian phenotypes obtained upon genetic perturbation experiments with topological characteristics of the network components. For perturbing the network experimentally and assigning an essentiality score (for circadian rhythmicity) to each component, I have (i) systematically knocked down and (ii) overexpressed every component of the core and the regulatory part of the network (see Methods for score criteria). These experiments were performed in human U2OS reporter cells (as described above) and the effect on circadian dynamics was analyzed. While I could reproduce most of the phenotypes that have been known from studies with classical knockout models (*e.g.* the opposite period phenotypes upon *Cry1* and *Cry2* deletion as well as arrhythmicity upon *Bmal1* and *Clock* knockout), I have detected interesting novel phenotypes such period shortening for *Per3* knockdown and period lengthening for *Rev-ErbB* (*Nr1d2*) downregulation (Figure 15 A and B; Figure 16 A and B).

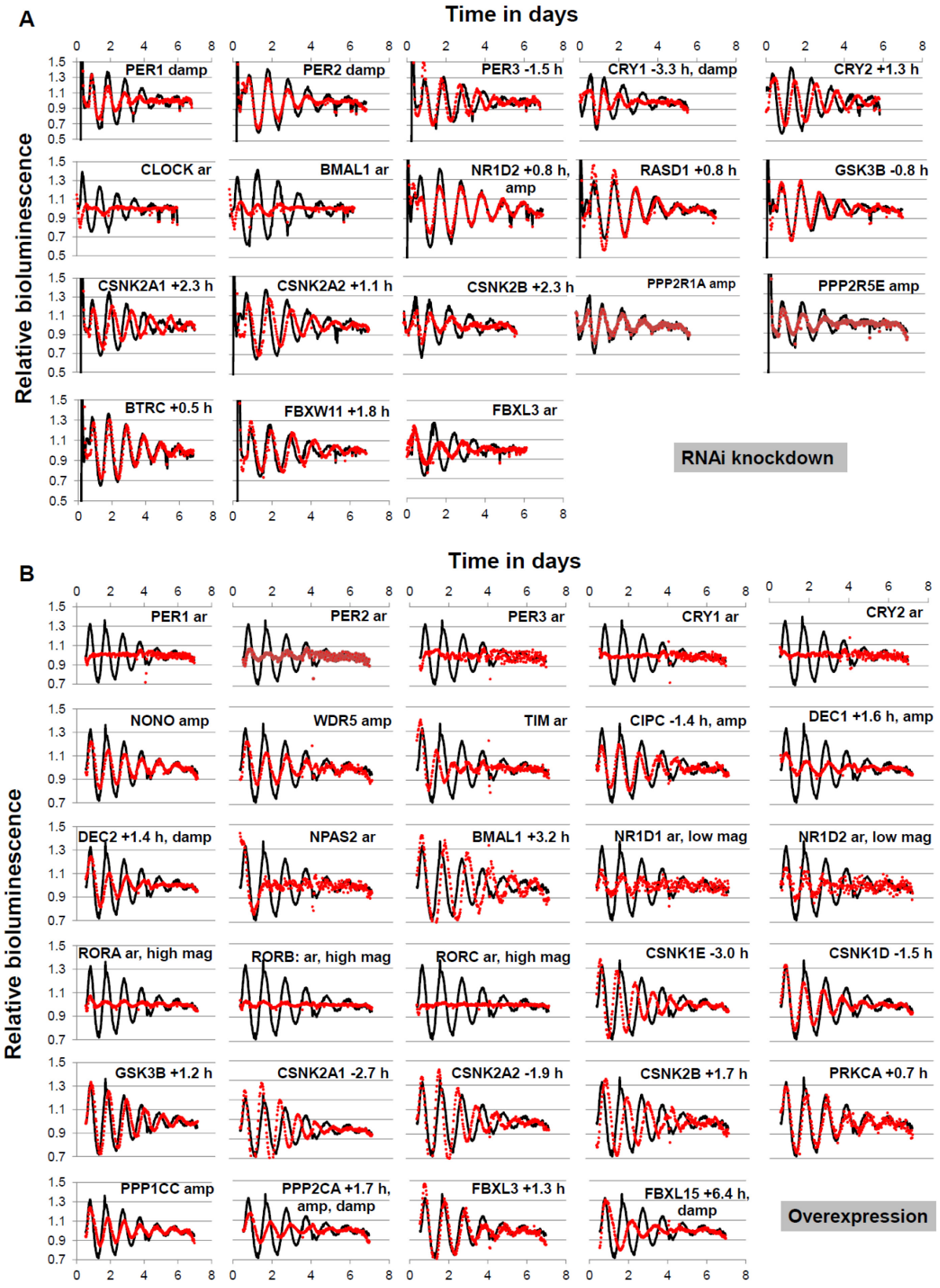
A
Time in days
Relative bioluminescence
PER1 damp
PER2 damp
PER3 -1.5 h
CRY1 -3.3 h, damp
CRY2 +1.3 h
CLOCK ar
BMAL1 ar
NR1D2 +0.8 h, amp
RASD1 +0.8 h
GSK3B -0.8 h
CSNK2A1 +2.3 h
CSNK2A2 +1.1 h
CSNK2B +2.3 h
PPP2R1A amp
PPP2R5E amp
BTRC +0.5 h
FBXW11 +1.8 h
FBXL3 ar
RNAi knockdown
B
Time in days
Relative bioluminescence
PER1 ar
PER2 ar
PER3 ar
CRY1 ar
CRY2 ar
NONO amp
WDR5 amp
TIM ar
CIPC -1.4 h, amp
DEC1 +1.6 h, amp
DEC2 +1.4 h, damp
NPAS2 ar
BMAL1 +3.2 h
NR1D1 ar, low mag
NR1D2 ar, low mag
RORA ar, high mag
RORB: ar, high mag
RORC ar, high mag
CSNK1E -3.0 h
CSNK1D -1.5 h
GSK3B +1.2 h
CSNK2A1 -2.7 h
CSNK2A2 -1.9 h
CSNK2B +1.7 h
PRKCA +0.7 h
PPP1CC amp
PPP2CA +1.7 h, amp, damp
FBXL3 +1.3 h
FBXL15 +6.4 h, damp
Overexpression

Figure 15. Visualization of Altered Circadian Phenotypes for Clock Core and Regulatory Components Upon Genetic Perturbation.
(A) Systematic gene silencing. RNAi constructs were lentivirally delivered into U2OS cells carrying the *Bmal1*-promoter luciferase reporter and oscillation dynamics were monitored for several days. Data were detrended using the Chronostar analysis software. Black lines show non-silencing controls. Red dotted lines depict phenotypes for one RNAi construct. Period differences from mean are given (ar: arrhythmic, amp: low amplitude, damp: high damping, mag: magnitude).
(B) Systematic overexpression. GFP overexpression was used as controls (black curves). Phenotypes were visualized as described in (A).

As examples for phenotypes detected upon clock protein overexpression, *Dec1* or *Dec2* as well as *Fbxl15* (the homolog to *Drosophila Jetlag*) led to a substantial period lengthening (~1.5 hrs and ~6 hrs, respectively) (Figure 15 B, Figure 16 B). For each network component, the downregulation and overexpression phenotypes were combined in a `phenotypic score´ (for rules, see Methods and also Appendix) to be able to correlate it with network properties of the individual components. There was no correlation of the phenotypic score with the number of interactions as it has been observed in more global networks of yeast, *Drosophila* and *C. elegans* [44]. In other words, `hub´ proteins apparently are not more important for circadian rhythmicity than components with a lower connectivity. However, proteins that are involved in dynamic interactions turned out to be more essential for circadian rhythm generation (*t*-test: $p < 0.01$; Mann-Whitney U test: $p < 0.01$; Figure 16 C).

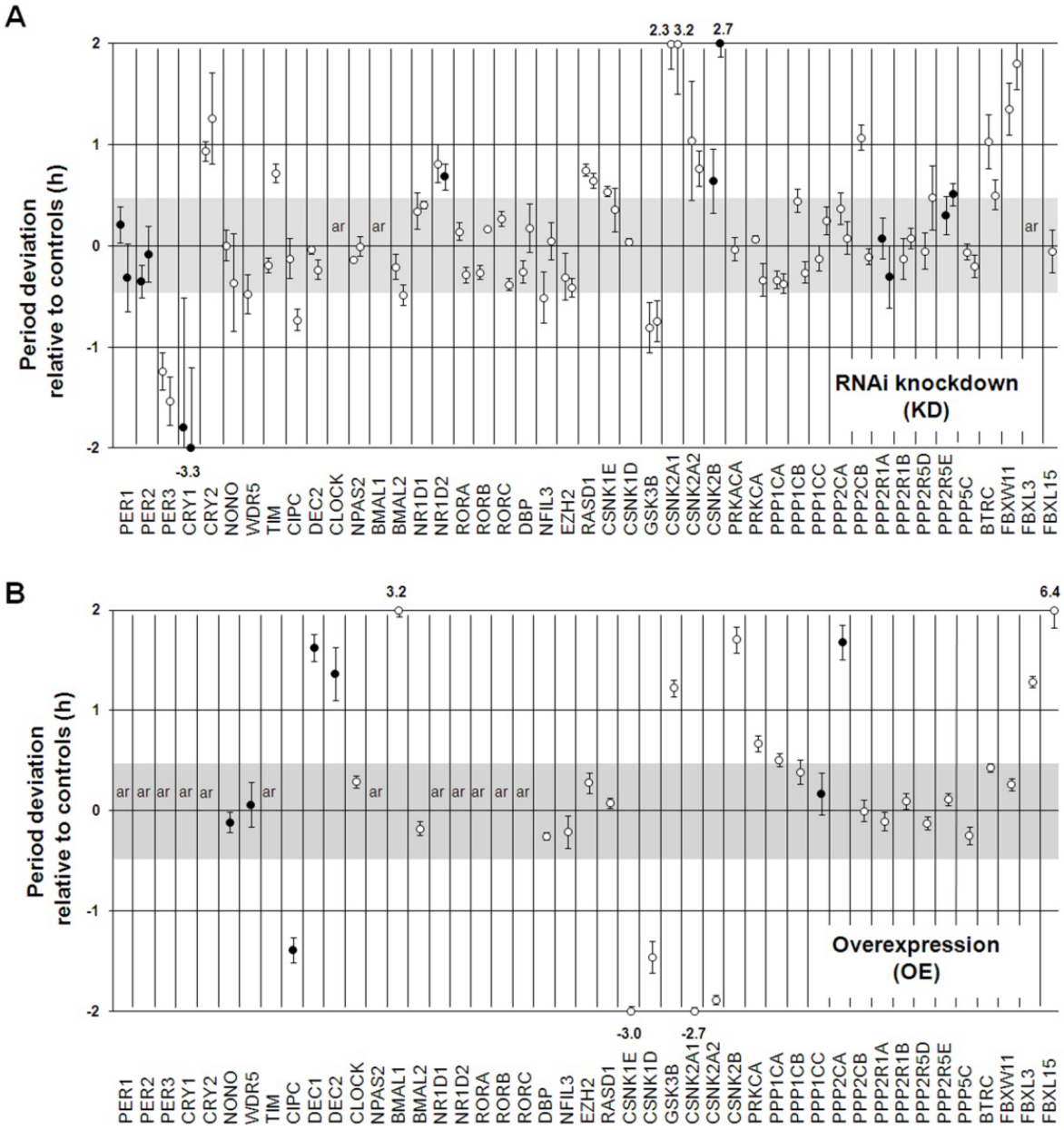

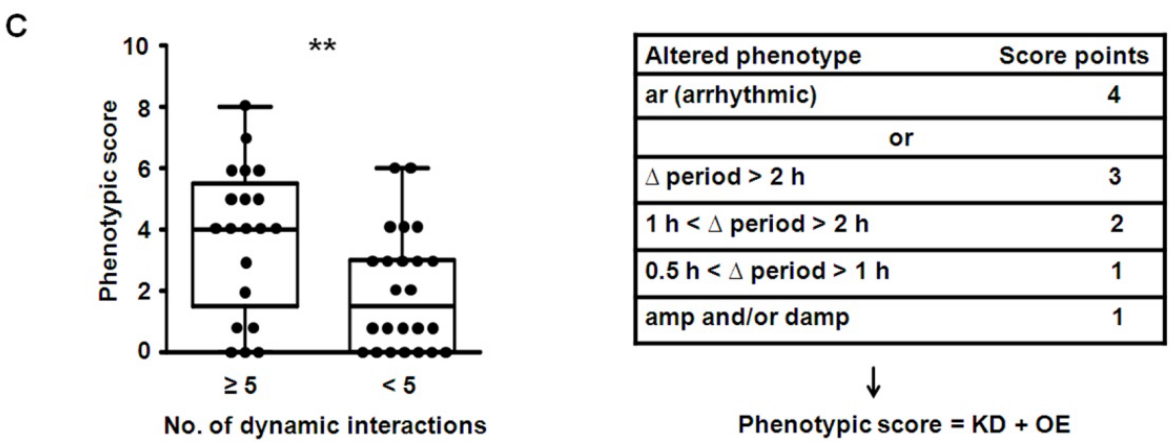

Altered phenotype	Score points
ar (arrhythmic)	4
or	
Δ period > 2 h	3
1 h < Δ period > 2 h	2
0.5 h < Δ period > 1 h	1
amp and/or damp	1

↓

Phenotypic score = KD + OE

Figure 16. Dynamic Interactions are Important for Circadian Rhythmicity.
(A) Systematic RNAi-mediated silencing of circadian clock core and regulatory components. RNAi constructs were lentivirally delivered into U2OS cells harboring a *Bmal1*-promoter luciferase reporter and oscillation dynamics were monitored for several days. Circles represent the difference in period (± s.e.m.; n = 3 independent experiments) relative to non-silencing controls (n > 10) for two RNAi constructs (if available). Filled circles show additional amplitude and/or damping phenotypes. Cells were classified as arrhythmic (ar) if the fit to a cosine function resulted in a low correlation coefficient (see Methods). Period deviations of more than 2 hrs are given.
(B) Systematic overexpression of circadian clock core and regulatory components. Experiments were performed with lentivirally delivered overexpression constructs as described in (A). Results of three independent experiments (± s.e.m.) are given.
(C) Correlation of circadian phenotype with number of dynamic interactions. The combined phenotypic score from silencing and overexpression experiments is significantly different for components with many dynamic interactions (≥ 5) compared to those with few (< 5) (*t*-test: ** $p < 0.01$; Mann Whitney test: ** $p < 0.01$).

For example, CLOCK, BMAL1, PER3 and CRY1 – which undergo 24, 21, 18 and 9 dynamic interactions, respectively – are especially important for circadian dynamics (Figure 16 A-C). This suggests that the more rhythmic interactions a protein is involved in the more important it is for normal circadian rhythmicity.

4.7 Regulation of Cellular Processes *via* Dynamic PPIs

Are dynamic PPIs also important for the regulation of cellular events? To identify such processes, we first assigned to each network component one or more specific GO categories. Secondly, using the information whether a PPI is dynamic or not (see Figure 14 B) we investigated, which cellular processes are significantly connected *via* dynamic PPIs. In other words, we tested whether dynamic interactions were over-represented in the total set of interactions between a pair of GO categories. This resulted in a network with twelve dynamic links between eleven biological processes with `Circadian rhythm´ as the central `hub´ rhythmically connected with processes such as `DNA repair´, `Transcriptional regulation´ and `Response to external stimulus´ (Figure 17 A) (see also Appendix section).

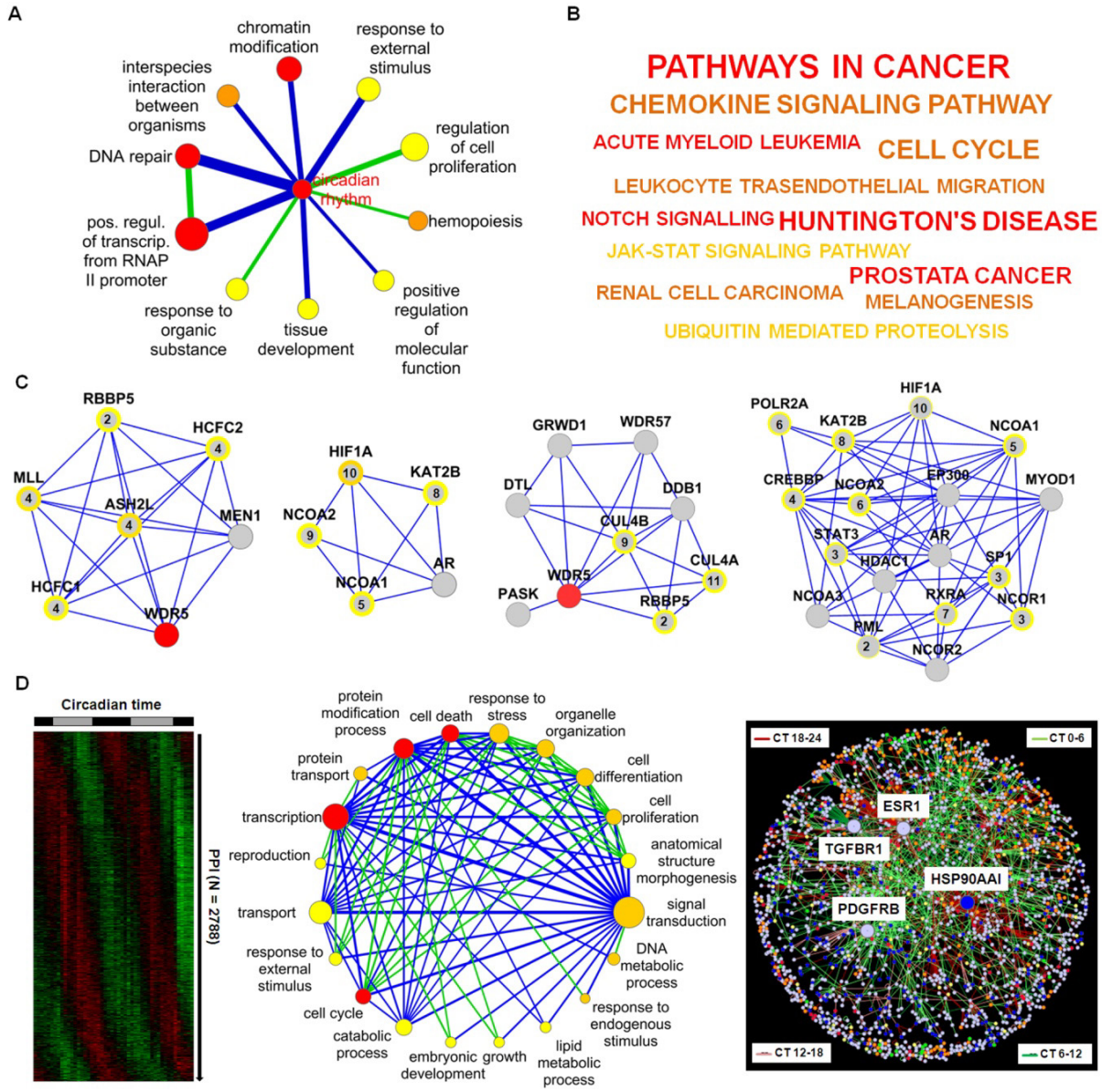

Figure 17. Dynamic Regulation of Circadian Output.
(A) Coupling of biological processes (as represented by the corresponding GO terms) *via* dynamic PPIs within the circadian PPI network. Node size represents the number of associated genes in the corresponding GO category. Nodes color shows significance of overrepresented GO category from yellow (low significance, FDR < 0.25) over orange (FDR < 0.01) to red (high significance, $p < 0.0001$). Edge width corresponds to the number of interactions between biological processes. Edge color represents enrichment in dynamic interactions between processes (blue: $p < 0.001$; green: $p < 0.1$). I prepared the figure. Analysis in (A) was conceptionally designed by me and performed by Dr. Matthias Futschik.
(B) KEGG pathway analysis of proteins within network neighborhood. Colors show significance of enrichment from yellow (low significance, $p < 0.02$) over orange ($p < 0.0005$) to red (high significance, $p < 0.0002$). Font size represents the number of components in each category.

(C) Identification of highly connected clusters within the circadian PPI network (for details see Methods). Depicted are four representative functional modules that show significant enrichment in the following GO categrory from left to right: `Histone methyltransferase complex´, `Transcription coactivator activity´, `Response to DNA damage stimulus´ as well as `Histone acetyltranferase activity´. Grey nodes: network neighborhood components; red nodes: core clock component. Yellow borders indicated a circadian transcript profile in murine liver with peak expression time (circadian time) given as numbers in the nodes. Border width represents the significance for rhythmic expression.
(D) Left: Identification of dynamic PPIs within the proteome. Identified interactions are visualized as a heat map. Middle: Coupling of biological processes *via* dynamic interactions within the proteome. 20 processes are linked with 89 connections. Node color: significance of enrichment in components with dynamic interactions (yellow: $p < 0.25$; orange: $p < 0.0001$; red: $p < 10^{-8}$); node size: number of genes per category; edge color: enrichment in dynamic interactions between processes (blue: $p < 10^{-16}$; green: $p < 10^{-5}$); edge width: number of dynamic interactions. Right: A dynamic global PPI network consisting of 1,979 proteins with 2,788 dynamic interactions. Interactions/edges were colored based on their peak times: dark red (CT 18-24), light green (CT 0-6), dark green (CT 6-12) and light red (CT 12-18). Proteins/nodes were colored with the respect to the five most significant biological processes and are associated with: `Cell cycle´ (green), `Cell death´ (red), `Protein modification´ (yellow), `Signal transduction´ (blue) and `Transcription´ (orange). The four proteins with most dynamic interactions (> 40) are highlighted. Analysis in (D) was conceptionally designed by me and performed by Dr. Matthias Futschik and Dr. Ravi Kalathur.

A strong association of the circadian clock network with these processes relevant for *e.g.* cancer and cell-cycle is supported by (i) KEGG pathway analysis of the network neighborhood only (Figure 17 B) and (ii) the significant ($p < 10^{-8}$; Chi-squared test) enrichment of the network neighborhood with cancer-associated genes (as reported in the Cancer Gene Census; for identity of cancer associated genes see Methods section).

Are these rhythmically regulated processes mediated by individual components or rather by functional modules within the network consisting of interconnected components? To answer this question, I have explored the circadian PPI network topology for clusters of highly connected proteins (structural modules) and identified eleven different modules within the circadian network (Figure 17 C, Figure 18 A).

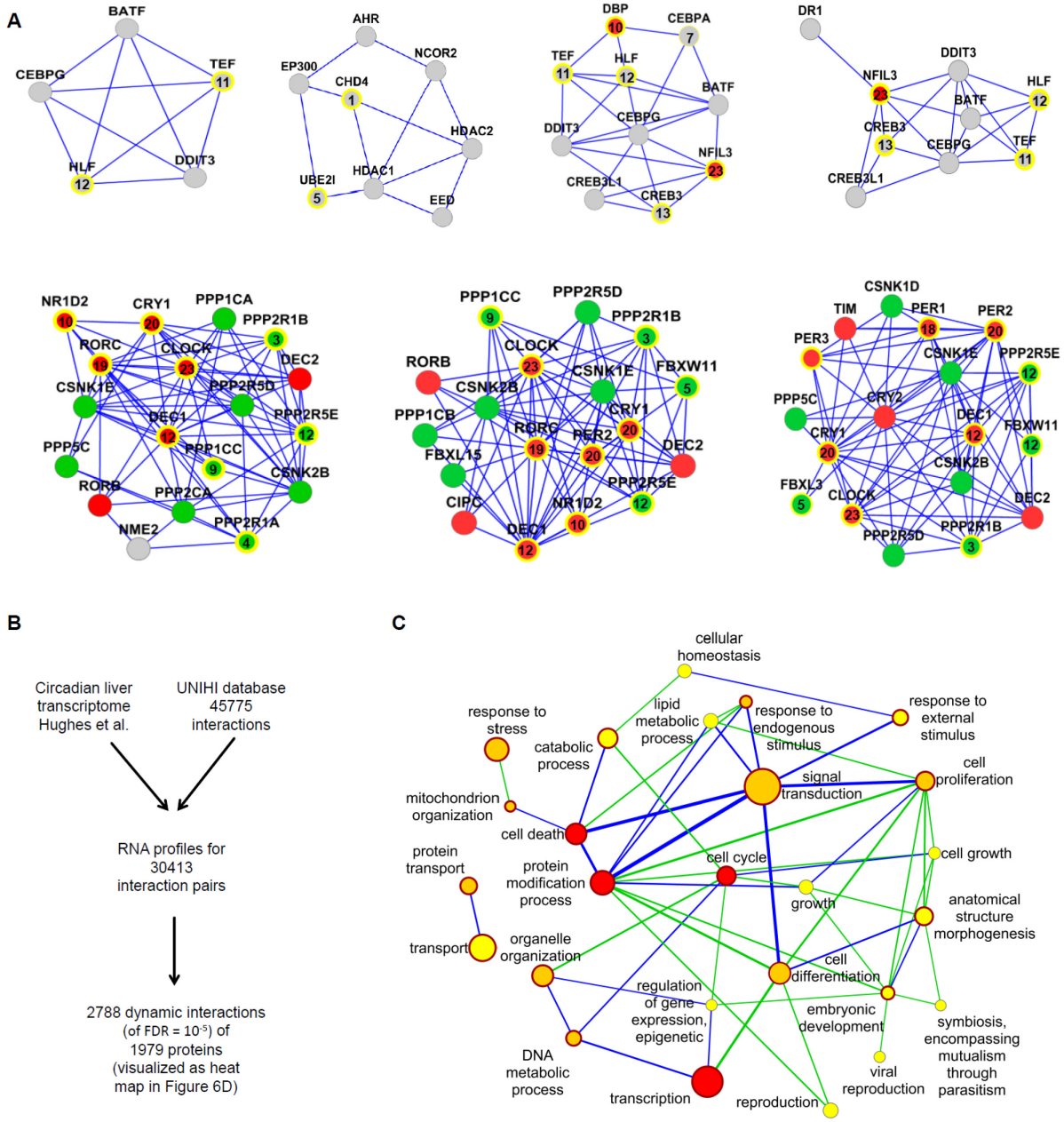

Figure 18. Identification of Functional Modules within the Circadian PPI Network and Dynamic Regulation within the Global Interactome.

(A) Highly connected clusters were identified using the Cytoscape plugins MCODE or the ClusterOne algorithm (for details on analysis see Methods). Node colors: grey – network neighborhood, red – clock core, green – regulatory components. Yellow circles highlight rhythmic RNA profiles. Numbers are mRNA peak times in circadian time (CT). Modules were analyzed for enrichment of processes using GO, KEGG and Pfam family annotations.

(B) Construction of a global dynamic protein-protein interactome.

(C) Coupling of biological processes within the interactome via rhythmic PPIs. Significance of connections was calculated based on the comparison with randomized versions of the dynamic interactome. Connections, for which no more than ten out of 1,000 random networks show a larger number of rhythmic interactions are displayed. In total, 26 processes are linked *via* 52 connections. Node color: significance of enrichment in components with dynamic interactions (yellow: $p < 0.25$; orange: $p < 10^{-4}$; red: $p < 10^{-8}$); node size: number of genes per category; edge color: number of random networks with larger number of rhythmic interactions between processes (blue: $n = 0$; green: $n \leq 10$); edge width: number of rhythmic interactions. Processes, for which $n \leq 10$ random networks have more internal dynamic interactions than observed in the global interaction network, were highlighted with a dark red border. I have prepared the figure. Analysis in (C) was performed by Dr. Matthias Futschik.

Modules were enriched with components *e.g.* relevant for the regulation of chromatin states (GO terms: `Histone methyltransferase complex´ and `Histone acetyltransferase activity´), DNA repair (GO term: `Nucleotide excision repair´) and transcriptional regulation (GO term: `Transcription coactivator activity´). Notably, the GO and KEGG terms derived from the analysis of the whole circadian network matched with the terms achieved for the structural modules. In addition, transcript levels of five of seven components of the `Histone methyltransferase´ module (consisting of ASH2L, HCFC1/2, MEN1, MLL, RBBP5 and WDR5; Figure 17 C left) are rhythmic and peak at similar circadian times. Co-expression in time was also observed within other highly connected clusters such as the `Histone acetyltransferase´ module (Figure 17 C right). Together, this suggests that modular organization within the circadian PPI network is contributing to a coherent functional regulation of cellular processes by the circadian clock.

Is a time-of-day dependent interaction of cellular processes *via* PPIs a general feature? To test this, we first identified 2,788 rhythmic PPIs (as described above – Figure 14 B) for the whole human proteome (Figure 17 D left) and then searched for biological processes that are significantly connected *via* dynamic PPIs (Figure 18 B). We constructed a network of 20 biological processes with 89 dynamic links. The central `hub´ of this `process network´ constitutes the term `Signal transduction´ (Figure 17 D middle) suggesting a time-of-day dependent modulation of a huge variety of cellular events such as `Protein transport´, `Response to stress´ and `Cell death´ by signaling pathways *via* rhythmic PPIs. This is also the case if we use randomized versions of our interactome as a background model (Figure 18 D). Interestingly, in this case we also observe an overrepresentation of dynamic PPIs within the individual processes (Figure 18 D).

To characterize the underlying PPI network properties, we constructed a dynamic PPI network for the whole proteome. We found that it again has `scale-free´ properties and

identified 269 dynamic `hubs´, *i.e.* proteins with at least five dynamic interactions. The protein with the most rhythmic interactions (79 of 105 in total) is heat-shock protein HSP90AA1 – a factor required for proper protein folding upon heat stress. Notably, three of the four interaction-richest proteins (with more than 40 interactions) are cell-surface receptors (ESR1, PDGFRB and TGFBR1) again highlighting the central role of signaling pathways for dynamic regulation (Figure 17 D right). The construction of the process networks and dynamic interactome was conceptionally designed by me and the analysis was performed by Dr. Matthias Futschik and Dr. Ravi Kalathur.

4.8 Protein Phosphatase 1 Modulates CLOCK/BMAL1-Dependent Transactivation

The Systems Biology analysis of the circadian interactome points to a timely regulated action of chromatin modifying enzymes (see Figure 17 A-C). It is known that at the heart of the circadian oscillator binding of the transcription factor heterodimer CLOCK/BMAL1 is controlled by methylation and acetylation states of histones at specific promoter regions [29, 61-64]. In addition, CLOCK/BMAL1 transactivation activity is modulated by a precisely timed acting repressor complex. In the Y2H screen, 15 new interaction partners for CLOCK/BMAL1 were discoverd, which might play a role in modulating their function in cells. Therefore, I have systematically tested whether these interactors (and their paralogs – in total 28 components) are able to modulate CLOCK/BMAL1 transactivation measured from an *E-box* containing artificial promoter with firefly luciferase as reporter.

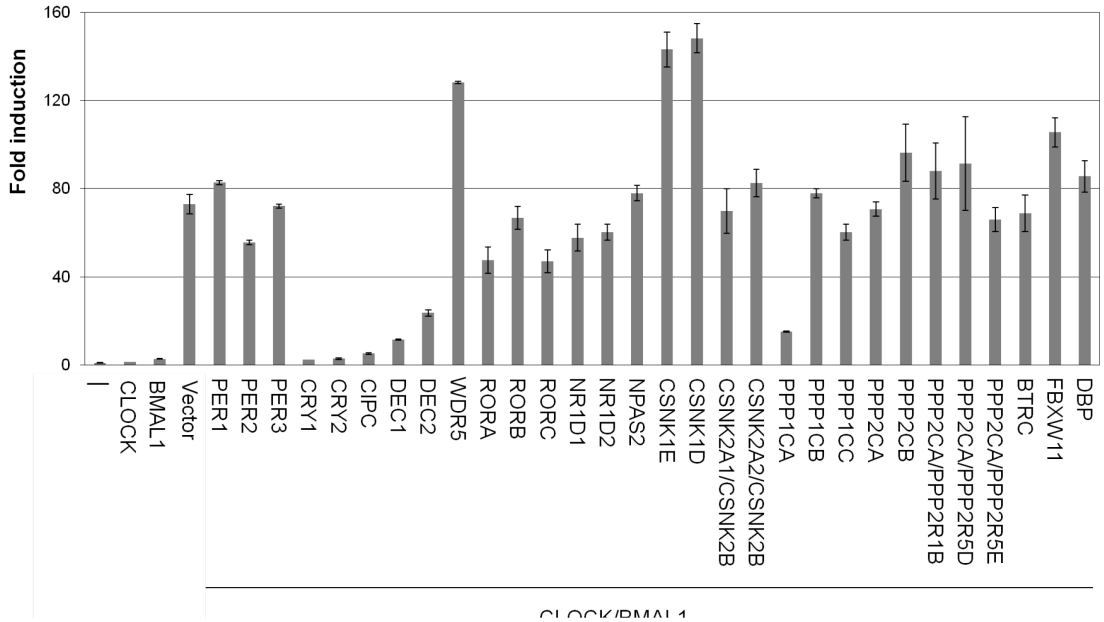

Figure 19. Systematic Screen for New Modulators of CLOCK/BMAL1 Transactivation.
All CLOCK and BMAL1 interactors identified in the Y2H experiments and their paralogs were co-transfected with CLOCK/BMAL1 together with an artificial 6 *E-box*-luciferase containing reporter. Normalization was performed to *Renilla*-luciferase signal. Shown is one representative result (n = 3; ± s.d.) of three independent experiments. Among new CLOCK/BMAL1 interactors RORs and PPP1CA showed consistent suppression of CLOCK/BMAL1 transactivation.

As expected, already characterized CLOCK/BMAL1 repressors such as CRYs, PER2 and DECs (Figure 19) [19, 55, 65] substantially inhibited transactivation. Interestingly, among the 15 new interactors (including their paralogs) PPP1CA (protein phosphatase 1 alpha, catalytic subunit), but not PPP1CB severely and RORs moderately reduced the reporter signal (Figure 20 A). The effect of PPP1CA on CLOCK/BMAL1-mediated transactivation was dose dependent (Figure 20 B).

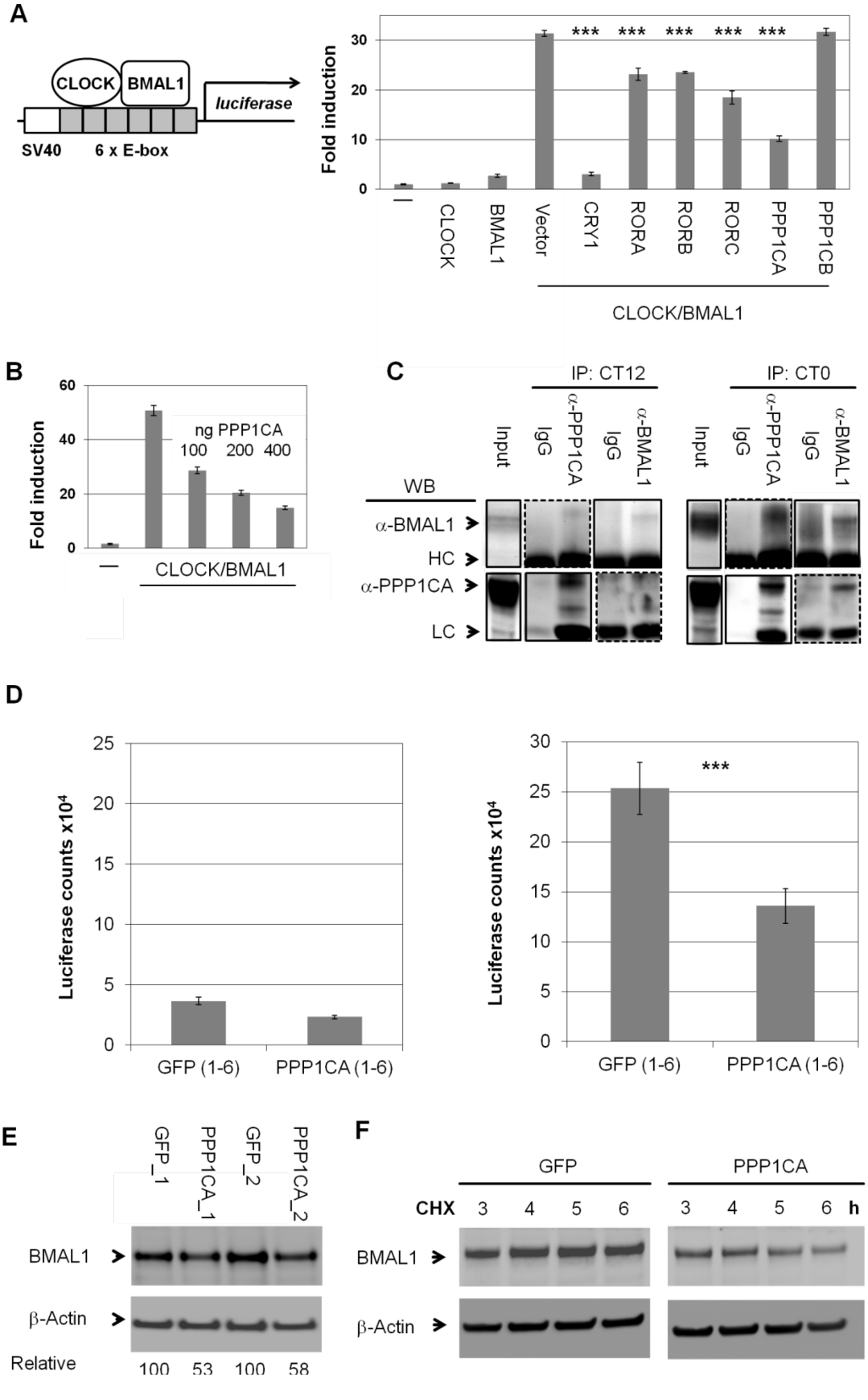
A
CLOCK
BMAL1
luciferase
SV40
6 x E-box
Fold induction
***
—
CLOCK
BMAL1
Vector
CRY1
RORA
RORB
RORC
PPP1CA
PPP1CB
CLOCK/BMAL1
B
Fold induction
ng PPP1CA
100 200 400
—
CLOCK/BMAL1
C
IP: CT12
IP: CT0
Input
IgG
α-PPP1CA
IgG
α-BMAL1
WB
α-BMAL1
HC
α-PPP1CA
LC
D
Luciferase counts x10⁴
GFP (1-6)
PPP1CA (1-6)
***
E
GFP_1
PPP1CA_1
GFP_2
PPP1CA_2
BMAL1
β-Actin
Relative
100 53 100 58
F
GFP
PPP1CA
CHX
3 4 5 6 h
BMAL1
β-Actin

Figure 20. Protein Phosphatase 1 Modulates CLOCK/BMAL1 Function.
(A) New modulators of CLOCK/BMAL1 function. All CLOCK and BMAL1 interactors identified in the Y2H screen and their paralogs were co-transfected with CLOCK/BMAL1 and an E-box containing luciferase reporter construct. Visualized is an experiment with those components interacting with CLOCK/BMAL1 that displayed a similar effect in three previously performed co-transactivation assays. Shown are means ± s.d. (n = 3; *** $p < 0.001$, *t*-test).
(B) PPP1CA dose-dependently reduces CLOCK/BMAL1 mediated co-transactivation of the luciferase reporter. Assay was performed as in (A) (n = 3; means ± s.d.).
(C) PPP1CA is present in the CLOCK/BMAL1 complex in mouse liver. Livers were harvested at indicated circadian time points (CT) and co-immunprecipitations and Western blots were performed with indicated antibodies. LC (antibody light chain) and HC (antibody heavy chain) of used antibodies. Dashed lines indicate higher exposure times. Shown is one representative of two independently performed experiments.
(D) PPP1CA destabilizes BMAL1. Left: HEK293 cells stably expressing CLOCK luciferase fusions were transduced with virus containing GFP or PPP1CA. After 24 hrs, luciferase activity was measured (n = 6; means ± s.d.; *** $p < 0.001$, *t*-test). Right: HEK293 cells stably expressing BMAL1 luciferase fusions were transduced with virus containing GFP or PPP1CA. After 24 hrs, luciferase activity was measured (n = 6; means ± s.d.).
(E) Endogenous BMAL1 levels are reduced upon stable PPP1CA overexpression in U2OS cells. β-Actin signals were used for quantification. Depicted are two independent experiments.
(F) PPP1CA leads to reduced BMAL1 stability. U2OS cells stably overexpressing PPP1CA or GFP were harvested at the indicated time points after CHX application and protein levels were analyzed by Western blot analysis. Shown is one representative of two independently performed experiments.

Endogenous PPP1CA binds to the CLOCK/BMAL1 complex in mouse liver, which was tested by co-IP experiments (Figure 20 C). As predicted by the dynamic interaction analysis based on transcript data (see Figure 14 B) I have detected an association of endogenous PPP1CA with CLOCK/BMAL1 at CT0 while only little PPP1CA-CLOCK/BMAL1 complex was present at CT12 suggesting a circadian time-dependent modulation on CLOCK/BMAL1 function. As CLOCK and BMAL1 phosphorylation have been described to affect their stability [66, 67], I have tested whether PPP1CA acts on this level. HEK293 cells stably expressing CLOCK or BMAL1-luciferase fusions were transduced with PPP1CA or GFP as a control and luciferase activity was measured as readout for protein abundance. Whereas no drastic difference of CLOCK-luciferase signal in the presence of PPP1CA was observed (Figure 20 D, left), a significant signal reduction was detected for the BMLA1-luciferase (Figure 20 D, right). In addition, endogenous BMAL1 levels were reduced by about 50% upon stably overexpression of PPP1CA in U2OS cells (Figure 20 E). Lower BMAL1 abundance in the presence of PPP1CA is likely due to reduced BMAL1 stability since CHX treated cells (in which *de novo* protein synthesis is blocked) revealed a much faster degradation of endogenous BMAL1 when PPP1CA is overexpressed (Figure 20 F). Circadian dynamics monitored with the *Bmal1*-luciferase reporter are unaffected in human U2OS cells (Figure 21 A) overexpressing PPP1CA (see Figure 21 B for overexpression efficiency). This is in line with the finding that the expression of a selection of clock output genes (*Per1*, *Dbp*

and *Nr1d1*) in U2OS is unaltered when PPP1CA is overexpressed 24 hrs after dexametasone treatment – where clock output gene levels are expected to be high (Figure 21 C left) – or 36 hrs after dexamethasone synchronization – where low levels in clock output gene expression are expected (Figure 21 C right) [68]. Differences in clock output gene expression between the two selected time points serve as proof-of-concept for the differences of mRNA levels of the indicated genes at the chosen time points (Figure 21 D).

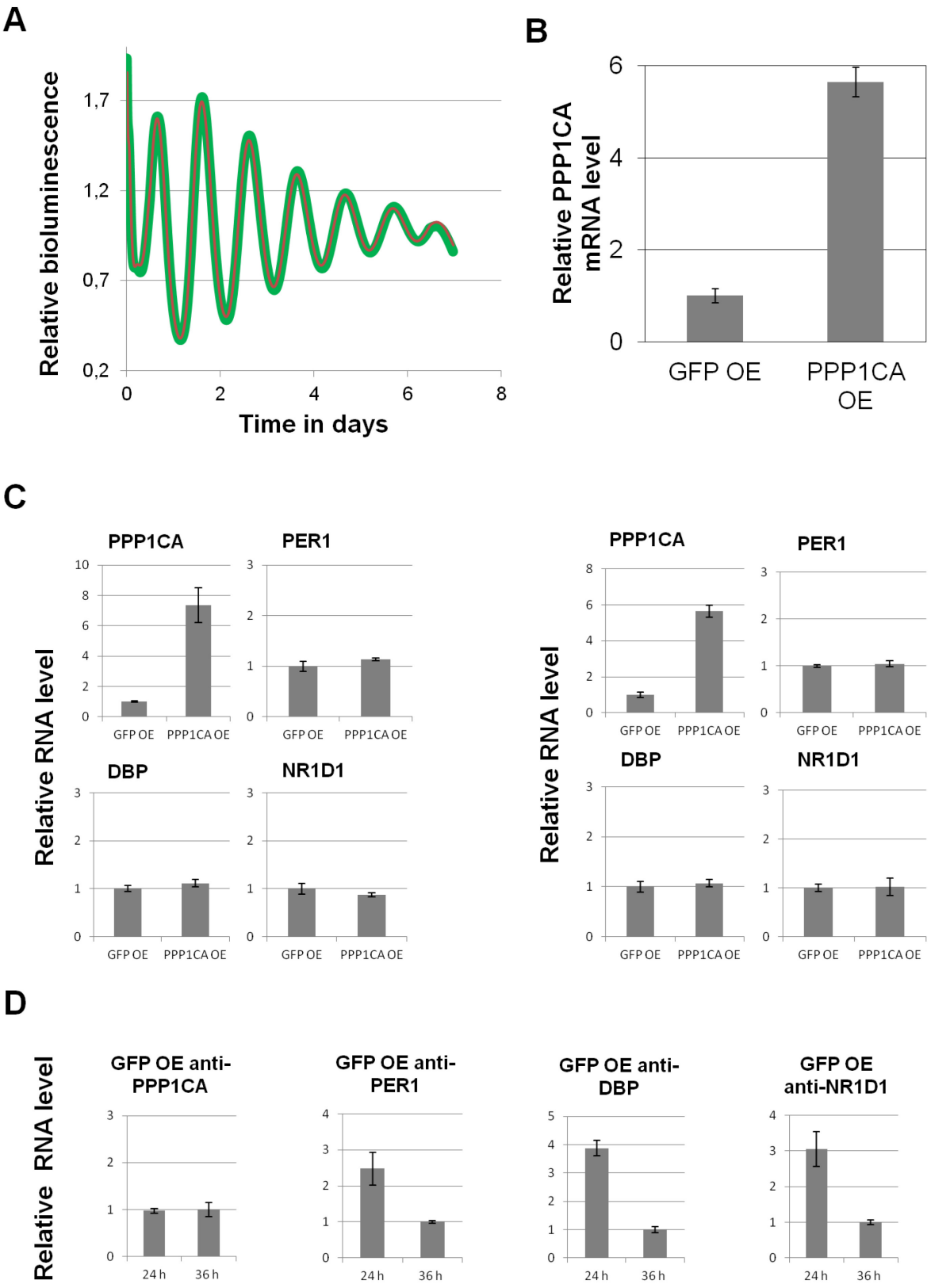
A
Relative bioluminescence
1,7
1,2
0,7
0,2
0
2
4
6
8
Time in days
B
Relative PPP1CA mRNA level
6
4
2
0
GFP OE
PPP1CA OE
C
Relative RNA level
PPP1CA
PER1
DBP
NR1D1
GFP OE
PPP1CA OE
D
Relative RNA level
GFP OE anti-PPP1CA
GFP OE anti-PER1
GFP OE anti-DBP
GFP OE anti-NR1D1
24 h
36 h

Figure 21. Protein Phospatase 1 Overexpression Does Not Affect Circadian Dynamics and Clock Output Gene Expression.
(A) U20S cells carrying the *Bmal1*-promoter luciferase reporter stably expressing GFP (green) or PPP1CA (red) in 35 mm dishes. Bioluminescence recordings were performed for several days.
(B) PPP1CA mRNA overexpression (OE) efficiency for cells used in (A) detected *via* q-PCR. Normalization was performed to GFP overexpressing cells.
(C) Left: Clock output gene RNA levels in U2OS cells overexpressing PPP1CA 24 hrs after dexametasone synchronization. Right: Clock output gene RNA levels in U2OS cells overexpressing PPP1CA 36 hrs after dexamethasone synchronization. Normalization was performed to the corresponding GFP controls.
(D) Clock output gene level at the indicated time point in GFP overexpressing cells (24 or 36 hrs after dexamethasone treatment). Normalization was performed to GFP signals at the 36 hrs-time points.
(B-D) Shown are means ± s.d (n = 3).

It is described that in the case of protein phosphatses (as PP1) substrate specifity is mediated by regulatory phosphatase subunits that form complexes with their corresponding catalytic subunits [69]. Gene silencing data of Zhang *et al*. [35] show an altered circadian phenotype (severe period lengthening effect) in U2OS cells when the PPP1R15B (protein phosphatase 1, regulatory subunit 15B) subunit is knocked-down (Figure 22 A) indicating an involvement of this subunit in the maintenance of circadian periodicity. Endogenous PPP1R15B is not rhythmically expressed in mouse liver neither at the transcript level (see [27]) nor at the protein level (Figure 22 B) but present at the CLOCK/BMAL1 complex at CT0.

Together, these data indicate that BMAL1 stability and probably thereby transactivation is regulated by the PPP1R15B/PPP1CA complex in a time-of-day dependent manner.

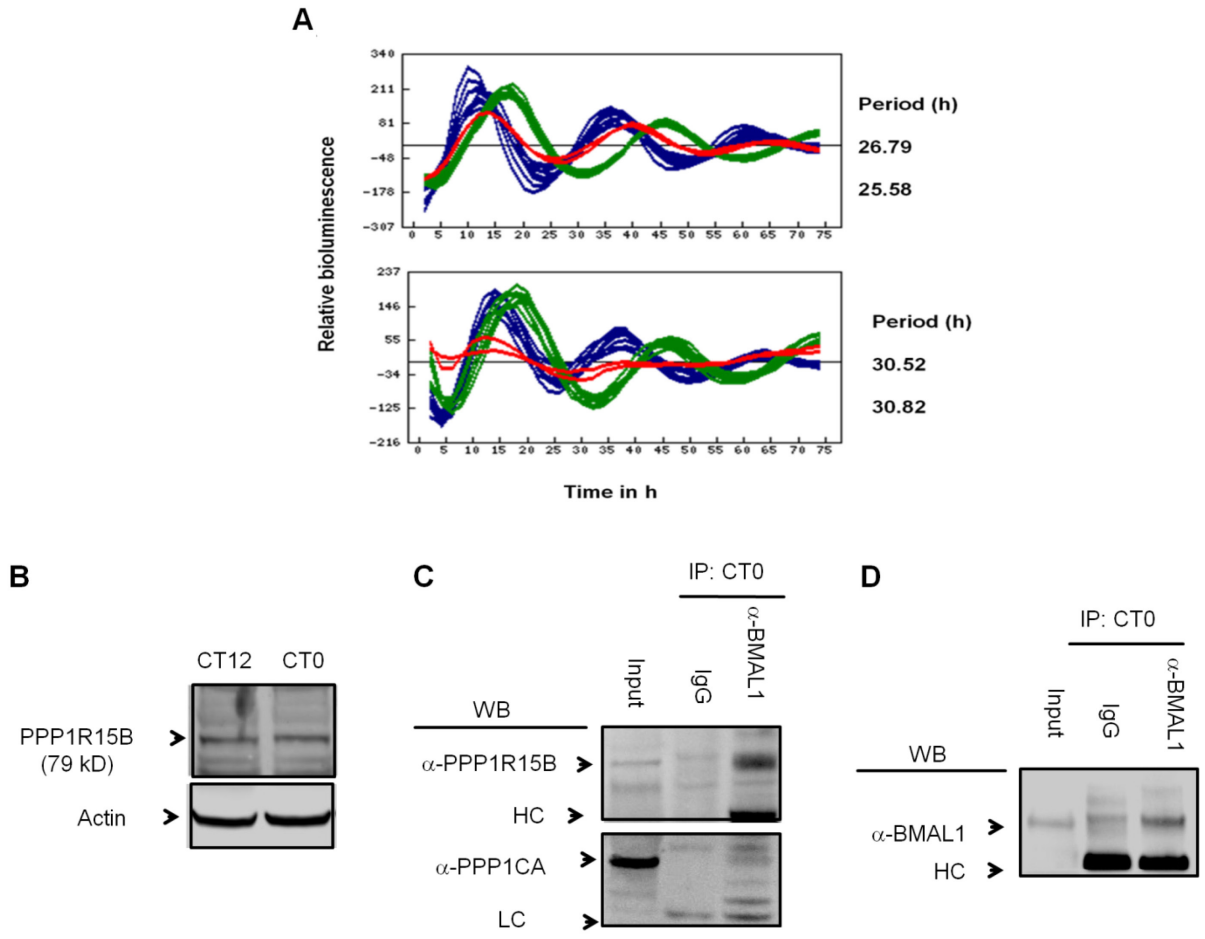

Figure 22. PPP1R15B Silencing Alters Circadian Dynamics and PPP1R15B is Present at the CLOCK/BMAL1 Complex.
(A) siRNA mediated gene silencing in U20S cells carrying the *Bmal1*-promoter luciferase reporter leads to severe period lengthening phenotypes (see red curves for effects of four individual siRNAs). Green curves: *Cry2* knockdown as positive control, blue curves: GL2 siRNA (designed against the *Luc* in the pGL2 vecotor) was used as a negative control. Period values for red curves are given from Circadian BIOGPS database [35].
(B) Endogenous PPP1R15B in mouse liver at the CT12 or CT0. Pull-downs and Western blot analysis were performed with the indicated antibodies (n = 2).
(C) PPP1R15B is present at CT20 at the CLOCK/BMAL1 complex. Pull-downs and Western blot analysis was performed with the indicated antibodies (n = 1). HC: heavy chain of used antibody, LC: light chain of used antibody.
(D) Determination of pull-down efficiency for co-IP experiments performed in (C). Western blot analysis was performed with the indicated antibody (n = 1).

5 DISCUSSION

5.1 Novel PPIs within the Molecular Oscillator

PPIs among circadian clock proteins are often time-of-day dependent, which is crucial for the function of the molecular circadian oscillator. While the recent years have witnessed the identification of an increasing number of clock proteins or modulators [22, 35, 61, 70, 71] a comprehensive analysis of PPIs within the circadian clockwork – in particular with respect to the timing of the PPIs – is still missing. Here, I have identified 109 so far uncharacterized interactions within the circadian clockwork in yeast and successfully validated a sub-fraction in mammalian cells. While the matrix screen design allowed me to perform independent replica experiments thereby reducing the risk of false positives, it is clear that due to the obvious limitations of the Y2H system [43] this network is likely still far away from saturation. For example, interactions that depend on posttranslational modifications or on more than two proteins are difficult to detect in Y2H assays. Nevertheless, Y2H approaches led to the discovery of crucial clock components such as BMAL1 [19] and large scale interaction networks have proven to be invaluable for a systems-wide understanding of physiology and disease [40, 48].

Interestingly, many of the new interactions occurred between core clock components and regulatory components such as kinases *e.g.*, CSNK2B, phosphatases (*e.g.*, PP2, PP1), and F-box proteins (*e.g.* FBXW11). Hence, these data should be a valuable resource for studying molecular events within the circadian system with so far uncharacterized posttranslational mechanisms being especially interesting. Whereas phosphorylation of clock proteins is increasingly recognized as crucial for circadian dynamics, de-phosphorylation events have not been studied as extensively [23]. Therefore, I have characterized the newly discovered interaction between PPP1CA and the CLOCK/BMAL1 heterodimer. The data suggest that a time-of-day specific action of PPP1CA negatively regulates BMAL1 abundance (see Figure 20), whereas others propose PER proteins as substrates of PP1 (Figure 23) [72, 73].

Furthermore, PPP1R15B was identified as a potential candidate that mediates BMAL1 substrate specifity for PP1 action. However, these findings suggest the existence of timely regulated stabilizing phosphosites, which are involved in the regulation of BMAL1 abundance

as proposed for other circadian proteins such as PER2 [22, 74]. Additional work using *state of the art* mass spectrometry approaches should be performed to identify the site/s of PP1 action on BMAL1 protein and the corresponding kinase/s acting at this site/s that regulate BMAL1 turnover.

In genetic perturbation studies, knockdown or overexpression of PPP1CA did not result in altered circadian dynamics in U2OS *Bmal1*-promoter luciferase reporter cells (see Figure 16 A and B; Figure 21 A) and clock output gene expression was unaffected (Figure 21 C).

In the case of gene silencing, one possible explanation for that observation could be paralog compensation effects by PPP1CB and/or PPP1CC (two additional PP1 catalytic subunits also expressed in these cells [73]). In line with my PPP1CA knockdown data, Schmutz *et al*. did not observe an altered circadian phenotype when PPP1CA was silenced *via* RNAi using the same reporter cell line [73]. Further investigations (*e.g*. single, double and triple knockdowns of PP1 catalytic subunits and the determination of the corresponding gene products *via* q-PCR experiments) are needed to support this interpretation.

In PPP1CA overexpression experiments, endogenous BMAL1 protein is reduced to about 50% (see Figure 20 E). Maier *et al*. [22] observe only a drastic altered circadian phenotype (arrhythmicity) when *Bmal1* mRMA is reduced in RNAi experiments by more than 50%. The remaining BMAL1 protein in my experiments could be still sufficient to drive normal circadian dynamics and output. In the overexpression experiments PPP1CA levels are about six-fold increased (Figure 21 B and C) which represents a relative low overexpression in comparison to overexpression rates usually achieved in transient transfection experiments. Dose dependent PPP1CA/PPP1R15B overexpression experiments combined with dynamic oscillation recordings should be addressed in this context.

However, a recent study suggests that *Bmal1* is not essential for the mammalian oscillator and that the circadian phenotype can be rescued by constitutive expression of its paralog *Bmal2* (= *Arntl2*) in a *Bmal1* knockout background [75]. The authors propose that *Baml1* and *Bmal2* are forming a circadian paralog pair that is functionally redundant and that *Bmal1* is a transcriptional regulator of *Bmal2*. In this scenario, a *Bmal1* knockout alone would result in a *Bmal1* and *Bmal2* double depletion that is probably responsible for the arrhythmic phenotype of *Bmal1* single knockout mice [76]. This could also be the case in the U2OS reporter cells

when *Bmal1* is silenced *via* RNAi. In my overexpression experiments a ~50% reduction in BMAL1 protein would imply that BMAL2 is also expressed to a certain extend and that the remaining BMAL1 and BMAL2 protein in concert could still drive normal circadian dynamics and cellular output processes. Further experiments are needed to clarify the role of PP1 action on BMAL1 and additively BMAL2 transcript and protein.

Clock output genes levels are not altered in U2OS cells when PPP1CA is overexpressed (Figure 21 C). But why does PPP1CA reduce severly the CLOCK/BMAL1 mediated reporter induction in the co-transactivation experiments (Figure 19 and Figure 20 A and B)?

One explanation might imply a higher overexpression efficiency reached by transient transfection in this artificial system (co-transactivation assay) and therefore a stronger destabilizing effect on BMAL1 protein. In addition, a change in the phosphorlyation state and stability of BMAL1 *via* PP1 could have additional effects on the CLOCK/BMAL1 heretodimer formation and function (*e.g.* DNA-binding and/or transactivation) or influence CLOCK stability. Such effects would also synergistically lead to a drastic reduction of CLOCK/BMAL1 transactivation. Precedence for such scenarios were described by Kondratov *et al*. where the formation of the CLOCK/BMAL1 heterodimer is leading to phosphorylation of both interactors as well as to CLOCK nuclear translocation and degradation [66]. Furthermore, Spengler *et al*. described that BMAL1 is involved in phosphorlylation-mediated degradation of CLOCK protein through a phosphor-degron site within the CLOCK protein [77].

It is also known that clock proteins have different phosphorylation states depending on the progress of the circadian cycle (see [20, 72]). *E.g*. recent data suggests that CLOCK is kept most of the time in a phosphorylated state whereas hyperphosporlyted CLOCK contributes to the suppression of CLOCK/BMAL1 mediated tranactivation [67]. Since different BMAL1 phosporylation states exist (see [20]) PP1 could possibly mediate its effect in U2OS cells on one BMAL1 protein fraction/state that could not be primarily involved in the regulation of transcription. Determinations of BMAL1 stability in nuclear and cytosolic fractions cloud reveal additional information of PP1 function.

In a simplified model, PP1 (complex of PPP1R15B and PPP1CA) dephosphorylates and therefore destabilizes BMAL1 at the end of a circadian cycle (late night) contributing to its

proteasomal degradation and therefore reduction of transactivation. In addition, it is described that phosphorylation of BMAL1 by GSK3B that was shown to destabilize BMAL1 protein is involved in the regulation of BMAL1 decay [78]. Further studies should be performed to uncover the mechanisms between the counterbalancing effects of PP1 and kinases for BMAL1 turnover and circadian functionality.

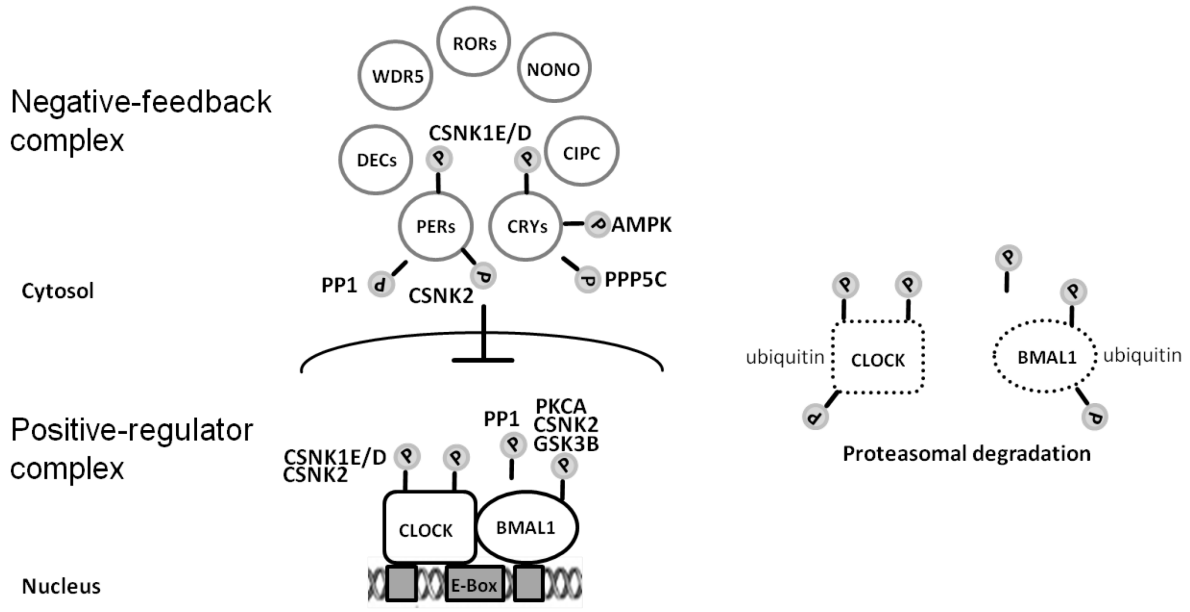

Figure 23. Speculative Model for the Negative-Feedback Mechanism with Kinase and Phosphatase Action. The Y2H screen led to the identification of circadian components newly present at the negative-feedback or positive-regulator complex (*e.g.* RORs, CSNK2 and PP1). In this model, PP1 action at the end of the night (as indicated by interaction experiments around CT0 (CT: circadian time)) dephosphorylates BMAL1 at potential stabilizing phosphosites leading to a less stable BMAL1 protein and therefore reduced transactivation. Furthermore, additional phosphorylation events as mediated by *e.g.* GSK3B are involved in the regulation of BMAL1 decay. Kinases: CSNK1E/D, CSNK2, PKCA, GSK3B, AMPK; phosphatases: PPP1; E-box: enhancer element in *Per* and *Cry* promoter.

5.2 Network Neighborhood Contains Genes that are Required for Normal Circadian Dynamics

Our systematically generated network extension/neighborhood contains 88 proteins that are linked to circadian clock core *via* physical interactions indicating a potential relevance for these components to be also involved in the regulation of circadian dynamics. Indeed after our systematic RNAi mediated perturbation study we could identify 21 genes that displayed an altered circadian phenotype of which several are described to be involved in transcriptional

and epigenetic regulation as well as nucleotide repair events. In agreement with this finding, three genes of our extension (DDB1, EPAS1 and HCFC1) have been previously shown to alter circadian dynamics when silenced by siRNA in U2OS cells [35]. Additionally, our neighborhood harbors six genes/or paralogs (CHD4, HDAC1, HSFPAA90, MLL, NCOR1 and PML), for which a role for the molecular clock as well as circadian physiology was proposed in different model organisms [61, 64, 79-82]. These findings together with our altered phenotypes support my hypothesis that the network neighborhood contains a relative high fraction of proteins mediating additional mechanisms that are involved in keeping the circadian pace. Interestingly, genes of our neighborhood that have been sensitive to RNAi mediated genetic perturbation are also present in the identified functional highly connected clusters (see Figure 17 and Figure 18) indicating a relevance for module function in keeping the circadian pace. It is apparent that the situation in the U2OS reporter cell line does not necessarily represent the conditions in a living organism and the relevance of the identified components for peripheral oscillators and SCN (and other tissues) still remains to be addressed. Interestingly, our neighborhood is highly significantly enriched in genes that are associated with Huntington's disease (see Figure 17 B) and one structural module is significantly enriched with *htt* related gens (see Methods for significance of enrichment). This is in line with observed altered circadian sleep-wake cycles in this disease [83]. Based on our liver specific trancriptome analysis, I can only speculate about the corresponding interaction dynamics within *e.g.* the CNS. However, network topology (not including dynamic information) can serve as a resource for interaction events *e.g.* within brain areas. In combination with other or newly generated expression profiles (from different tissues than liver) at RNA and protein level (or with the integration of information of different disease progression states) the constructed network could again be used to study network dynamics.

5.3 Circadian Protein-Protein Networks

The circadian PPI network is very densely connected. How can such a network function? We analyzed both temporal organization, which separate PPIs in time as well as modular organization, which organize the network in functional complexes. To investigate temporal organization, we have integrated circadian expression profiles from mouse liver for the interacting pairs of proteins assuming that co-expression on transcript level can represent

individual protein abundance probably as one limiting factor for physical interaction. Such an approach has been used when large-scale protein abundance data are lacking [47]. Our transcript-based analysis led to the construction of a dynamic circadian (albeit only liver-specific) PPI network, in which PPIs are formed at all circadian phases (see Figure 14 B). Obviously, our analysis harbors several limitations, since PPIs *in vivo* depend on a variety of factors such as spatial restrains, restriction to specific tissues, relative protein abundance, mRNA processing, stoichiometry and interaction kinetics, complex formation and posttranslational modifications. All these parameters are not represented by the corresponding mRNA profiles of interaction partners. However, our assumption that indeed dynamic binding events can be approximated by such an approach is supported by (i) our finding that co-expression of transcripts at similar circadian phases more often occurs among interacting proteins (see Figure 14 A) and (ii) known interaction dynamics between components of the circadian system can be reproduced (see Figure 14 B), *e.g.* the circadian phase-specific CLOCK/CRY1 interaction [20].

Beyond the dynamic interactions that occur among circadian core components, we have identified many time-of-day specific PPIs between core and neighborhood proteins. For example, the circadian core component BMAL1 binds to EPAS1 (endothelial PAS domain protein 1) and HIF1A (hypoxia inducible factor 1, alpha subunit), two proteins involved in hemopoiesis during the late night (see Appendix and Figure 17 A). Interestingly, Bozek *et al*. [30] proposed a circadian regulation of the *Erythropoietin* (*Epo*) gene with HIF1A (and not the CLOCK/BMAL1 hererodimer) being its transcritonal activator. The construction of the dynamic circadian protein-protein network suggests that BMAL1 could recruit HIF1A to DNA to drive *Epo* transcription in a dynamic range. Hemopoetic *Epo* expression is restricted to the adult kidney [84]. Therefore, systematic circadian chromatin binding studies using CLOCK/BMAL1 and HIF1A antibodies for pull-downs in chromatin immunoprecipitation assays as performed by Rey *et al*. [29] in mouse liver would represent experiments to support this hypothesis. However, further validations of our predicted interaction dynamics *e.g*. *via* rhythmic co-IPs or FRET (fluorescence resonance energy transfer) experiments are needed.

5.4 Dynamic Hubs

Dynamic `hubs´ (proteins involved in many rhythmic PPIs) are especially important for

circadian rhythms (see Figure 16 C) as revealed by my genetic perturbation analyses. Thus, it seems that not the absolute number of interactions is crucial for the importance of a clock protein but the degree of dynamic PPIs. This is not too surprising, since precisely timed interactions between activators and their repressors is the fundamental principle of the circadian negative feedback mechanism. Interestingly, this principle may be translated to the global proteome: we find that proteins with a rhythmic transcript have significantly more interaction partners than non-rhythmic proteins ($p < 10^{-10}$, Wilcoxon Rank test). In addition, proteins that qualify as regulatory components (as defined by their GO category `Regulation of biological process´) have significantly more interaction partners than non-regulatory proteins ($p < 10^{-15}$, Wilcoxon Rank test). Together, this indicates that rhythmic control of PPIs is an essential feature of biological networks.

5.5 Regulation of Cellular Physiology by Dynamic Protein-Protein Interactions

In the last decade, transcriptome analyses were successfully used to study circadian dynamics on a systems-wide level [27, 28] with mRNA rhythms serving as indicators for output control. Corresponding comprehensive studies on the level of the proteome are still largely missing. To get novel insights into the time-of-day dependent regulation of cellular processes, we have constructed a circadian interactome (see Figure 17 D) allowing us to study circadian regulation at the level of protein complexes rather than looking at mRNA profiles of individual components. Based on this dynamic interactome, we have constructed a process network demonstrating that many important processes are strongly connected by dynamic PPIs (see Figure 17 D and Figure 18 C). Interestingly, `Signal transduction´ is the central hub in this process network and cellular surface receptors are the proteins with the most dynamic interactions. This implies that circadian regulation is especially important for cells responding to external stimuli. Reported examples include the daytime dependent response to UV-induced DNA damage [85] – for which I have also identified a clock-controlled module in our network (Figure 17 C) – or endotoxin-triggered secretion of proinflammatory cytokines [13].

Timing of biological functions *via* PPIs that occur at specific circadian phases seems to be accomplished by co-expression of module components (see Figure 17 C), but also in more general terms: interacting proteins are expressed significantly more likely at similar times (Figure 14 A) probably to restrict regulatory interactions to specific circadian phases.

Overall, data accumulated during my PhD work provide a global view and valualbe resource on the circadian control of PPIs important not only for the circadian oscillator but also for the temporal orchestration of many essential cellular processes.

6 REFERENCES

[1] Gallego M, Virshup DM. Post-translational modifications regulate the ticking of the circadian clock. Nat Rev Mol Cell Biol 2007;8:139.

[2] Reppert SM, Weaver DR. Coordination of circadian timing in mammals. Nature 2002;418:935.

[3] Zhang EE, Kay SA. Clocks not winding down: unravelling circadian networks. Nat Rev Mol Cell Biol 2010;11:764.

[4] DeMairan J. Observation Botanique. Hist Acad R Sci 1729:35–36.

[5] Bünning E. Zur Kenntnis der erblichen Tagesperiodizität bei den Primärblättern Phaseolus multiflorus. Jb wiss Bot 1935;81:411–418.

[6] Hastings JW, Sweeny BM. A persistent dirunal rhythm on luminescence in Gonyaulax polyedra. Biol Bull 1958: 440.

[7] Kramer G. Experiments on bird orientation. Ibs 1952:265.

[8] Aschoff J. Circadian Rhythms in Man - A Self-Sustained Oscillator with An Inherent Frequency Underlies Human 24-Hour Periodicity. Science 1965;148:1427–&.

[9] Aschoff J, Wever R. Spontanperiodik des Menschen Bei Ausschluss Aller Zeitgeber. Naturwissenschaften 1962;49:337–&.

[10] Konopka RJ, Benzer S. Clock Mutants of Drosophila-Melanogaster. PNAS 1971;68:2112–2116.

[11] Feldman JF, Hoyle MN. Isolation of circadian clock mutants of Neurospora crassa. Genetics 1973;75:605–613.

[12] Beersma DGM, Daan S, Gordijn MCM, Gerkema MP. EU-CLOCK Summer School Chronobiology. Course text book Choronobiology Summer School 2007 2007.

[13] Keller M, Mazuch J, Abraham U, Eom GD, Herzog ED, Volk HD, Kramer A, Maier B. A circadian clock in macrophages controls inflammatory immune responses. Proc Natl Acad Sci U S A 2009;106:21407.

[14] Sahar S, Sassone-Corsi P. Regulation of metabolism: the circadian clock dictates the time. Trends Endocrinol Metab 2012;23:1.

[15] Lamia KA, Sachdeva UM, DiTacchio L, Williams EC, Alvarez JG, Egan DF, Vasquez DS, Juguilon H, Panda S, Shaw RJ, Thompson CB, Evans RM. AMPK regulates the circadian clock by cryptochrome phosphorylation and degradation. Science 2009;326:437.

[16] Lamia KA, Storch KF, Weitz CJ. Physiological significance of a peripheral tissue circadian clock. Proc Natl Acad Sci U S A 2008;105:15172.

[17] Vollmers C, Gill S, DiTacchio L, Pulivarthy SR, Le HD, Panda S. Time of feeding and the intrinsic circadian clock drive rhythms in hepatic gene expression. Proc Natl Acad Sci U S A 2009;106:21453.

[18] Liu AC, Lewis WG, Kay SA. Mammalian circadian signaling networks and therapeutic

targets. Nat Chem Biol 2007;3:630.

[19] Gekakis N, Staknis D, Nguyen HB, Davis FC, Wilsbacher LD, King DP, Takahashi JS, Weitz CJ. Role of the CLOCK protein in the mammalian circadian mechanism. Science 1998;280:1564.

[20] Lee C, Etchegaray JP, Cagampang FR, Loudon AS, Reppert SM. Posttranslational mechanisms regulate the mammalian circadian clock. Cell 2001;107:855.

[21] Godinho SI, Maywood ES, Shaw L, Tucci V, Barnard AR, Busino L, Pagano M, Kendall R, Quwailid MM, Romero MR, O'Neill J, Chesham JE, Brooker D, Lalanne Z, Hastings MH, Nolan PM. The after-hours mutant reveals a role for Fbxl3 in determining mammalian circadian period. Science 2007;316:897.

[22] Maier B, Wendt S, Vanselow JT, Wallach T, Reischl S, Oehmke S, Schlosser A, Kramer A. A large-scale functional RNAi screen reveals a role for CK2 in the mammalian circadian clock. Genes Dev 2009;23:708.

[23] Reischl S, Kramer A. Kinases and phosphatases in the mammalian circadian clock. FEBS Lett 2011;585:1393.

[24] Edgar RS, Green EW, Zhao Y, van Ooijen G, Olmedo M, Qin X, Xu Y, Pan M, Valekunja UK, Feeney KA, Maywood ES, Hastings MH, Baliga NS, Merrow M, Millar AJ, Johnson CH, Kyriacou CP, O'Neill JS, Reddy AB. Peroxiredoxins are conserved markers of circadian rhythms. Nature 2012;485:459.

[25] O'Neill JS, Reddy AB. Circadian clocks in human red blood cells. Nature 2011;469:498.

[26] O'Neill JS, van Ooijen G, Dixon LE, Troein C, Corellou F, Bouget FY, Reddy AB, Millar AJ. Circadian rhythms persist without transcription in a eukaryote. Nature 2011;469:554.

[27] Hughes ME, DiTacchio L, Hayes KR, Vollmers C, Pulivarthy S, Baggs JE, Panda S, Hogenesch JB. Harmonics of circadian gene transcription in mammals. PLoS Genet 2009;5:e1000442.

[28] Panda S, Antoch MP, Miller BH, Su AI, Schook AB, Straume M, Schultz PG, Kay SA, Takahashi JS, Hogenesch JB. Coordinated transcription of key pathways in the mouse by the circadian clock. Cell 2002;109:307.

[29] Rey G, Cesbron F, Rougemont J, Reinke H, Brunner M, Naef F. Genome-wide and phase-specific DNA-binding rhythms of BMAL1 control circadian output functions in mouse liver. PLoS Biol 2011;9:e1000595.

[30] Bozek K, Kielbasa SM, Kramer A, Herzel H. Promoter analysis of Mammalian clock controlled genes. Genome Inform 2007;18:65.

[31] Dallmann R, Viola AU, Tarokh L, Cajochen C, Brown SA. The human circadian metabolome. Proc Natl Acad Sci U S A 2012;109:2625.

[32] Eckel-Mahan KL, Patel VR, Mohney RP, Vignola KS, Baldi P, Sassone-Corsi P. Coordination of the transcriptome and metabolome by the circadian clock. Proc Natl Acad Sci U S A 2012;109:5541.

[33] Antoch MP, Song EJ, Chang AM, Vitaterna MH, Zhao Y, Wilsbacher LD, Sangoram

AM, King DP, Pinto LH, Takahashi JS. Functional identification of the mouse circadian Clock gene by transgenic BAC rescue. Cell 1997;89:655.

[34] Reddy AB, Karp NA, Maywood ES, Sage EA, Deery M, O'Neill JS, Wong GK, Chesham J, Odell M, Lilley KS, Kyriacou CP, Hastings MH. Circadian orchestration of the hepatic proteome. Curr Biol 2006;16:1107.

[35] Zhang EE, Liu AC, Hirota T, Miraglia LJ, Welch G, Pongsawakul PY, Liu X, Atwood A, Huss JW, 3rd, Janes J, Su AI, Hogenesch JB, Kay SA. A genome-wide RNAi screen for modifiers of the circadian clock in human cells. Cell 2009;139:199.

[36] Baggs JE, Price TS, DiTacchio L, Panda S, Fitzgerald GA, Hogenesch JB. Network features of the mammalian circadian clock. PLoS Biol 2009;7:e52.

[37] Baggs JE, Hogenesch JB. Genomics and systems approaches in the mammalian circadian clock. Curr Opin Genet Dev 2010;20:581.

[38] Ueda HR. Systems biology of mammalian circadian clocks. Cold Spring Harb Symp Quant Biol 2007;72:365.

[39] Goehler H, Lalowski M, Stelzl U, Waelter S, Stroedicke M, Worm U, Droege A, Lindenberg KS, Knoblich M, Haenig C, Herbst M, Suopanki J, Scherzinger E, Abraham C, Bauer B, Hasenbank R, Fritzsche A, Ludewig AH, Bussow K, Coleman SH, Gutekunst CA, Landwehrmeyer BG, Lehrach H, Wanker EE. A protein interaction network links GIT1, an enhancer of huntingtin aggregation, to Huntington's disease. Mol Cell 2004;15:853.

[40] Rual JF, Venkatesan K, Hao T, Hirozane-Kishikawa T, Dricot A, Li N, Berriz GF, Gibbons FD, Dreze M, Ayivi-Guedehoussou N, Klitgord N, Simon C, Boxem M, Milstein S, Rosenberg J, Goldberg DS, Zhang LV, Wong SL, Franklin G, Li S, Albala JS, Lim J, Fraughton C, Llamosas E, Cevik S, Bex C, Lamesch P, Sikorski RS, Vandenhaute J, Zoghbi HY, Smolyar A, Bosak S, Sequerra R, Doucette-Stamm L, Cusick ME, Hill DE, Roth FP, Vidal M. Towards a proteome-scale map of the human protein-protein interaction network. Nature 2005;437:1173.

[41] Stelzl U, Worm U, Lalowski M, Haenig C, Brembeck FH, Goehler H, Stroedicke M, Zenkner M, Schoenherr A, Koeppen S, Timm J, Mintzlaff S, Abraham C, Bock N, Kietzmann S, Goedde A, Toksoz E, Droege A, Krobitsch S, Korn B, Birchmeier W, Lehrach H, Wanker EE. A human protein-protein interaction network: a resource for annotating the proteome. Cell 2005;122:957.

[42] Barabasi AL, Oltvai ZN. Network biology: understanding the cell's functional organization. Nat Rev Genet 2004;5:101.

[43] Stelzl U, Wanker EE. The value of high quality protein-protein interaction networks for systems biology. Curr Opin Chem Biol 2006;10:551.

[44] Hahn MW, Kern AD. Comparative genomics of centrality and essentiality in three eukaryotic protein-interaction networks. Mol Biol Evol 2005;22:803.

[45] Przytycka TM, Singh M, Slonim DK. Toward the dynamic interactome: it's about time. Brief Bioinform 2010;11:15.

[46] Atwood A, DeConde R, Wang SS, Mockler TC, Sabir JS, Ideker T, Kay SA. Cell-autonomous circadian clock of hepatocytes drives rhythms in transcription and polyamine synthesis. Proc Natl Acad Sci U S A 2011;108:18560.

[47] de Lichtenberg U, Jensen LJ, Brunak S, Bork P. Dynamic complex formation during the yeast cell cycle. Science 2005;307:724.

[48] Venkatesan K, Rual JF, Vazquez A, Stelzl U, Lemmens I, Hirozane-Kishikawa T, Hao T, Zenkner M, Xin X, Goh KI, Yildirim MA, Simonis N, Heinzmann K, Gebreab F, Sahalie JM, Cevik S, Simon C, de Smet AS, Dann E, Smolyar A, Vinayagam A, Yu H, Szeto D, Borick H, Dricot A, Klitgord N, Murray RR, Lin C, Lalowski M, Timm J, Rau K, Boone C, Braun P, Cusick ME, Roth FP, Hill DE, Tavernier J, Wanker EE, Barabasi AL, Vidal M. An empirical framework for binary interactome mapping. Nat Methods 2009;6:83.

[49] Hofmann KP, Spahn CM, Heinrich R, Heinemann U. Building functional modules from molecular interactions. Trends Biochem Sci 2006;31:497.

[50] Jakubcakova V, Oster H, Tamanini F, Cadenas C, Leitges M, van der Horst GT, Eichele G. Light entrainment of the mammalian circadian clock by a PRKCA-dependent posttranslational mechanism. Neuron 2007;54:831.

[51] Huang G, Chen S, Li S, Cha J, Long C, Li L, He Q, Liu Y. Protein kinase A and casein kinases mediate sequential phosphorylation events in the circadian negative feedback loop. Genes Dev 2007;21:3283.

[52] Busino L, Bassermann F, Maiolica A, Lee C, Nolan PM, Godinho SI, Draetta GF, Pagano M. SCFFbxl3 controls the oscillation of the circadian clock by directing the degradation of cryptochrome proteins. Science 2007;316:900.

[53] Koh K, Zheng X, Sehgal A. JETLAG resets the Drosophila circadian clock by promoting light-induced degradation of TIMELESS. Science 2006;312:1809.

[54] Barnes JW, Tischkau SA, Barnes JA, Mitchell JW, Burgoon PW, Hickok JR, Gillette MU. Requirement of mammalian Timeless for circadian rhythmicity. Science 2003;302:439.

[55] Zhao WN, Malinin N, Yang FC, Staknis D, Gekakis N, Maier B, Reischl S, Kramer A, Weitz CJ. CIPC is a mammalian circadian clock protein without invertebrate homologues. Nat Cell Biol 2007;9:268.

[56] Chaurasia G, Malhotra S, Russ J, Schnoegl S, Hanig C, Wanker EE, Futschik ME. UniHI 4: new tools for query, analysis and visualization of the human protein-protein interactome. Nucleic Acids Res 2009;37:D657.

[57] Futschik ME, Herzel H. Are we overestimating the number of cell-cycling genes? The impact of background models on time-series analysis. Bioinformatics 2008;24:1063.

[58] Strogatz SH. Exploring complex networks. Nature 2001;410:268.

[59] Schwanhausser B, Busse D, Li N, Dittmar G, Schuchhardt J, Wolf J, Chen W, Selbach M. Global quantification of mammalian gene expression control. Nature 2011;473:337.

[60] Han JD, Bertin N, Hao T, Goldberg DS, Berriz GF, Zhang LV, Dupuy D, Walhout AJ, Cusick ME, Roth FP, Vidal M. Evidence for dynamically organized modularity in the yeast protein-protein interaction network. Nature 2004;430:88.

[61] Katada S, Sassone-Corsi P. The histone methyltransferase MLL1 permits the oscillation of circadian gene expression. Nat Struct Mol Biol 2010;17:1414.

[62] Brown SA, Ripperger J, Kadener S, Fleury-Olela F, Vilbois F, Rosbash M, Schibler U. PERIOD1-associated proteins modulate the negative limb of the mammalian circadian

oscillator. Science 2005;308:693.

[63] DiTacchio L, Le HD, Vollmers C, Hatori M, Witcher M, Secombe J, Panda S. Histone lysine demethylase JARID1a activates CLOCK-BMAL1 and influences the circadian clock. Science 2011;333:1881.

[64] Duong HA, Robles MS, Knutti D, Weitz CJ. A molecular mechanism for circadian clock negative feedback. Science 2011;332:1436.

[65] Honma S, Kawamoto T, Takagi Y, Fujimoto K, Sato F, Noshiro M, Kato Y, Honma K. Dec1 and Dec2 are regulators of the mammalian molecular clock. Nature 2002;419:841.

[66] Kondratov RV, Chernov MV, Kondratova AA, Gorbacheva VY, Gudkov AV, Antoch MP. BMAL1-dependent circadian oscillation of nuclear CLOCK: posttranslational events induced by dimerization of transcriptional activators of the mammalian clock system. Genes Dev 2003;17:1921.

[67] Yoshitane H, Takao T, Satomi Y, Du NH, Okano T, Fukada Y. Roles of CLOCK phosphorylation in suppression of E-box-dependent transcription. Mol Cell Biol 2009;29:3675.

[68] Ripperger JA, Schibler U. Rhythmic CLOCK-BMAL1 binding to multiple E-box motifs drives circadian Dbp transcription and chromatin transitions. Nat Genet 2006;38:369.

[69] Cohen PT. Protein phosphatase 1--targeted in many directions. J Cell Sci 2002;115:241.

[70] Asher G, Gatfield D, Stratmann M, Reinke H, Dibner C, Kreppel F, Mostoslavsky R, Alt FW, Schibler U. SIRT1 regulates circadian clock gene expression through PER2 deacetylation. Cell 2008;134:317.

[71] Robles MS, Boyault C, Knutti D, Padmanabhan K, Weitz CJ. Identification of RACK1 and protein kinase Calpha as integral components of the mammalian circadian clock. Science 2010;327:463.

[72] Lee HM, Chen R, Kim H, Etchegaray JP, Weaver DR, Lee C. The period of the circadian oscillator is primarily determined by the balance between casein kinase 1 and protein phosphatase 1. Proc Natl Acad Sci U S A 2011;108:16451.

[73] Schmutz I, Wendt S, Schnell A, Kramer A, Mansuy IM, Albrecht U. Protein phosphatase 1 (PP1) is a post-translational regulator of the mammalian circadian clock. PLoS One 2011;6:e21325.

[74] Vanselow K, Kramer A. Role of phosphorylation in the mammalian circadian clock. Cold Spring Harb Symp Quant Biol 2007;72:167.

[75] Shi S, Hida A, McGuinness OP, Wasserman DH, Yamazaki S, Johnson CH. Circadian clock gene Bmal1 is not essential; functional replacement with its paralog, Bmal2. Curr Biol 2010;20:316.

[76] Bunger MK, Wilsbacher LD, Moran SM, Clendenin C, Radcliffe LA, Hogenesch JB, Simon MC, Takahashi JS, Bradfield CA. Mop3 is an essential component of the master circadian pacemaker in mammals. Cell 2000;103:1009.

[77] Spengler ML, Kuropatwinski KK, Schumer M, Antoch MP. A serine cluster mediates BMAL1-dependent CLOCK phosphorylation and degradation. Cell Cycle 2009;8:4138.

[78] Sahar S, Zocchi L, Kinoshita C, Borrelli E, Sassone-Corsi P. Regulation of BMAL1 protein stability and circadian function by GSK3beta-mediated phosphorylation. PLoS One 2010;5:e8561.

[79] Miki T, Xu Z, Chen-Goodspeed M, Liu M, Van Oort-Jansen A, Rea MA, Zhao Z, Lee CC, Chang KS. PML regulates PER2 nuclear localization and circadian function. Embo J 2012;31:1427.

[80] Alenghat T, Meyers K, Mullican SE, Leitner K, Adeniji-Adele A, Avila J, Bucan M, Ahima RS, Kaestner KH, Lazar MA. Nuclear receptor corepressor and histone deacetylase 3 govern circadian metabolic physiology. Nature 2008;456:997.

[81] Belden WJ, Lewis ZA, Selker EU, Loros JJ, Dunlap JC. CHD1 remodels chromatin and influences transient DNA methylation at the clock gene frequency. PLoS Genet 2011;7:e1002166.

[82] Kim TS, Kim WY, Fujiwara S, Kim J, Cha JY, Park JH, Lee SY, Somers DE. HSP90 functions in the circadian clock through stabilization of the client F-box protein ZEITLUPE. Proc Natl Acad Sci U S A 2011;108:16843.

[83] Kudo T, Schroeder A, Loh DH, Kuljis D, Jordan MC, Roos KP, Colwell CS. Dysfunctions in circadian behavior and physiology in mouse models of Huntington's disease. Exp Neurol 2011;228:80.

[84] Dame C, Sola MC, Lim KC, Leach KM, Fandrey J, Ma Y, Knopfle G, Engel JD, Bungert J. Hepatic erythropoietin gene regulation by GATA-4. J Biol Chem 2004;279:2955.

[85] Gaddameedhi S, Selby CP, Kaufmann WK, Smart RC, Sancar A. Control of skin cancer by the circadian rhythm. Proc Natl Acad Sci U S A 2011;108:18790.

[86] Yin L, Wang J, Klein PS, Lazar MA. Nuclear receptor Rev-erbalpha is a critical lithium-sensitive component of the circadian clock. Science 2006;311:1002.

[87] Lopez-Molina L, Conquet F, Dubois-Dauphin M, Schibler U. The DBP gene is expressed according to a circadian rhythm in the suprachiasmatic nucleus and influences circadian behavior. Embo J 1997;16:6762.

[88] Ohno T, Onishi Y, Ishida N. The negative transcription factor E4BP4 is associated with circadian clock protein PERIOD2. Biochem Biophys Res Commun 2007;354:1010.

[89] Etchegaray JP, Yang X, DeBruyne JP, Peters AH, Weaver DR, Jenuwein T, Reppert SM. The polycomb group protein EZH2 is required for mammalian circadian clock function. J Biol Chem 2006;281:21209.

[90] Cheng HY, Dziema H, Papp J, Mathur DP, Koletar M, Ralph MR, Penninger JM, Obrietan K. The molecular gatekeeper Dexras1 sculpts the photic responsiveness of the mammalian circadian clock. J Neurosci 2006;26:12984.

[91] Partch CL, Shields KF, Thompson CL, Selby CP, Sancar A. Posttranslational regulation of the mammalian circadian clock by cryptochrome and protein phosphatase 5. Proc Natl Acad Sci U S A 2006;103:10467.

[92] Reischl S, Vanselow K, Westermark PO, Thierfelder N, Maier B, Herzel H, Kramer A. Beta-TrCP1-mediated degradation of PERIOD2 is essential for circadian dynamics. J Biol Rhythms 2007;22:375.

[93] Vielhaber E, Eide E, Rivers A, Gao ZH, Virshup DM. Nuclear entry of the circadian regulator mPER1 is controlled by mammalian casein kinase I epsilon. Mol Cell Biol 2000;20:4888.

[94] Akashi M, Tsuchiya Y, Yoshino T, Nishida E. Control of intracellular dynamics of mammalian period proteins by casein kinase I epsilon (CKIepsilon) and CKIdelta in cultured cells. Mol Cell Biol 2002;22:1693.

[95] Griffin EA, Jr., Staknis D, Weitz CJ. Light-independent role of CRY1 and CRY2 in the mammalian circadian clock. Science 1999;286:768.

[96] Oster H, Baeriswyl S, Van Der Horst GT, Albrecht U. Loss of circadian rhythmicity in aging mPer1-/-mCry2-/- mutant mice. Genes Dev 2003;17:1366.

[97] Toh KL, Jones CR, He Y, Eide EJ, Hinz WA, Virshup DM, Ptacek LJ, Fu YH. An hPer2 phosphorylation site mutation in familial advanced sleep phase syndrome. Science 2001;291:1040.

[98] Vanselow K, Vanselow JT, Westermark PO, Reischl S, Maier B, Korte T, Herrmann A, Herzel H, Schlosser A, Kramer A. Differential effects of PER2 phosphorylation: molecular basis for the human familial advanced sleep phase syndrome (FASPS). Genes Dev 2006;20:2660.

[99] Xu Y, Toh KL, Jones CR, Shin JY, Fu YH, Ptacek LJ. Modeling of a human circadian mutation yields insights into clock regulation by PER2. Cell 2007;128:59.

[100] Kume K, Zylka MJ, Sriram S, Shearman LP, Weaver DR, Jin X, Maywood ES, Hastings MH, Reppert SM. mCRY1 and mCRY2 are essential components of the negative limb of the circadian clock feedback loop. Cell 1999;98:193.

[101] Miyazaki K, Mesaki M, Ishida N. Nuclear entry mechanism of rat PER2 (rPER2): role of rPER2 in nuclear localization of CRY protein. Mol Cell Biol 2001;21:6651.

[102] Xu Y, Padiath QS, Shapiro RE, Jones CR, Wu SC, Saigoh N, Saigoh K, Ptacek LJ, Fu YH. Functional consequences of a CKIdelta mutation causing familial advanced sleep phase syndrome. Nature 2005;434:640.

[103] Shearman LP, Sriram S, Weaver DR, Maywood ES, Chaves I, Zheng B, Kume K, Lee CC, van der Horst GT, Hastings MH, Reppert SM. Interacting molecular loops in the mammalian circadian clock. Science 2000;288:1013.

[104] Eide EJ, Kang H, Crapo S, Gallego M, Virshup DM. Casein kinase I in the mammalian circadian clock. Methods Enzymol 2005;393:408.

[105] Eide EJ, Vielhaber EL, Hinz WA, Virshup DM. The circadian regulatory proteins BMAL1 and cryptochromes are substrates of casein kinase Iepsilon. J Biol Chem 2002;277:17248.

[106] St-Pierre B, Flock G, Zacksenhaus E, Egan SE. Stra13 homodimers repress transcription through class B E-box elements. J Biol Chem 2002;277:46544.

[107] Hogenesch JB, Gu YZ, Jain S, Bradfield CA. The basic-helix-loop-helix-PAS orphan MOP3 forms transcriptionally active complexes with circadian and hypoxia factors. Proc Natl Acad Sci U S A 1998;95:5474.

[108] McNamara P, Seo SB, Rudic RD, Sehgal A, Chakravarti D, FitzGerald GA. Regulation

of CLOCK and MOP4 by nuclear hormone receptors in the vasculature: a humoral mechanism to reset a peripheral clock. Cell 2001;105:877.

[109] Gietzen KF, Virshup DM. Identification of inhibitory autophosphorylation sites in casein kinase I epsilon. J Biol Chem 1999;274:32063.

[110] Kim MS, Lee YT, Kim JM, Cha JY, Bae YS. Characterization of protein interaction among subunits of protein kinase CKII in vivo and in vitro. Mol Cells 1998;8:43.

[111] Lehner B, Semple JI, Brown SE, Counsell D, Campbell RD, Sanderson CM. Analysis of a high-throughput yeast two-hybrid system and its use to predict the function of intracellular proteins encoded within the human MHC class III region. Genomics 2004;83:153.

[112] Marin O, Meggio F, Sarno S, Pinna LA. Physical dissection of the structural elements responsible for regulatory properties and intersubunit interactions of protein kinase CK2 beta-subunit. Biochemistry 1997;36:7192.

[113] Ahn BH, Kim TH, Bae YS. Mapping of the interaction domain of the protein kinase CKII beta subunit with target proteins. Mol Cells 2001;12:158.

[114] Litchfield DW, Lozeman FJ, Cicirelli MF, Harrylock M, Ericsson LH, Piening CJ, Krebs EG. Phosphorylation of the beta subunit of casein kinase II in human A431 cells. Identification of the autophosphorylation site and a site phosphorylated by p34cdc2. J Biol Chem 1991;266:20380.

[115] Sablina AA, Chen W, Arroyo JD, Corral L, Hector M, Bulmer SE, DeCaprio JA, Hahn WC. The tumor suppressor PP2A Abeta regulates the RalA GTPase. Cell 2007;129:969.

[116] Kitajima TS, Sakuno T, Ishiguro K, Iemura S, Natsume T, Kawashima SA, Watanabe Y. Shugoshin collaborates with protein phosphatase 2A to protect cohesin. Nature 2006;441:46.

[117] Shern JF, Sharer JD, Pallas DC, Bartolini F, Cowan NJ, Reed MS, Pohl J, Kahn RA. Cytosolic Arl2 is complexed with cofactor D and protein phosphatase 2A. J Biol Chem 2003;278:40829.

[118] McCright B, Rivers AM, Audlin S, Virshup DM. The B56 family of protein phosphatase 2A (PP2A) regulatory subunits encodes differentiation-induced phosphoproteins that target PP2A to both nucleus and cytoplasm. J Biol Chem 1996;271:22081.

[119] Tamaru T, Hirayama J, Isojima Y, Nagai K, Norioka S, Takamatsu K, Sassone-Corsi P. CK2alpha phosphorylates BMAL1 to regulate the mammalian clock. Nat Struct Mol Biol 2009;16:446.

[120] Langmesser S, Tallone T, Bordon A, Rusconi S, Albrecht U. Interaction of circadian clock proteins PER2 and CRY with BMAL1 and CLOCK. BMC Mol Biol 2008;9:41.

[121] Chaurasia G, Futschik M. The integration and annotation of the human interactome in the UniHI Database. Methods Mol Biol 2012;812:175.

[122] Zylka MJ, Shearman LP, Levine JD, Jin X, Weaver DR, Reppert SM. Molecular analysis of mammalian timeless. Neuron 1998;21:1115.

[123] Gallego M, Kang H, Virshup DM. Protein phosphatase 1 regulates the stability of the circadian protein PER2. Biochem J 2006;399:169.

[124] Iitaka C, Miyazaki K, Akaike T, Ishida N. A role for glycogen synthase kinase-3beta in the mammalian circadian clock. J Biol Chem 2005;280:29397.

[125] Ohno T, Onishi Y, Ishida N. A novel E4BP4 element drives circadian expression of mPeriod2. Nucleic Acids Res 2007;35:648.

[126] Harada Y, Sakai M, Kurabayashi N, Hirota T, Fukada Y. Ser-557-phosphorylated mCRY2 is degraded upon synergistic phosphorylation by glycogen synthase kinase-3 beta. J Biol Chem 2005;280:31714.

[127] Heriche JK, Lebrin F, Rabilloud T, Leroy D, Chambaz EM, Goldberg Y. Regulation of protein phosphatase 2A by direct interaction with casein kinase 2alpha. Science 1997;276:952.

[128] Zhou J, Pham HT, Ruediger R, Walter G. Characterization of the Aalpha and Abeta subunit isoforms of protein phosphatase 2A: differences in expression, subunit interaction, and evolution. Biochem J 2003;369:387.

[129] Lubert EJ, Hong Y, Sarge KD. Interaction between protein phosphatase 5 and the A subunit of protein phosphatase 2A: evidence for a heterotrimeric form of protein phosphatase 5. J Biol Chem 2001;276:38582.

[130] Wang J, Yin L, Lazar MA. The orphan nuclear receptor Rev-erb alpha regulates circadian expression of plasminogen activator inhibitor type 1. J Biol Chem 2006;281:33842.

[131] Schmutz I, Ripperger JA, Baeriswyl-Aebischer S, Albrecht U. The mammalian clock component PERIOD2 coordinates circadian output by interaction with nuclear receptors. Genes Dev 2009;24:345.

[132] Suzuki H, Chiba T, Suzuki T, Fujita T, Ikenoue T, Omata M, Furuichi K, Shikama H, Tanaka K. Homodimer of two F-box proteins betaTrCP1 or betaTrCP2 binds to IkappaBalpha for signal-dependent ubiquitination. J Biol Chem 2000;275:2877.

APPENDIX

Table 1. 46 Components for Interaction Mapping.

Gene ID h	Gene ID m	Symbol h	Symbol m	References
5187	18626	PER1	Per1	[1]
8864	18627	PER2	Per2	[1]
8863	18628	PER3	Per3	[1]
1407	12952	CRY1	Cry1	[1]
1408	12953	CRY2	Cry2	[1]
4841	53610	NONO	Nono	[62]
11091	140858	WDR5	Wdr5	[62]
8914	21853	TIMELESS	Timeless	[1, 54]
85457	217732	CIPC	Cipc	[55]
8553	20893	DEC1	Dec1	[65]
79365	79362	DEC2	Dec2	[65]
9575	12753	CLOCK	Clock	[1]
4862	18143	NPAS2	Npas2	[1]
406	11865	BMAL1	Bmal1	[1, 19]
56938	272322	BMAL2	Bmal2	[1, 19]
9572	217166	NR1D1	Nr1d1	[1, 86]
9975	353187	NR1D2	Nr1d2	[1]
6095	19883	RORA	Rora	[1]
6096	225998	RORB	Rorb	[1]
6097	19885	RORC	Rorc	[1]
1628	13170	DBP	Dbp	[87]
4783	18030	NFIL3	Nfil3	[88]
2146	14056	EZH2	Ezh2	[89]
51655	19416	RASD1	Rasd1	[90]
1453	104318	CSNK1D	Csnk1d	[1]
1454	27373	CSNK1E	Csnk1e	[1]
2932	56637	GSK3B	Gsk3b	[1]
1457	12995	CSNK2A1	Csnk2a1	[1, 22]
1459	13000	CSNK2A2	Csnk2a2	[22]
1460	13001	CSNK2B	Csnk2b	[22]
5566	18747	PRKACA	Prkaca	[51]
5578	18750	PRKCA	Prkca	[50]
5499	19045	PPP1CA	Ppp1ca	[1]
5500	19046	PPP1CB	Ppp1cb	[1]
5501	19047	PPP1CC	Ppp1cc	[1]
5515	19052	PPP2CA	Ppp2ca	[1]
5516	19053	PPP2CB	Ppp2cb	[1]

5518	51792	PPP2R1A	Ppp2r1a	[1]
5519	73699	PPP2R1B	Ppp2r1b	[1]
5528	21770	PPP2R5D	Ppp2r5d	[1]
5529	26932	PPP2R5E	Ppp2r5e	[1]
5536	19060	PPP5C	Ppp5c	[91]
8945	12234	BTRC	Btrc	[92]
23291	103583	FBXW11	Fbxw11	[92]
26224	50789	FBXL3	Fbxl3	[21, 52]
79176	68431	FBXL15	Fbxl15	[53]

Table 2. Detected Interactions in Y2H Screen and Interaction Score.

No.	**Gene A h**	**Gene B**	**Gene ID A h**	**Gene ID B h**	**Score**
1	BMAL1	CLOCK	406	9575	4
2	BMAL1	CRY1	406	1407	4
3	BMAL1	CRY2	406	1408	4
4	BMAL1	CSNK2B	406	1460	4
5	BMAL1	DEC1	406	8553	4
6	BMAL1	NPAS2	406	4862	4
7	CIPC	CLOCK	85457	9575	4
8	CIPC	CSNK2B	85457	1460	4
9	CIPC	DEC1	85457	8553	4
10	CIPC	RORC	85457	6097	4
11	CLOCK	CRY1	9575	1407	4
12	CLOCK	CRY2	9575	1408	4
13	CLOCK	DEC1	9575	8553	4
14	CLOCK	DEC2	9575	79365	4
15	CLOCK	NPAS2	9575	4862	4
16	CLOCK	PPP2R5D	9575	5528	4
17	CLOCK	PPP2R5E	9575	5529	4
18	CRY1	CSNK2B	1407	1460	4
19	CRY1	DEC1	1407	8553	4
20	CRY1	DEC2	1407	79365	4
21	CRY1	NPAS2	1407	4862	4
22	CRY1	PER2	1407	8864	4
23	CRY1	PPP2R5E	1407	5529	4
24	CRY2	DEC1	1408	8553	4
25	CRY2	DEC2	1408	79365	4
26	CRY2	PER1	1408	5187	4
27	CRY2	PER2	1408	8864	4
28	CSNK1E	DEC1	1454	8553	4
29	CSNK1E	DEC2	1454	79365	4
30	CSNK1E	PER1	1454	5187	4

31	CSNK1E	PER2	1454	8864	4
32	CSNK1E	PPP1CC	1454	5501	4
33	CSNK1E	PPP2R5E	1454	5529	4
34	CSNK1E	RORC	1454	6097	4
35	CSNK2A1	CSNK2B	1457	1460	4
36	CSNK2A1	DEC1	1457	8553	4
37	CSNK2A1	DEC2	1457	79365	4
38	CSNK2A2	CSNK2B	1459	1460	4
39	CSNK2A2	DEC1	1459	8553	4
40	CSNK2A2	DEC2	1459	79365	4
41	CSNK2A2	NR1D2	1459	9975	4
42	CSNK2B	DEC1	1460	8553	4
43	CSNK2B	DEC2	1460	79365	4
44	CSNK2B	EZH2	1460	2146	4
45	CSNK2B	FBXL15	1460	79176	4
46	CSNK2B	NPAS2	1460	4862	4
47	CSNK2B	PER1	1460	5187	4
48	CSNK2B	PER2	1460	8864	4
49	CSNK2B	PPP1CA	1460	5499	4
50	CSNK2B	PPP1CB	1460	5500	4
51	CSNK2B	PPP1CC	1460	5501	4
52	CSNK2B	PPP2R1A	1460	5518	4
53	CSNK2B	PPP2R1B	1460	5519	4
54	CSNK2B	PPP2R5D	1460	5528	4
55	CSNK2B	PPP2R5E	1460	5529	4
56	DEC1	DEC1	8553	8553	4
57	DEC1	DEC2	8553	79365	4
58	DEC1	EZH2	8553	2146	4
59	DEC1	FBXL15	8553	79176	4
60	DEC1	GSK3B	8553	2932	4
61	DEC1	NPAS2	8553	4862	4
62	DEC1	PER1	8553	5187	4
63	DEC1	PER2	8553	8864	4
64	DEC1	PPP1CA	8553	5499	4
65	DEC1	PPP1CB	8553	5500	4
66	DEC1	PPP1CC	8553	5501	4
67	DEC1	PPP2R1A	8553	5518	4
68	DEC1	PPP2R1B	8553	5519	4
69	DEC1	PPP2R5D	8553	5528	4
70	DEC1	PPP2R5E	8553	5529	4
71	DEC1	RORC	8553	6097	4
72	DEC2	FBXW11	79365	23291	4
73	DEC2	GSK3B	79365	2932	4

74	DEC2	NONO	79365	4841	4
75	DEC2	PPP2R5E	79365	5529	4
76	DEC2	RORC	79365	6097	4
77	FBXW11	PPP1CC	23291	5501	4
78	FBXW11	PPP2R5E	23291	5529	4
79	NONO	NONO	4841	4841	4
80	NPAS2	RORC	4862	6097	4
81	NR1D2	RORC	9975	6097	4
82	PPP1CA	RORC	5499	6097	4
83	PPP1CC	RORC	5501	6097	4
84	PPP2R1A	PPP2R5D	5518	5528	4
85	PPP2R1A	PPP2R5E	5518	5529	4
86	PPP2R1B	PPP2R5D	5519	5528	4
87	PPP2R1B	PPP2R5E	5519	5529	4
88	PPP2R1B	RORC	5519	6097	4
89	PPP2R5D	RORC	5528	6097	4
90	PPP2R5E	RORC	5529	6097	4
91	BMAL1	WDR5	406	11091	3
92	CLOCK	CSNK2B	9575	1460	3
93	CLOCK	PPP2R1B	9575	5519	3
94	CRY2	PPP2R5D	1408	5528	3
95	CSNK1D	PER2	1453	8864	3
96	CSNK2B	PPP2CA	1460	5515	3
97	DEC1	NONO	8553	4841	3
98	DEC1	PPP2CA	8553	5515	3
99	DEC2	DEC2	79365	79365	3
100	DEC2	WDR5	79365	11091	3
101	PER2	RORC	8864	6097	3
102	RORB	RORC	6096	6097	3
103	BMAL1	RORC	406	6097	2
104	CLOCK	NR1D2	9575	9975	2
105	CLOCK	PER2	9575	8864	2
106	CLOCK	PPP1CA	9575	5499	2
107	CLOCK	PPP1CB	9575	5500	2
108	CLOCK	PPP1CC	9575	5501	2
109	CLOCK	RORB	9575	6096	2
110	CRY1	CSNK1E	1407	1454	2
111	CRY1	PER1	1407	5187	2
112	CRY1	PPP2R1B	1407	5519	2
113	CRY1	PPP2R5D	1407	5528	2
114	CRY2	PPP2R1B	1408	5519	2
115	CRY2	PPP2R5E	1408	5529	2
116	CSNK1E	CSNK2B	1454	1460	2

117	CSNK1E	FBXW11	1454	23291	2
118	CSNK1E	NR1D2	1454	9975	2
119	CSNK2B	CSNK2B	1460	1460	2
120	CSNK2B	RORB	1460	6096	2
121	DEC1	NFIL3	8553	4783	2
122	DEC1	NR1D2	8553	9975	2
123	DEC1	RORB	8553	6096	2
124	DEC2	PER2	79365	8864	2
125	DEC2	PPP2R1B	79365	5519	2
126	DEC2	RASD1	79365	51655	2
127	FBXW11	PPP2R1B	23291	5519	2
128	FBXW11	PRKACA	23291	5566	2
129	PPP2R1A	RORC	5518	6097	2
130	PPP2R1B	PPP2R1B	5519	5519	2
131	PPP2R5E	PPP2R5E	5529	5529	2
132	BMAL1	CSNK1E	406	1454	1
133	BMAL2	RORC	56938	6097	1
134	CLOCK	CSNK1E	9575	1454	1
135	CLOCK	DBP	9575	1628	1
136	CLOCK	RORC	9575	6097	1
137	CRY1	NR1D2	1407	9975	1
138	CRY2	EZH2	1408	2146	1
139	CRY2	NPAS2	1408	4862	1
140	CSNK1E	CSNK1E	1454	1454	1
141	CSNK1E	PPP2R5D	1454	5528	1
142	CSNK1E	RORA	1454	6095	1
143	CSNK2B	GSK3B	1460	2932	1
144	DEC2	PPP2CB	79365	5516	1
145	DEC2	RORA	79365	6095	1
146	FBXL15	RORC	79176	6097	1
147	FBXW11	GSK3B	23291	2932	1
148	PPP1CA	PPP2R5E	5499	5529	1
149	PPP1CB	RORC	5500	6097	1
150	PPP2CA	RORC	5515	6097	1

Table 3. Reproduced Protein-Protein Interactions by Y2H Screen.

No.	**Gene A h**	**Gene B h**	**ID A h**	**ID B h**	**Exp. type**	**References**
1	PER1	CSNK1E	5187	1454	In Vivo; In Vitro	[93, 94]
2	PER1	PER2	5187	8864	In Vivo	[93]
3	PER1	CRY2	5187	1408	In Vivo; In Vitro	[95, 96]
4	PER1	CRY1	5187	1407	Y2H; In Vivo	[95, 96]
5	PER2	CSNK1E	8864	1454	In Vitro; In Vivo	[97-99]

6	PER2	CRY2	8864	1408	Y2H; In Vivo	[95, 100]
7	PER2	CRY1	8864	1407	Y2H; In Vivo	[95, 100, 101]
8	PER2	CSNK1D	8864	1453	In Vitro	[102]
9	CRY1	BMAL1	1407	406	Y2H	[103]
10	CRY1	CSNK1E	1407	1454	In Vivo	[104, 105]
11	CRY1	PER1	1407	5187	Y2H; In Vivo	[95, 96]
12	CRY1	PER2	1407	8864	Y2H; In Vivo	[95, 100, 101]
13	DEC1	BMAL1	8553	406	Y2H	[65]
14	DEC1	DEC2	8553	79365	In Vivo	[106]
15	DEC1	DEC1	8553	8553	In Vivo	[106]
16	CLOCK	BMAL1	9575	406	Y2H	[19]
17	NPAS2	BMAL1	4862	406	Y2H; In Vivo	[107, 108]
18	BMAL1	CSNK1E	406	1454	In Vitro	[104, 105]
19	CSNK1E	CSNK1E	1454	1454	In Vitro	[109]
20	CSNK2A1	CSNK2B	1457	1460	Y2H; In Vivo	[110-112]
21	CSNK2B	CSNK2A2	1460	1459	Y2H; In Vivo	[110-112]
22	CSNK2B	CSNK2B	1460	1460	Y2H; In Vivo	[112-114]
23	PPP2R1B	PPP2R5E	5519	5529	In Vivo	[115]
24	PPP2R1B	PPP2R5D	5519	5528	Y2H	[116]
25	PPP2R1B	PPP2R1B	5519	5519	In Vitro	[117]
26	PPP2R5D	PPP2R1A	5528	5518	In Vivo	[118]
27	PPP2R5E	PPP2R1A	5529	5518	In Vivo	[118]
28	PPP2R1B	PPP2R5D	5519	5528	In Vivo	[118]
29	CRY2	CLOCK	1408	9575	Y2H	[95]
30	BMAL1	CRY2	406	1408	Y2H	[103]
31	CLOCK	CRY1	9575	1407	Y2H	[103]
32	CLOCK	CRY2	9575	1408	Y2H	[103]
33	NPAS2	CRY1	4862	1407	Y2H	[103]
34	NPAS2	CRY2	4862	1408	Y2H	[103]
35	DEC1	CLOCK	8553	9575	Y2H	[65]
36	DEC2	CLOCK	79365	9575	Y2H	[65]
37	CIPC	CLOCK	85457	9575	Y2H	[55]
38	NONO	NONO	4841	4841	Y2H	[40]
39	PER2	CSNK2B	8864	1460	In Vivo	[22]
40	BMAL1	CSNK2B	406	1460	In Vivo	[119]
41	CLOCK	PER2	9575	8864	In Vivo	[20, 120]

Table 4. Enriched Interactions from UNIHI Database.

No.	**Gene A h**	**Gene B h**	**Gene ID A h**	**Gene ID B h**	**Source**	**References**
1	ARNTL	PER3	406	8863	UNIHI	[56, 121]
2	CRY1	PER3	1407	8863	UNIHI	[56, 121]
3	CRY1	TIMELESS	1407	8914	UNIHI	[56, 121]
4	CRY2	PPP5C	1408	5536	UNIHI	[56, 121]
5	CRY2	PER3	1408	8863	UNIHI	[56, 121]

6	CRY2	TIMELESS	1408	8914	UNIHI	[56, 121]
7	CSNK1D	PER1	1453	5187	UNIHI	[56, 121]
8	CSNK1D	PER3	1453	8863	UNIHI	[56, 121]
9	CSNK1E	PER3	1454	8863	UNIHI	[56, 121]
10	CSNK2A1	CSNK2A1	1457	1457	UNIHI	[56, 121]
11	GSK3B	PRKACA	2932	5566	UNIHI	[56, 121]
12	GSK3B	GSK3B	2932	2932	UNIHI	[56, 121]
13	GSK3B	PPP1CA	2932	5499	UNIHI	[56, 121]
14	NFIL3	NFIL3	4783	4783	UNIHI	[56, 121]
15	PER1	PER3	5187	8863	UNIHI	[56, 121]
16	PER1	PER2	5187	8864	UNIHI	[56, 121]
17	PER1	TIMELESS	5187	8914	UNIHI	[56, 121]
18	PPP1CA	PPP2CA	5499	5515	UNIHI	[56, 121]
19	PPP1CA	PPP1CA	5499	5499	UNIHI	[56, 121]
20	PPP2CA	PPP2R5E	5515	5529	UNIHI	[56, 121]
21	PPP2CA	PPP2R1A	5515	5518	UNIHI	[56, 121]
22	PPP2R1A	PPP5C	5518	5536	UNIHI	[56, 121]
23	PPP5C	PPP5C	5536	5536	UNIHI	[56, 121]
24	PRKCA	PRKCA	5578	5578	UNIHI	[56, 121]
25	RORA	RORA	6095	6095	UNIHI	[56, 121]
26	PER3	CLOCK	8863	9575	UNIHI	[56, 121]
27	PER3	PER2	8863	8864	UNIHI	[56, 121]
28	PER2	TIMELESS	8864	8914	UNIHI	[56, 121]
29	BTRC	BTRC	8945	8945	UNIHI	[56, 121]
30	NR1D1	NR1D1	9572	9572	UNIHI	[56, 121]
31	CLOCK	ARNTL2	9575	56938	UNIHI	[56, 121]

Table 5. Enriched Interactions from Manual Curation.

No.	**Gene A h**	**Gene B h**	**Gene ID A h**	**Gene ID B h**	**Source**	**References**
1	PER1	PER1	5187	5187	MAN	[122]
2	PER1	PER2	5187	8864	MAN	[122]
3	PER2	PER2	8864	8864	MAN	[122]
4	NONO	PER1	4841	5187	MAN	[122]
5	PER1	WDR5	5187	11091	MAN	[122]
6	NONO	PER2	4841	8864	MAN	[62]
7	PER2	WDR5	8864	11091	MAN	[62]
8	PPP1CA	PER2	5499	8864	MAN	[123]
9	GSK3B	PER2	2932	8864	MAN	[124]
10	CSNK2A1	PER2	1457	8864	MAN	[22]
11	PER2	BTRC	8864	8945	MAN	[92]
12	NFIL3	PER2	4783	8864	MAN	[88, 125]
13	PRKCA	PER2	5578	8864	MAN	[50]
14	CRY1	PPP5C	1407	5536	MAN	[91]
15	CRY2	GSK3B	1408	2932	MAN	[126]

16	CRY1	FBXL3	1407	26224	MAN	[21, 52]
17	CRY2	FBXL3	1408	26224	MAN	[21, 52]
18	CRY2	NFIL3	1408	4783	MAN	[88]
19	ARNTL	DEC2	406	79365	MAN	[65]
20	ARNTL	CSNK2A1	406	1457	MAN	[119]
21	CSNK2A1	PPP2CA	1457	5515	MAN	[127]
22	EZH2	CLOCK	2146	9575	MAN	[89]
23	ARNTL	EZH2	406	2146	MAN	[89]
24	PPP2CA	PPP2CA	5515	5515	MAN	[128]
25	PPP2CA	PPP5C	5515	5536	MAN	[129]
26	PER2	FBXW11	8864	23291	MAN	[92]
27	GSK3B	NR1D1	2932	9572	MAN	[86, 130]
28	PER2	NR1D1	8864	9572	MAN	[131]
29	BTRC	FBXW11	8945	23291	MAN	[132]
30	CRY1	CSNK1D	1407	1453	MAN	[20]
31	CRY2	CSNK1D	1408	1453	MAN	[20]
32	CSNK1E	PPP5C	1454	5536	MAN	[91]

Table 6. Components of Network Extension.

No.	**Gene ID h**	**Gene ID m**	**Symbol h**	**Symbol m**	**Source**
1	207	11651	AKT1	Akt1	UNIHI
2	367	11835	AR	Ar	UNIHI
3	466	11908	ATF1	Atf1	UNIHI
4	1050	12606	CEBPA	Cebpa	UNIHI
5	1111	12649	CHEK1	Chek1	UNIHI
6	1387	12914	CREBBP	Crebbp	UNIHI
7	1390	12916	CREM	Crem	UNIHI
8	1649	13198	DDIT3	Ddit3	UNIHI
9	2033	328572	EP300	Ep300	UNIHI
10	2034	13819	EPAS1	Epas1	UNIHI
11	3054	15161	HCFC1	Hcfc1	UNIHI
12	3065	433759	HDAC1	Hdac1	UNIHI
13	3091	15251	HIF1A	Hif1a	UNIHI
14	3320	15519	HSP90AA1	Hsp90aa1	UNIHI
15	4163	328949	MCC	Mcc	UNIHI
16	4609	17869	MYC	Myc	UNIHI
17	4654	17927	MYOD1	Myod1	UNIHI
18	4830	18102	NME1	Nme1	UNIHI
19	4831	18103	NME2	Nme2	UNIHI
20	4842	18125	NOS1	Nos1	UNIHI
21	5111	18538	PCNA	Pcna	UNIHI
22	6667	20683	SP1	Sp1	UNIHI
23	8850	18519	KAT2B	Kat2b	UNIHI
24	9611	20185	NCOR1	Ncor1	UNIHI

25	190	11614	NR0B1	Nr0b1	UNIHI
26	196	11622	AHR	Ahr	UNIHI
27	546	22589	ATRX	Atrx	UNIHI
28	760	12349	CA2	Car2	UNIHI
29	1054	12611	CEBPG	Cebpg	UNIHI
30	1108	107932	CHD4	Chd4	UNIHI
31	1642	13194	DDB1	Ddb1	UNIHI
32	1786	13433	DNMT1	Dnmt1	UNIHI
33	1788	13435	DNMT3A	Dnmt3a	UNIHI
34	1789	13436	DNMT3B	Dnmt3b	UNIHI
35	1810	13486	DR1	Dr1	UNIHI
36	1822	13498	ATN1	Atn1	UNIHI
37	1876	50496	E2F6	E2f6	UNIHI
38	2770	14677	GNAI1	Gnai1	UNIHI
39	2771	14678	GNAI2	Gnai2	UNIHI
40	2782	14688	GNB1	Gnb1	UNIHI
41	4221	17283	MEN1	Men1	UNIHI
42	4297	214162	MLL	Mll1	UNIHI
43	5469	19014	MED1	Med1	UNIHI
44	5705	19184	PSMC5	Psmc5	UNIHI
45	5929	213464	RBBP5	Rbbp5	UNIHI
46	6774	20848	STAT3	Stat3	UNIHI
47	7329	22196	UBE2I	Ube2i	UNIHI
48	8450	72584	CUL4B	Cul4b	UNIHI
49	8451	99375	CUL4A	Cul4a	UNIHI
50	9070	23808	ASH2L	Ash2l	UNIHI
51	9410	66585	WDR57	Wdr57	UNIHI
52	9722	70729	NOS1AP	Nos1ap	UNIHI
53	3131	217082	HLF	Hlf	UNIHI
54	3066	15182	HDAC2	Hdac2	UNIHI
55	6688	20375	SPI1	Sfpi1	UNIHI
56	5914	19401	RARA	Rara	UNIHI
57	8726	13626	EED	Eed	UNIHI
58	5829	19303	PXN	Pxn	UNIHI
59	7414	22330	VCL	Vcl	UNIHI
60	266743	225872	NPAS4	Npas4	UNIHI
61	7008	21685	TEF	Tef	UNIHI
62	5371	18854	PML	Pml	UNIHI
63	7409	22324	VAV1	Vav1	UNIHI
64	23512	52615	SUZ12	Suz12	UNIHI
65	23649	18969	POLA2	Pola2	UNIHI
66	5252	21652	PHF1	Phf1	UNIHI
67	10538	53314	BATF	Batf	UNIHI
68	90993	26427	CREB3L1	Creb3l1	UNIHI
69	10488	12913	CREB3	Creb3	UNIHI

70	5430	20020	POLR2A	Polr2a	UNIHI
71	6421	71514	SFPQ	Sfpq	UNIHI
72	55269	66645	PSPC1	Pspc1	UNIHI
73	6256	20181	RXRA	Rxra	UNIHI
74	8202	17979	NCOA3	Ncoa3	UNIHI
75	9737	67298	GPRASP1	Gprasp1	UNIHI
76	10499	17978	NCOA2	Ncoa2	UNIHI
77	55885	109593	LMO3	Lmo3	UNIHI
78	8648	17977	NCOA1	Ncoa1	UNIHI
79	83714	60345	NRIP2	Nrip2	UNIHI
80	11277	22040	TREX1	Trex1	UNIHI
81	54962	66131	TIPIN	Tipin	UNIHI
82	9612	20602	NCOR2	Ncor2	UNIHI
83	10002	23958	NR2E3	Nr2e3	UNIHI
84	57727	228869	NCOA5	Ncoa5	UNIHI
85	23178	269224	PASK	Pask	UNIHI
86	29915	67933	HCFC2	Hcfc2	UNIHI
87	51514	76843	DTL	Dtl	UNIHI
88	83743	101612	GRWD1	Grwd1	UNIHI

Table 7. Additional Interactions of Neighborhood Components.

No.	**Gene ID A h**	**Gene ID B h**	**Gene A h**	**Gene B h**	**Source**
1	190	6095	NR0B1	RORA	UNIHI
2	196	406	AHR	ARNTL	UNIHI
3	207	2146	AKT1	EZH2	UNIHI
4	367	4841	AR	NONO	UNIHI
5	406	2033	ARNTL	EP300	UNIHI
6	406	2034	ARNTL	EPAS1	UNIHI
7	406	3091	ARNTL	HIF1A	UNIHI
8	406	3320	ARNTL	HSP90AA1	UNIHI
9	406	8850	ARNTL	KAT2B	UNIHI
10	406	3131	ARNTL	HLF	UNIHI
11	406	266743	ARNTL	NPAS4	UNIHI
12	466	4783	ATF1	NFIL3	UNIHI
13	546	2146	ATRX	EZH2	UNIHI
14	760	4841	CA2	NONO	UNIHI
15	1050	1628	CEBPA	DBP	UNIHI
16	1054	4783	CEBPG	NFIL3	UNIHI
17	1108	6097	CHD4	RORC	UNIHI
18	1111	8914	CHEK1	TIMELESS	UNIHI
19	1387	4862	CREBBP	NPAS2	UNIHI
20	1390	4783	CREM	NFIL3	UNIHI
21	1628	2033	DBP	EP300	UNIHI

22	1628	3131	DBP	HLF	UNIHI
23	1628	7008	DBP	TEF	UNIHI
24	1642	11091	DDB1	WDR5	UNIHI
25	1649	4783	DDIT3	NFIL3	UNIHI
26	1786	2146	DNMT1	EZH2	UNIHI
27	1788	2146	DNMT3A	EZH2	UNIHI
28	1789	2146	DNMT3B	EZH2	UNIHI
29	1810	4783	DR1	NFIL3	UNIHI
30	1822	11091	ATN1	WDR5	UNIHI
31	1876	2146	E2F6	EZH2	UNIHI
32	2033	9575	EP300	CLOCK	UNIHI
33	2033	4862	EP300	NPAS2	UNIHI
34	2033	6095	EP300	RORA	UNIHI
35	2034	56938	EPAS1	ARNTL2	UNIHI
36	2146	3065	EZH2	HDAC1	UNIHI
37	2146	3066	EZH2	HDAC2	UNIHI
38	2146	5371	EZH2	PML	UNIHI
39	2146	5914	EZH2	RARA	UNIHI
40	2146	7409	EZH2	VAV1	UNIHI
41	2146	8726	EZH2	EED	UNIHI
42	2146	23512	EZH2	SUZ12	UNIHI
43	2146	23649	EZH2	POLA2	UNIHI
44	2146	5252	EZH2	PHF1	UNIHI
45	2770	51655	GNAI1	RASD1	UNIHI
46	2771	51655	GNAI2	RASD1	UNIHI
47	2782	51655	GNB1	RASD1	UNIHI
48	3054	11091	HCFC1	WDR5	UNIHI
49	3091	5187	HIF1A	PER1	UNIHI
50	3320	4862	HSP90AA1	NPAS2	UNIHI
51	4163	11091	MCC	WDR5	UNIHI
52	4221	11091	MEN1	WDR5	UNIHI
53	4297	11091	MLL	WDR5	UNIHI
54	4609	11091	MYC	WDR5	UNIHI
55	4654	79365	MYOD1	BHLHE41	UNIHI
56	4654	6095	MYOD1	RORA	UNIHI
57	4783	10538	NFIL3	BATF	UNIHI
58	4783	90993	NFIL3	CREB3L1	UNIHI
59	4783	10488	NFIL3	CREB3	UNIHI
60	4830	6095	NME1	RORA	UNIHI
61	4830	6096	NME1	RORB	UNIHI
62	4831	6095	NME2	RORA	UNIHI
63	4831	6096	NME2	RORB	UNIHI
64	4841	5111	NONO	PCNA	UNIHI

65	4841	5430	NONO	POLR2A	UNIHI
66	4841	5829	NONO	PXN	UNIHI
67	4841	6421	NONO	SFPQ	UNIHI
68	4841	6688	NONO	SPI1	UNIHI
69	4841	7414	NONO	VCL	UNIHI
70	4841	55269	NONO	PSPC1	UNIHI
71	4842	51655	NOS1	RASD1	UNIHI
72	4862	5914	NPAS2	RARA	UNIHI
73	4862	6256	NPAS2	RXRA	UNIHI
74	4862	8202	NPAS2	NCOA3	UNIHI
75	4862	8850	NPAS2	KAT2B	UNIHI
76	5187	9737	PER1	GPRASP1	UNIHI
77	5469	6095	MED1	RORA	UNIHI
78	5705	6095	PSMC5	RORA	UNIHI
79	5929	11091	RBBP5	WDR5	UNIHI
80	6095	10499	RORA	NCOA2	UNIHI
81	6095	55885	RORA	LMO3	UNIHI
82	6096	8648	RORB	NCOA1	UNIHI
83	6096	83714	RORB	NRIP2	UNIHI
84	6667	8863	SP1	PER3	UNIHI
85	6774	8553	STAT3	BHLHE40	UNIHI
86	7329	8553	UBE2I	BHLHE40	UNIHI
87	8450	11091	CUL4B	WDR5	UNIHI
88	8451	11091	CUL4A	WDR5	UNIHI
89	8850	9575	KAT2B	CLOCK	UNIHI
90	8914	11277	TIMELESS	TREX1	UNIHI
91	8914	54962	TIMELESS	TIPIN	UNIHI
92	9070	11091	ASH2L	WDR5	UNIHI
93	9410	11091	SNRNP40	WDR5	UNIHI
94	9572	9611	NR1D1	NCOR1	UNIHI
95	9572	9612	NR1D1	NCOR2	UNIHI
96	9572	10002	NR1D1	NR2E3	UNIHI
97	9611	9975	NCOR1	NR1D2	UNIHI
98	9722	51655	NOS1AP	RASD1	UNIHI
99	9975	57727	NR1D2	NCOA5	UNIHI
100	11091	23178	WDR5	PASK	UNIHI
101	11091	29915	WDR5	HCFC2	UNIHI
102	11091	51514	WDR5	DTL	UNIHI
103	11091	83743	WDR5	GRWD1	UNIHI
104	190	367	NR0B1	AR	UNIHI
105	196	10499	AHR	NCOA2	UNIHI
106	196	9612	AHR	NCOR2	UNIHI
107	196	2033	AHR	EP300	UNIHI

108	196	3320	AHR	HSP90AA1	UNIHI
109	196	8648	AHR	NCOA1	UNIHI
110	196	196	AHR	AHR	UNIHI
111	196	6667	AHR	SP1	UNIHI
112	207	2033	AKT1	EP300	UNIHI
113	207	3320	AKT1	HSP90AA1	UNIHI
114	207	367	AKT1	AR	UNIHI
115	207	2932	AKT1	GSK3B	UNIHI
116	207	1111	AKT1	CHEK1	UNIHI
117	207	207	AKT1	AKT1	UNIHI
118	207	5515	AKT1	PPP2CA	UNIHI
119	367	10499	AR	NCOA2	UNIHI
120	367	1387	AR	CREBBP	UNIHI
121	367	9612	AR	NCOR2	UNIHI
122	367	9611	AR	NCOR1	UNIHI
123	367	6667	AR	SP1	UNIHI
124	367	2033	AR	EP300	UNIHI
125	367	3065	AR	HDAC1	UNIHI
126	367	6774	AR	STAT3	UNIHI
127	367	3320	AR	HSP90AA1	UNIHI
128	367	367	AR	AR	UNIHI
129	367	5829	AR	PXN	UNIHI
130	367	8850	AR	KAT2B	UNIHI
131	367	8202	AR	NCOA3	UNIHI
132	367	8648	AR	NCOA1	UNIHI
133	367	5469	AR	MED1	UNIHI
134	367	7329	AR	UBE2I	UNIHI
135	367	55269	AR	PSPC1	UNIHI
136	367	2932	AR	GSK3B	UNIHI
137	367	3091	AR	HIF1A	UNIHI
138	466	1457	ATF1	CSNK2A1	UNIHI
139	466	1387	ATF1	CREBBP	UNIHI
140	466	5566	ATF1	PRKACA	UNIHI
141	466	1459	ATF1	CSNK2A2	UNIHI
142	466	466	ATF1	ATF1	UNIHI
143	466	1390	ATF1	CREM	UNIHI
144	466	6688	ATF1	SPI1	UNIHI
145	466	1460	ATF1	CSNK2B	UNIHI
146	546	3065	ATRX	HDAC1	UNIHI
147	546	1822	ATRX	ATN1	UNIHI
148	1050	1387	CEBPA	CREBBP	UNIHI
149	1050	4609	CEBPA	MYC	UNIHI
150	1050	2033	CEBPA	EP300	UNIHI

151	1050	1050	CEBPA	CEBPA	UNIHI
152	1050	6688	CEBPA	SPI1	UNIHI
153	1050	2932	CEBPA	GSK3B	UNIHI
154	1050	1054	CEBPA	CEBPG	UNIHI
155	1050	10538	CEBPA	BATF	UNIHI
156	1054	1054	CEBPG	CEBPG	UNIHI
157	1054	3131	CEBPG	HLF	UNIHI
158	1054	7008	CEBPG	TEF	UNIHI
159	1054	10488	CEBPG	CREB3	UNIHI
160	1054	10538	CEBPG	BATF	UNIHI
161	1054	90993	CEBPG	CREB3L1	UNIHI
162	1054	1649	CEBPG	DDIT3	UNIHI
163	1108	2033	CHD4	EP300	UNIHI
164	1108	3065	CHD4	HDAC1	UNIHI
165	1108	3066	CHD4	HDAC2	UNIHI
166	1108	4609	CHD4	MYC	UNIHI
167	1111	3320	CHEK1	HSP90AA1	UNIHI
168	1111	1460	CHEK1	CSNK2B	UNIHI
169	1111	8451	CHEK1	CUL4A	UNIHI
170	1111	1457	CHEK1	CSNK2A1	UNIHI
171	1387	1457	CREBBP	CSNK2A1	UNIHI
172	1387	10499	CREBBP	NCOA2	UNIHI
173	1387	5371	CREBBP	PML	UNIHI
174	1387	6774	CREBBP	STAT3	UNIHI
175	1387	1459	CREBBP	CSNK2A2	UNIHI
176	1387	4297	CREBBP	MLL	UNIHI
177	1387	4654	CREBBP	MYOD1	UNIHI
178	1387	1387	CREBBP	CREBBP	UNIHI
179	1387	8648	CREBBP	NCOA1	UNIHI
180	1387	2033	CREBBP	EP300	UNIHI
181	1387	8850	CREBBP	KAT2B	UNIHI
182	1387	3065	CREBBP	HDAC1	UNIHI
183	1387	1390	CREBBP	CREM	UNIHI
184	1387	3131	CREBBP	HLF	UNIHI
185	1387	6688	CREBBP	SPI1	UNIHI
186	1387	4609	CREBBP	MYC	UNIHI
187	1387	8202	CREBBP	NCOA3	UNIHI
188	1387	3091	CREBBP	HIF1A	UNIHI
189	1387	5430	CREBBP	POLR2A	UNIHI
190	1390	1457	CREM	CSNK2A1	UNIHI
191	1390	5578	CREM	PRKCA	UNIHI
192	1390	5566	CREM	PRKACA	UNIHI
193	1390	2932	CREM	GSK3B	UNIHI

194	1390	1459	CREM	CSNK2A2	UNIHI
195	1390	6688	CREM	SPI1	UNIHI
196	1390	1390	CREM	CREM	UNIHI
197	1390	90993	CREM	CREB3L1	UNIHI
198	1453	4163	CSNK1D	MCC	UNIHI
199	1454	4163	CSNK1E	MCC	UNIHI
200	1457	3065	CSNK2A1	HDAC1	UNIHI
201	1457	3066	CSNK2A1	HDAC2	UNIHI
202	1457	1649	CSNK2A1	DDIT3	UNIHI
203	1457	3320	CSNK2A1	HSP90AA1	UNIHI
204	1457	6667	CSNK2A1	SP1	UNIHI
205	1457	4609	CSNK2A1	MYC	UNIHI
206	1457	3091	CSNK2A1	HIF1A	UNIHI
207	1457	6688	CSNK2A1	SPI1	UNIHI
208	1459	4609	CSNK2A2	MYC	UNIHI
209	1459	3065	CSNK2A2	HDAC1	UNIHI
210	1459	3320	CSNK2A2	HSP90AA1	UNIHI
211	1459	3066	CSNK2A2	HDAC2	UNIHI
212	1642	8451	DDB1	CUL4A	UNIHI
213	1642	9410	DDB1	SNRNP40	UNIHI
214	1642	5929	DDB1	RBBP5	UNIHI
215	1642	8450	DDB1	CUL4B	UNIHI
216	1642	51514	DDB1	DTL	UNIHI
217	1649	10538	DDIT3	BATF	UNIHI
218	1649	3131	DDIT3	HLF	UNIHI
219	1649	1649	DDIT3	DDIT3	UNIHI
220	1649	7008	DDIT3	TEF	UNIHI
221	1649	10488	DDIT3	CREB3	UNIHI
222	1786	5111	DNMT1	PCNA	UNIHI
223	1786	3065	DNMT1	HDAC1	UNIHI
224	1786	3066	DNMT1	HDAC2	UNIHI
225	1786	1786	DNMT1	DNMT1	UNIHI
226	1786	1788	DNMT1	DNMT3A	UNIHI
227	1786	1789	DNMT1	DNMT3B	UNIHI
228	1788	4609	DNMT3A	MYC	UNIHI
229	1788	3065	DNMT3A	HDAC1	UNIHI
230	1788	7329	DNMT3A	UBE2I	UNIHI
231	1788	1789	DNMT3A	DNMT3B	UNIHI
232	1789	3065	DNMT3B	HDAC1	UNIHI
233	1789	3066	DNMT3B	HDAC2	UNIHI
234	1789	7329	DNMT3B	UBE2I	UNIHI
235	1822	1822	ATN1	ATN1	UNIHI
236	2033	10499	EP300	NCOA2	UNIHI

237	2033	5371	EP300	PML	UNIHI
238	2033	6667	EP300	SP1	UNIHI
239	2033	4609	EP300	MYC	UNIHI
240	2033	6774	EP300	STAT3	UNIHI
241	2033	4654	EP300	MYOD1	UNIHI
242	2033	5111	EP300	PCNA	UNIHI
243	2033	8202	EP300	NCOA3	UNIHI
244	2033	3091	EP300	HIF1A	UNIHI
245	2033	8850	EP300	KAT2B	UNIHI
246	2033	2033	EP300	EP300	UNIHI
247	2033	8648	EP300	NCOA1	UNIHI
248	2033	2034	EP300	EPAS1	UNIHI
249	2033	7329	EP300	UBE2I	UNIHI
250	2033	5430	EP300	POLR2A	UNIHI
251	2770	2770	GNAI1	GNAI1	UNIHI
252	2782	4831	GNB1	NME2	UNIHI
253	2782	4163	GNB1	MCC	UNIHI
254	2932	4609	GSK3B	MYC	UNIHI
255	2932	5829	GSK3B	PXN	UNIHI
256	3054	6667	HCFC1	SP1	UNIHI
257	3054	3054	HCFC1	HCFC1	UNIHI
258	3054	10488	HCFC1	CREB3	UNIHI
259	3054	5501	HCFC1	PPP1CC	UNIHI
260	3054	3065	HCFC1	HDAC1	UNIHI
261	3054	3320	HCFC1	HSP90AA1	UNIHI
262	3054	3066	HCFC1	HDAC2	UNIHI
263	3054	29915	HCFC1	HCFC2	UNIHI
264	3054	4221	HCFC1	MEN1	UNIHI
265	3054	5929	HCFC1	RBBP5	UNIHI
266	3054	9070	HCFC1	ASH2L	UNIHI
267	3054	4297	HCFC1	MLL	UNIHI
268	3065	5371	HDAC1	PML	UNIHI
269	3065	9612	HDAC1	NCOR2	UNIHI
270	3065	6667	HDAC1	SP1	UNIHI
271	3065	5111	HDAC1	PCNA	UNIHI
272	3065	6774	HDAC1	STAT3	UNIHI
273	3065	4654	HDAC1	MYOD1	UNIHI
274	3065	3065	HDAC1	HDAC1	UNIHI
275	3065	3066	HDAC1	HDAC2	UNIHI
276	3065	7329	HDAC1	UBE2I	UNIHI
277	3065	8726	HDAC1	EED	UNIHI
278	3065	3091	HDAC1	HIF1A	UNIHI
279	3065	4297	HDAC1	MLL	UNIHI

280	3065	4609	HDAC1	MYC	UNIHI
281	3065	5519	HDAC1	PPP2R1B	UNIHI
282	3065	5518	HDAC1	PPP2R1A	UNIHI
283	3066	5371	HDAC2	PML	UNIHI
284	3066	6667	HDAC2	SP1	UNIHI
285	3066	6774	HDAC2	STAT3	UNIHI
286	3066	8726	HDAC2	EED	UNIHI
287	3066	9612	HDAC2	NCOR2	UNIHI
288	3066	3091	HDAC2	HIF1A	UNIHI
289	3066	3066	HDAC2	HDAC2	UNIHI
290	3066	4609	HDAC2	MYC	UNIHI
291	3091	10499	HIF1A	NCOA2	UNIHI
292	3091	3320	HIF1A	HSP90AA1	UNIHI
293	3091	8648	HIF1A	NCOA1	UNIHI
294	3091	8850	HIF1A	KAT2B	UNIHI
295	3131	10538	HLF	BATF	UNIHI
296	3131	3131	HLF	HLF	UNIHI
297	3131	7008	HLF	TEF	UNIHI
298	3320	4609	HSP90AA1	MYC	UNIHI
299	3320	6774	HSP90AA1	STAT3	UNIHI
300	3320	3320	HSP90AA1	HSP90AA1	UNIHI
301	3320	4842	HSP90AA1	NOS1	UNIHI
302	3320	4654	HSP90AA1	MYOD1	UNIHI
303	3320	5536	HSP90AA1	PPP5C	UNIHI
304	4163	5518	MCC	PPP2R1A	UNIHI
305	4163	5516	MCC	PPP2CB	UNIHI
306	4163	5111	MCC	PCNA	UNIHI
307	4221	5929	MEN1	RBBP5	UNIHI
308	4221	9070	MEN1	ASH2L	UNIHI
309	4221	29915	MEN1	HCFC2	UNIHI
310	4221	4297	MEN1	MLL	UNIHI
311	4297	4297	MLL	MLL	UNIHI
312	4297	5929	MLL	RBBP5	UNIHI
313	4297	9070	MLL	ASH2L	UNIHI
314	4297	29915	MLL	HCFC2	UNIHI
315	4609	5371	MYC	PML	UNIHI
316	4609	6667	MYC	SP1	UNIHI
317	4609	8850	MYC	KAT2B	UNIHI
318	4609	5430	MYC	POLR2A	UNIHI
319	4609	5499	MYC	PPP1CA	UNIHI
320	4654	9612	MYOD1	NCOR2	UNIHI
321	4654	6667	MYOD1	SP1	UNIHI
322	4654	6774	MYOD1	STAT3	UNIHI

323	4654	4654	MYOD1	MYOD1	UNIHI
324	4654	5578	MYOD1	PRKCA	UNIHI
325	4654	6256	MYOD1	RXRA	UNIHI
326	4654	8850	MYOD1	KAT2B	UNIHI
327	4654	9611	MYOD1	NCOR1	UNIHI
328	4830	4830	NME1	NME1	UNIHI
329	4831	5515	NME2	PPP2CA	UNIHI
330	4831	4831	NME2	NME2	UNIHI
331	4831	5518	NME2	PPP2R1A	UNIHI
332	4842	5578	NOS1	PRKCA	UNIHI
333	4842	5566	NOS1	PRKACA	UNIHI
334	4842	9722	NOS1	NOS1AP	UNIHI
335	5111	5111	PCNA	PCNA	UNIHI
336	5111	5501	PCNA	PPP1CC	UNIHI
337	5371	5371	PML	PML	UNIHI
338	5371	6774	PML	STAT3	UNIHI
339	5371	9612	PML	NCOR2	UNIHI
340	5371	9611	PML	NCOR1	UNIHI
341	5371	5914	PML	RARA	UNIHI
342	5371	6667	PML	SP1	UNIHI
343	5371	6256	PML	RXRA	UNIHI
344	5371	23512	PML	SUZ12	UNIHI
345	5430	8850	POLR2A	KAT2B	UNIHI
346	5469	5914	MED1	RARA	UNIHI
347	5469	6256	MED1	RXRA	UNIHI
348	5469	5469	MED1	MED1	UNIHI
349	5499	8726	PPP1CA	EED	UNIHI
350	5515	5829	PPP2CA	PXN	UNIHI
351	5578	5914	PRKCA	RARA	UNIHI
352	5578	7414	PRKCA	VCL	UNIHI
353	5705	6667	PSMC5	SP1	UNIHI
354	5705	6256	PSMC5	RXRA	UNIHI
355	5829	7414	PXN	VCL	UNIHI
356	5829	5829	PXN	PXN	UNIHI
357	5829	6421	PXN	SFPQ	UNIHI
358	5914	9612	RARA	NCOR2	UNIHI
359	5914	6256	RARA	RXRA	UNIHI
360	5914	6667	RARA	SP1	UNIHI
361	5914	8648	RARA	NCOA1	UNIHI
362	5914	10002	RARA	NR2E3	UNIHI
363	5914	8850	RARA	KAT2B	UNIHI
364	5914	83714	RARA	NRIP2	UNIHI
365	5914	8202	RARA	NCOA3	UNIHI

366	5914	5914	RARA	RARA	UNIHI
367	5929	8450	RBBP5	CUL4B	UNIHI
368	5929	8451	RBBP5	CUL4A	UNIHI
369	5929	9070	RBBP5	ASH2L	UNIHI
370	5929	29915	RBBP5	HCFC2	UNIHI
371	6256	10499	RXRA	NCOA2	UNIHI
372	6256	9612	RXRA	NCOR2	UNIHI
373	6256	6667	RXRA	SP1	UNIHI
374	6256	8648	RXRA	NCOA1	UNIHI
375	6256	8202	RXRA	NCOA3	UNIHI
376	6256	6256	RXRA	RXRA	UNIHI
377	6421	55269	SFPQ	PSPC1	UNIHI
378	6667	9612	SP1	NCOR2	UNIHI
379	6667	9611	SP1	NCOR1	UNIHI
380	6667	6667	SP1	SP1	UNIHI
381	6667	9070	SP1	ASH2L	UNIHI
382	6774	6774	STAT3	STAT3	UNIHI
383	6774	8648	STAT3	NCOA1	UNIHI
384	7008	10538	TEF	BATF	UNIHI
385	7008	7008	TEF	TEF	UNIHI
386	7414	7414	VCL	VCL	UNIHI
387	8202	9612	NCOA3	NCOR2	UNIHI
388	8202	8202	NCOA3	NCOA3	UNIHI
389	8202	8850	NCOA3	KAT2B	UNIHI
390	8450	9410	CUL4B	SNRNP40	UNIHI
391	8450	8451	CUL4B	CUL4A	UNIHI
392	8450	83743	CUL4B	GRWD1	UNIHI
393	8450	51514	CUL4B	DTL	UNIHI
394	8648	8648	NCOA1	NCOA1	UNIHI
395	8648	8850	NCOA1	KAT2B	UNIHI
396	8648	9611	NCOA1	NCOR1	UNIHI
397	8648	10499	NCOA1	NCOA2	UNIHI
398	8726	8726	EED	EED	UNIHI
399	8850	8850	KAT2B	KAT2B	UNIHI
400	9070	9070	ASH2L	ASH2L	UNIHI
401	9070	29915	ASH2L	HCFC2	UNIHI
402	9410	9410	SNRNP40	SNRNP40	UNIHI
403	9410	83743	SNRNP40	GRWD1	UNIHI
404	9611	9611	NCOR1	NCOR1	UNIHI
405	9611	9612	NCOR1	NCOR2	UNIHI
406	10488	90993	CREB3	CREB3L1	UNIHI
407	10488	10488	CREB3	CREB3	UNIHI
408	10499	10499	NCOA2	NCOA2	UNIHI

409	10538	10538	BATF	BATF	UNIHI
410	23178	23178	PASK	PASK	UNIHI
411	51514	83743	DTL	GRWD1	UNIHI
412	90993	90993	CREB3L1	CREB3L1	UNIHI

Table 8. Hits of RNAi Screen of Network Neighborhood.

Gene ID h	**RNAi construt**	**Period**	**Delta period**	**Amp**	**Damp**	**Corr. coeff.**	**Hit**
367	AR_1	23.22	-0.78	0.53	55.55	0.98	sp
367	AR_2	23.07	-0.93	0.44	35.72	0.96	sp
1108	CHD4_1	24.58	0.58	0.31	47.15	0.93	lp
1108	CHD4_2	25.55	1.55	0.49	29.98	0.93	lp
1111	CHEK1_1	23.06	-0.94	0.36	48.17	0.95	sp
1111	CHEK1_2	22.56	-1.44	0.41	32.16	0.94	sp
90993	CREB3L1	23.48	-0.52	0.44	38.10	0.98	sp
8450	CUL4B	23.41	-0.59	0.36	32.47	0.97	sp
1642	DDB1_1	23.21	-0.79	0.64	35.33	0.96	sp
1642	DDB1_2	23.75	-0.25	0.33	28.98	0.859	ar
1810	DR1	23.33	-0.67	0.48	34.28	0.97	sp
9737	GPRASP1	23.17	-0.83	0.45	32.41	0.94	sp
3066	HDAC2	24.88	0.88	0.41	32.03	0.98	lp
4654	MYOD1	24.56	0.56	0.57	41.58	0.98	lp
8202	NCOA3_1	24.77	0.77	0.46	43.33	0.98	lp
8202	NCOA3_2	24.56	0.56	0.54	34.76	0.98	lp
190	NR0B1_1	24.85	0.85	0.52	39.83	0.97	lp
190	NR0B1_2	25.29	1.29	0.43	43.24	0.93	lp
23178	PASK	23.44	-0.56	0.55	43.52	0.95	sp
5111	PCNA	22.12	-1.88	0.35	22.27	0.95	sp
5111	PCNA	23.34	-0.66	0.48	34.88	0.95	sp
5430	POLR2A	25.38	1.38	0.63	40.65	0.98	lp
5705	PSMC5_1	25.57	1.57	0.38	17.08	0.91	lp
5705	PSMC5_2	25.11	1.11	0.22	8.38	0.96	lp
5929	RBBP5_1	23.41	-0.59	0.56	45.34	0.97	sp
5929	RBBP5_2	23.49	-0.51	0.57	40.86	0.97	sp
6688	SPI1	25.00	1.00	0.50	34.84	0.98	lp
7008	TEF_1	23.19	-0.81	0.53	34.36	0.96	sp
7008	TEF_2	23.05	-0.95	0.54	33.32	0.95	sp
7329	UBE2I_2	24.52	0.52	0.51	39.22	0.98	lp
7329	UBE2I_2	26.53	2.53	0.19	274.01	0.75	lp, ar
7409	VAV1_1	25.13	1.13	0.52	41.71	0.97	lp
7409	VAV1_2	25.39	1.39	0.64	44.22	0.96	lp

Table 9. Interaction Dynamics within the Circadian PPI Network.

No.	Gene ID h A	Gene ID h B	Sym. h A	Sym. h B	FDR PPI	Time PPI CT
1	406	9575	ARNTL	CLOCK	0.00000	22.6
2	406	4862	ARNTL	NPAS2	0.00000	23.5
3	406	1407	ARNTL	CRY1	0.00000	21.2
4	406	1408	ARNTL	CRY2	0.00000	22.5
5	406	1460	ARNTL	CSNK2B	0.00000	22.5
6	406	8553	ARNTL	BHLHE40	0.00000	21.5
7	406	11091	ARNTL	WDR5	0.00000	22.5
8	406	6097	ARNTL	RORC	0.00000	21.1
9	406	1454	ARNTL	CSNK1E	0.00000	22.1
10	1407	5528	CRY1	PPP2R5D	0.00000	19.8
11	1407	5529	CRY1	PPP2R5E	0.00000	19.4
12	1407	9575	CRY1	CLOCK	0.00000	20.7
13	1407	4862	CRY1	NPAS2	0.00000	22.1
14	1407	79365	CRY1	BHLHE41	0.00000	19.6
15	1407	5519	CRY1	PPP2R1B	0.00000	20.5
16	1407	5187	CRY1	PER1	0.00000	18.6
17	1407	1460	CRY1	CSNK2B	0.00000	19.9
18	1407	1454	CRY1	CSNK1E	0.00000	19.6
19	1407	9975	CRY1	NR1D2	0.00000	16.7
20	1407	8553	CRY1	BHLHE40	0.00000	18.6
21	1407	8864	CRY1	PER2	0.00000	17.1
22	1408	9575	CRY2	CLOCK	0.00000	0
23	1408	4862	CRY2	NPAS2	0.00000	1.6
24	1408	8864	CRY2	PER2	0.00000	13.5
25	1453	8864	CSNK1D	PER2	0.00000	14
26	1454	5529	CSNK1E	PPP2R5E	0.00000	13.3
27	1454	9575	CSNK1E	CLOCK	0.00000	22.4
28	1454	5187	CSNK1E	PER1	0.00000	12.4
29	1454	8864	CSNK1E	PER2	0.00000	14.2
30	1454	6097	CSNK1E	RORC	0.00000	18.5
31	1454	9975	CSNK1E	NR1D2	0.00000	10.1
32	1459	9975	CSNK2A2	NR1D2	0.00000	9.1
33	1460	9575	CSNK2B	CLOCK	0.00000	23.5
34	1460	4862	CSNK2B	NPAS2	0.00000	1.1
35	1460	8864	CSNK2B	PER2	0.00000	13.9
36	1628	9575	DBP	CLOCK	0.00000	9.9
37	4841	4841	NONO	NONO	0.00000	4.1
38	4862	9575	NPAS2	CLOCK	0.00000	0.3
39	4862	6097	NPAS2	RORC	0.00000	22.2
40	5187	8553	PER1	BHLHE40	0.00000	11.9
41	5499	9575	PPP1CA	CLOCK	0.00000	23.5
42	5499	6097	PPP1CA	RORC	0.00000	18.9

43	5500	9575	PPP1CB	CLOCK	0.00000	22.8
44	5500	6097	PPP1CB	RORC	0.00000	18.6
45	5501	9575	PPP1CC	CLOCK	0.00000	23.6
46	5501	6097	PPP1CC	RORC	0.00000	18.4
47	5501	23291	PPP1CC	FBXW11	0.00000	6.9
48	5515	6097	PPP2CA	RORC	0.00000	18.4
49	5518	6097	PPP2R1A	RORC	0.00000	19.5
50	5519	5528	PPP2R1B	PPP2R5D	0.00000	3.5
51	5519	9575	PPP2R1B	CLOCK	0.00000	0.1
52	5519	6097	PPP2R1B	RORC	0.00000	19.7
53	5519	5519	PPP2R1B	PPP2R1B	0.00000	2.7
54	5519	23291	PPP2R1B	FBXW11	0.00000	3.2
55	5528	6097	PPP2R5D	RORC	0.00000	18.6
56	5528	9575	PPP2R5D	CLOCK	0.00000	23.3
57	5529	6097	PPP2R5E	RORC	0.00000	18
58	5529	9575	PPP2R5E	CLOCK	0.00000	22.8
59	5529	8553	PPP2R5E	BHLHE40	0.00000	12.1
60	5529	5529	PPP2R5E	PPP2R5E	0.00000	11.7
61	6096	9575	RORB	CLOCK	0.00000	23
62	6096	6097	RORB	RORC	0.00000	18.9
63	6097	79365	RORC	BHLHE41	0.00000	18.4
64	6097	56938	RORC	ARNTL2	0.00000	18.6
65	6097	85457	RORC	KIAA1737	0.00000	18.3
66	6097	79176	RORC	FBXL15	0.00000	18.7
67	6097	8864	RORC	PER2	0.00000	15.9
68	6097	8553	RORC	BHLHE40	0.00000	16.9
69	6097	9975	RORC	NR1D2	0.00000	13.5
70	6097	9575	RORC	CLOCK	0.00000	20.3
71	8553	9975	BHLHE40	NR1D2	0.00000	10.4
72	8553	8864	BHLHE40	PER2	0.00000	13.6
73	8864	9575	PER2	CLOCK	0.00000	15.8
74	8864	79365	PER2	BHLHE41	0.00000	14.1
75	9575	79365	CLOCK	BHLHE41	0.00000	22.4
76	9575	85457	CLOCK	KIAA1737	0.00000	21.7
77	9575	9975	CLOCK	NR1D2	0.00000	8.5
78	5187	5187	PER1	PER1	0.00000	11.6
79	5187	8864	PER1	PER2	0.00000	13.3
80	8864	8864	PER2	PER2	0.00000	14
81	4841	5187	NONO	PER1	0.00000	11.3
82	5187	11091	PER1	WDR5	0.00000	11.2
83	4841	8864	NONO	PER2	0.00000	14
84	8864	11091	PER2	WDR5	0.00000	13.9
85	5499	8864	PPP1CA	PER2	0.00000	13.9
86	2932	8864	GSK3B	PER2	0.00000	13.7
87	1457	8864	CSNK2A1	PER2	0.00000	13.5

88	8864	8945	PER2	BTRC	0.00000	13.8
89	4783	8864	NFIL3	PER2	0.00000	16.7
90	5578	8864	PRKCA	PER2	0.00000	13.6
91	1407	5536	CRY1	PPP5C	0.00000	19.9
92	1407	26224	CRY1	FBXL3	0.00000	20.1
93	406	79365	ARNTL	BHLHE41	0.00000	22.1
94	406	1457	ARNTL	CSNK2A1	0.00000	22.8
95	2146	9575	EZH2	CLOCK	0.00000	0.4
96	406	2146	ARNTL	EZH2	0.00000	22.8
97	8864	23291	PER2	FBXW11	0.00000	13.9
98	2932	9572	GSK3B	NR1D1	0.00000	6.3
99	8864	9572	PER2	NR1D1	0.00000	10.8
100	1407	1453	CRY1	CSNK1D	0.00000	20.2
101	406	8863	ARNTL	PER3	0.00000	20
102	1407	8863	CRY1	PER3	0.00000	16.7
103	1407	8914	CRY1	TIMELESS	0.00000	19.8
104	1408	8863	CRY2	PER3	0.00000	11.4
105	1453	8863	CSNK1D	PER3	0.00000	11.5
106	1454	8863	CSNK1E	PER3	0.00000	12.2
107	4783	4783	NFIL3	NFIL3	0.00000	22.9
108	5187	8863	PER1	PER3	0.00000	11.7
109	5515	5529	PPP2CA	PPP2R5E	0.00000	10.8
110	8863	9575	PER3	CLOCK	0.00000	12.9
111	8863	8864	PER3	PER2	0.00000	13
112	8864	8914	PER2	TIMELESS	0.00000	14.4
113	9572	9572	NR1D1	NR1D1	0.00000	6.7
114	9575	56938	CLOCK	ARNTL2	0.00000	22.6
115	190	6095	NR0B1	RORA	0.00000	21.1
116	196	406	AHR	ARNTL	0.00000	22.8
117	406	2033	ARNTL	EP300	0.00000	22.9
118	406	2034	ARNTL	EPAS1	0.00000	22.5
119	406	3091	ARNTL	HIF1A	0.00000	22.4
120	406	3320	ARNTL	HSP90AA1	0.00000	21.7
121	406	8850	ARNTL	KAT2B	0.00000	22.6
122	406	3131	ARNTL	HLF	0.00000	22.1
123	406	266743	ARNTL	NPAS4	0.00000	22.2
124	466	4783	ATF1	NFIL3	0.00000	23.2
125	1050	1628	CEBPA	DBP	0.00000	9.9
126	1054	4783	CEBPG	NFIL3	0.00000	22.5
127	1108	6097	CHD4	RORC	0.00000	19.9
128	1387	4862	CREBBP	NPAS2	0.00000	1.8
129	1390	4783	CREM	NFIL3	0.00000	22.9
130	1628	2033	DBP	EP300	0.00000	9.8
131	1628	3131	DBP	HLF	0.00000	10.2
132	1628	7008	DBP	TEF	0.00000	10.3

133	1649	4783	DDIT3	NFIL3	0.00000	22.5
134	1788	2146	DNMT3A	EZH2	0.00000	5
135	1789	2146	DNMT3B	EZH2	0.00000	23.6
136	1810	4783	DR1	NFIL3	0.00000	22.6
137	2033	9575	EP300	CLOCK	0.00000	0.6
138	2033	4862	EP300	NPAS2	0.00000	1.6
139	3091	5187	HIF1A	PER1	0.00000	11.4
140	3320	4862	HSP90AA1	NPAS2	0.00000	23.5
141	4783	10538	NFIL3	BATF	0.00000	22.7
142	4783	90993	NFIL3	CREB3L1	0.00000	23
143	4783	10488	NFIL3	CREB3	0.00000	22.6
144	4830	6095	NME1	RORA	0.00000	21.3
145	4831	6095	NME2	RORA	0.00000	21.8
146	4841	5829	NONO	PXN	0.00000	4.4
147	4841	55269	NONO	PSPC1	0.00000	5.8
148	4862	5914	NPAS2	RARA	0.00000	0.6
149	4862	6256	NPAS2	RXRA	0.00000	1.6
150	4862	8202	NPAS2	NCOA3	0.00000	1.3
151	4862	8850	NPAS2	KAT2B	0.00000	1.6
152	6095	55885	RORA	LMO3	0.00000	20.8
153	6667	8863	SP1	PER3	0.00000	11.3
154	8450	11091	CUL4B	WDR5	0.00000	7.9
155	8850	9575	KAT2B	CLOCK	0.00000	0.3
156	9572	9611	NR1D1	NCOR1	0.00000	6.4
157	9572	9612	NR1D1	NCOR2	0.00000	6.6
158	9572	10002	NR1D1	NR2E3	0.00000	6.9
159	9611	9975	NCOR1	NR1D2	0.00000	9.1
160	9975	57727	NR1D2	NCOA5	0.00000	9.7
161	196	3320	AHR	HSP90AA1	0.00000	20.7
162	207	3320	AKT1	HSP90AA1	0.00000	18.5
163	367	3320	AR	HSP90AA1	0.00000	18.4
164	466	1390	ATF1	CREM	0.00000	0.1
165	1054	7008	CEBPG	TEF	0.00000	11.7
166	1054	10488	CEBPG	CREB3	0.00000	13.2
167	1108	3065	CHD4	HDAC1	0.00000	0.6
168	1111	3320	CHEK1	HSP90AA1	0.00000	18.2
169	1111	8451	CHEK1	CUL4A	0.00000	11.3
170	1387	1390	CREBBP	CREM	0.00000	2.3
171	1390	5566	CREM	PRKACA	0.00000	0.5
172	1390	2932	CREM	GSK3B	0.00000	1.1
173	1390	1459	CREM	CSNK2A2	0.00000	1.7
174	1390	1390	CREM	CREM	0.00000	23.2
175	1457	6667	CSNK2A1	SP1	0.00000	4.6
176	1457	3091	CSNK2A1	HIF1A	0.00000	7.4
177	1649	7008	DDIT3	TEF	0.00000	11.9

178	1786	1789	DNMT1	DNMT3B	0.00000	23.8
179	1788	3065	DNMT3A	HDAC1	0.00000	4.7
180	1788	7329	DNMT3A	UBE2I	0.00000	4.8
181	1788	1789	DNMT3A	DNMT3B	0.00000	0.3
182	1789	3065	DNMT3B	HDAC1	0.00000	22.7
183	1789	3066	DNMT3B	HDAC2	0.00000	23.1
184	1789	7329	DNMT3B	UBE2I	0.00000	23.5
185	3065	5519	HDAC1	PPP2R1B	0.00000	2.8
186	3091	3320	HIF1A	HSP90AA1	0.00000	18.7
187	3091	8850	HIF1A	KAT2B	0.00000	8.8
188	3131	7008	HLF	TEF	0.00000	11.6
189	3320	4609	HSP90AA1	MYC	0.00000	18.7
190	3320	3320	HSP90AA1	HSP90AA1	0.00000	19.1
191	3320	4842	HSP90AA1	NOS1	0.00000	18.3
192	3320	4654	HSP90AA1	MYOD1	0.00000	18.6
193	3320	5536	HSP90AA1	PPP5C	0.00000	19.5
194	5430	8850	POLR2A	KAT2B	0.00000	7.1
195	6667	9611	SP1	NCOR1	0.00000	2.9
196	6667	6667	SP1	SP1	0.00000	2.8
197	7008	10538	TEF	BATF	0.00000	11.7
198	7008	7008	TEF	TEF	0.00000	11.4
199	8450	8451	CUL4B	CUL4A	0.00000	9.4
200	8648	8850	NCOA1	KAT2B	0.00000	6.3
201	8850	8850	KAT2B	KAT2B	0.00000	8.4
202	10499	10499	NCOA2	NCOA2	0.00000	5.7
203	5529	79365	PPP2R5E	BHLHE41	0.00000	13
204	4830	4830	NME1	NME1	0.00000	20.3
205	6095	6095	RORA	RORA	0.00000	21.9
206	4163	5518	MCC	PPP2R1A	0.00000	2.6
207	1459	3065	CSNK2A2	HDAC1	0.00000	5.5
208	3054	29915	HCFC1	HCFC2	0.00000	4.3
209	5929	29915	RBBP5	HCFC2	0.00001	3.2
210	1453	4163	CSNK1D	MCC	0.00001	2.2
211	1459	3320	CSNK2A2	HSP90AA1	0.00001	20.7
212	3320	6774	HSP90AA1	STAT3	0.00001	22.3
213	466	1457	ATF1	CSNK2A1	0.00002	5.4
214	2033	8850	EP300	KAT2B	0.00002	7
215	4654	8850	MYOD1	KAT2B	0.00003	10
216	5500	8553	PPP1CB	BHLHE40	0.00003	12.5
217	1408	5187	CRY2	PER1	0.00003	10.9
218	6667	9070	SP1	ASH2L	0.00003	3.6
219	1408	4783	CRY2	NFIL3	0.00003	23.3
220	546	1822	ATRX	ATN1	0.00003	6.5
221	466	1459	ATF1	CSNK2A2	0.00003	4.7
222	8553	79365	BHLHE40	BHLHE41	0.00003	12.9

223	5469	6095	MED1	RORA	0.00003	22.4
224	4163	11091	MCC	WDR5	0.00003	2.5
225	196	10499	AHR	NCOA2	0.00003	5.4
226	1457	1457	CSNK2A1	CSNK2A1	0.00003	6.5
227	8648	10499	NCOA1	NCOA2	0.00003	5.3
228	11091	29915	WDR5	HCFC2	0.00003	4.9
229	1387	1459	CREBBP	CSNK2A2	0.00003	4.1
230	1054	3131	CEBPG	HLF	0.00003	12.7
231	1387	8850	CREBBP	KAT2B	0.00003	4.7
232	5501	8553	PPP1CC	BHLHE40	0.00003	11.6
233	1387	1457	CREBBP	CSNK2A1	0.00003	4.3
234	196	6667	AHR	SP1	0.00004	3.8
235	5515	8553	PPP2CA	BHLHE40	0.00004	11.9
236	3054	5929	HCFC1	RBBP5	0.00004	3.5
237	5371	9611	PML	NCOR1	0.00004	2.6
238	5371	6667	PML	SP1	0.00005	2.5
239	5705	6667	PSMC5	SP1	0.00005	2.5
240	3054	5501	HCFC1	PPP1CC	0.00005	5.3
241	1387	10499	CREBBP	NCOA2	0.00005	4.4
242	546	2146	ATRX	EZH2	0.00005	6.4
243	1460	5187	CSNK2B	PER1	0.00005	11.2
244	9611	9611	NCOR1	NCOR1	0.00005	3.1
245	3065	6667	HDAC1	SP1	0.00005	3
246	6256	10499	RXRA	NCOA2	0.00005	6.2
247	8553	85457	BHLHE40	KIAA1737	0.00005	13.6
248	5187	8914	PER1	TIMELESS	0.00005	12.4
249	9070	29915	ASH2L	HCFC2	0.00005	4.4
250	1786	1788	DNMT1	DNMT3A	0.00005	3.8
251	1390	1457	CREM	CSNK2A1	0.00005	1.9
252	3054	6667	HCFC1	SP1	0.00005	3.7
253	4841	5430	NONO	POLR2A	0.00005	5.6
254	8648	9611	NCOA1	NCOR1	0.00005	4.1
255	4297	29915	MLL	HCFC2	0.00005	4.2
256	1390	90993	CREM	CREB3L1	0.00006	23.4
257	3091	10499	HIF1A	NCOA2	0.00006	6.5
258	1457	5515	CSNK2A1	PPP2CA	0.00006	7.3
259	1387	5371	CREBBP	PML	0.00006	3.3
260	5929	9070	RBBP5	ASH2L	0.00006	3.3
261	4297	9070	MLL	ASH2L	0.00006	4.2
262	1387	8648	CREBBP	NCOA1	0.00006	4
263	1387	3065	CREBBP	HDAC1	0.00008	3.7
264	4221	5929	MEN1	RBBP5	0.00008	1.9
265	3131	3131	HLF	HLF	0.00008	12.2
266	4831	5518	NME2	PPP2R1A	0.00008	3.5
267	2782	4163	GNB1	MCC	0.00009	1.1

268	1387	1387	CREBBP	CREBBP	0.00009	3.7
269	466	1387	ATF1	CREBBP	0.00009	3.6
270	4862	8553	NPAS2	BHLHE40	0.00009	1.1
271	8945	23291	BTRC	FBXW11	0.00009	5
272	5187	9737	PER1	GPRASP1	0.00009	10.7
273	4163	5516	MCC	PPP2CB	0.00009	2.8
274	1387	6774	CREBBP	STAT3	0.00010	3.5
275	1454	8553	CSNK1E	BHLHE40	0.00010	13
276	4163	5111	MCC	PCNA	0.00010	1.7
277	1108	3066	CHD4	HDAC2	0.00010	0.9
278	1457	3065	CSNK2A1	HDAC1	0.00010	6.7
279	1387	4297	CREBBP	MLL	0.00010	3.9
280	5829	5829	PXN	PXN	0.00010	4.5
281	4841	7414	NONO	VCL	0.00011	1
282	3054	9070	HCFC1	ASH2L	0.00011	4.3
283	1454	4163	CSNK1E	MCC	0.00011	1.3
284	8451	11091	CUL4A	WDR5	0.00011	9.2
285	1457	8553	CSNK2A1	BHLHE40	0.00011	10.8
286	2146	23512	EZH2	SUZ12	0.00011	5.4
287	1387	6688	CREBBP	SPI1	0.00011	3.6
288	2932	5566	GSK3B	PRKACA	0.00011	3.2
289	3066	6774	HDAC2	STAT3	0.00012	3
290	2932	23291	GSK3B	FBXW11	0.00013	3.8
291	5929	11091	RBBP5	WDR5	0.00013	3.1
292	2146	5371	EZH2	PML	0.00014	4
293	3054	4297	HCFC1	MLL	0.00014	4.1
294	1454	6095	CSNK1E	RORA	0.00014	20.2
295	5566	23291	PRKACA	FBXW11	0.00014	3.4
296	1387	5430	CREBBP	POLR2A	0.00014	4.3
297	466	5566	ATF1	PRKACA	0.00015	2.9
298	1390	6688	CREM	SPI1	0.00015	23.6
299	2033	10499	EP300	NCOA2	0.00016	5.7
300	4297	5929	MLL	RBBP5	0.00016	3.5
301	8553	8553	BHLHE40	BHLHE40	0.00016	12.3
302	8648	8648	NCOA1	NCOA1	0.00017	4.7
303	2932	5829	GSK3B	PXN	0.00017	4
304	6421	55269	SFPQ	PSPC1	0.00017	5.8
305	3131	10538	HLF	BATF	0.00017	13
306	196	8648	AHR	NCOA1	0.00017	4.8
307	1408	5529	CRY2	PPP2R5E	0.00019	10.3
308	546	3065	ATRX	HDAC1	0.00020	7.6
309	10488	10488	CREB3	CREB3	0.00020	12.4
310	3054	3054	HCFC1	HCFC1	0.00020	4.2
311	6774	8648	STAT3	NCOA1	0.00021	3.9
312	4221	29915	MEN1	HCFC2	0.00021	3.2

313	1457	1460	CSNK2A1	CSNK2B	0.00026	6.3
314	5705	6095	PSMC5	RORA	0.00026	22.9
315	1387	2033	CREBBP	EP300	0.00027	4.2
316	6256	8648	RXRA	NCOA1	0.00029	5.8
317	51514	83743	DTL	GRWD1	0.00030	16
318	3054	3320	HCFC1	HSP90AA1	0.00031	22.3
319	367	8850	AR	KAT2B	0.00032	11.6
320	5371	23512	PML	SUZ12	0.00032	3.4
321	5528	8553	PPP2R5D	BHLHE40	0.00032	12
322	5515	5829	PPP2CA	PXN	0.00034	5.5
323	207	1111	AKT1	CHEK1	0.00034	11.2
324	4841	8553	NONO	BHLHE40	0.00035	11.9
325	3054	3066	HCFC1	HDAC2	0.00036	3.7
326	2146	5252	EZH2	PHF1	0.00038	5.8
327	6256	6667	RXRA	SP1	0.00039	5
328	5529	23291	PPP2R5E	FBXW11	0.00039	9.7
329	1050	1387	CEBPA	CREBBP	0.00039	4.3
330	2146	8726	EZH2	EED	0.00039	6.2
331	4783	8553	NFIL3	BHLHE40	0.00040	20.9
332	1387	3091	CREBBP	HIF1A	0.00041	4.1
333	1390	5578	CREM	PRKCA	0.00042	1.4
334	6256	6256	RXRA	RXRA	0.00043	7
335	5111	5501	PCNA	PPP1CC	0.00045	10.5
336	3065	7329	HDAC1	UBE2I	0.00046	5.4
337	3066	5371	HDAC2	PML	0.00047	2.2
338	3054	11091	HCFC1	WDR5	0.00047	4.5
339	1108	2033	CHD4	EP300	0.00047	2.7
340	3054	3065	HCFC1	HDAC1	0.00050	4.3
341	23291	23291	FBXW11	FBXW11	0.00052	4.6
342	1457	3320	CSNK2A1	HSP90AA1	0.00053	19.8
343	4221	4297	MEN1	MLL	0.00053	3.5
344	2932	5499	GSK3B	PPP1CA	0.00055	3.7
345	5371	6774	PML	STAT3	0.00058	2.9
346	1111	1457	CHEK1	CSNK2A1	0.00058	8.5
347	6774	6774	STAT3	STAT3	0.00059	3.3
348	9070	11091	ASH2L	WDR5	0.00062	4.9
349	1457	6688	CSNK2A1	SPI1	0.00065	5.8
350	2770	2770	GNAI1	GNAI1	0.00065	10.9
351	2033	6667	EP300	SP1	0.00066	4.3
352	3054	4221	HCFC1	MEN1	0.00069	3.5
353	2033	8648	EP300	NCOA1	0.00071	5.1
354	1408	8553	CRY2	BHLHE40	0.00071	11.3
355	5929	8450	RBBP5	CUL4B	0.00072	5.7
356	2932	2932	GSK3B	GSK3B	0.00072	3.5
357	1453	5187	CSNK1D	PER1	0.00075	10.8

358	3065	6774	HDAC1	STAT3	0.00075	3.3
359	6095	79365	RORA	BHLHE41	0.00079	19.7
360	1387	4654	CREBBP	MYOD1	0.00079	3.7
361	2033	7329	EP300	UBE2I	0.00080	5.4
362	7414	7414	VCL	VCL	0.00080	0.4
363	5499	5529	PPP1CA	PPP2R5E	0.00080	10.2
364	1408	2146	CRY2	EZH2	0.00085	7.6
365	1786	2146	DNMT1	EZH2	0.00086	4
366	3091	8648	HIF1A	NCOA1	0.00087	5.8
367	2146	8553	EZH2	BHLHE40	0.00088	10.6
368	2146	23649	EZH2	POLA2	0.00088	5.2
369	3065	4297	HDAC1	MLL	0.00088	4.2
370	196	2033	AHR	EP300	0.00088	5.3
371	1387	8202	CREBBP	NCOA3	0.00088	3.8
372	1649	3131	DDIT3	HLF	0.00089	13.1
373	4297	11091	MLL	WDR5	0.00091	4.3
374	2033	5430	EP300	POLR2A	0.00091	5.8
375	3054	10488	HCFC1	CREB3	0.00091	5.2
376	3065	5518	HDAC1	PPP2R1A	0.00092	3.9
377	8202	8850	NCOA3	KAT2B	0.00094	6.6
378	5518	5528	PPP2R1A	PPP2R5D	0.00096	4.6
379	6096	8553	RORB	BHLHE40	0.00098	12.7
380	5515	5518	PPP2CA	PPP2R1A	0.00098	5.1
381	4297	4297	MLL	MLL	0.00100	4.1
382	2033	6774	EP300	STAT3	0.00102	4.2
383	5829	6421	PXN	SFPQ	0.00110	4.9
384	207	2146	AKT1	EZH2	0.00111	7.2
385	8553	79176	BHLHE40	FBXL15	0.00113	13.8
386	1459	3066	CSNK2A2	HDAC2	0.00114	4.3
387	9070	9070	ASH2L	ASH2L	0.00114	4.4
388	1460	5519	CSNK2B	PPP2R1B	0.00114	3.3
389	5519	5529	PPP2R1B	PPP2R5E	0.00120	5.6
390	4221	9070	MEN1	ASH2L	0.00122	3.3
391	1460	2146	CSNK2B	EZH2	0.00127	5.8
392	3066	6667	HDAC2	SP1	0.00128	2.6
393	1459	1460	CSNK2A2	CSNK2B	0.00142	5.5
394	5829	7414	PXN	VCL	0.00143	2.4
395	466	466	ATF1	ATF1	0.00167	3.2
396	5578	5578	PRKCA	PRKCA	0.00171	7.5
397	5499	8553	PPP1CA	BHLHE40	0.00173	11.9
398	5371	5371	PML	PML	0.00173	2.2
399	6095	10499	RORA	NCOA2	0.00175	3.4
400	2033	5371	EP300	PML	0.00179	4
401	6096	8648	RORB	NCOA1	0.00181	3.9
402	367	3091	AR	HIF1A	0.00189	14.2

403	1459	8553	CSNK2A2	BHLHE40	0.00190	10.5
404	1050	1050	CEBPA	CEBPA	0.00192	7.4
405	1642	8450	DDB1	CUL4B	0.00199	8
406	8450	9410	CUL4B	SNRNP40	0.00204	6.4
407	367	1387	AR	CREBBP	0.00210	3.4
408	4842	51655	NOS1	RASD1	0.00215	15.4
409	1050	2033	CEBPA	EP300	0.00242	6.3
410	5578	7414	PRKCA	VCL	0.00250	2.8
411	5914	8850	RARA	KAT2B	0.00268	9.4
412	1050	2932	CEBPA	GSK3B	0.00276	5
413	4841	6421	NONO	SFPQ	0.00283	5
414	207	367	AKT1	AR	0.00292	14
415	1457	79365	CSNK2A1	BHLHE41	0.00325	8.6
416	1786	3066	DNMT1	HDAC2	0.00335	2.8
417	2770	51655	GNAI1	RASD1	0.00343	12.1
418	5371	6256	PML	RXRA	0.00353	4.6
419	196	196	AHR	AHR	0.00359	4.9
420	1054	10538	CEBPG	BATF	0.00362	15.9
421	8945	8945	BTRC	BTRC	0.00369	5.3
422	367	367	AR	AR	0.00371	16.1
423	1822	11091	ATN1	WDR5	0.00372	5.8
424	5705	6256	PSMC5	RXRA	0.00372	5.9
425	7329	8553	UBE2I	BHLHE40	0.00409	10.8
426	207	5515	AKT1	PPP2CA	0.00412	9.7
427	2146	3065	EZH2	HDAC1	0.00415	5.9
428	1054	1054	CEBPG	CEBPG	0.00426	14
429	1460	5501	CSNK2B	PPP1CC	0.00467	7.7
430	190	367	NR0B1	AR	0.00509	17.5
431	1786	1786	DNMT1	DNMT1	0.00533	3
432	1460	8553	CSNK2B	BHLHE40	0.00534	11.8
433	1408	79365	CRY2	BHLHE41	0.00559	10.9
434	2033	2033	EP300	EP300	0.00575	5.6
435	5499	8726	PPP1CA	EED	0.00575	6
436	2033	3091	EP300	HIF1A	0.00620	6.6
437	3065	5371	HDAC1	PML	0.00621	2.4
438	5499	5515	PPP1CA	PPP2CA	0.00656	7.2
439	1822	1822	ATN1	ATN1	0.00672	5.6
440	5914	83714	RARA	NRIP2	0.00673	16.2
441	1408	5528	CRY2	PPP2R5D	0.00712	9.1
442	8450	51514	CUL4B	DTL	0.00734	12
443	5515	5515	PPP2CA	PPP2CA	0.00742	9.1
444	1786	3065	DNMT1	HDAC1	0.00838	3.1
445	4830	6096	NME1	RORB	0.00911	20.9
446	9410	9410	SNRNP40	SNRNP40	0.00920	1
447	1454	79365	CSNK1E	BHLHE41	0.00942	15.9

448	5518	5536	PPP2R1A	PPP5C	0.00966	4.2
449	367	5469	AR	MED1	0.00982	18.3
450	4654	79365	MYOD1	BHLHE41	0.00988	15.1
451	1460	5529	CSNK2B	PPP2R5E	0.00989	10.3
452	1408	26224	CRY2	FBXL3	0.00990	7.3
453	5518	5529	PPP2R1A	PPP2R5E	0.00994	6.9
454	4654	6256	MYOD1	RXRA	0.01024	8.5
455	1387	3131	CREBBP	HLF	0.01027	5
456	1454	5501	CSNK1E	PPP1CC	0.01031	12
457	3065	3091	HDAC1	HIF1A	0.01076	9.9
458	1408	5519	CRY2	PPP2R1B	0.01086	5.8
459	4221	11091	MEN1	WDR5	0.01102	3.1
460	367	3065	AR	HDAC1	0.01115	15.8
461	4654	6095	MYOD1	RORA	0.01243	19.9
462	1460	2932	CSNK2B	GSK3B	0.01354	4
463	6256	8202	RXRA	NCOA3	0.01377	5.8
464	1459	79365	CSNK2A2	BHLHE41	0.01460	6.9
465	9410	11091	SNRNP40	WDR5	0.01498	3
466	8726	8726	EED	EED	0.01575	7.5
467	2146	3066	EZH2	HDAC2	0.01635	4.6
468	1460	5518	CSNK2B	PPP2R1A	0.01638	4.3
469	5469	5469	MED1	MED1	0.01805	23.2
470	11091	51514	WDR5	DTL	0.01862	14.1
471	4654	6774	MYOD1	STAT3	0.01936	3.4
472	5516	79365	PPP2CB	BHLHE41	0.01942	12.5
473	5519	79365	PPP2R1B	BHLHE41	0.01960	2.3
474	2033	8202	EP300	NCOA3	0.01978	5
475	1642	5929	DDB1	RBBP5	0.01981	3.1
476	1786	5111	DNMT1	PCNA	0.01990	2.8
477	2033	6095	EP300	RORA	0.02050	2.6
478	1457	3066	CSNK2A1	HDAC2	0.02160	5.2
479	1054	1649	CEBPG	DDIT3	0.02164	14.7
480	1649	10488	DDIT3	CREB3	0.02168	13.8
481	1050	6688	CEBPA	SPI1	0.02241	6.4
482	207	2033	AKT1	EP300	0.02244	7
483	367	10499	AR	NCOA2	0.02318	7.2
484	1050	1054	CEBPA	CEBPG	0.02423	9.4
485	2033	2034	EP300	EPAS1	0.02480	6.3
486	51655	79365	RASD1	BHLHE41	0.02499	15.5
487	1111	1460	CHEK1	CSNK2B	0.02517	10.1
488	6667	9612	SP1	NCOR2	0.02527	4.1
489	196	9612	AHR	NCOR2	0.02550	5.3
490	207	207	AKT1	AKT1	0.02572	10.3
491	1642	8451	DDB1	CUL4A	0.02679	9.3
492	5499	5499	PPP1CA	PPP1CA	0.02796	4.4

493	6256	9612	RXRA	NCOR2	0.02816	6.4
494	5914	6667	RARA	SP1	0.02825	1.5
495	2782	51655	GNB1	RASD1	0.02838	16.9
496	4842	5578	NOS1	PRKCA	0.02873	11.4
497	9611	9612	NCOR1	NCOR2	0.02882	4.4
498	5518	8553	PPP2R1A	BHLHE40	0.02900	10.6
499	4831	5515	NME2	PPP2CA	0.02929	9.4
500	2033	5111	EP300	PCNA	0.02989	6.1
501	1454	1454	CSNK1E	CSNK1E	0.03016	16.6
502	5929	8451	RBBP5	CUL4A	0.03082	5.8
503	1408	2932	CRY2	GSK3B	0.03279	6.3
504	5914	8648	RARA	NCOA1	0.03287	4.3
505	466	6688	ATF1	SPI1	0.03346	3
506	207	2932	AKT1	GSK3B	0.03423	5.2
507	8450	83743	CUL4B	GRWD1	0.03752	10.3
508	79365	79365	BHLHE41	BHLHE41	0.03763	15.2
509	5469	6256	MED1	RXRA	0.03801	5.3
510	1642	51514	DDB1	DTL	0.03820	14.1
511	5469	5914	MED1	RARA	0.03884	21.1
512	1050	10538	CEBPA	BATF	0.03919	7.5
513	2782	4831	GNB1	NME2	0.03978	18.1
514	2033	4654	EP300	MYOD1	0.03981	6.8
515	1457	1649	CSNK2A1	DDIT3	0.04126	8.1
516	8553	9575	BHLHE40	CLOCK	0.04525	19.8
517	5515	5536	PPP2CA	PPP5C	0.04570	7.6
518	5371	9612	PML	NCOR2	0.04665	3.7
519	1460	5515	CSNK2B	PPP2CA	0.04779	7.8
520	4841	6688	NONO	SPI1	0.05013	3.4
521	1408	5536	CRY2	PPP5C	0.05065	8.5
522	2932	8553	GSK3B	BHLHE40	0.05720	10.3
523	367	4841	AR	NONO	0.06169	16.1
524	5111	5111	PCNA	PCNA	0.06488	15.9
525	5914	10002	RARA	NR2E3	0.06528	17.7
526	367	6774	AR	STAT3	0.06574	2.5
527	2932	79365	GSK3B	BHLHE41	0.06601	3.7
528	5519	8553	PPP2R1B	BHLHE40	0.06837	10.5
529	2146	7409	EZH2	VAV1	0.06989	4.6
530	466	1460	ATF1	CSNK2B	0.07002	4.3
531	10538	10538	BATF	BATF	0.07411	19.2
532	8202	8202	NCOA3	NCOA3	0.07578	4.2
533	5371	5914	PML	RARA	0.07940	1
534	1408	1453	CRY2	CSNK1D	0.08198	7.1
535	4654	5578	MYOD1	PRKCA	0.08753	9.7
536	3065	8726	HDAC1	EED	0.09452	8.1
537	1387	4609	CREBBP	MYC	0.09501	3.3

538	3066	9612	HDAC2	NCOR2	0.10113	4.4
539	5914	6256	RARA	RXRA	0.11084	7.3
540	4654	6667	MYOD1	SP1	0.11097	2.7
541	760	4841	CA2	NONO	0.11148	22.4
542	4842	9722	NOS1	NOS1AP	0.11363	17.1
543	1649	10538	DDIT3	BATF	0.11451	16.7
544	6096	83714	RORB	NRIP2	0.11496	16.9
545	1642	11091	DDB1	WDR5	0.11506	6.2
546	1108	4609	CHD4	MYC	0.12002	22.4
547	367	55269	AR	PSPC1	0.12376	8.5
548	1111	8914	CHEK1	TIMELESS	0.12388	14.8
549	8202	9612	NCOA3	NCOR2	0.12540	5
550	3065	4654	HDAC1	MYOD1	0.12707	14.5
551	1876	2146	E2F6	EZH2	0.13082	6.2
552	1454	5528	CSNK1E	PPP2R5D	0.13304	14.3
553	1642	9410	DDB1	SNRNP40	0.13761	3
554	4654	4654	MYOD1	MYOD1	0.14013	14.9
555	1460	5528	CSNK2B	PPP2R5D	0.14494	7.1
556	9410	83743	SNRNP40	GRWD1	0.15728	21.7
557	1460	5499	CSNK2B	PPP1CA	0.15760	5.2
558	6774	8553	STAT3	BHLHE40	0.17728	9.1
559	4654	9611	MYOD1	NCOR1	0.19612	3.3
560	3065	9612	HDAC1	NCOR2	0.20420	5.9
561	2146	5914	EZH2	RARA	0.20932	5.5
562	1788	4609	DNMT3A	MYC	0.21010	4.6
563	11091	79365	WDR5	BHLHE41	0.21458	12.5
564	5914	5914	RARA	RARA	0.22076	18
565	1649	1649	DDIT3	DDIT3	0.22308	15.4
566	1460	85457	CSNK2B	KIAA1737	0.22873	15.9
567	3066	8726	HDAC2	EED	0.23436	4.4
568	3065	5111	HDAC1	PCNA	0.24236	15.1
569	367	8648	AR	NCOA1	0.24738	5.7
570	4609	8850	MYC	KAT2B	0.25294	11.2
571	5578	5914	PRKCA	RARA	0.26351	8.5
572	9722	51655	NOS1AP	RASD1	0.26424	18.8
573	4831	4831	NME2	NME2	0.26884	19.5
574	5536	5536	PPP5C	PPP5C	0.27750	5.8
575	3065	4609	HDAC1	MYC	0.32005	16.4
576	11091	23178	WDR5	PASK	0.32149	6.3
577	3066	3091	HDAC2	HIF1A	0.32396	5.6
578	367	5829	AR	PXN	0.32469	5.1
579	4831	6096	NME2	RORB	0.32521	21.6
580	3066	3066	HDAC2	HDAC2	0.33227	2.2
581	1408	8914	CRY2	TIMELESS	0.34715	10.3
582	1460	5500	CSNK2B	PPP1CB	0.35403	7.9

583	367	2932	AR	GSK3B	0.36136	2.2
584	367	6667	AR	SP1	0.36143	23.2
585	1460	1460	CSNK2B	CSNK2B	0.37420	6.1
586	367	2033	AR	EP300	0.38343	8.2
587	8914	11277	TIMELESS	TREX1	0.38536	23.8
588	2034	56938	EPAS1	ARNTL2	0.39896	9.4
589	4841	79365	NONO	BHLHE41	0.41593	14.2
590	4654	9612	MYOD1	NCOR2	0.42311	7.4
591	3065	3066	HDAC1	HDAC2	0.42424	2.6
592	1460	79176	CSNK2B	FBXL15	0.43850	18.6
593	5914	8202	RARA	NCOA3	0.46803	3
594	1460	79365	CSNK2B	BHLHE41	0.48701	12.7
595	90993	90993	CREB3L1	CREB3L1	0.53640	23.9
596	1460	6096	CSNK2B	RORB	0.55999	2.5
597	2771	51655	GNAI2	RASD1	0.56085	6.2
598	8914	54962	TIMELESS	TIPIN	0.57695	0.3
599	367	9611	AR	NCOR1	0.59594	22.2
600	5914	9612	RARA	NCOR2	0.59873	5.4
601	23291	79365	FBXW11	BHLHE41	0.61187	11.4
602	367	7329	AR	UBE2I	0.63770	9.5
603	4609	5371	MYC	PML	0.66318	23.1
604	4609	5430	MYC	POLR2A	0.70136	7.7
605	1457	4609	CSNK2A1	MYC	0.71785	9.5
606	1050	4609	CEBPA	MYC	0.72718	11.7
607	3066	4609	HDAC2	MYC	0.75330	19.3
608	4609	6667	MYC	SP1	0.75748	23.6
609	1054	90993	CEBPG	CREB3L1	0.75767	17.2
610	4609	5499	MYC	PPP1CA	0.76405	16.9
611	4609	11091	MYC	WDR5	0.76588	15.5
612	367	9612	AR	NCOR2	0.76665	10
613	2932	4609	GSK3B	MYC	0.79008	1.8
614	2033	4609	EP300	MYC	0.79695	7.3
615	1454	1460	CSNK1E	CSNK2B	0.79800	14.6
616	3065	3065	HDAC1	HDAC1	0.81467	11.7
617	1459	4609	CSNK2A2	MYC	0.82263	6.9
618	1454	5536	CSNK1E	PPP5C	0.82865	14.3
619	10488	90993	CREB3	CREB3L1	0.84222	13
620	4842	5566	NOS1	PRKACA	0.90796	0
621	11091	83743	WDR5	GRWD1	0.91140	16
622	23178	23178	PASK	PASK	0.97684	16.6
623	4841	5111	NONO	PCNA	0.99172	7.6
624	1454	23291	CSNK1E	FBXW11	0.99264	17.9
625	367	8202	AR	NCOA3	0.99928	15.1

Table 10. Score for RNAi Mediated Perturbation of 46 Network Components.

Gene ID h	Sym. h	Degree	Dyn. degree	Corr. Coeff.	Period	Amp/damp	Score
5187	PER1	14	9	0	0	1	1
8864	PER2	23	23	0	0	1	1
8863	PER3	9	9	0	2	0	2
1407	CRY1	18	18	0	3	1	4
1408	CRY2	18	5	0	2	0	2
4841	NONO	14	5	0	0	0	0
11091	WDR5	20	4	0	0	0	0
8914	TIM	7	2	0	0	0	0
85457	CIPC	4	2	0	0	0	0
8553	DEC1	32	7	no construct			
79365	DEC2	22	6	0	0	0	0
9575	CLOCK	25	24	4	0	0	4
4862	NPAS2	14	13	0	0	0	0
406	BMAL1	21	21	4	0	0	4
56938	BMAL2	3	2	0	0	0	0
9572	NR1D1	6	6	0	0	0	0
9975	NR1D2	8	8	0	1	0	1
6095	RORA	12	5	0	0	0	0
6096	RORB	8	2	0	0	0	0
6097	RORC	21	21	0	0	0	0
1628	DBP	5	5	0	0	0	0
4783	NFIL3	12	10	0	0	0	0
2146	EZH2	20	4	0	0	0	0
51655	RASD1	6	0	0	1	0	1
1453	CSNK1E	6	3	0	0	0	0
1454	CSNK1D	19	9	0	0	0	0
2932	GSK3B	16	3	0	1	0	1
1457	CSNK2A1	19	4	0	3	0	3
1459	CSNK2A2	11	3	0	2	0	2
1460	CSNK2B	27	5	0	3	1	4
5566	PRKACA	5	1				
5578	PRKCA	7	1	0	0	0	0
5499	PPP1CA	11	3	0	0	0	0
5500	PPP1CB	4	2	0	0	0	0
5501	PPP1CC	8	3	0	0	0	0
5515	PPP2CA	12	2	0	0	0	0
5516	PPP2CB	2	0	0	0	0	0
5518	PPP2R1A	10	2	0	0	1	1
5519	PPP2R1B	12	7	0	0	0	0
5528	PPP2R5D	9	4	0	0	0	0

5529	PPP2R5E	14	8	0	0	1	1
5536	PPP5C	7	2	0	0	0	0
8945	BTRC	3	1	0	2	0	2
23291	FBXW11	10	3	0	2	0	2
26224	FBXL3	2	1	4	0	0	4
79176	FBXL15	3	1	0	0	0	0

Table 11. Score for Overexpression of 46 Experimental Network Components.

Gene ID h	**Sym. h**	**Degree**	**Dyn. degree**	**Corr. Coeff.**	**Period**	**Amp/damp**	**Score**
5187	PER1	14	9	4	0	0	4
8864	PER2	23	23	4	0	0	4
8863	PER3	9	9	4	0	0	4
1407	CRY1	18	18	4	0	0	4
1408	CRY2	18	5	4	0	0	4
4841	NONO	14	5	0	0	1	1
11091	WDR5	20	4	0	0	1	1
8914	TIM	7	2	4	0	0	4
85457	CIPC	4	2	0	2	1	3
8553	DEC1	32	7	0	2	1	3
79365	DEC2	22	6	0	2	1	3
9575	CLOCK	25	24	0	0	0	0
4862	NPAS2	14	13	4	0	0	4
406	BMAL1	21	21	0	3	0	3
56938	BMAL2	3	2	0	0	0	0
9572	NR1D1	6	6	4	0	0	4
9975	NR1D2	8	8	4	0	0	4
6095	RORA	12	5	4	0	0	4
6096	RORB	8	2	4	0	0	4
6097	RORC	21	21	4	0	0	4
1628	DBP	5	5	0	0	0	0
4783	NFIL3	12	10	0	0	0	0
2146	EZH2	20	4	0	0	0	0
51655	RASD1	6	0	0	0	0	0
1453	CSNK1E	6	3	0	3	0	3
1454	CSNK1D	19	9	0	2	0	2
2932	GSK3B	16	3	0	2	0	2
1457	CSNK2A1	19	4	0	3	0	3
1459	CSNK2A2	11	3	0	2	0	2
1460	CSNK2B	27	5	0	2	0	2
5566	PRKACA	5	1	lethal			
5578	PRKCA	7	1	0	1	0	1
5499	PPP1CA	11	3	0	0	0	0

5500	PPP1CB	4	2	0	0	0	0
5501	PPP1CC	8	3	0	1	0	1
5515	PPP2CA	12	2	0	2	1	3
5516	PPP2CB	2	0	0	0	0	0
5518	PPP2R1A	10	2	0	0	0	0
5519	PPP2R1B	12	7	0	0	0	0
5528	PPP2R5D	9	4	0	0	0	0
5529	PPP2R5E	14	8	0	0	0	0
5536	PPP5C	7	2	0	0	0	0
8945	BTRC	3	1	0	0	0	0
23291	FBXW11	10	3	0	0	0	0
26224	FBXL3	2	1	0	2	0	2
79176	FBXL15	3	1	0	3	0	3

Table 12. Phenotypic Score for 46 Network Components.
The knockdown and overexpression score was combined to the phenotypic score.

Gene ID h	**Sym. h**	**Degree**	**Dyn. degree**	**Phenotypic score**
5187	PER1	14	9	5
8864	PER2	23	23	5
8863	PER3	9	9	6
1407	CRY1	18	18	8
1408	CRY2	18	5	6
4841	NONO	14	5	1
11091	WDR5	20	4	1
8914	TIM	7	2	4
85457	CIPC	4	2	3
8553	DEC1	32	7	
79365	DEC2	22	6	3
9575	CLOCK	25	24	4
4862	NPAS2	14	13	4
406	BMAL1	21	21	7
56938	BMAL2	3	2	0
9572	NR1D1	6	6	4
9975	NR1D2	8	8	5
6095	RORA	12	5	4
6096	RORB	8	2	4
6097	RORC	21	21	4
1628	DBP	5	5	0
4783	NFIL3	12	10	0
2146	EZH2	20	4	0
51655	RASD1	6	0	1
1453	CSNK1E	6	3	3

1454	CSNK1D	19	9	2
2932	GSK3B	16	3	3
1457	CSNK2A1	19	4	6
1459	CSNK2A2	11	3	4
1460	CSNK2B	27	5	6
5566	PRKACA	5	1	
5578	PRKCA	7	1	1
5499	PPP1CA	11	3	0
5500	PPP1CB	4	2	0
5501	PPP1CC	8	3	1
5515	PPP2CA	12	2	3
5516	PPP2CB	2	0	0
5518	PPP2R1A	10	2	1
5519	PPP2R1B	12	7	0
5528	PPP2R5D	9	4	0
5529	PPP2R5E	14	8	1
5536	PPP5C	7	2	0
8945	BTRC	3	1	2
23291	FBXW11	10	3	2
26224	FBXL3	2	1	6
79176	FBXL15	3	1	3

Table 13. Process Network Underlying the Dynamic Circadian PPI Network.

Sym. h A	**Sym. h B**	**Time PPI CT**	**GO A**	**GO B**
ARNTL	CLOCK	22.6	circadian rhythm	circadian rhythm
ARNTL	NPAS2	23.5	circadian rhythm	circadian rhythm
ARNTL	CRY1	21.2	circadian rhythm	circadian rhythm
ARNTL	CRY2	22.5	circadian rhythm	circadian rhythm
ARNTL	BHLHE40	21.5	circadian rhythm	circadian rhythm
CRY1	CLOCK	20.7	circadian rhythm	circadian rhythm
CRY1	NPAS2	22.1	circadian rhythm	circadian rhythm
CRY1	PER1	18.6	circadian rhythm	circadian rhythm
CRY1	BHLHE40	18.6	circadian rhythm	circadian rhythm
CRY1	PER2	17.1	circadian rhythm	circadian rhythm
CRY2	CLOCK	0	circadian rhythm	circadian rhythm
CRY2	NPAS2	1.6	circadian rhythm	circadian rhythm
CRY2	PER1	10.9	circadian rhythm	circadian rhythm
CRY2	BHLHE40	11.3	circadian rhythm	circadian rhythm
CRY2	PER2	13.5	circadian rhythm	circadian rhythm
NPAS2	CLOCK	0.3	circadian rhythm	circadian rhythm
NPAS2	BHLHE40	1.1	circadian rhythm	circadian rhythm
PER1	BHLHE40	11.9	circadian rhythm	circadian rhythm

BHLHE40	CLOCK	19.8	circadian rhythm	circadian rhythm
BHLHE40	PER2	13.6	circadian rhythm	circadian rhythm
PER2	CLOCK	15.8	circadian rhythm	circadian rhythm
PER1	PER2	13.3	circadian rhythm	circadian rhythm
PER2	NR1D1	10.8	circadian rhythm	circadian rhythm
CRY1	TIMELESS	19.8	circadian rhythm	circadian rhythm
CRY2	TIMELESS	10.3	circadian rhythm	circadian rhythm
PER1	TIMELESS	12.4	circadian rhythm	circadian rhythm
PER2	TIMELESS	14.4	circadian rhythm	circadian rhythm
CLOCK	ARNTL2	22.6	circadian rhythm	circadian rhythm
CRY2	EZH2	7.6	circadian rhythm	chromatin modification
ARNTL	EZH2	22.8	circadian rhythm	chromatin modification
ARNTL	EP300	22.9	circadian rhythm	chromatin modification
ARNTL	KAT2B	22.6	circadian rhythm	chromatin modification
NPAS2	KAT2B	1.6	circadian rhythm	chromatin modification
NR1D1	NCOR1	6.4	circadian rhythm	chromatin modification
EZH2	BHLHE40	10.6	chromatin modification	circadian rhythm
EZH2	CLOCK	0.4	chromatin modification	circadian rhythm
CREBBP	NPAS2	1.8	chromatin modification	circadian rhythm
EP300	CLOCK	0.6	chromatin modification	circadian rhythm
EP300	NPAS2	1.6	chromatin modification	circadian rhythm
KAT2B	CLOCK	0.3	chromatin modification	circadian rhythm
ARNTL	CRY1	21.2	circadian rhythm	DNA repair
ARNTL	CRY2	22.5	circadian rhythm	DNA repair
ARNTL	CSNK1E	22.1	circadian rhythm	DNA repair
CRY1	CSNK1E	19.6	circadian rhythm	DNA repair
CRY1	CSNK1D	20.2	circadian rhythm	DNA repair
CRY2	CSNK1D	7.1	circadian rhythm	DNA repair
TIM	TREX1	23.8	circadian rhythm	DNA repair
CRY1	CLOCK	20.7	DNA repair	circadian rhythm
CRY1	NPAS2	22.1	DNA repair	circadian rhythm
CRY1	PER1	18.6	DNA repair	circadian rhythm
CRY1	BHLHE40	18.6	DNA repair	circadian rhythm
CRY1	PER2	17.1	DNA repair	circadian rhythm
CRY2	CLOCK	0	DNA repair	circadian rhythm
CRY2	NPAS2	1.6	DNA repair	circadian rhythm
CRY2	PER1	10.9	DNA repair	circadian rhythm
CRY2	BHLHE40	11.3	DNA repair	circadian rhythm
CRY2	PER2	13.5	DNA repair	circadian rhythm
CSNK1D	PER2	14	DNA repair	circadian rhythm
CSNK1E	CLOCK	22.4	DNA repair	circadian rhythm
CSNK1E	PER1	12.4	DNA repair	circadian rhythm
CSNK1E	PER2	14.2	DNA repair	circadian rhythm

CSNK1E	BHLHE40	13	DNA repair	circadian rhythm
NONO	BHLHE40	11.9	DNA repair	circadian rhythm
NONO	PER1	11.3	DNA repair	circadian rhythm
NONO	PER2	14	DNA repair	circadian rhythm
CRY1	TIM	19.8	DNA repair	circadian rhythm
CRY2	TIM	10.3	DNA repair	circadian rhythm
CSNK1D	PER1	10.8	DNA repair	circadian rhythm
CHEK1	TIM	14.8	DNA repair	circadian rhythm
ARNTL	EPAS1	22.5	circadian rhythm	hemopoiesis
ARNTL	HIF1A	22.4	circadian rhythm	hemopoiesis
NPAS2	RARA	0.6	circadian rhythm	hemopoiesis
EPAS1	ARNTL2	9.4	hemopoiesis	circadian rhythm
HIF1A	PER1	11.4	hemopoiesis	circadian rhythm
PER2	BTRC	13.8	circadian rhythm	interaction between organisms
ARNTL	EP300	22.9	circadian rhythm	interaction between organisms
ARNTL	KAT2B	22.6	circadian rhythm	interaction between organisms
NPAS2	RXRA	1.6	circadian rhythm	interaction between organisms
NPAS2	KAT2B	1.6	circadian rhythm	interaction between organisms
CREBBP	NPAS2	1.8	interaction between organisms	circadian rhythm
EP300	CLOCK	0.6	interaction between organisms	circadian rhythm
EP300	NPAS2	1.6	interaction between organisms	circadian rhythm
STAT3	BHLHE40	9.1	interaction between organisms	circadian rhythm
UBE2I	BHLHE40	10.8	interaction between organisms	circadian rhythm
KAT2B	CLOCK	0.3	interaction between organisms	circadian rhythm
ARNTL	HSP90AA1	21.7	circadian rhythm	response to organic substance
NPAS2	RARA	0.6	circadian rhythm	response to organic substance
PPP2CA	BHLHE40	11.9	response to organic substance	circadian rhythm
PPP2R1A	BHLHE40	10.6	response to organic substance	circadian rhythm
PRKCA	PER2	13.6	response to organic substance	circadian rhythm
HSP90AA1	NPAS2	23.5	response to organic substance	circadian rhythm
STAT3	BHLHE40	9.1	response to organic substance	circadian rhythm
PER2	BTRC	13.8	circadian rhythm	positive regulation of molecular function
ARNTL	EP300	22.9	circadian rhythm	positive regulation of molecular function
ARNTL	HIF1A	22.4	circadian rhythm	positive regulation of molecular function
EP300	CLOCK	0.6	regulation of molecular function	circadian rhythm
EP300	NPAS2	1.6	regulation of molecular function	circadian rhythm
HIF1A	PER1	11.4	regulation of molecular function	circadian rhythm
ARNTL	CLOCK	22.6	circadian rhythm	transcrip. from RNA poly. II promot.

ARNTL	NPAS2	23.5	circadian rhythm	transcrip. from RNA poly. II promot.
CRY1	CLOCK	20.7	circadian rhythm	transcrip. from RNA poly. II promot.
CRY1	NPAS2	22.1	circadian rhythm	transcrip. from RNA poly. II promot.
CRY2	CLOCK	0	circadian rhythm	transcrip. from RNA poly. II promot.
CRY2	NPAS2	1.6	circadian rhythm	transcrip. from RNA poly. II promot.
NPAS2	CLOCK	0.3	circadian rhythm	transcrip. from RNA poly. II promot.
BHLHE40	CLOCK	19.8	circadian rhythm	transcrip. from RNA poly. II promot.
PER2	CLOCK	15.8	circadian rhythm	transcrip. from RNA poly. II promot.
ARNTL	EP300	22.9	circadian rhythm	transcrip. from RNA poly. II promot.
ARNTL	EPAS1	22.5	circadian rhythm	transcrip. from RNA poly. II promot.
ARNTL	HIF1A	22.4	circadian rhythm	transcrip. from RNA poly. II promot.
ARNTL	NPAS4	22.2	circadian rhythm	transcrip. from RNA poly. II promot.
NPAS2	RXRA	1.6	circadian rhythm	transcrip. from RNA poly. II promot.
ARNTL	CRY1	21.2	transcrip. from RNA poly. II promot.	circadian rhythm
ARNTL	CRY2	22.5	transcrip. from RNA poly. II promot.	circadian rhythm
ARNTL	BHLHE40	21.5	transcrip. from RNA poly. II promot.	circadian rhythm
NPAS2	BHLHE40	1.1	transcrip. from RNA poly. II promot.	circadian rhythm
CLOCK	ARNTL2	22.6	transcrip. from RNA poly. II promot.	circadian rhythm
AHR	ARNTL	22.8	transcrip. from RNA poly. II promot.	circadian rhythm
EP300	CLOCK	0.6	transcrip. from RNA poly. II promot.	circadian rhythm
EP300	NPAS2	1.6	transcrip. from RNA poly. II promot.	circadian rhythm
EPAS1	ARNTL2	9.4	transcrip. from RNA poly. II promot.	circadian rhythm
HIF1A	PER1	11.4	transcrip. from RNA poly. II promot.	circadian rhythm
CRY1	TIM	19.8	circadian rhythm	regulation of cell proliferation
CRY2	TIM	10.3	circadian rhythm	regulation of cell proliferation
PER1	TIM	12.4	circadian rhythm	regulation of cell proliferation
PER2	TIM	14.4	circadian rhythm	regulation of cell proliferation
ARNTL	HIF1A	22.4	circadian rhythm	regulation of cell proliferation
ARNTL	KAT2B	22.6	circadian rhythm	regulation of cell proliferation
NPAS2	KAT2B	1.6	circadian rhythm	regulation of cell proliferation
TIM	TIPIN	0.3	circadian rhythm	regulation of cell proliferation
DBP	CLOCK	9.9	regulation of cell proliferation	circadian rhythm
PRKCA	PER2	13.6	regulation of cell proliferation	circadian rhythm
CHEK1	TIM	14.8	regulation of cell proliferation	circadian rhythm
HIF1A	PER1	11.4	regulation of cell proliferation	circadian rhythm
KAT2B	CLOCK	0.3	regulation of cell proliferation	circadian rhythm
CRY1	CLOCK	20.7	DNA repair	transcrip. from RNA poly. II promot.
CRY1	NPAS2	22.1	DNA repair	transcrip. from RNA poly. II promot.

CRY2	CLOCK	0	DNA repair	transcrip. from RNA poly. II promot.
CRY2	NPAS2	1.6	DNA repair	transcrip. from RNA poly. II promot.
CSNK1E	CLOCK	22.4	DNA repair	transcrip. from RNA poly. II promot.
CSNK1E	RORA	20.2	DNA repair	transcrip. from RNA poly. II promot.
ATRX	HDAC1	7.6	DNA repair	transcrip. from RNA poly. II promot.
ARNTL	CRY1	21.2	transcrip. from RNA poly. II promot.	DNA repair
ARNTL	CRY2	22.5	transcrip. from RNA poly. II promot.	DNA repair
ARNTL	CSNK1E	22.1	transcrip. from RNA poly. II promot.	DNA repair
AR	NONO	16.1	transcrip. from RNA poly. II promot.	DNA repair
CEBPA	CEBPG	9.4	transcrip. from RNA poly. II promot.	DNA repair
EP300	PCNA	6.1	transcrip. from RNA poly. II promot.	DNA repair
HDAC1	PCNA	15.1	transcrip. from RNA poly. II promot.	DNA repair

Table 14. KEGG Pathway Analysis of Network Extension Components.

KEGG ID	**p-value**	**FDR**	**Term**
5200	0.0000	0.0000	Pathways in cancer
5221	0.0000	0.0001	Acute myeloid leukemia
4330	0.0000	0.0002	Notch signaling pathway
5215	0.0001	0.0003	Prostate cancer
5016	0.0001	0.0004	Huntington's disease
4110	0.0006	0.0058	Cell cycle
4916	0.0006	0.0058	Melanogenesis
5211	0.0013	0.0106	Renal cell carcinoma
4062	0.0054	0.0318	Chemokine signaling pathway
4670	0.0071	0.0382	Leukocyte transendothelial migration
4120	0.0149	0.0645	Ubiquitin mediated proteolysis
4630	0.0279	0.1009	Jak-STAT signaling pathway

Table 15. RNAi Constructs Used for Systematic Screen for Network Neighborhood Components.

Gene ID h	**Sym. h**	**RNAi clone ID**	**Supplier**
196	AHR	V2LHS_132480	Open Biosystems
196	AHR	V2LHS_132482	Open Biosystems
207	AKT1	V2LHS_192049	Open Biosystems
367	AR	V2LHS_149847	Open Biosystems
367	AR	V2LHS_149850	Open Biosystems
367	AR	V2LHS_239220	Open Biosystems
367	AR	V2LHS_239574	Open Biosystems
9070	ASH2L	V2LHS_245205	Open Biosystems
9070	ASH2L	V2LHS_41272	Open Biosystems

466	ATF1	V2LHS_244510	Open Biosystems
466	ATF1	V2LHS_48799	Open Biosystems
466	ATF1	V2LHS_48799	Open Biosystems
466	ATF1	V2LHS_48801	Open Biosystems
1822	ATN1	V2LHS_151237	Open Biosystems
546	ATRX	V2LHS_11512	Open Biosystems
546	ATRX	V2LHS_201895	Open Biosystems
546	ATRX	V2LHS_202296	Open Biosystems
546	ATRX	V2LHS_202335	Open Biosystems
546	ATRX	V2LHS_202920	Open Biosystems
546	ATRX	V2LHS_228887	Open Biosystems
546	ATRX	V2LHS_93286	Open Biosystems
10538	BATF	V2LHS_197450	Open Biosystems
10538	BATF	V2LHS_200084	Open Biosystems
10538	BATF	V2LHS_254489	Open Biosystems
760	CA2	V2LHS_89120	Open Biosystems
1054	CEBPG	V2LHS_150519	Open Biosystems
1054	CEBPG	V2LHS_150521	Open Biosystems
1054	CEBPG	V2LHS_150523	Open Biosystems
1108	CHD4	V2LHS_112987	Open Biosystems
1108	CHD4	V2LHS_112988	Open Biosystems
1108	CHD4	V2LHS_112990	Open Biosystems
1108	CHD4	V2LHS_14657	Open Biosystems
1111	CHEK1	V2LHS_112994	Open Biosystems
1111	CHEK1	V2LHS_112996	Open Biosystems
10488	CREB3	V2LHS_197887	Open Biosystems
10488	CREB3	V2LHS_199720	Open Biosystems
90993	CREB3L1	V2LHS_99572	Open Biosystems
1387	CREBBP	V2LHS_24251	Open Biosystems
1390	CREM	V2LHS_150902	Open Biosystems
1390	CREM	V2LHS_150904	Open Biosystems
1390	CREM	V2LHS_150907	Open Biosystems
1390	CREM	V2LHS_7070	Open Biosystems
8451	CUL4A	V2LHS_32526	Open Biosystems
8451	CUL4A	V2LHS_32527	Open Biosystems
8451	CUL4A	V2LHS_32529	Open Biosystems
8450	CUL4B	V2LHS_32515	Open Biosystems
8450	CUL4B	V2LHS_32517	Open Biosystems
1642	DDB1	V2LHS_151130	Open Biosystems
1642	DDB1	V2LHS_151132	Open Biosystems
1786	DNMT1	V2LHS_113503	Open Biosystems
1786	DNMT1	V2LHS_113505	Open Biosystems
1788	DNMT3A	V2LHS_189136	Open Biosystems

1788	DNMT3A	V2LHS_200445	Open Biosystems
1788	DNMT3A	V2LHS_201692	Open Biosystems
1788	DNMT3A	V2LHS_202364	Open Biosystems
1788	DNMT3A	V2LHS_202453	Open Biosystems
1788	DNMT3A	V2LHS_202509	Open Biosystems
1788	DNMT3A	V2LHS_74666	Open Biosystems
1788	DNMT3A	V2LHS_74667	Open Biosystems
1788	DNMT3A	V2LHS_74668	Open Biosystems
1789	DNMT3B	V2LHS_11913	Open Biosystems
1789	DNMT3B	V2LHS_77230	Open Biosystems
1789	DNMT3B	V2LHS_77233	Open Biosystems
1789	DNMT3B	V2LHS_77234	Open Biosystems
1810	DR1	V2LHS_151221	Open Biosystems
51514	DTL	V2LHS_225424	Open Biosystems
1876	E2F6	V2LHS_151292	Open Biosystems
1876	E2F6	V2LHS_151297	Open Biosystems
8726	EED	V2LHS_23172	Open Biosystems
2034	EPAS1	V2LHS_113750	Open Biosystems
2034	EPAS1	V2LHS_113753	Open Biosystems
2034	EPAS1	V2LHS_225592	Open Biosystems
2770	GNAI1	V2LHS_114161	Open Biosystems
2770	GNAI1	V2LHS_114162	Open Biosystems
2771	GNAI2	V2LHS_114165	Open Biosystems
2782	GNB1	V2LHS_114181	Open Biosystems
2782	GNB1	V2LHS_114185	Open Biosystems
2782	GNB1	V2LHS_114186	Open Biosystems
9737	GPRASP1	V2LHS_259021	Open Biosystems
83743	GRWD1	V2LHS_117549	Open Biosystems
3054	HCFC1	V2LHS_37684	Open Biosystems
3054	HCFC1	V2LHS_37685	Open Biosystems
29915	HCFC2	V2LHS_247453	Open Biosystems
29915	HCFC2	V2LHS_65548	Open Biosystems
29915	HCFC2	V2LHS_65550	Open Biosystems
3065	HDAC1	V2LHS_61808	Open Biosystems
3065	HDAC1	V2LHS_61809	Open Biosystems
3065	HDAC1	V2LHS_61813	Open Biosystems
3066	HDAC2	V2LHS_132136	Open Biosystems
3091	HIF1A	V2LHS_132150	Open Biosystems
3091	HIF1A	V2LHS_132151	Open Biosystems
3091	HIF1A	V2LHS_132152	Open Biosystems
3091	HIF1A	V2LHS_236718	Open Biosystems
3131	HLF	V2LHS_133079	Open Biosystems
3131	HLF	V2LHS_133080	Open Biosystems

3131	HLF	V2LHS_133082	Open Biosystems
3131	HLF	V2LHS_133083	Open Biosystems
8850	KAT2B	V2LHS_53088	Open Biosystems
8850	KAT2B	V2LHS_53089	Open Biosystems
8850	KAT2B	V2LHS_53090	Open Biosystems
8850	KAT2B	V2LHS_53091	Open Biosystems
55885	LMO3	V2LHS_240458	Open Biosystems
55885	LMO3	V2LHS_30925	Open Biosystems
4163	MCC	V2LHS_151622	Open Biosystems
4163	MCC	V2LHS_151627	Open Biosystems
4163	MCC	V2LHS_261826	Open Biosystems
4163	MCC	V2LHS_262535	Open Biosystems
4163	MCC	V2LHS_263032	Open Biosystems
5469	MED1	V2LHS_35711	Open Biosystems
5469	MED1	V2LHS_35711	Open Biosystems
5469	MED1	V2LHS_35712	Open Biosystems
5469	MED1	V2LHS_35713	Open Biosystems
5469	MED1	V2LHS_35715	Open Biosystems
4221	MEN1	V2LHS_76605	Open Biosystems
4297	MLL	V2LHS_196843	Open Biosystems
4297	MLL	V2LHS_198242	Open Biosystems
4297	MLL	V2LHS_198375	Open Biosystems
4609	MYC	V2LHS_152050	Open Biosystems
4609	MYC	V2LHS_152051	Open Biosystems
4654	MYOD1	V2LHS_152109	Open Biosystems
8648	NCOA1	V2LHS_23965	Open Biosystems
8648	NCOA1	V2LHS_23968	Open Biosystems
8648	NCOA1	V2LHS_23970	Open Biosystems
10499	NCOA2	V2LHS_12526	Open Biosystems
10499	NCOA2	V2LHS_199743	Open Biosystems
8202	NCOA3	V2LHS_206733	Open Biosystems
8202	NCOA3	V2LHS_206740	Open Biosystems
8202	NCOA3	V2LHS_206781	Open Biosystems
8202	NCOA3	V2LHS_207128	Open Biosystems
8202	NCOA3	V2LHS_261936	Open Biosystems
57727	NCOA5	V2LHS_200338	Open Biosystems
57727	NCOA5	V2LHS_200715	Open Biosystems
9611	NCOR1	V2LHS_196602	Open Biosystems
9611	NCOR1	V2LHS_91777	Open Biosystems
9611	NCOR1	V2LHS_91778	Open Biosystems
9611	NCOR1	V2LHS_91779	Open Biosystems
9612	NCOR2	V2LHS_196739	Open Biosystems
9612	NCOR2	V2LHS_251658	Open Biosystems

4830	NME1	V2LHS_76045	Open Biosystems
4830	NME1	V2LHS_76046	Open Biosystems
4830	NME1	V2LHS_76050	Open Biosystems
4831	NME2	V2LHS_152291	Open Biosystems
9722	NOS1AP	V2LHS_103917	Open Biosystems
9722	NOS1AP	V2LHS_103920	Open Biosystems
266743	NPAS4	V2LHS_118806	Open Biosystems
266743	NPAS4	V2LHS_118807	Open Biosystems
266743	NPAS4	V2LHS_118808	Open Biosystems
190	NR0B1	V2LHS_239255	Open Biosystems
190	NR0B1	V2LHS_239628	Open Biosystems
190	NR0B1	V2LHS_93206	Open Biosystems
190	NR0B1	V2LHS_93207	Open Biosystems
10002	NR2E3	V2LHS_199322	Open Biosystems
10002	NR2E3	V2LHS_239554	Open Biosystems
83714	NRIP2	V2LHS_117487	Open Biosystems
83714	NRIP2	V2LHS_117489	Open Biosystems
83714	NRIP2	V2LHS_117492	Open Biosystems
23178	PASK	V2LHS_87444	Open Biosystems
23178	PASK	V2LHS_87445	Open Biosystems
5111	PCNA	V2LHS_152708	Open Biosystems
5111	PCNA	V2LHS_152710	Open Biosystems
5111	PCNA	V2LHS_261970	Open Biosystems
5252	PHF1	V2LHS_221739	Open Biosystems
5371	PML	V2LHS_194094	Open Biosystems
23649	POLA2	V2LHS_170195	Open Biosystems
23649	POLA2	V2LHS_170199	Open Biosystems
5430	POLR2A	V2LHS_131390	Open Biosystems
5430	POLR2A	V2LHS_131391	Open Biosystems
5705	PSMC5	V2LHS_170781	Open Biosystems
5705	PSMC5	V2LHS_170782	Open Biosystems
5705	PSMC5	V2LHS_170783	Open Biosystems
5705	PSMC5	V2LHS_170785	Open Biosystems
5705	PSMC5	V2LHS_302	Open Biosystems
5705	PSMC5	V2LHS_304	Open Biosystems
55269	PSPC1	V2LHS_156677	Open Biosystems
5914	RARA	V2LHS_131536	Open Biosystems
5929	RBBP5	V2LHS_19053	Open Biosystems
5929	RBBP5	V2LHS_19056	Open Biosystems
5929	RBBP5	V2LHS_19057	Open Biosystems
6256	RXRA	V2LHS_239551	Open Biosystems
6256	RXRA	V2LHS_31972	Open Biosystems
6256	RXRA	V2LHS_31973	Open Biosystems

6421	SFPQ	V2LHS_18691	Open Biosystems
6421	SFPQ	V2LHS_18692	Open Biosystems
6421	SFPQ	V2LHS_240572	Open Biosystems
6421	SFPQ	V2LHS_241826	Open Biosystems
9410	SNRNP40	V2LHS_68716	Open Biosystems
9410	SNRNP40	V2LHS_68717	Open Biosystems
9410	SNRNP40	V2LHS_68720	Open Biosystems
6667	SP1	V2LHS_179659	Open Biosystems
6667	SP1	V2LHS_179661	Open Biosystems
6667	SP1	V2LHS_179662	Open Biosystems
6667	SP1	V2LHS_221748	Open Biosystems
6667	SP1	V2LHS_68650	Open Biosystems
6688	SPI1	V2LHS_278676	Open Biosystems
6774	STAT3	V2LHS_262105	Open Biosystems
6774	STAT3	V2LHS_88502	Open Biosystems
23512	SUZ12	V2LHS_256397	Open Biosystems
23512	SUZ12	V2LHS_74301	Open Biosystems
7008	TEF	V2LHS_153880	Open Biosystems
7008	TEF	V2LHS_153884	Open Biosystems
7008	TEF	V2LHS_153885	Open Biosystems
54962	TIPIN	V2LHS_174169	Open Biosystems
54962	TIPIN	V2LHS_174170	Open Biosystems
54962	TIPIN	V2LHS_222044	Open Biosystems
11277	TREX1	V2LHS_115659	Open Biosystems
11277	TREX1	V2LHS_115661	Open Biosystems
11277	TREX1	V2LHS_263865	Open Biosystems
7329	UBE2I	V2LHS_171776	Open Biosystems
7329	UBE2I	V2LHS_171781	Open Biosystems
7329	UBE2I	V2LHS_254973	Open Biosystems
7329	UBE2I	V2LHS_8129	Open Biosystems
7409	VAV1	V2LHS_69841	Open Biosystems
7409	VAV1	V2LHS_69842	Open Biosystems
7409	VAV1	V2LHS_69844	Open Biosystems
7414	VCL	V2LHS_171918	Open Biosystems
7414	VCL	V2LHS_171919	Open Biosystems

Table 16. RNAi Constructs Used for Systematic Screen for 46 Network Components.

Gene ID h	**Sym. h**	**RNAi clone ID**	**Supplier**
5187	PER1	V2HS_169842	Open Biosystems
5187	PER1	V2HS_169845	Open Biosystems
5187	PER1	V2MM_67435	Open Biosystems
5187	PER1	V2LHS_169842	Open Biosystems

5187	PER1	V2LHS_169845	Open Biosystems
8864	PER2	V2HS_52938	Open Biosystems
8864	PER2	V2HS_52937	Open Biosystems
8864	PER2	V2HS_53009	Open Biosystems
8864	PER2	V2HS_52939	Open Biosystems
8864	PER2	V2LHS_52937	Open Biosystems
8863	PER3	V2HS_154125	Open Biosystems
8863	PER3	V2HS_154121	Open Biosystems
8863	PER3	V2LHS_154120	Open Biosystems
1407	CRY1	V2HS_172866	Open Biosystems
1407	CRY1	V2HS_172863	Open Biosystems
1407	CRY1	V2HS_172862	Open Biosystems
1408	CRY2	V2HS_67007	Open Biosystems
1408	CRY2	V2HS_67010	Open Biosystems
1408	CRY2	V2HS_67009	Open Biosystems
1408	CRY2	V2LHS_67005	Open Biosystems
8914	TIM	V2HS_47525	Open Biosystems
8914	TIM	V2HS_47526	Open Biosystems
8914	TIM	V2LHS_245690	Open Biosystems
9572	NR1D1	V2HS_239439	Open Biosystems
9572	NR1D1	V2HS_87199	Open Biosystems
9572	NR1D1	V2HS_239200	Open Biosystems
9572	NR1D1	V2HS_239561	Open Biosystems
9975	NR1D2	V2HS_239239	Open Biosystems
9975	NR1D2	V2HS_239468	Open Biosystems
9975	NR1D2	V2HS_49993	Open Biosystems
9975	NR1D2	V2HS_239350	Open Biosystems
9975	NR1D2	V2LHS_239488	Open Biosystems
9975	NR1D2	V2LHS_239383	Open Biosystems
9975	NR1D2	V2LHS_239570	Open Biosystems
9975	NR1D2	V2LHS_49921	Open Biosystems
9975	NR1D2	V2LHS_49922	Open Biosystems
9975	NR1D2	V2LHS_49994	Open Biosystems
85457	CIPC	V2HS_178395	Open Biosystems
85457	CIPC	V2HS_178399	Open Biosystems
85457	CIPC	V2HS_275456	Open Biosystems
85457	CIPC	V2LHS_178399	Open Biosystems
79365	DEC2	V2HS_116724	Open Biosystems
79365	DEC2	V2LHS_116721	Open Biosystems
79365	DEC2	V2LHS_116719	Open Biosystems
79365	DEC2	V2LHS_116724	Open Biosystems
9575	CLOCK	V2HS_67386	Open Biosystems
9575	CLOCK	V2HS_67391	Open Biosystems
4862	NPAS2	V2MM_38437	Open Biosystems
4862	NPAS2	V2HS_152327	Open Biosystems

4862	NPAS2	V2HS_138097	Open Biosystems
4862	NPAS2	V2HS_152324	Open Biosystems
406	ARNTL	V2HS_94645	Open Biosystems
406	ARNTL	V2HS_94643	Open Biosystems
406	ARNTL	V2HS_94640	Open Biosystems
56938	ARNTL2	V2HS_50998	Open Biosystems
56938	ARNTL2	V2HS_51001	Open Biosystems
56938	ARNTL2	V2LHS_51000	Open Biosystems
6095	RORA	V2HS_32210	Open Biosystems
6095	RORA	V2HS_239080	Open Biosystems
6095	RORA	V2HS_202956	Open Biosystems
6095	RORA	V2LHS_239222	Open Biosystems
6095	RORA	V2LHS_239238	Open Biosystems
6095	RORA	V2LHS_239416	Open Biosystems
6095	RORA	V2LHS_202317	Open Biosystems
6095	RORA	V2LHS_32209	Open Biosystems
6095	RORA	V2LHS_239707	Open Biosystems
6096	RORB	V2HS_94815	Open Biosystems
6096	RORB	V2HS_239246	Open Biosystems
6096	RORB	V2MM_24349	Open Biosystems
6096	RORB	V2LHS_94818	Open Biosystems
6096	RORB	V2LHS_8643	Open Biosystems
6096	RORB	V2LHS_94819	Open Biosystems
6096	RORB	V2LHS_239259	Open Biosystems
6096	RORB	V2LHS_239511	Open Biosystems
6096	RORB	V2LHS_94816	Open Biosystems
6096	RORB	V2LHS_239362	Open Biosystems
6097	RORC	V2HS_239620	Open Biosystems
6097	RORC	V2HS_18863	Open Biosystems
6097	RORC	V2HS_239366	Open Biosystems
6097	RORC	V2LHS_239280	Open Biosystems
6097	RORC	V2LHS_18859	Open Biosystems
6097	RORC	V2LHS_18861	Open Biosystems
1454	CSNK1E	V2HS_192204	Open Biosystems
1454	CSNK1E	V2MM_72981	Open Biosystems
1453	CSNK1D	V2LHS_150979	Open Biosystems
2932	GSK3B	V2HS_114291	Open Biosystems
2932	GSK3B	V2HS_114293	Open Biosystems
2932	GSK3B	V2HS_114292	Open Biosystems
2932	GSK3B	V2HS_114290	Open Biosystems
1457	CSNK2A1	V2LHS_150990	Open Biosystems
1457	CSNK2A1	V2LHS_283708	Open Biosystems
1457	CSNK2A1	V2HS_200683	Open Biosystems
1457	CSNK2A1	V2MM_34225	Open Biosystems
1457	CSNK2A1	V2HS_150988	Open Biosystems

1459	CSNK2A2	V2LHS_150997	Open Biosystems
1459	CSNK2A2	V2MM_70928	Open Biosystems
1460	CSNK2B_1	Prof. Kramer	Open Biosystems
1460	CSNK2B_2	Prof. Kramer	Open Biosystems
1460	CSNK2B_3	Prof. Kramer	Open Biosystems
1460	CSNK2B_4	Prof. Kramer	Open Biosystems
5578	PRKCA	V2LHS_218226	Open Biosystems
5578	PRKCA	V2LHS_87125	Open Biosystems
5578	PRKCA	V2LHS_87125	Open Biosystems
5578	PRKCA	V2LHS_170435	Open Biosystems
5578	PRKCA	V2LHS_218656	Open Biosystems
5578	PRKCA	V2LHS_218656	Open Biosystems
5566	PRKACA	V2LHS_170398	Open Biosystems
5499	PPP1CA	V2HS_170297	Open Biosystems
5499	PPP1CA	V2HS_262414	Open Biosystems
5500	PPP1CB	V2HS_220925	Open Biosystems
5500	PPP1CB	V2HS_223243	Open Biosystems
5500	PPP1CB	V2HS_276133	Open Biosystems
5501	PPP1CC	V2HS_170308	Open Biosystems
5501	PPP1CC	V2HS_170309	Open Biosystems
5501	PPP1CC	V2HS_170312	Open Biosystems
5515	PPP2CA	V2HS_170340	Open Biosystems
5515	PPP2CA	V2HS_170343	Open Biosystems
5515	PPP2CA	V2HS_170338	Open Biosystems
5515	PPP2CA	V2LHS_218016	Open Biosystems
5515	PPP2CA	V2LHS_170340	Open Biosystems
5516	PPP2CB	V2HS_173254	Open Biosystems
5516	PPP2CB	V2HS_173251	Open Biosystems
5516	PPP2CB	V2HS_220461	Open Biosystems
5516	PPP2CB	V2LHS_173252	Open Biosystems
5516	PPP2CB	V2LHS_262386	Open Biosystems
5516	PPP2CB	V2LHS_173256	Open Biosystems
5518	PPP2R1A	V2LHS_197495	Open Biosystems
5518	PPP2R1A	V2LHS_198701	Open Biosystems
5519	PPP2R1B	V2LHS_170346	Open Biosystems
5528	PPP2R5D	V2LHS_57934	Open Biosystems
5528	PPP2R5D	V2LHS_57937	Open Biosystems
5529	PPP2R5E	V2LHS_57881	Open Biosystems
5529	PPP2R5E	V2LHS_276146	Open Biosystems
5529	PPP2R5E	V2LHS_170347	Open Biosystems
5529	PPP2R5E	V2LHS_57882	Open Biosystems
5529	PPP2R5E	V2LHS_57880	Open Biosystems
5536	PPP5C	V2HS_57831	Open Biosystems
5536	PPP5C	V2HS_247322	Open Biosystems
8945	BTRC	V2LHS_277057	Open Biosystems

8945	BTRC	V2LHS_177228	Open Biosystems
8945	BTRC	V2LHS_33329	Open Biosystems
8945	BTRC	V2LHS_33325	Open Biosystems
8945	BTRC	V2LHS_33330	Open Biosystems
8945	BTRC	V2LHS_177233	Open Biosystems
23291	FBXW11	V2LHS_254528	Open Biosystems
23291	FBXW11	V2LHS_265946	Open Biosystems
23291	FBXW11	V2LHS_51187	Open Biosystems
23291	FBXW11	V2LHS_51191	Open Biosystems
26224	FBXL3	V2LHS_254736	Open Biosystems
26224	FBXL3	V2LHS_16078	Open Biosystems
26224	FBXL3	V2LHS_16079	Open Biosystems
26224	FBXL3	V2LHS_254741	Open Biosystems
26224	FBXL3	V2LHS_254986	Open Biosystems
26224	FBXL3	V2LHS_16077	Open Biosystems
79176	FBXL15	V2HS_135909	Open Biosystems
79176	FBXL15	V2LHS_135909	Open Biosystems
4841	NONO	V2HS_52657	Open Biosystems
4841	NONO	V2HS_52659	Open Biosystems
11091	WDR5	V2HS_140181	Open Biosystems
51655	RASD1	V2HS_97482	Open Biosystems
51655	RASD1	V2MM_19224	Open Biosystems
51655	RASD1	V2LHS_97478	Open Biosystems
51655	RASD1	V2LHS_97482	Open Biosystems
2146	EZH2	V2LHS_63067	Open Biosystems
2146	EZH2	V2LHS_63068	Open Biosystems
2146	EZH2	V2LHS_17510	Open Biosystems
2146	EZH2	V2LHS_63066	Open Biosystems
2146	EZH2	V2LHS_238994	Open Biosystems
2146	EZH2	V2LHS_17509	Open Biosystems
2146	EZH2	V2LHS_17507	Open Biosystems
4783	NFIL3	V2HS_243549	Open Biosystems
4783	NFIL3	V2LHS_36553	Open Biosystems
4783	NFIL3	V2LHS_243549	Open Biosystems
1628	DBP	V2LHS_113404	Open Biosystems
1628	DBP	V2LHS_113406	Open Biosystems

Table 17. Expression Plasmids.

No.	**Vector**	**Source**
1	pACT4-DM	Prof. Wanker
2	pBTM116-D9	Prof. Wanker
3	pcMYC-CMV-D12	Prof. Wanker
4	pFLAG-CMV-D11	Prof. Wanker

5	pENTR/D-TOPO	Invitrogen
6	pDEST 26	Invitrogen
7	pLenti6	Invitrogen
8	pGL3-Promoter Vector	Promega
9	phRL-SV40 Vector	Promega
10	pGL3-Basic Vector	Promega
11	pGIPZ constructs	Open Biosystems

Expression vector maps:

Yeast expression vectors:

Prey configuration [39]:

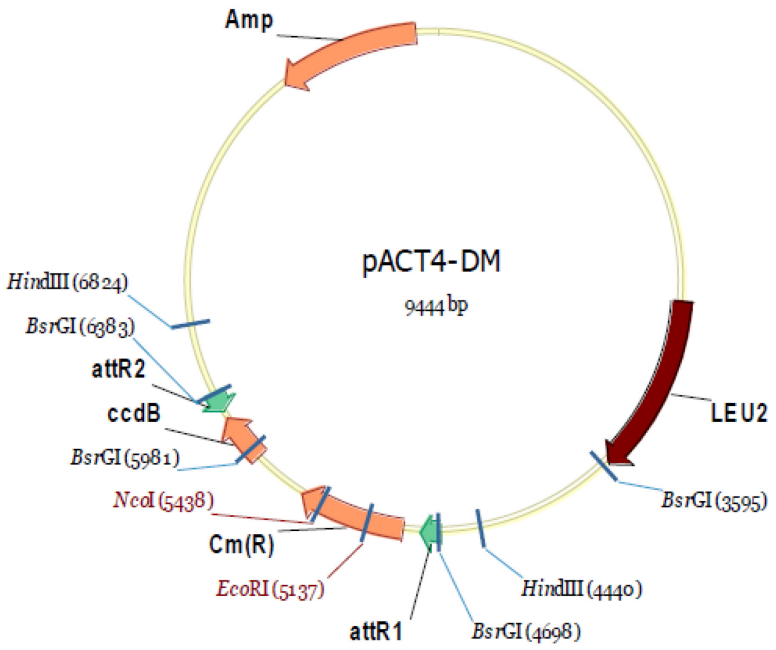

Bait configuration [39]:

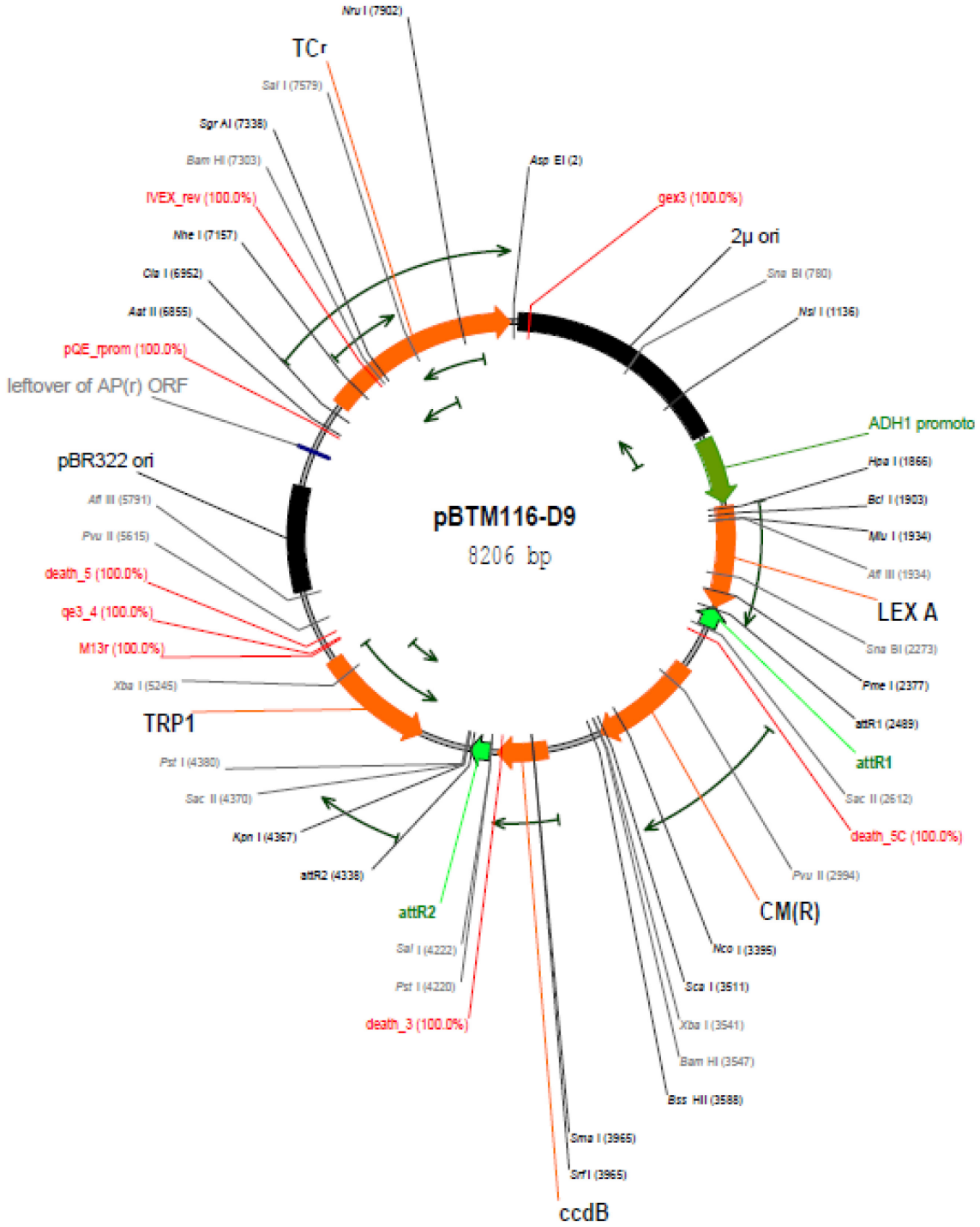

Mammalian expression vectors:

MYC-fusion expression (Prof. Wanker):

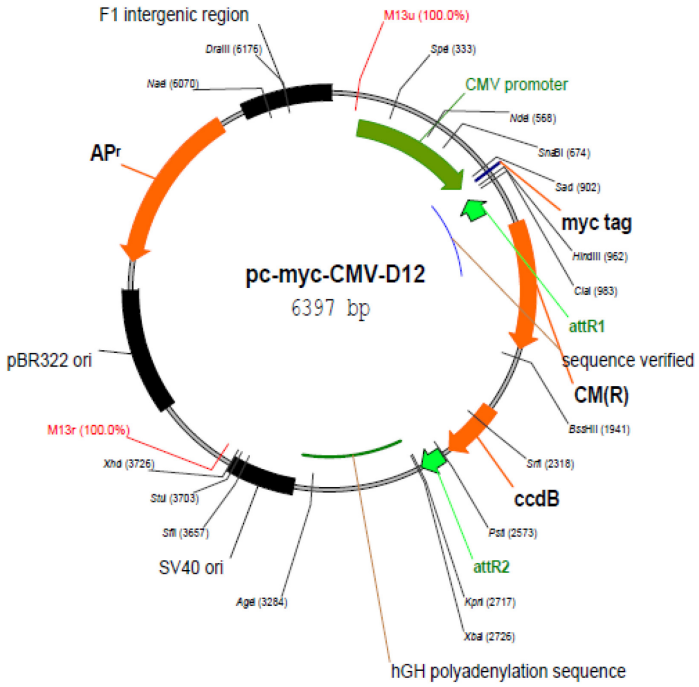

FLAG-fusion expression (Prof. Wanker):

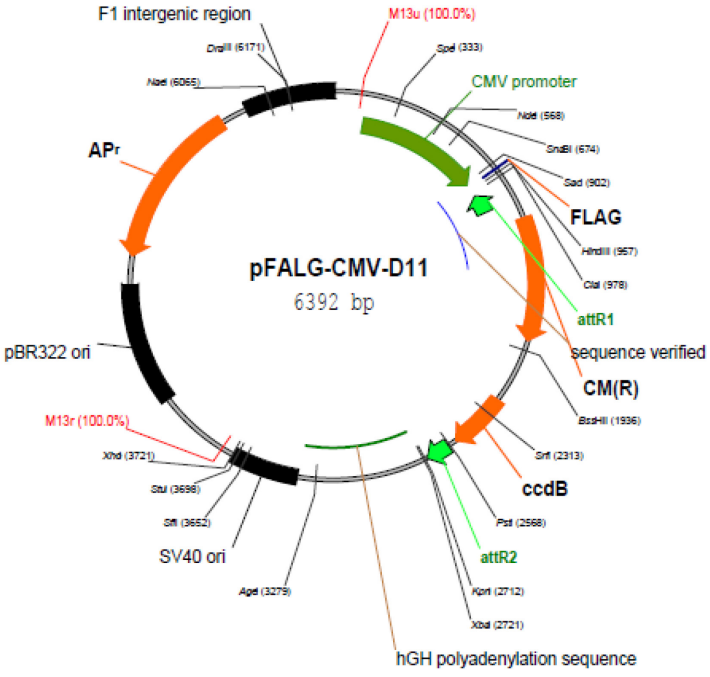

Vector maps were taken from Ivitrogen user's manual.

pENTR/D-TOPO (Invitrogen):

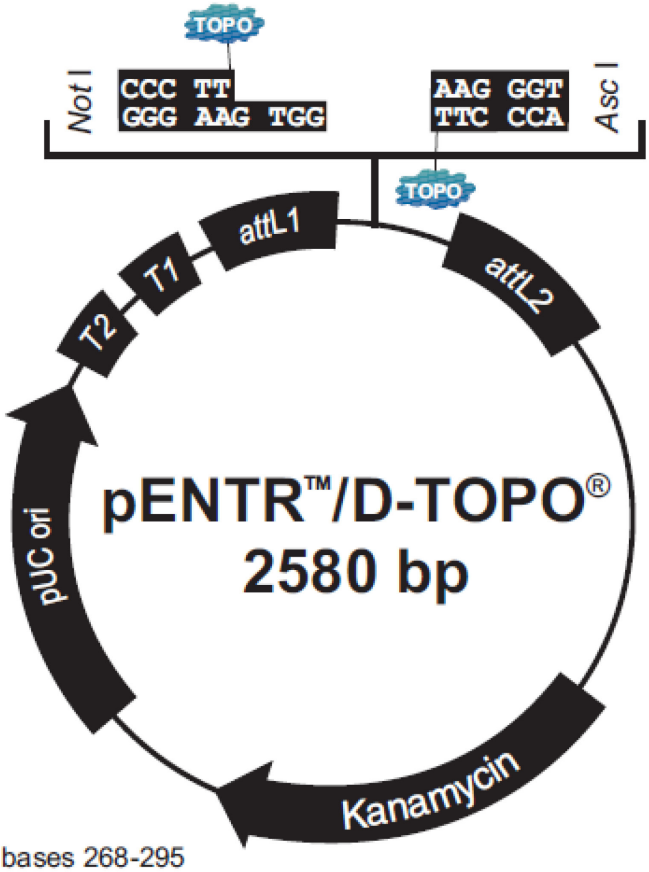

Comments for pENTR™/D-TOPO®
2580 nucleotides

*rrn*B T2 transcription termination sequence: bases 268-295
*rrn*B T1 transcription termination sequence: bases 427-470
M13 forward (-20) priming site: bases 537-552
*att*L1: bases 569-668 (c)
TOPO® recognition site 1: bases 680-684
Overhang: bases 685-688
TOPO® recognition site 2: bases 689-693
*att*L2: bases 705-804
T7 Promoter/priming site: bases 821-840 (c)
M13 reverse priming site: bases 845-861
Kanamycin resistance gene: bases 974-1783
pUC origin: bases 1904-2577

(c) = complementary sequence

pDEST 26 (Invitrogen):

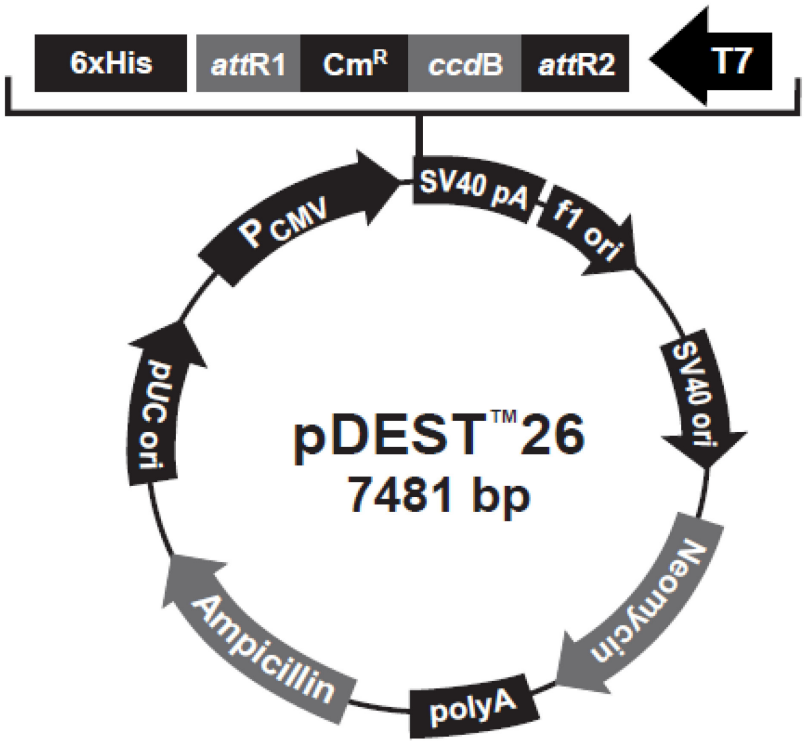

Comments for pDEST™26:
7481 nucleotides

CMV promoter: bases 15-608
6xHis tag: bases 644-661
*att*R1 site: bases 671-795
Chloramphenicol resistance gene (Cm^R): bases 904-1563
*ccd*B gene: bases 1905-2210
*att*R2 site: bases 2251-2375
T7 promoter: bases 2407-2426 (C)
SV40 early polyadenylation signal: bases 2726-2992
f1 intergenic region: bases 3118-3573
SV40 early promoter and origin: bases 3733-4041
Neomycin resistance gene: bases 4100-4894
Synthetic polyadenylation signal: bases 4958-5006
bla promoter: bases 5318-5416
Ampicillin (*bla*) resistance gene: bases 5417-6277
pUC origin: bases 6422-7095
(C) = complementary strand

pLenti6 (Invitrogen):

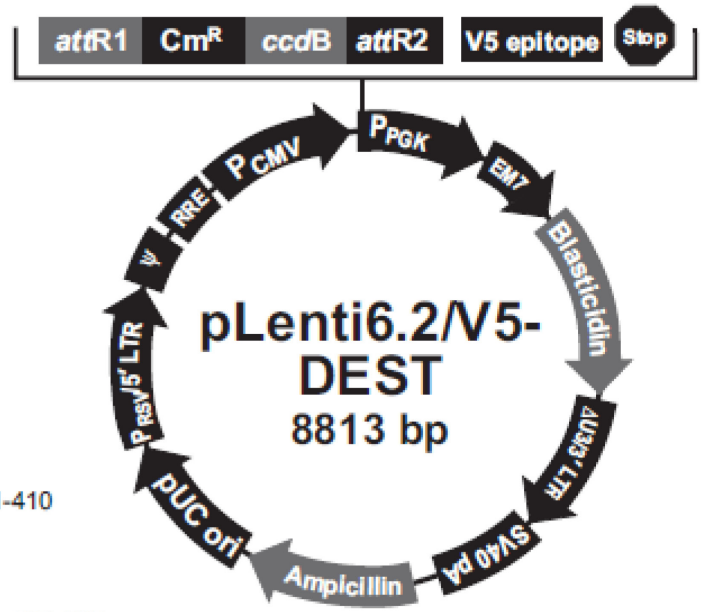

Comments for pLenti6.2/V5-DEST
8813 nucleotides

RSV/5′ LTR hybrid promoter: bases 1-410
RSV promoter: bases 1-229
HIV-1 5′ LTR: bases 230-410
5′ splice donor: base 520
HIV-1 psi (ψ) packaging signal: bases 521-565
HIV-1 Rev response element (RRE): bases 1075-1308
3′ splice acceptor: base 1656
3′ splice acceptor: base 1684
CMV promoter: bases 1809-2392
attR1 site: bases 2440-2564
Chloramphenicol resistance gene (Cm^R): bases 2673-3332
ccdB gene: bases 3674-3979
attR2 site: bases 4020-4144
V5 epitope: bases 4197-4238
PGK promoter: bases 4266-4771
EM7 promoter: bases 4782-4848
Blasticidin resistance gene: bases 4849-5247
ΔU3/3′ LTR: bases 5333-5567
ΔU3: bases 5333-5386
3′ LTR: bases 5387-5567
SV40 polyadenylation signal: bases 5639-5770
bla promoter: bases 6629-6727
Ampicillin (*bla*) resistance gene: bases 6728-7588
pUC origin: bases 7733-8406

Reporter vectors:

Vector maps were taken from Promega users's manual.

Promega Dual-Luciferase Reporter Assay System (firefly luciferase reporter):

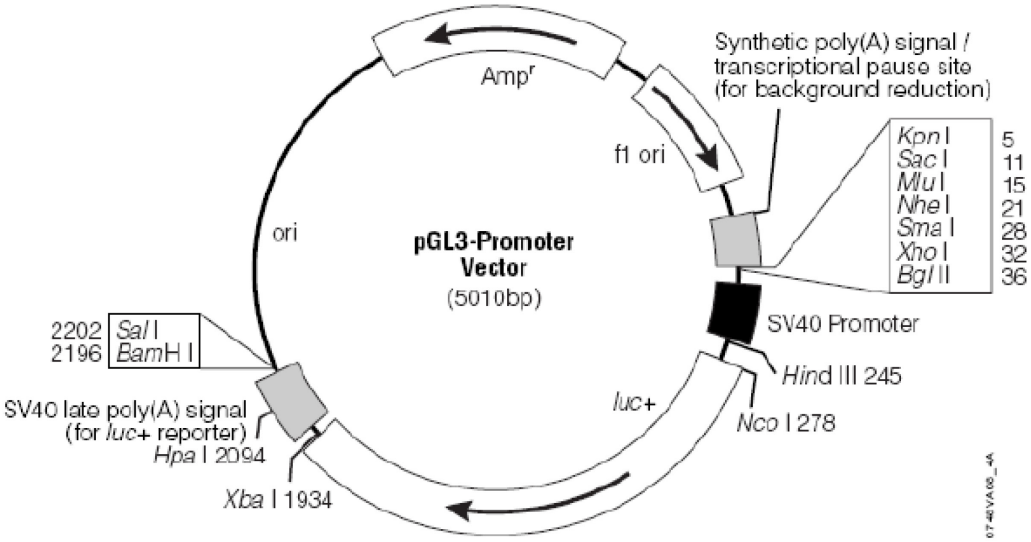

Promega Dual-Luciferase Reporter Assay System (*Renilla* luciferase reporter):

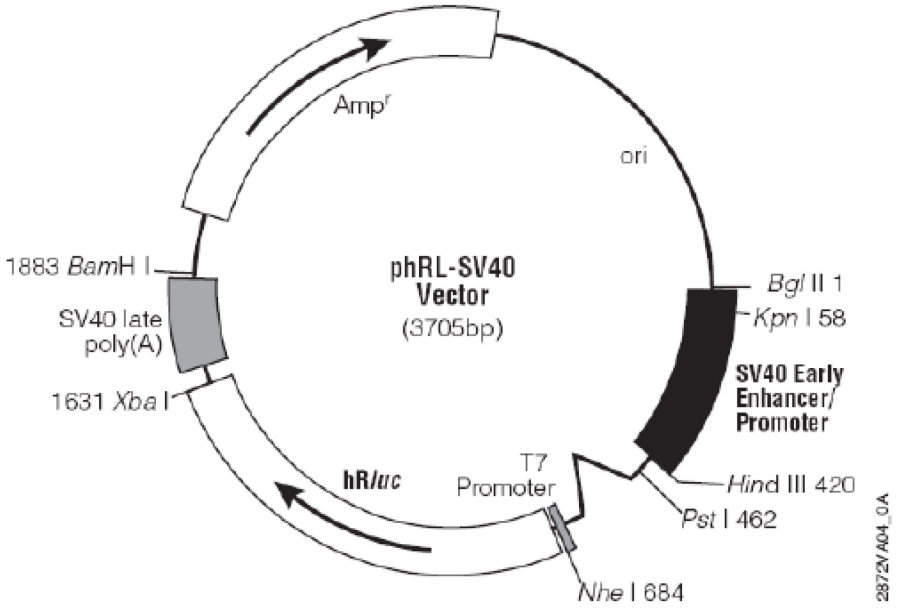

Promega Dual-Luciferase Reporter Assay System (pGL3-Basic Vector):

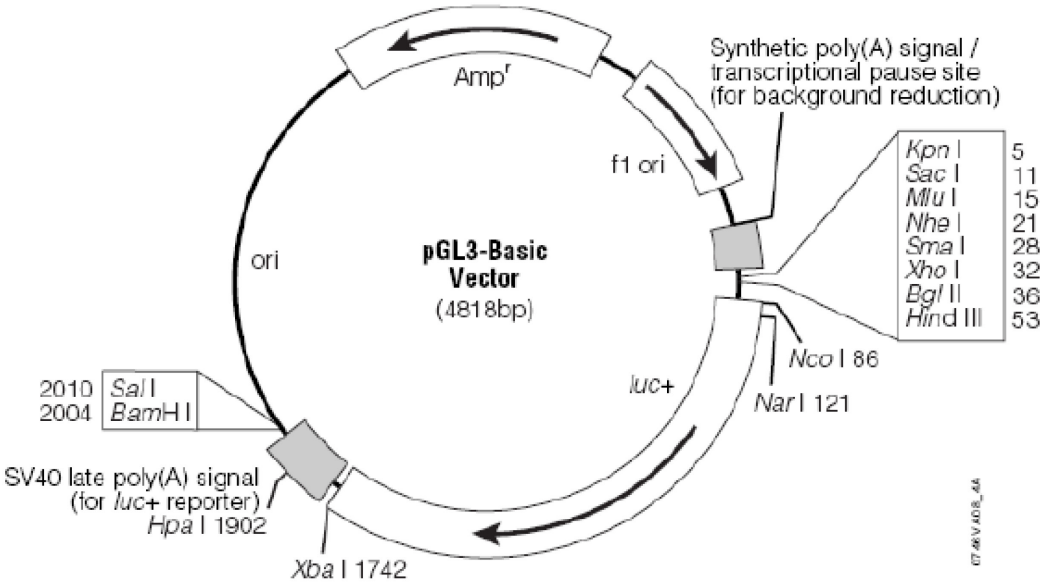

pGIPZ empty vector (Open Biosystems):

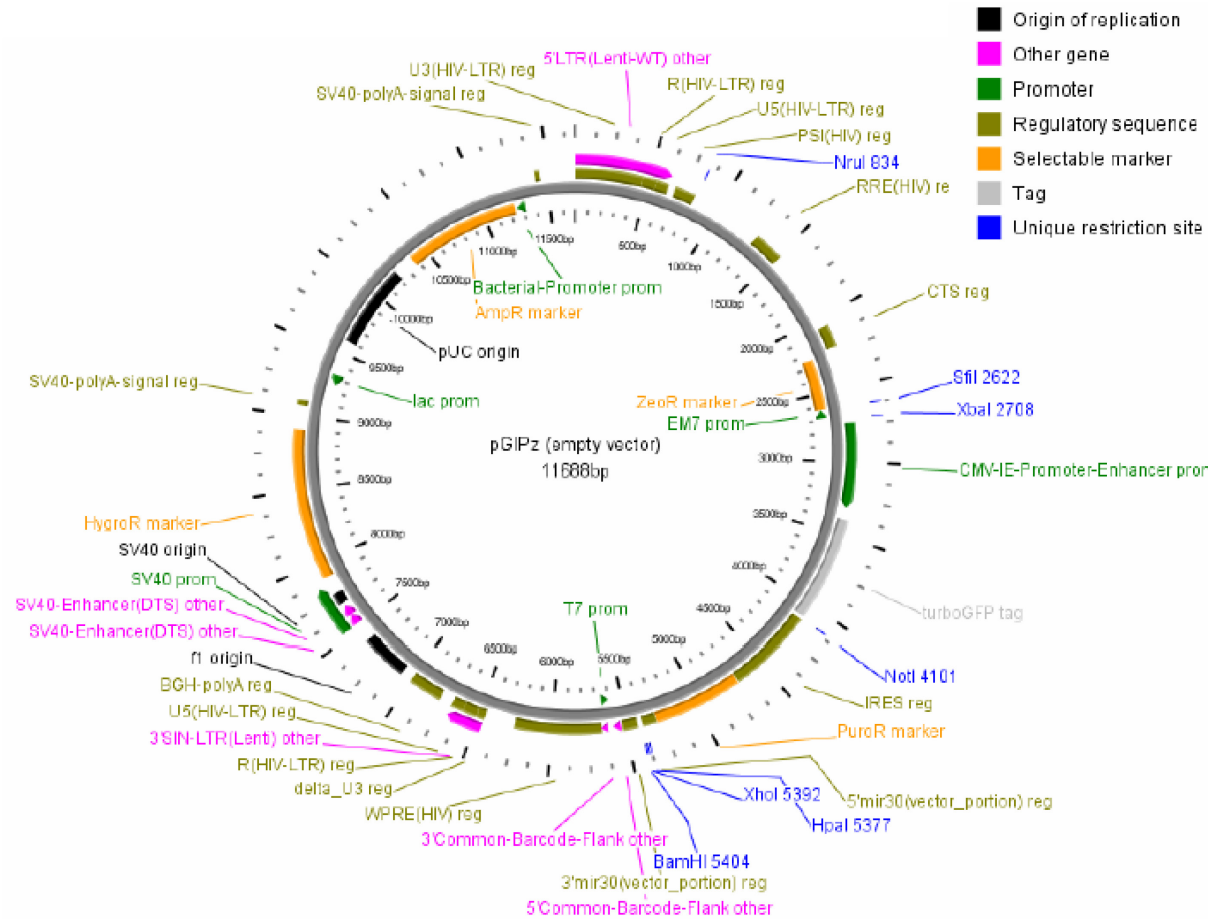

PUBLIKATIONEN, PRÄSENTATIONEN UND PREISE

Publikationen in Fachzeitschriften

- Wallach T, Schellenberg K, Maier B, Kalathur R, Porras P, Wanker EE, Futschik M, Kramer A. Dynamic Circadian Protein-Protein Interaction Networks Reveal Temporal Organization of Cellular Functions. In Vorbereitung.

- Relógio A, Westermark PO, Wallach T, Schellenberg K, Kramer A, Herzel H.Tuning the mammalian circadian clock: robust synergy of two loops. *PLoS Comput Biol*. 2011 Dec; **7** (12):e1002309

- Wallach T, Porras Milan P, Wanker EE, Kramer A. A Mammalian circadian interactome. Abstract in *Eur J Med Research* 2009, **14** (Supplement II): I-XXII, 1-208

- Maier B, Wendt S, Vanselow JT, Wallach T, Reischl S, Oehmke S, Schlosser A, Kramer A. A large-scale functional RNAi screen reveals a role for CK2 in the mammalian clock. *Genes Dev*. 2009, 23(6):708-18.

- Hoene V, Fischer M, Ivanova A, Wallach T, Berthold F, Dame C. GATA factors in human neuroblastoma: distinctive expression patterns in clinical subtypes. *Br J Cancer* 2009, **101**(8):1481-9.

- Wallach T, Porras Milan P, Wanker EE, Kramer A. Circadian protein-protein interaction networks. Abstarct in *Eur J Med Research* 2008, **13** (Supplement I): I-XX, 5

- Dame C, Kirscher K.M, Bartz KV, Wallach T, Hussels CS, Scholz H. Wilms tumor suppressor is an activator of the erythropoietin gene. *Blood* 2006, **107** (11): 4282-90

Präsentationen

- Wallach T. From Molecules to Modules: Organization and Dynamics of Functional Units in Cells. Poster im Rahmen der Begutachtung des SFB740 durch die DFG. Berlin, 08/2010

- Wallach T, Futschik M, Porras Milan P, Wanker EE, Kramer A. A dynamic circadian interactome. Poster bei International Symposium “Membranes and Modules” Berlin, 12/2009

- Wallach T, Futschik M, Porras Millan P, Wanker EE, Kramer A. A mammalian circadian interactome. Poster bei Gordon Research Conference on Chronobilogy, Salve Regina University, Newport, RI, USA, 07/2009

- Wallach T, Porras Milan P, Wanker EE, Kramer A. A circadian mammalian interactome. Vortrag bei 20th European Student’s Conference, Charité – Universitätsmedizin Berlin, 10/2009

- Wallach T, Porras Milan P, Wanker EE, Kramer A. Circadian protein-protein interaction networks. Vortrag bei 19th European Student's Conference, Charité – Universitätsmedizin Berlin, 10/2008

- Wallach T, Porras Milan P, Wanker EE, Kramer A. Circadian protein-protein interaction networks. Vortrag im Institut für Medizinische Immunologie, Charité – Universitätsmedizin Berlin, Germany, 06/2008

- Wallach T, Porras Milan P, Wanker EE, Kramer A. Circadian protein-protein interaction networks. Poster bei SRBR, Destin, Florida, USA, 05/2008

- Wallach T. Introduction into Chronobiology. Vortrag an The Rockefeller University, New York, NY, USA, 05/2008

- Wallach T, Porras Milan P, Wanker EE, Kramer A. Circadian protein-protein interaction networks. Vortrag an The Rockefeller University, New York, NY, USA, 05/2008

- Wallach T, Porras Milan P, Wanker EE, Kramer A. Circadian protein-protein interaction networks. Vortrag und Poster bei EUCLOCK Summer School, Matrahaza, Hungary, 10/2007

Auszeichnungen

- Gewinner in der Vortragsreihe Biochemie. 19th European Student's Conference, Charité – Universitätsmedizin Berlin, 10/2008

DANKSAGUNG

Die hier vorliegende Arbeit wurde von mir in der Arbeitsgruppe Chronobiologie von Prof. Dr. Achim Kamer am Institut für Medizinische Immunologie, Charité – Universitätsmedizin, Berlin im Zeitraum vom Mai 2007 bis Juni 2012 angefertigt.

Zuallererst möchte ich mich bei Prof. Dr. Achim Kramer für die Möglichkeit bedanken, meine Doktorarbeit auf dem sehr interessanten Gebiet der circadianen Rhythmen in seiner Gruppe anfertigen zu dürfen. Vielen Dank für die intensive Betreuung und stetiges Interesse an meinem Projekt sowie die Möglichkeit, an zahlreichen Konferenzen teilzunehmen.

Prof. Dr. Hanspeter Herzel möchte ich für die freundliche Übernahme der Betreuung dieser Arbeit an der Mathematisch-Naturwissenschaftlichen Fakultät I der Humboldt-Universität zu Berlin danken.

Dr. Matthias Futschik und Dr. Ravi Kalathur danke ich für die gute Zusammenarbeit und die Anfertigung der bioinformatischen Analysen für mein Projekt.

Vielen Dank auch an Prof. Dr. Erich Wanker, in dessen Labor ich die Interaktionsexperimente in Hefe durchführen durfte.

Dr. Bert Maier danke ich für die Zurverfügungstellung der RNAi-Daten für die Komponenten der Netzwerknachbarschaft.

Ich möchte auch allen Mitgliedern der AG Chronobiologie danken, die mich während meiner Doktorarbeit begleitet haben. Vielen Dank für die gute Zusammenarbeit, die zahlreichen Diskussionen sowie Unterstützung in allen Lagen und freundliche wie lustige Arbeitsatmosphäre.

Astrid, Katja und Bert danke ich außerdem noch für ihre Unterstützung bei der Anfertigung meiner Publikation und die vielen konstruktiven Diskussionen und Hilfestellungen. Ute, Silke, Maike, Roman und Ruppert vielen Dank für Euer stets offenes Ohr und Eure hilfreichen Tipps und Tricks, die mir eine große Hilfe waren. Ich danke auch meinen Mitstreiterinnen Sabrina, Jeannine und Manjana für die gemeinsam erlebten Erfahrungen mit vielen freudigen Momenten und wünsche Euch alles Gute für den Abschluss Eurer Arbeiten.

Veronika, Sandra und Sebastian wünsche ich viel Spaß und Erfolg bei der circadianen Forschung in den noch kommenden Jahren. Kathrin, Sandra und Barbara gilt mein Dank für die „Hiwiarbeiten“, die meinem Projekt im Laufe der Zeit zugutegekommen sind.

Annette danke ich für ihre Hilfe bei vielen administrativen Angelegenheiten und Rolf für seinen unermüdlichen Einsatz für die Sicherheit und das reibungslose Funktionieren der „Computerwelt“.

Der Arbeitsgruppe „Molekulare Bibliotheken“ danke ich für die fachübergreifenden Gespräche und die vielen Zusammenkünfte.

Zu guter Letzt möchte ich meiner Frau Iwona, meinen Kindern Kilian und Stella sowie Freunden und Familie für ihr großes Verständnis und Hilfsbreitschaft während meiner Doktorarbeit sehr herzlich danken.

ERKLÄRUNG

Hiermit erkläre ich, dass ich die vorliegende Arbeit selbstständig und nur unter der Verwendung der angegebenen Hilfen und Hilfsmittel angefertigt habe. Ich habe mich außerdem weder anderwärts um einen Doktorgrad beworben noch besitze ich bereits einen entsprechenden Doktorgrad. Die dem angestrebten Verfahren zugrunde liegende Promotionsordnung ist mir bekannt.